Recent Developments in NDA Strategy, Technology and Innovation

Dr Rick Short

10th November 2021

Who we are

The Nuclear Decommissioning Authority (NDA) is a non-departmental public body created through the Energy Act 2004.

Our business model:

Where we operate

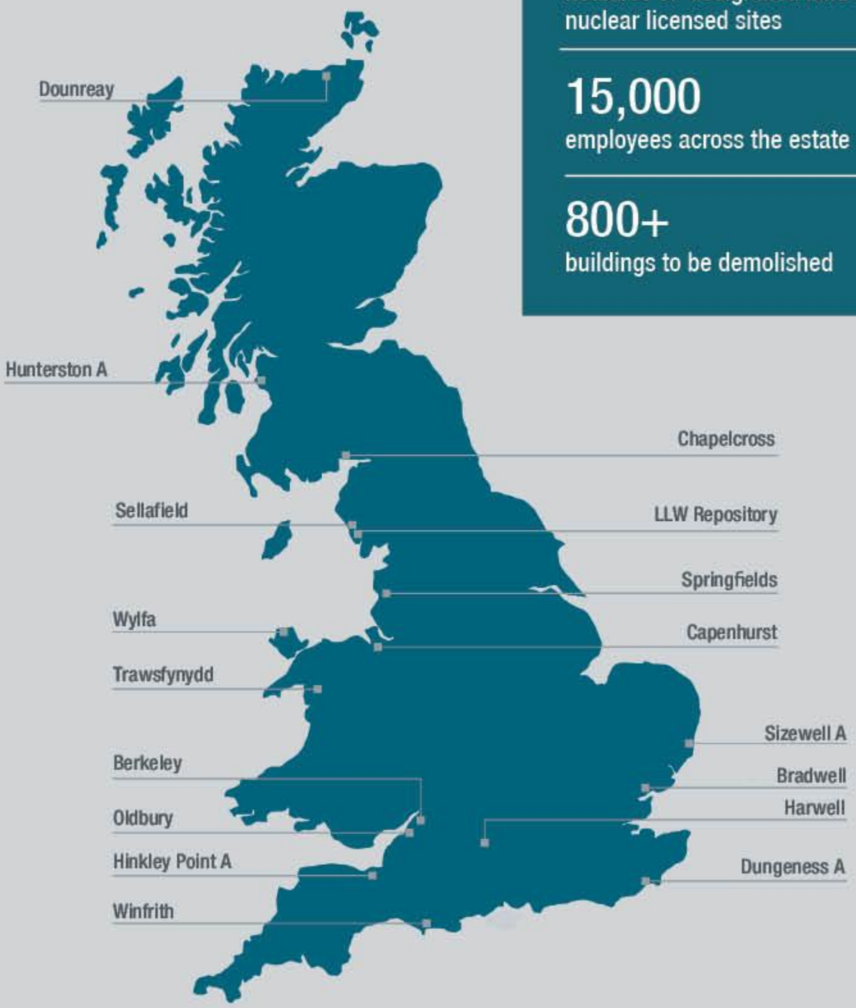

17
nuclear sites across the UK

1,046
hectares of designated land on nuclear licensed sites

15,000
employees across the estate

800+
buildings to be demolished

Our Mission

We're cleaning up the UK's earliest nuclear sites safely, securely and cost-effectively with care for people and the environment.

Our work to clean up the UK's nuclear legacy is the largest, most important environmental restoration project in Europe. And our mission is so long-term it spans the next century and beyond.

Our 17 sites are at different stages of decommissioning and all have unique challenges.

We're also engaging with communities to establish a long-term storage solution for higher-level wastes, making our environment safer for future generations.

How we work

We deliver our mission through our site licence companies and subsidiaries.

NDA's role is to support our sites, businesses and employees, optimising delivery and managing performance by providing group leadership, focus and governance.

We support research and development, seek innovation and work to standardise and simplify processes.

LLW Repository Ltd

Dounreay

NTS Nuclear Transport Solutions

Sellafield Ltd

Magnox

Radioactive Waste Management

Our Challenge

"Our mission will be complete when we release our sites for other uses."

NDA Strategy, effective from April 2016, p19

We break down our mission into 4 key strategic areas which help us to more clearly define and prioritise our work.

Our most urgent task is dealing with the highest hazard materials across our sites: spent fuel, nuclear materials and highly radioactive wastes.

Once the inventory has been made safe, the redundant nuclear facilities can be dismantled and demolished and land released for other uses.

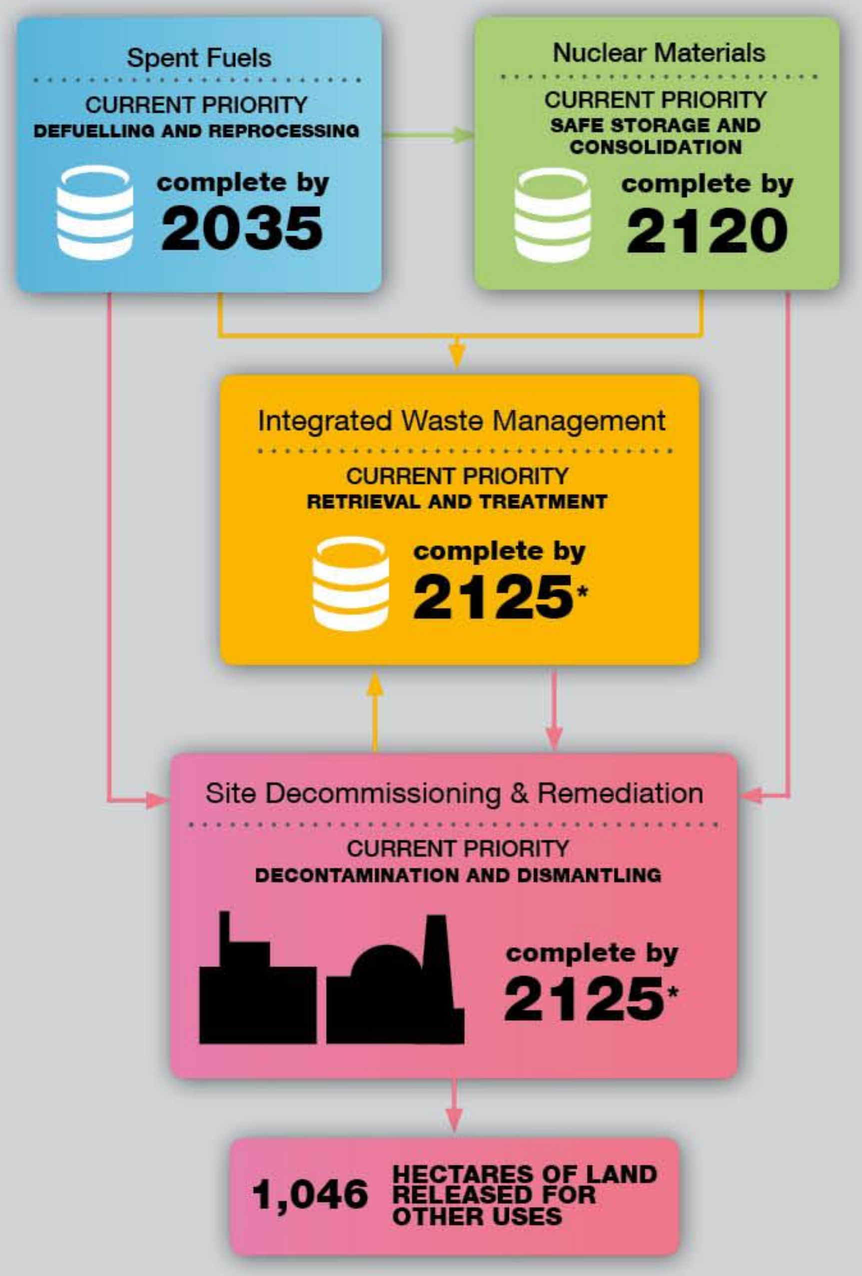

*the policy for Scotland is to have near surface disposal, the final decision on which is not accounted for in this date.

Recent developments

- Move to One NDA
- Mission evolution
- Strategy & Technology becomes Technology & Innovation

One NDA group structure

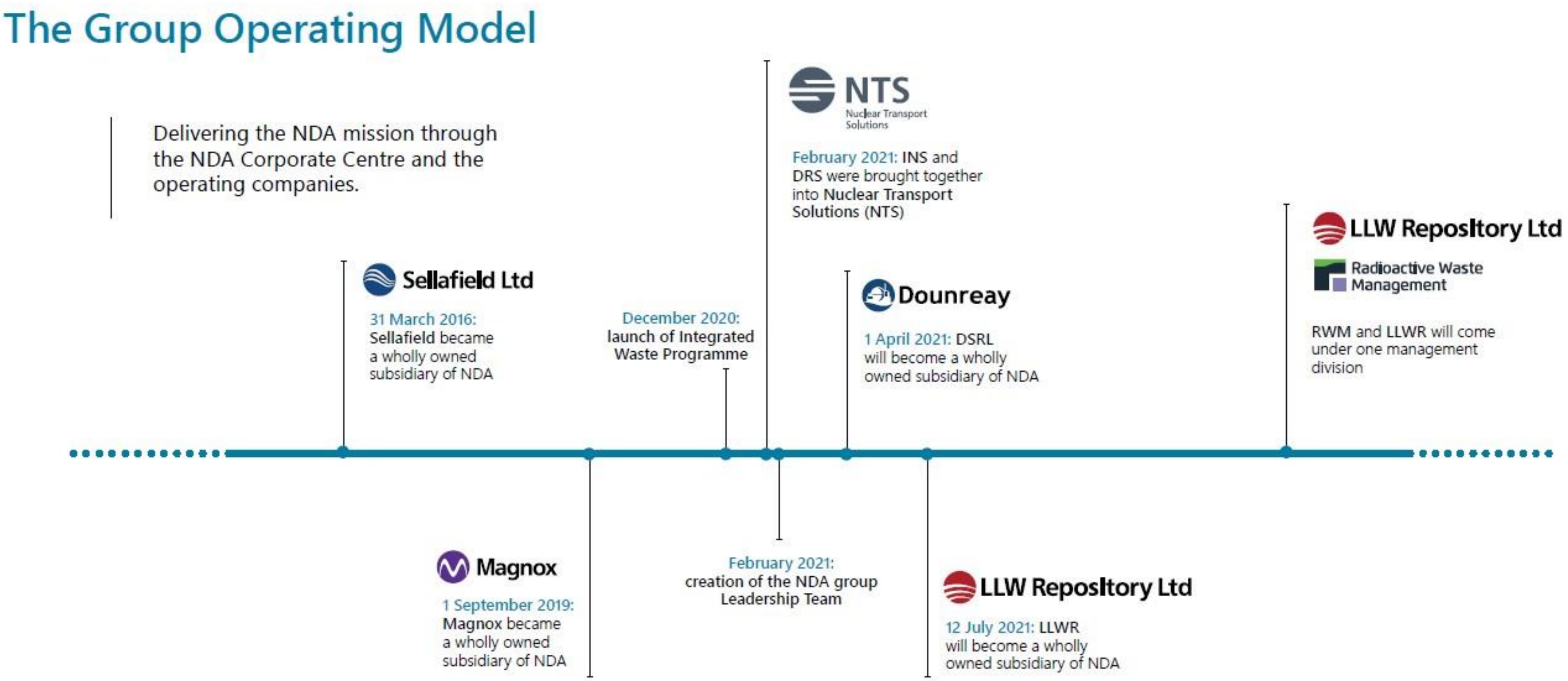

Recent publications

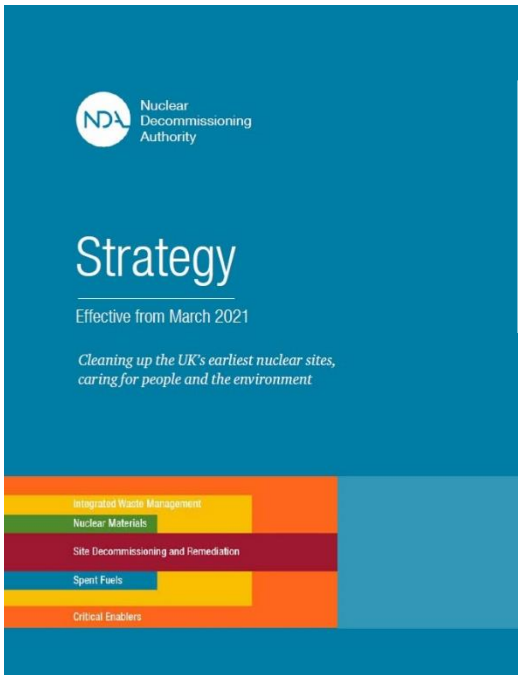

https://www.gov.uk/government/publications/nuclear-decommissioning-authority-strategy-effective-from-march-2021/nuclear-decommissioning-authority-strategy-effective-from-march-2021

https://www.gov.uk/government/publications/nuclear-decommissioning-authority-mission-progress-report-2021

Sustainability and Inclusion

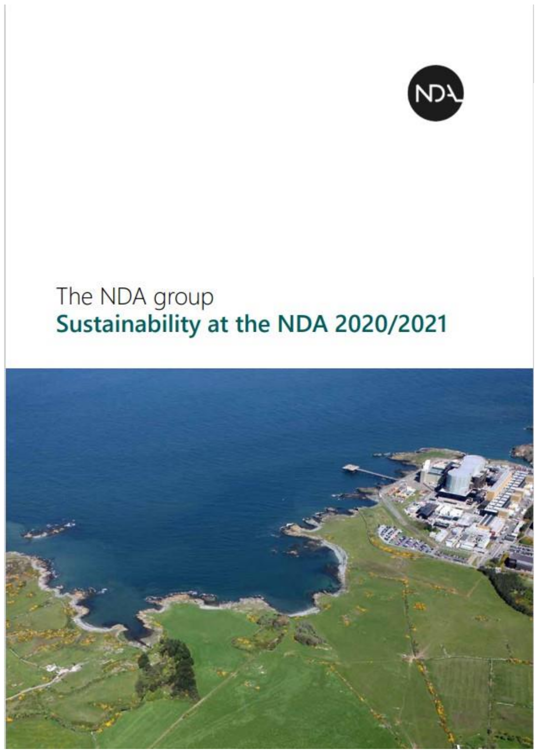

https://www.gov.uk/government/publications/nda-sustainability-report-financial-year-april-2020-to-march-2021

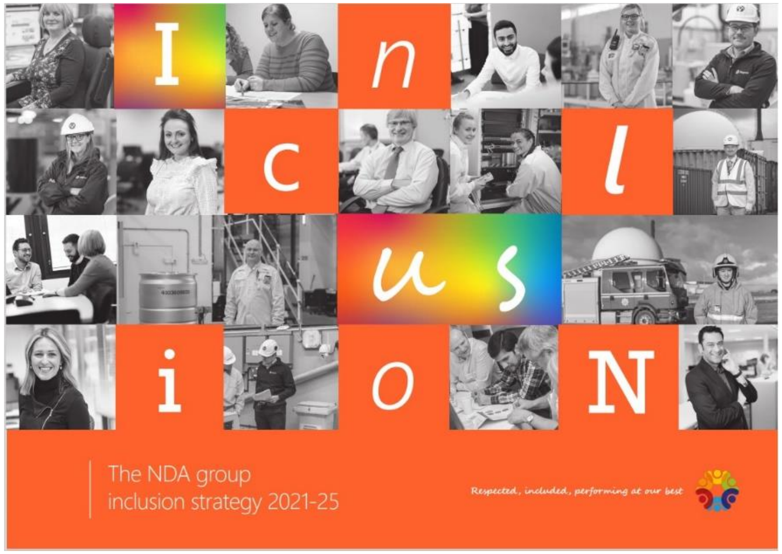

https://www.gov.uk/government/publications/the-nda-group-inclusion-strategy-2021-to-2025

Mission evolution

- Risk-informed radioactive waste strategy developed

https://www.gov.uk/government/consultations/nda-radioactive-waste-management-strategy/outcome/radioactive-waste-strategy-september-2019

- Magnox reprocessing nearing completion (2022 end date)

- Accelerated decommissioning of Magnox sites

- NDA to take on the future ownership of the 7 EDF Energy Advance Gas-cooled Reactor stations after defueling for decommissioning

Technology and Innovation

Changes over last 12 months

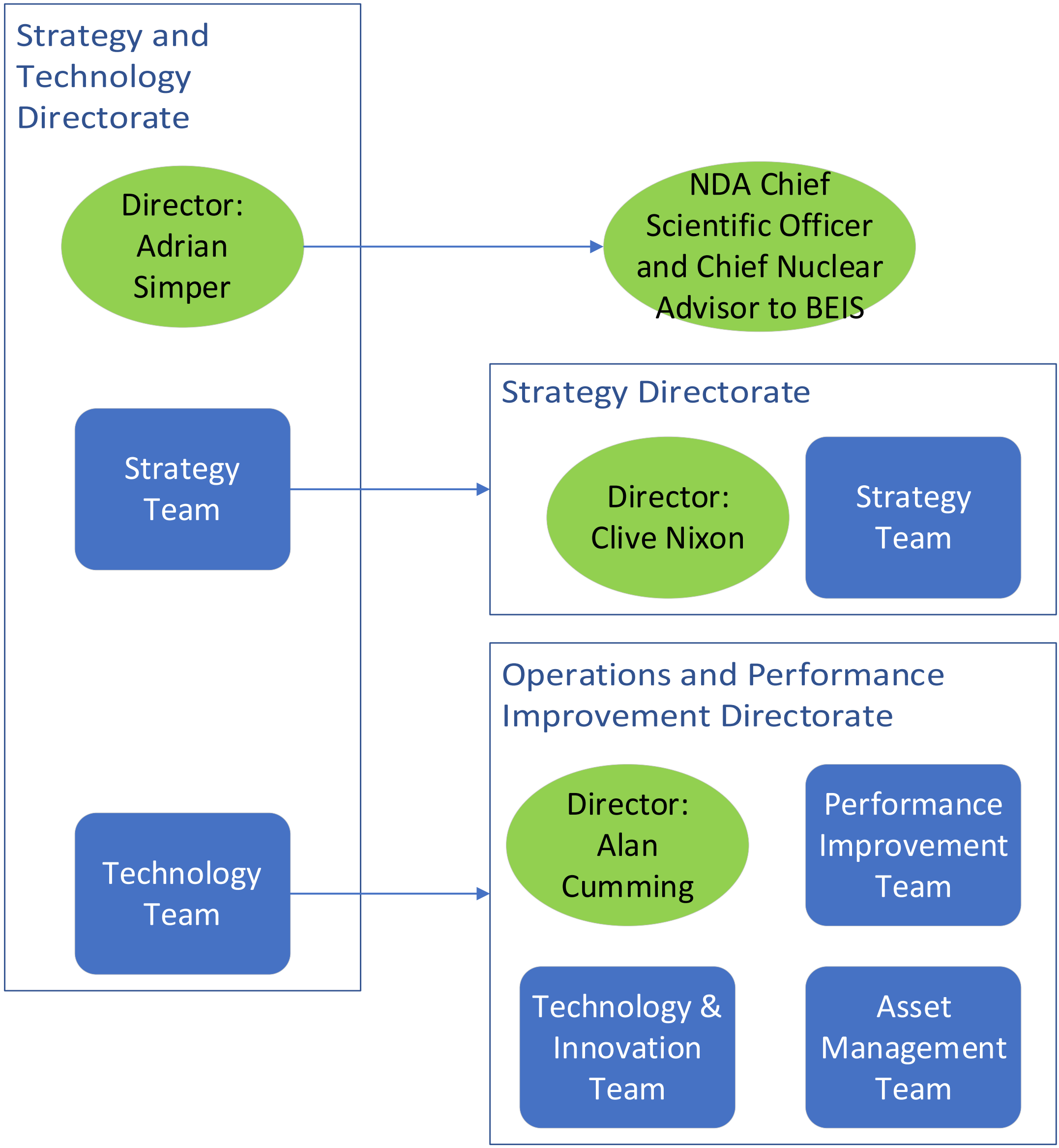

Technology and Innovation

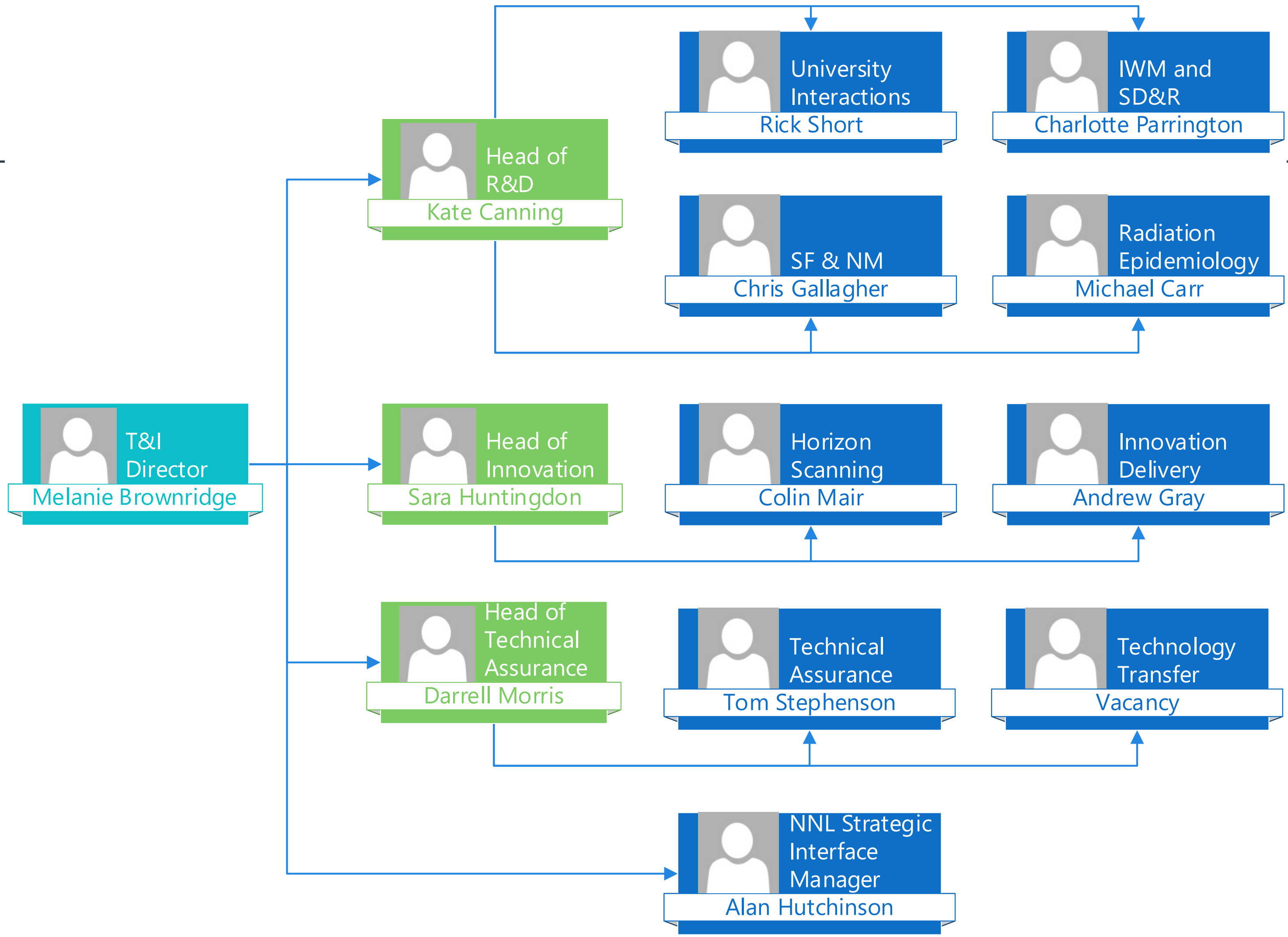

R&D team

Key new members for academic community

Kate Canning
Head of R&D

Charlotte Parrington
Research Manager for Integrated Waste Management and Site Decommissioning & Remediation

Chris Gallagher
Research Manager for Spent Fuels and Nuclear Materials

Moving forward

Increased focus on Innovation

Theme	2025	2030
Reduce and reshape our waste hierarchy	Characterisation done in- situ	50% of waste from decommissioning is recycled
Intelligent infrastructure	All buildings monitored remotely	All new buildings self-monitoring and energy neutral in 10 years
Move humans away from harm	Gloveboxes decommissioned remotely	Decommissioning activities carried out by humans reduced by 50%
Digital Delivery	3-D virtual models for key sites	All data captured at source to drive decisions

Cross Sector Remote Sort & Segregation of Waste

What is it?

Volume?

Radioactivity?

Material?

Surface area?

How do we manage the records?

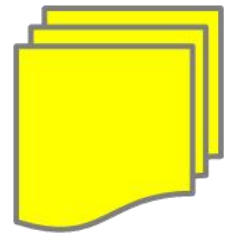

How do we integrate it together?

How do we sort and segregate the waste without touching it?

How do we pack it?

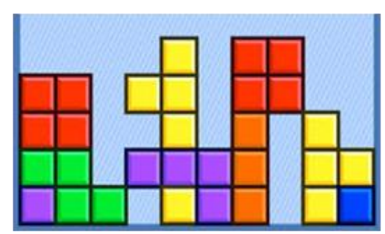

More collaborative working

Working with UK and international partners

- LongOps
  - UK/Japan collaborative programme on long reach robotics exploring synergies between fission and fusion – end use cases at SL and Fukushima

    https://www.gov.uk/government/news/3-million-nuclear-robotics-contract-is-first-tranche-in-longops-uk-japan-deal

- Telexistence
  - With Defence (DASA) looking at telepresence, haptics and robotics

    https://www.gov.uk/government/news/cutting-edge-telexistence-technology-given-funding-boost

Working with academia

- Annual NDA PhD Bursary Call **NOW LIVE** for 2021/22

https://www.nnl.co.uk/2021/11/nda-phd-bursary-2022/

- “Non-STEM” PDRA call going live soon
  >Broadening scope of academic engagement

- Improving coordination across the NDA group

- Expect ~35 PhDs per year across NDA group

- Continued engagement with EPSRC and wider UKRI

Making a difference

Costs: A UK view over 120+ years

Total cost of our clean-up mission: £131.6 billion over 120+ years

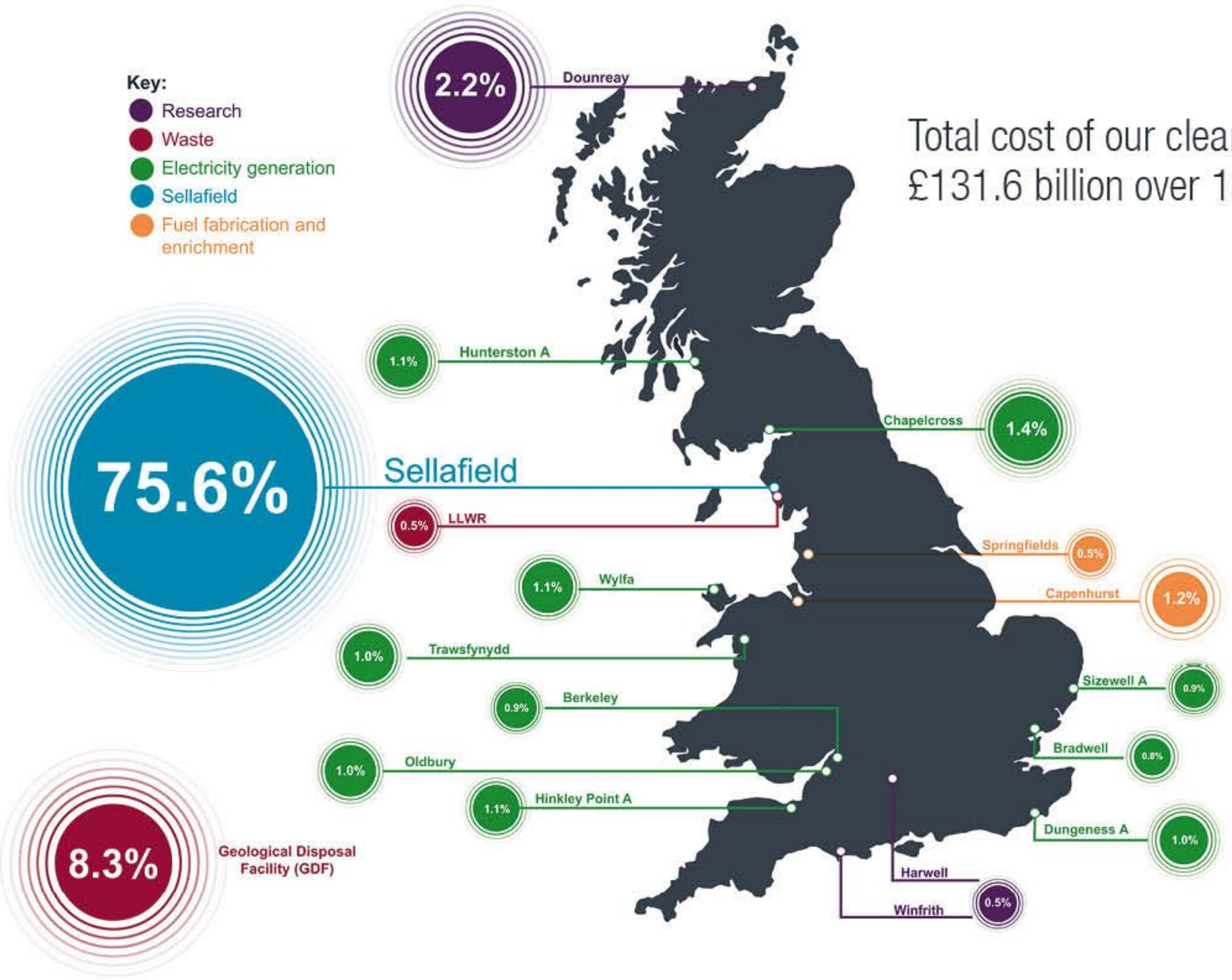

Transformative Science and Engineering for Nuclear Decommissioning

New materials and methods for decontamination of effluent

Antony Nearchou, University of Birmingham

10/11/21
TRANSCEND Annual Meeting

Energy
For a Low Carbon Future

Waste Management

- ^{235}U fission produces fission products such as Ba, Kr, Sr, Cs, I and Xe, with atomic masses distributed around 95 and 135.
- **^{137}Cs** and **^{90}Sr** have half-lives of *ca.* 30 years and produce most of the medium-lived radioactivity in spent fuel. Require removal from liquid waste.
- The radionuclides can be immobilised in a solid. Reduces waste volume as well as risk of environmental leaching.
- Current removal methods make use of **ion exchange** with **zeolite** materials. This is a facile, inexpensive, selective, consistent and high-capacity approach.

Spent fuel cooling pond at Sellafield. Source: Sellafield Ltd.

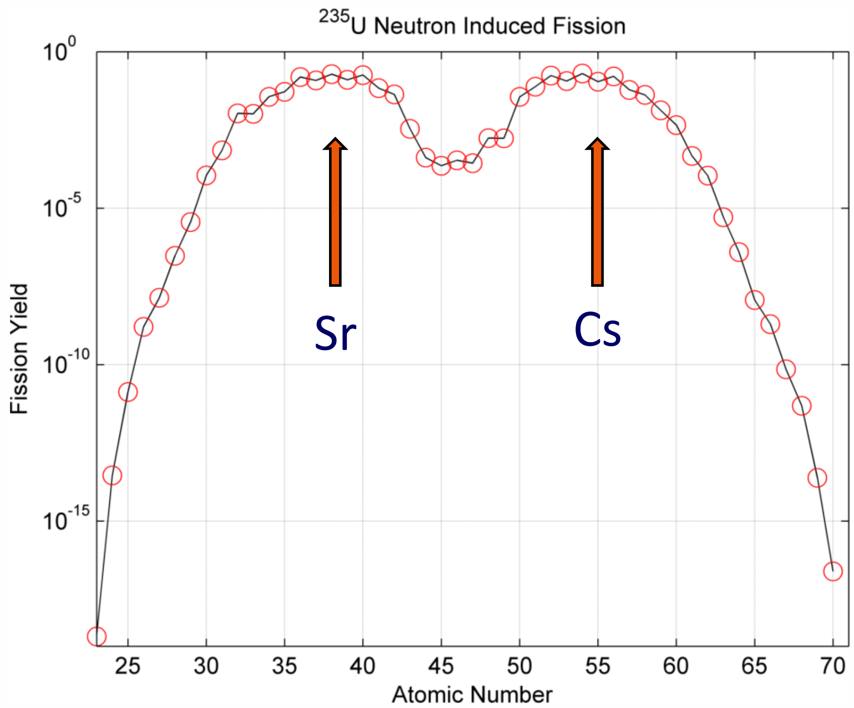

Zeolites and Ion Exchange

Zeolite Clino: $Na_6[Al_6Si_{30}O_{72}](H_2O)_9$

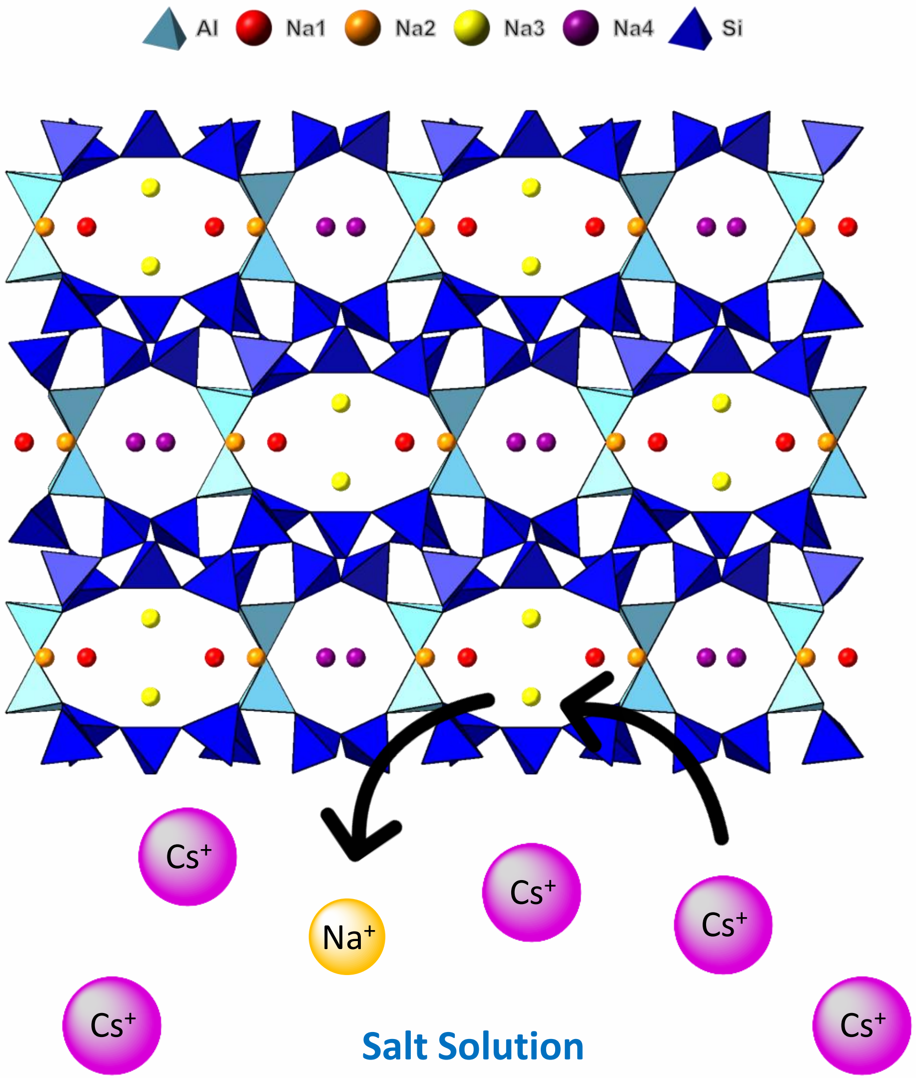

What are Zeolites?

- Crystalline, microporous (< 2nm) aluminosilicates.
- 3D network of connected SiO_4 and AlO_4 tetrahedra.
- Negatively charged framework, balanced by extra-framework cations.

Ion Exchange

- Interchange between the zeolite cations and the cations in a salt solution – i.e. Cs^+ and Sr^{2+}.
- Mud Hills clinoptilolite (clino) is used on the SIXEP plant at Sellafield.
- Clino has the best performance of natural zeolites.[1] Pore diameter is 3.5-3.9 Å, similar to hydrated Cs^+.

[1] L.L. Ames, *Am. Miner.*, 1962, **47**, 1310-1326

Zeolites and Ion Exchange

Zeolite Clino: $Na_6[Al_6Si_{30}O_{72}](H_2O)_9$

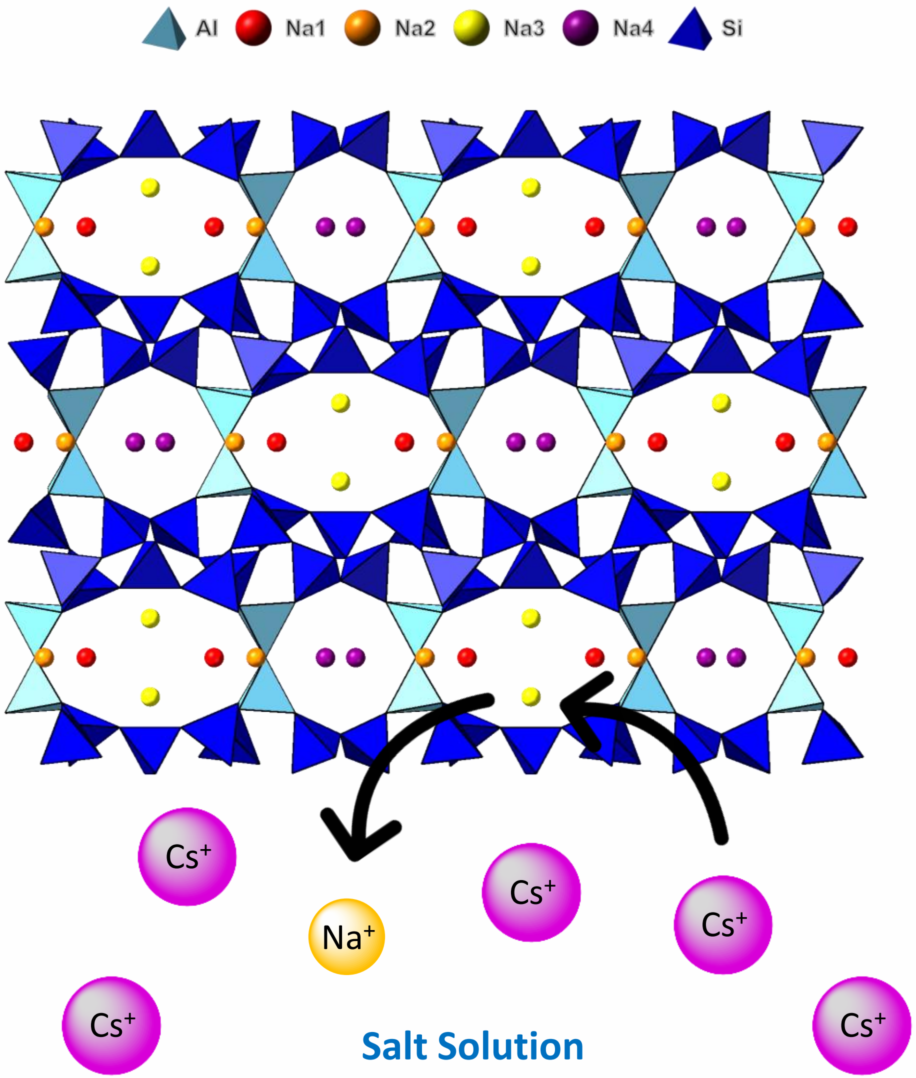

Project Objectives

- Researching new materials for uptake of Cs^+ and Sr^{2+} cations.
- Ensure selective uptake against excess competitors.
- Focus on **Cs^+ vs K^+ selectivity** – similar hydrated radii.
- Performance at different pH.
- Means of deployment.
- Potential waste forms.

Transformative Science and Engineering for Nuclear Decommissioning

New Material: Doped Umbites

$$K_2MSi_3O_9 \cdot H_2O$$

Where M = Zr, Ti, Sn, Ge

Dope M site with +5 element for enhanced **cation affinity**.

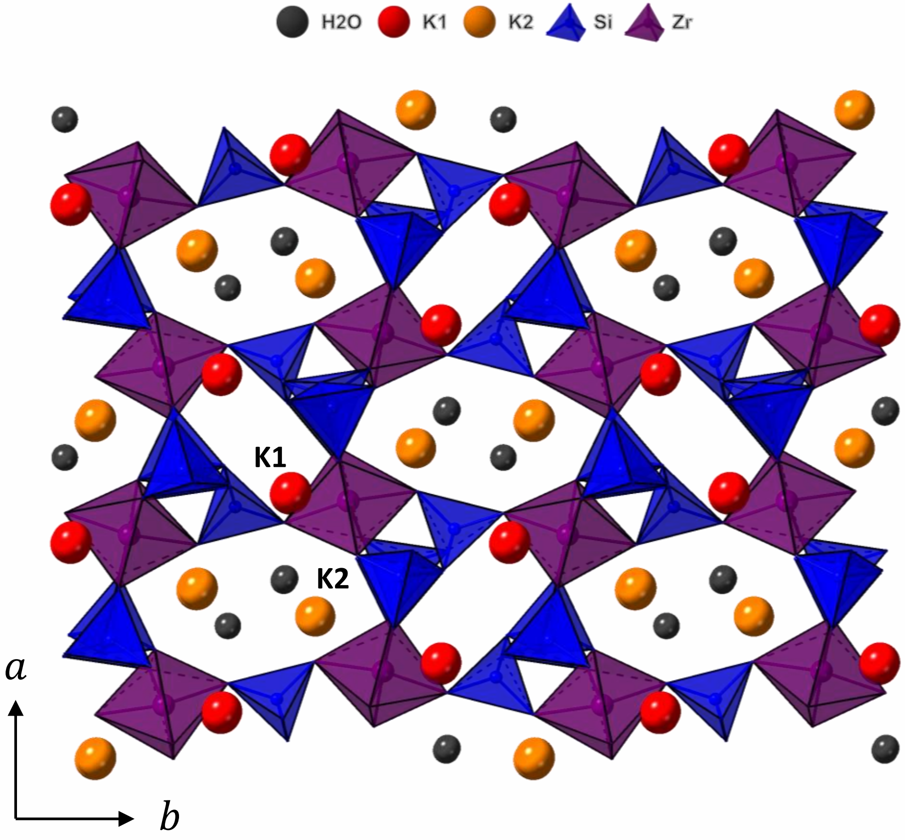

A. Nearchou *et al.* Manuscript in preparation, 2021
T-Y. Chen *et al.* Unpublished work, 2019

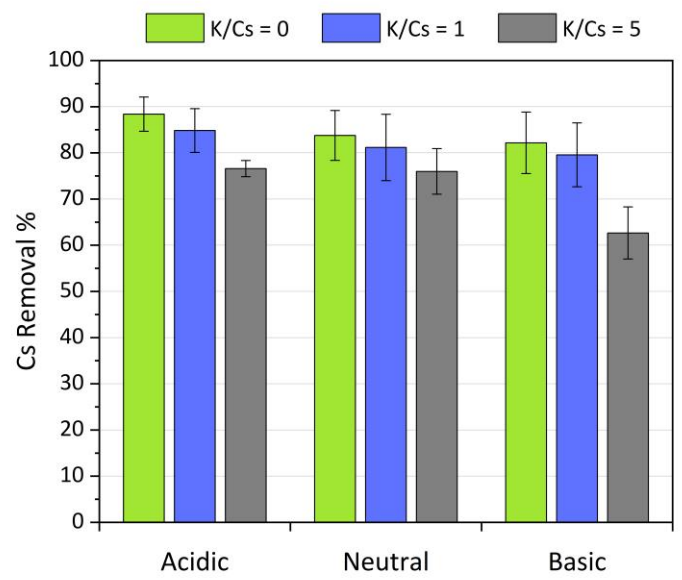

Cs Vs K selectivity pH

Cs selectivity mostly retained with increasing K content and across pH range.

Sr uptake vastly impeded by K.

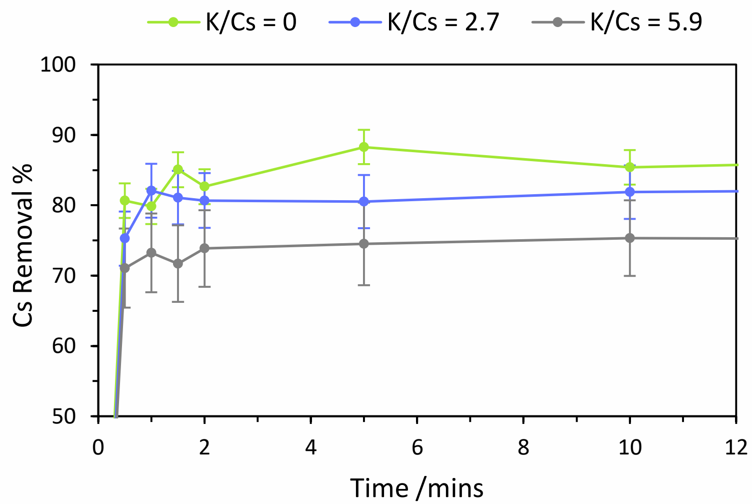

Kinetics IX

Eqm achieved within 5 mins of contact.
K reduces eqm removal%

Pre-treatment of Umbite

- Replace K sites with smaller cations H, Na.
- "**Activates**" the exchange sites.
- H pre-treatment has been shown to enhance kinetics.[2, 3]
- Pre-treat with 1 M HNO_3 or NaCl – Clino method.[1]
- 1 g in 100 ml, 3 hrs, 140 rpm.

Shannon radii of cations.

Cation	H^+	Na^+	K^+	Cs^+
Ionic radius /Å	<0.01	1.02	1.38	1.67

Exchange Mechanism[3]

Cation travels down the 001 *c*-axis channel.
K1 exchange site in pocket.

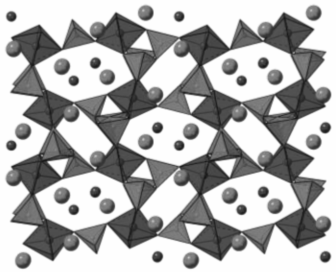

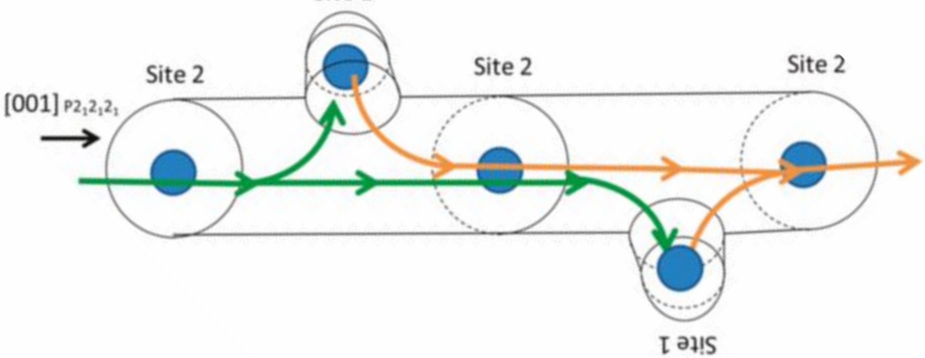

K1 exchange site

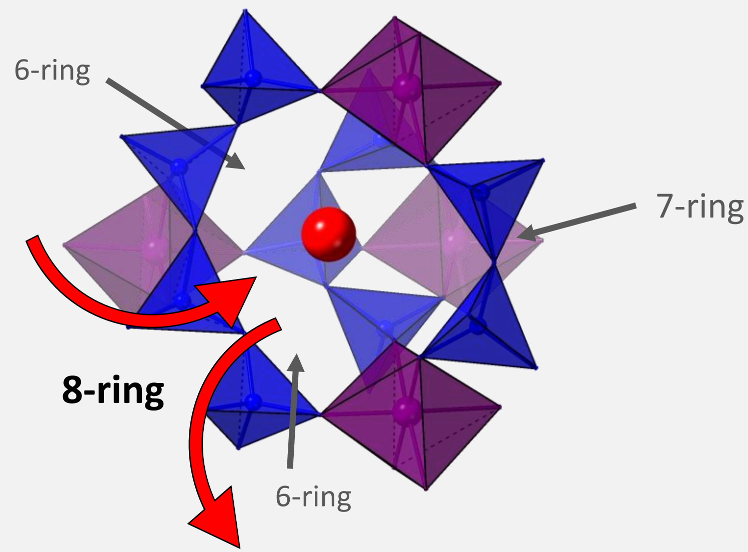

[1] P. Sylvester. RDR0418. May 1995.
[2] C. S. Fewox *et al. Chem. Mater.* 2007, **19**(3), 384-392.
[3] C. S. Fewox *et al.*, *Inorg. Chem.*, 2011, **50**(8), 3596-3604.

Pre-treatment of Umbite

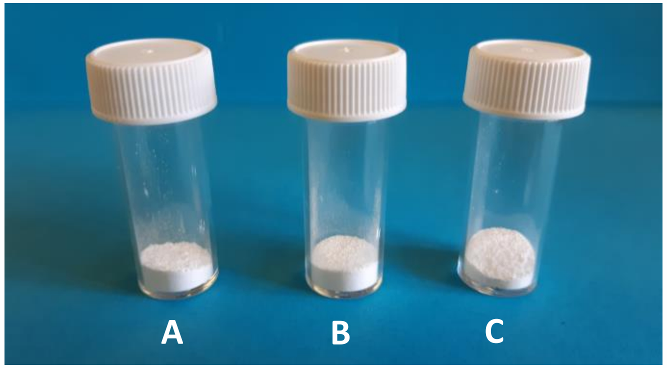

(A) SbSnUmb
(B) H-SbSnUmb
(C) Na-SbSnUmb

- 0.03g sample in 15ml solution, 24 hrs, 140 rpm.
- Cs 10 ppm, with K 0, 10 and 50 ppm.
- K/Cs = 0, 1, 5.

- Awaiting results of Sr exchanges.

Powder X-ray Diffraction

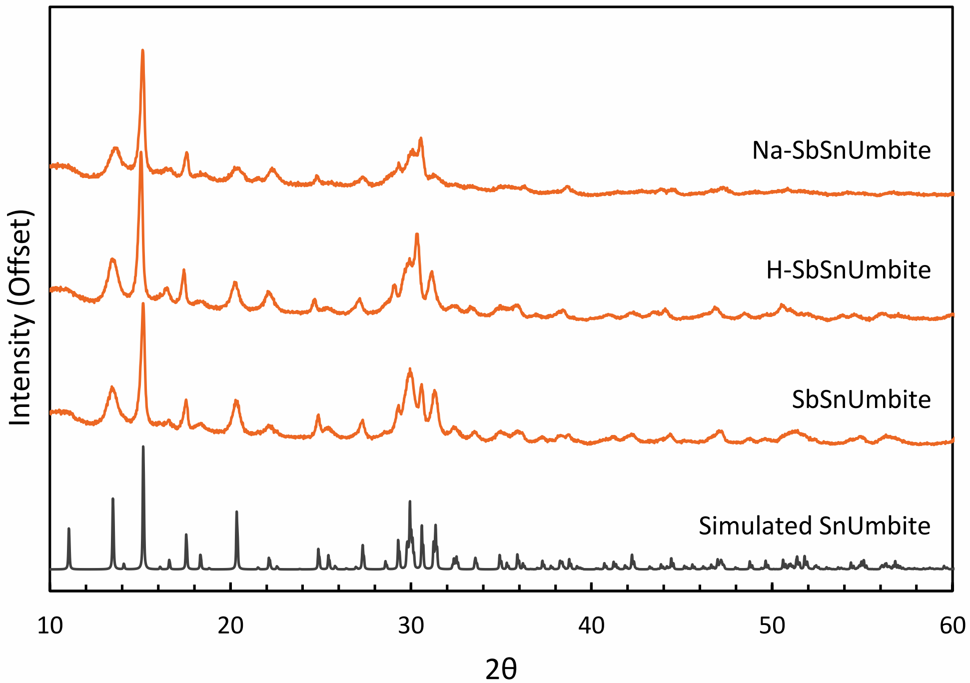

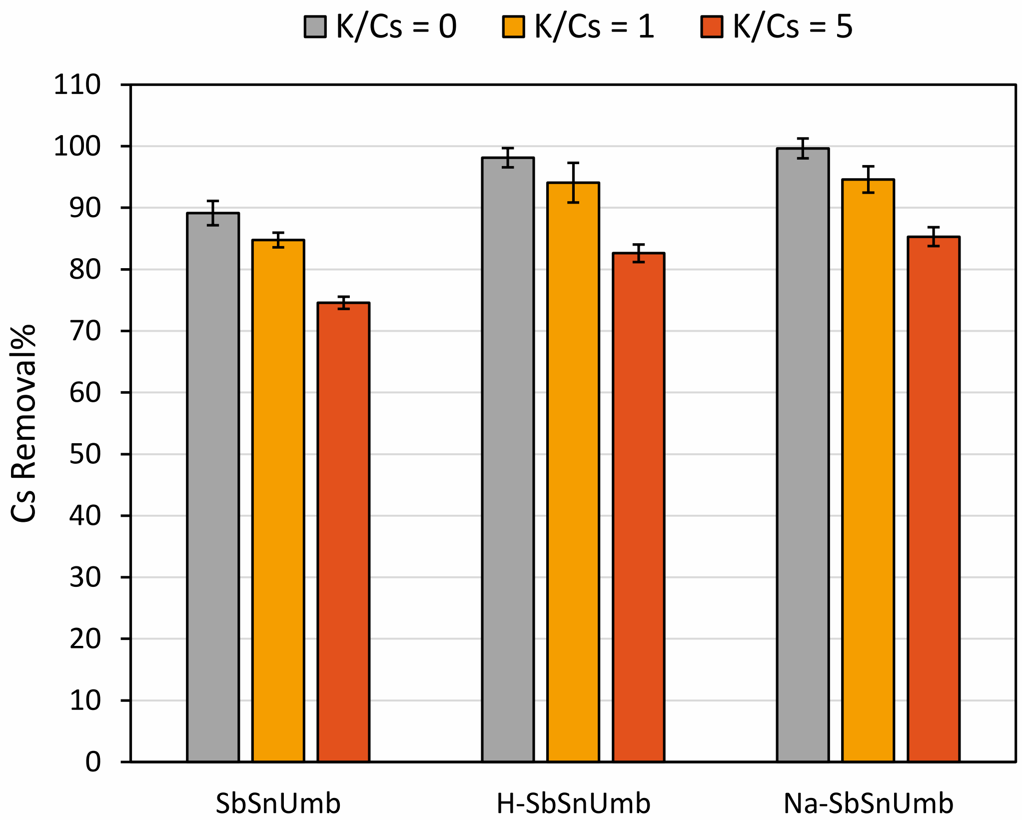

Groundwater Simulant

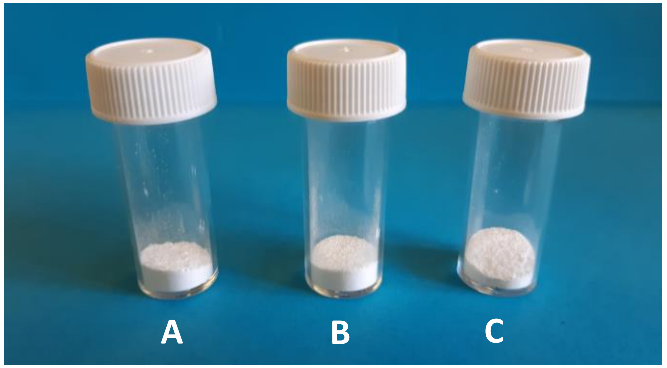

(A) SbSnUmb
(B) H-SbSnUmb
(C) Na-SbSnUmb

- 0.03g sample in 15ml solution, 24 hrs, 140 rpm.
- Cs 1 ppm from groundwater simulant[1]
- Awaiting results for Sr 1 ppm from GW.

Composition of groundwater simulant (GW) solution.[1]

Cation	/ppm
Cs^+	1
Na^+	125
K^+	5
Mg^{2+}	10
Ca^{2+}	25

pH 6-7
Cs – nitrate source.
Na, K, Mg, Ca – chloride sources.

Anions
NO_3^- ~0.5 ppm
Cl^- ~190 ppm

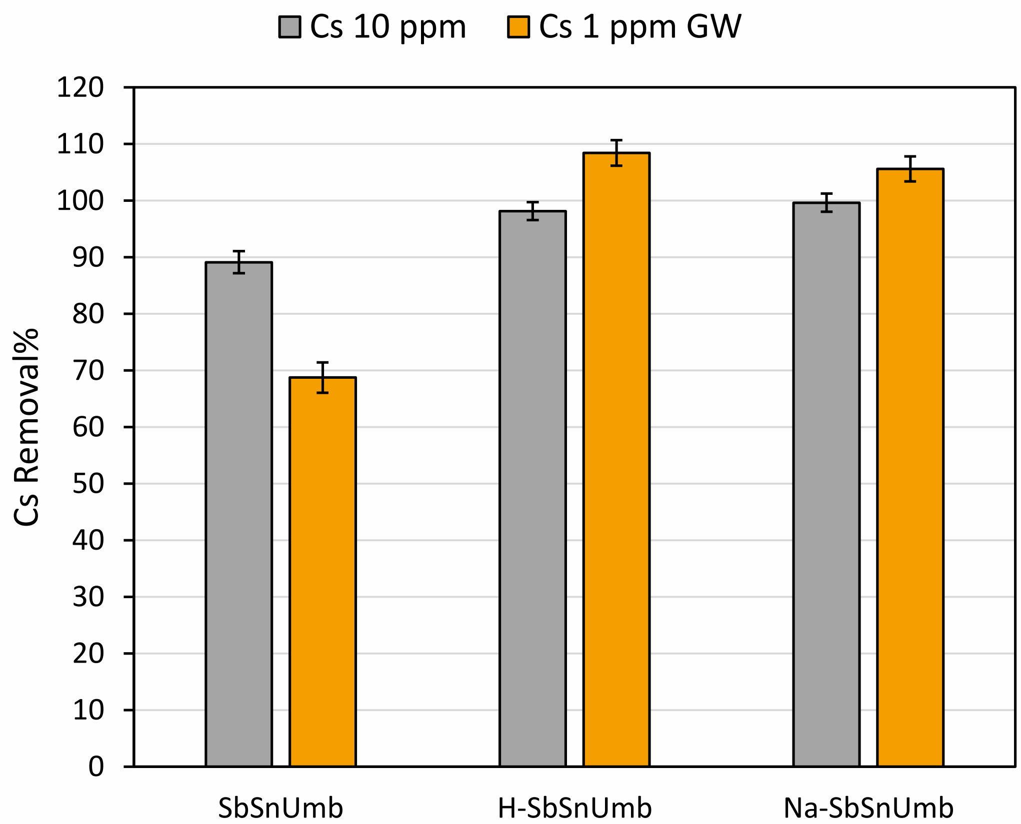

[1] S. Kwon *et al. J. Hazard. Mater.* 2021, **408**, 124419.

Pellet Production

- Loose powder particle size too small for flow system.
- Production of **monoliths/pellets** for use in an exchange bed.

Average crystal ~1.65 µm length
Too small for flow system

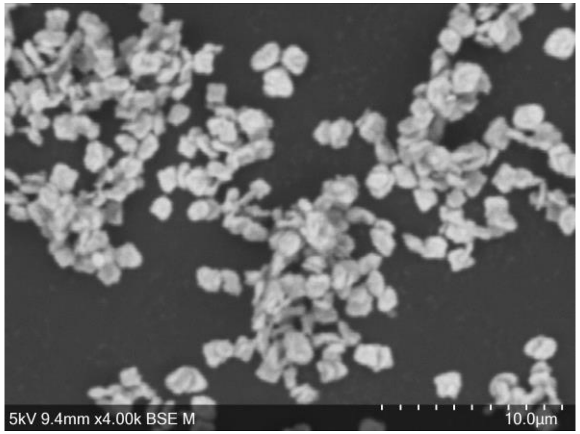

Fired Umbite Pellet ~2 mm diameter

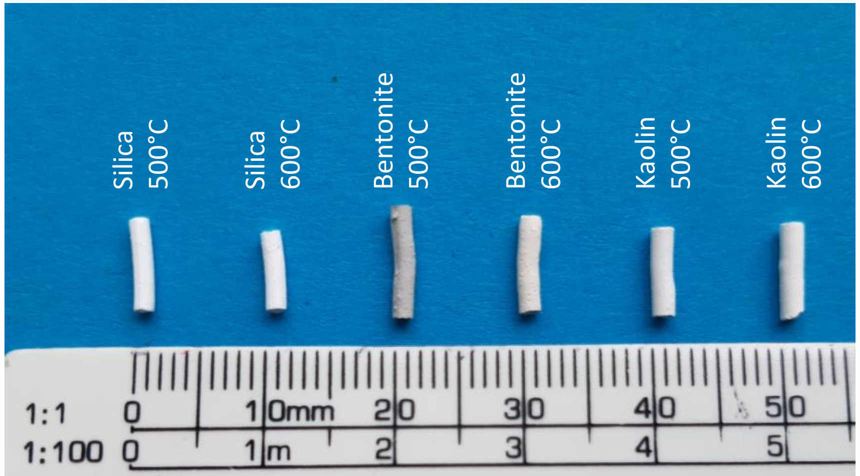

- Pellet paste composition:
  - ❖ Umbite powder.
  - ❖ Plasticiser – Poly vinyl acohol (PVA) solution.
  - ❖ Peptiser – 2% acetic acid.
  - ❖ Permanent binder – silica, bentonite, kaolin.
- Paste extruded through a 2 mm diameter syringe.
- Extrudates dried, and fired in a furnace at 500°C-600°C.
- Umbite structure retained – powder X-ray diffraction.

Powder X-ray Diffraction

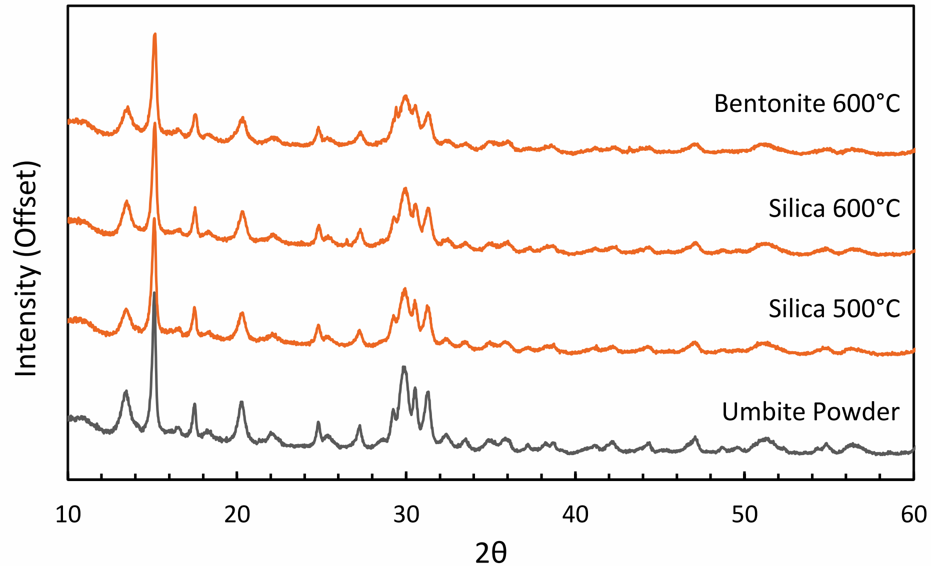

Pellet Stability

50 mg of pellets in 10 ml of 0.1 M HNO_3 or NaOH
140 rpm agitation

Observations

- Green: Pellet intact.
- Yellow: Pellet intact, but solution cloudy.
- Orange: Pellet broken into large fragments.
- Red: Pellet disintegrated.

Acid Stability – 0.1 M HNO_3

	1hr	3hr	5hr	1d	3d	4d	7d	8d	10d	14d	16d
Silica 500°C	Green	Green	Green	Green	Green	Green	Green	Green	Green	Green	Green
Silica 600°C	Green	Green	Green	Green	Green	Green	Green	Green	Green	Green	Green
Bent. 500°C	Orange	Orange	Orange	Orange	Orange	Orange	Orange	Orange	Orange	Orange	Orange
Bent. 600°C	Green	Green	Green	Green	Green	Green	Green	Green	Green	Green	Green
Kaolin 500°C	Orange	Orange	Orange	Orange	Orange	Orange	Orange	Orange	Orange	Orange	Orange
Kaolin 600°C	Orange	Orange	Orange	Orange	Orange	Orange	Orange	Orange	Orange	Orange	Orange

Base Stability – 0.1 M NaOH

Silica 500°C	Green	Green	Green	Green	Green	Green	Yellow	Yellow	Yellow	Yellow	Yellow
Silica 600°C	Green	Green	Green	Green	Green	Green	Yellow	Yellow	Yellow	Yellow	Yellow
Bent. 500°C	Orange	Orange	Red								
Bent. 600°C	Green	Green	Green	Green	Green	Green	Green	Green	Green	Green	Green
Kaolin 500°C	Green	Green	Green	Green	Yellow	Yellow	Yellow	Yellow	Yellow	Yellow	Yellow
Kaolin 600°C	Green	Green	Green	Green	Yellow	Yellow	Yellow	Yellow	Yellow	Yellow	Yellow

Fired Umbite Pellet ~2 mm diameter

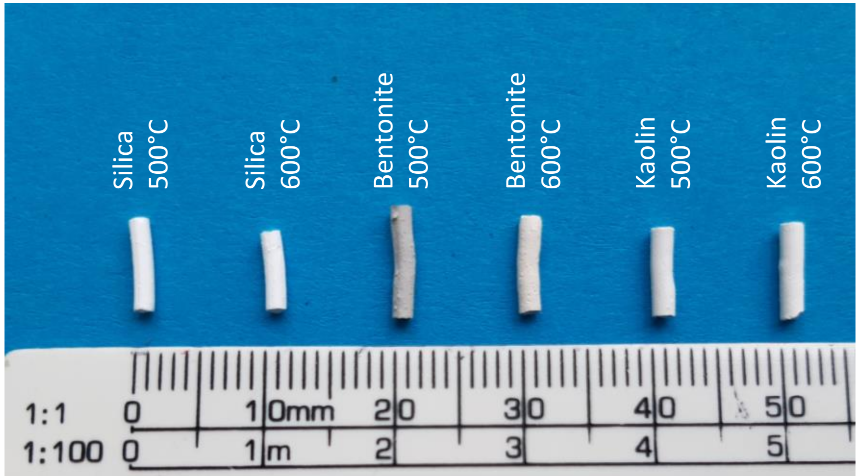

Powder X-ray Diffraction

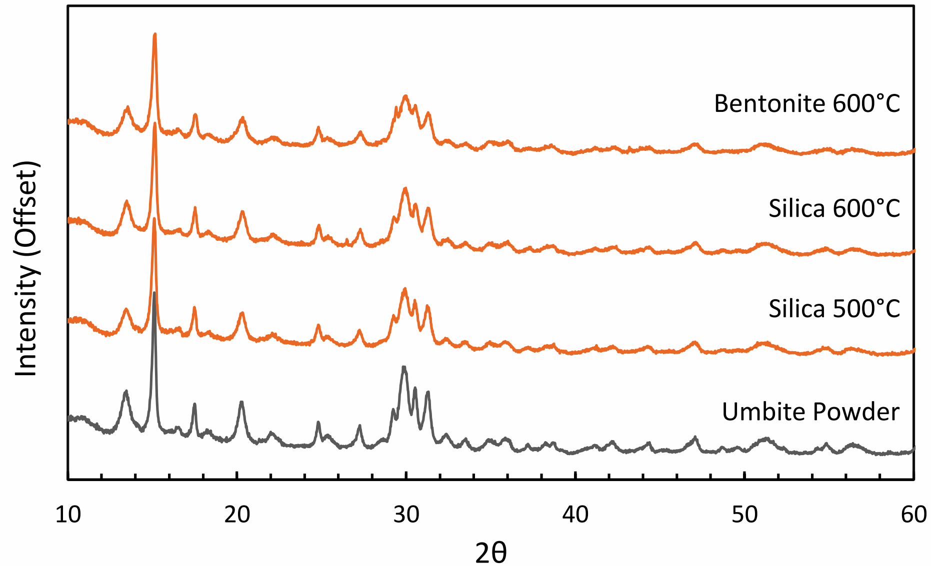

Pellet Surface and Performance

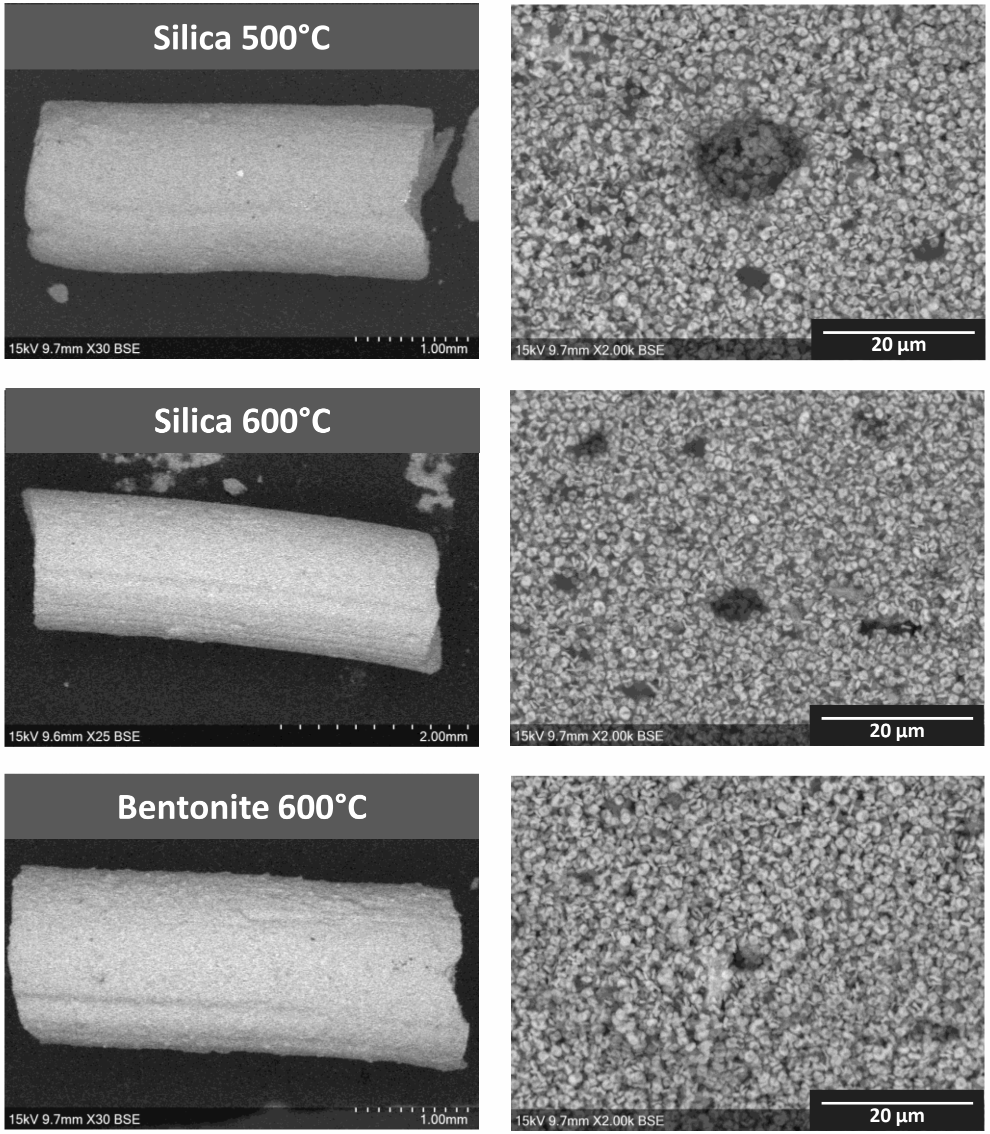

- Cs 10 ppm, with K 0, 10, 50 ppm.
- ~30 mg in 15 ml solution, 24 hrs, 140rpm agitation.
- Three runs, average Cs Removal% and standard deviation (error bar) recorded.
- Pellets show larger variance in Cs removal.
- Cs selectivity mostly retained.

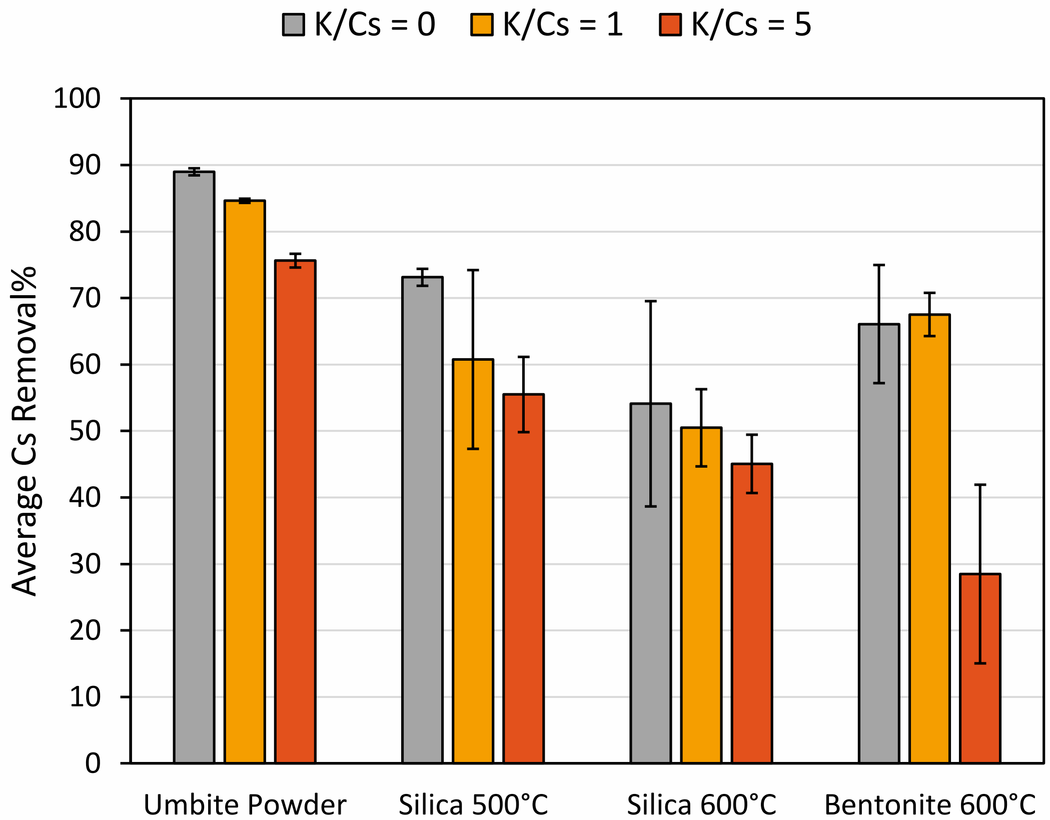

Some Other Work

AFCP
Advanced Fuel Cycle Programme

About Us | Our Partners | Our Impact | Fuel Cycle Themes | News and Highlights

NATIONAL NUCLEAR LABORATORY

CASE STUDIES

Cleaning up our act: Materialising new ideas for a better planet

INNOVATION | NNL | SOLVENT AND EFFLUENT TREATMENT | UNIVERSITIES AND ACADEMIA

As the need for nuclear energy expands to meet Net Zero, so does the need to manage stored nuclear materials. However, this also raises an opportunity to do things differently. AFCP's Advanced Solvent and Effluent Treatment team is exploring novel decontamination materials that are both sustainably sourced and industry optimised. Antony Nearchou, Research Fellow at the University of Birmingham, discusses how sharing strengths has enabled this impactful innovation.

https://afcp.nnl.co.uk/case-study/materialising-new-ideas-for-a-better-planet/

Tweet

Advanced Fuel Cycle Programme
@afcp_uknnl

Antony Nearchou, AFCP researcher at @unibirmingham, is driving industry-ready innovation on our Advanced Solvent & Effluent Treatment team. With @UKNNL, the team is materialising new decontamination solutions for a better planet 💡

Read his case study ➡️ afcp.nnl.co.uk/case-study/mat ...

11:58 AM · Jun 16, 2021 · Twitter Web App

A. Nearchou *et al.* Manuscript in preparation, 2021

Transformative Science and Engineering for Nuclear Decommissioning

Summary and Future Work

Achievements

- Use of pre-treatment to improve ion exchange properties of umbites.
- Enhancing Cs selectivity against K as well as uptake from groundwater simulant.
- Successful preparation of chemically stable umbite pellets.
- Pellets exhibit moderate retention of Cs selectivity.

Ongoing and Future Work

- Papers.
- Analysis of Sr exchanges.
- Active testing if possible.
- Assess mechanical stability of pellets.
- Potential waste forms and Cs/Sr leach testing.
- Currently looking into some new materials of interest – hopefully next time!

TRANSCEND

EPSRC Pioneering research and skills

UNIVERSITY OF BIRMINGHAM

NATIONAL NUCLEAR LABORATORY

AFCP Advanced Fuel Cycle Programme

Research Councils UK Energy For a Low Carbon Future

Acknowledgements

Funding Bodies

University of Birmingham - Chemistry:

- Joe Hriljac
- Phoebe Allan
- Tzu-Yu Chen
- James Reed
- Dan Parsons
- Ryan George

UOB – FENAC Facility: ICP-MS

- Norman Day
- Chris Stark

National Nuclear Laboratory (NNL)

- Luke O’Brien
- Nicholas Hodge
- Keith Cuthell
- Liam Abrahamsen-Mills

TRANSCEND

Transformative Science and Engineering for Nuclear Decommissioning

Thank you

Email: A.Nearchou@bham.ac.uk

TRANSCEND

Transformative Science and Engineering for Nuclear Decommissioning

Assessing the feasibility of ex-situ vitrification of soils grouted with colloidal silica

Arianna Gea Pagano, University of Strathclyde

2nd Annual Meeting

10/11/2021
Harrogate

Energy
For a Low Carbon Future

TRANSCEND

Transformative Science and Engineering for Nuclear Decommissioning

University of Strathclyde Glasgow

Prof Becky Lunn

Dr Grainne El Mountassir

Dr Arianna Gea Pagano

The University Of Sheffield.

Dr Claire Corkhill

Dr Josh Radford

Access to the HADES facility (University of Sheffield) funded by NNUF

NNUF

National Nuclear User Facility

What is colloidal silica?

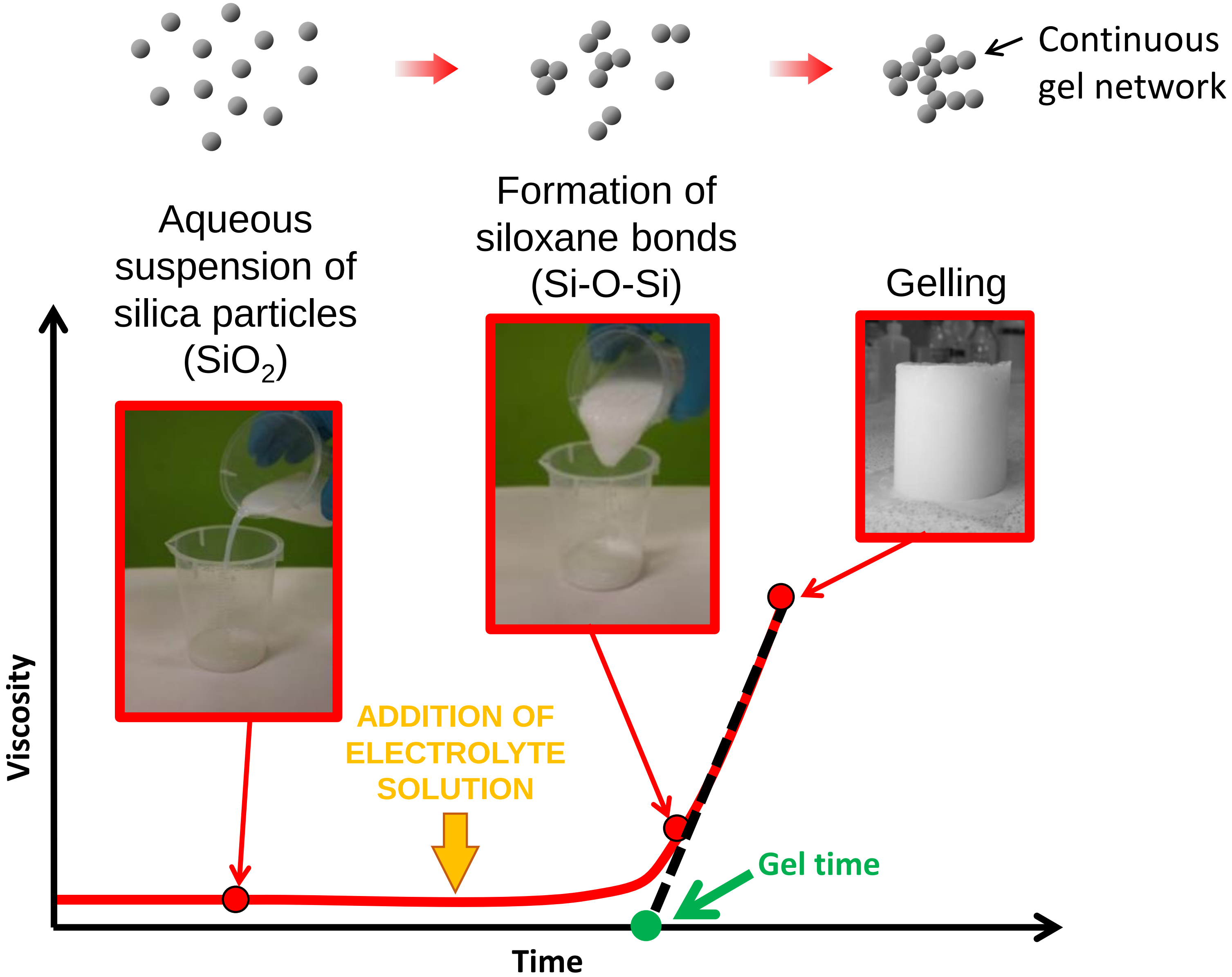

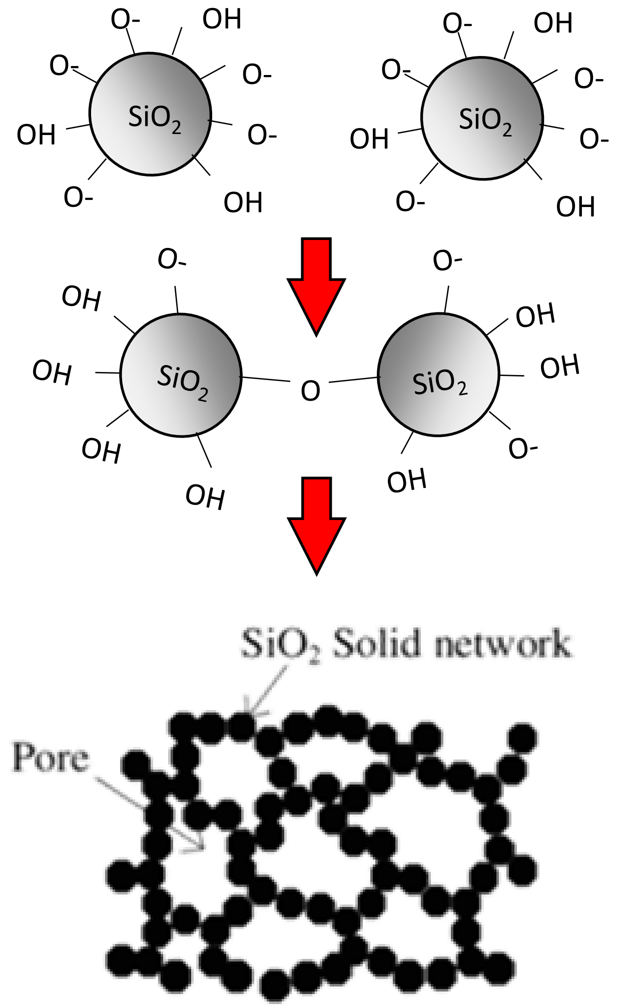

Soil grouting with colloidal silica

- Turns loose soil into 'cohesive' soil
- The grout gains strength overtime as the gelation process evolves -> grouted soils gain strength overtime
- Lowers soil permeability (gel permeability: 10^{-17} to 10^{-18} m^2)
- Enhances sorption capacity -> beneficial effect towards radionuclide retention

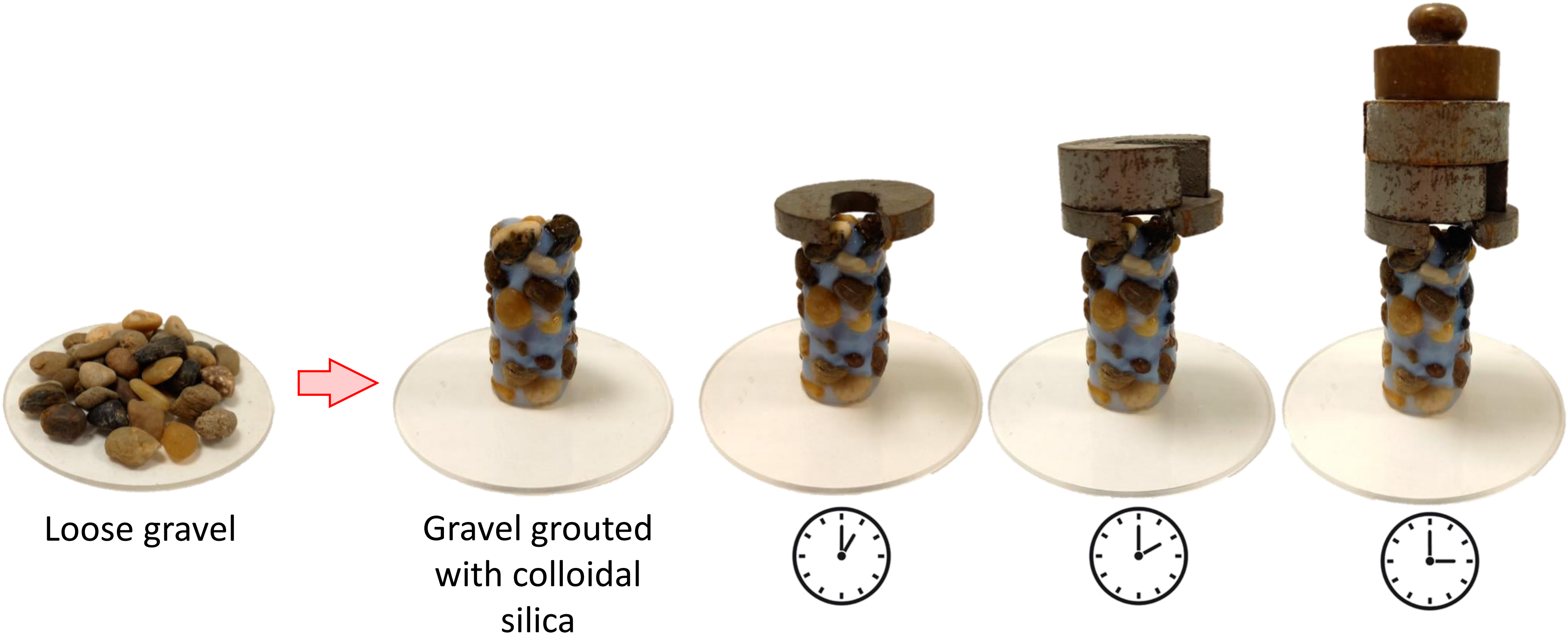

Ex-situ vitrification of contaminated soils

Ex-situ soil vitrification: thermal treatment that converts contaminated soil masses into glassy solid matrices, carried out in a melting chamber.

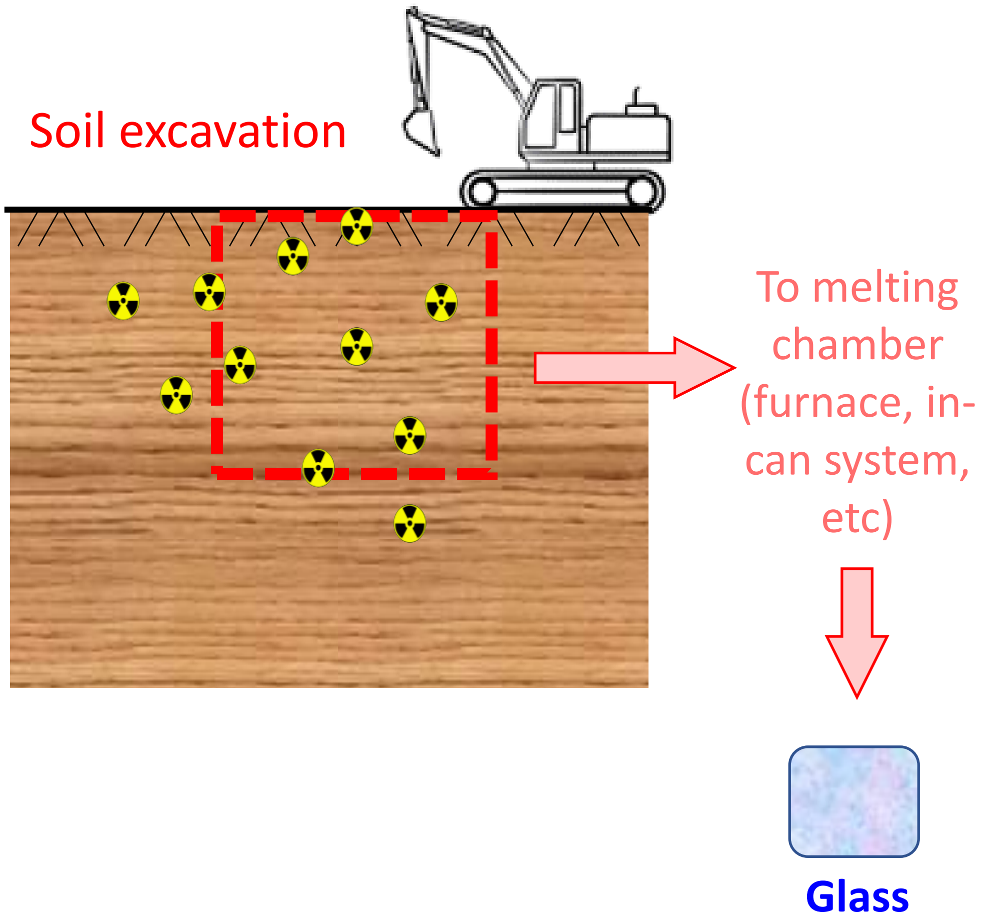

Advantages:

- Excellent **stability and durability** of the wasteform
- Significant **volume reduction** (up to 96% compared to other stabilisation strategies)
- Potential **cost savings**

Disadvantages:

- Ex-situ vitrification requires **soil excavation and transport** to a melting system.
- Excavation of radioactively contaminated soils poses serious **risks of radiation exposure** from fugitive hazardous gases and dust emissions.

Ex-situ vitrification of contaminated soils grouted with colloidal silica

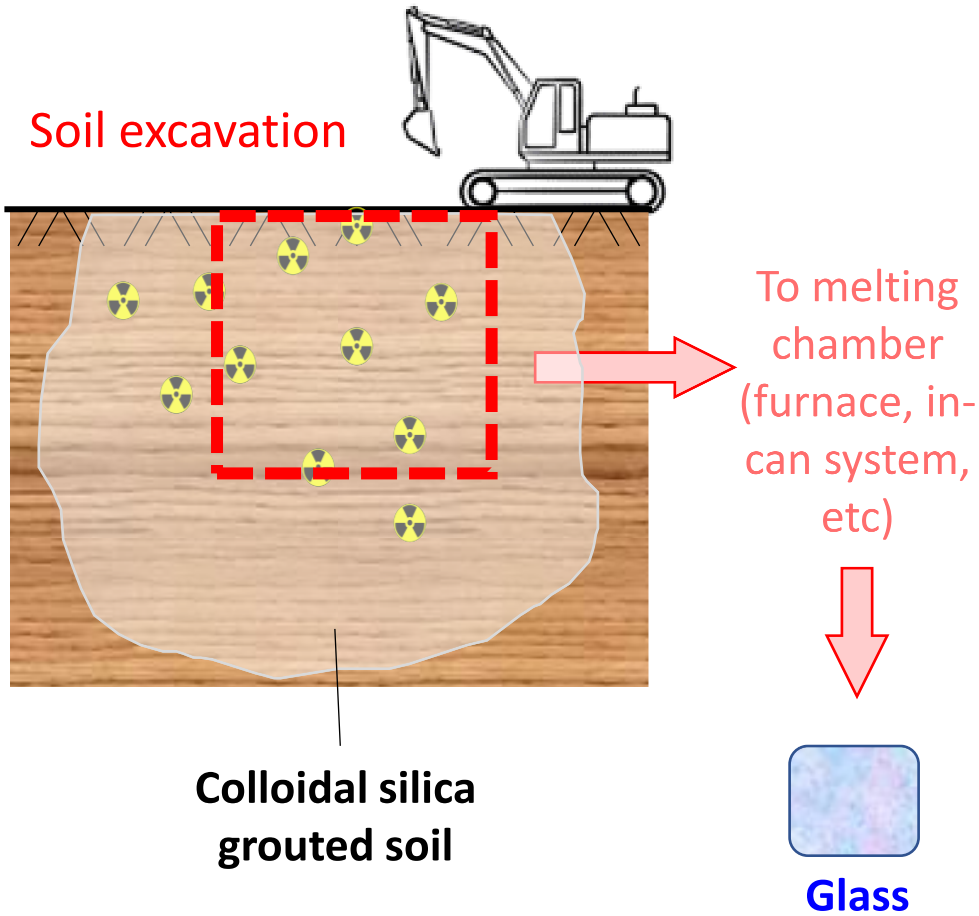

Advantages:

- Excellent **stability and durability** of the wasteform
- Significant **volume reduction** (up to 96% compared to other stabilisation strategies)
- Potential **cost savings**
- *Enhanced radionuclide retention upon glass formation (?)*

Disadvantages:

- Ex-situ vitrification requires **soil excavation and transport** to a melting system.
- ~~Excavation of radioactively contaminated soils poses serious **risks of radiation exposure** from fugitive hazardous gases and dust emissions.~~

Mitigated by inhibiting dust formation upon excavation

Feasibility of vitrification of CS-grouted soils

Soil grouted with colloidal silica

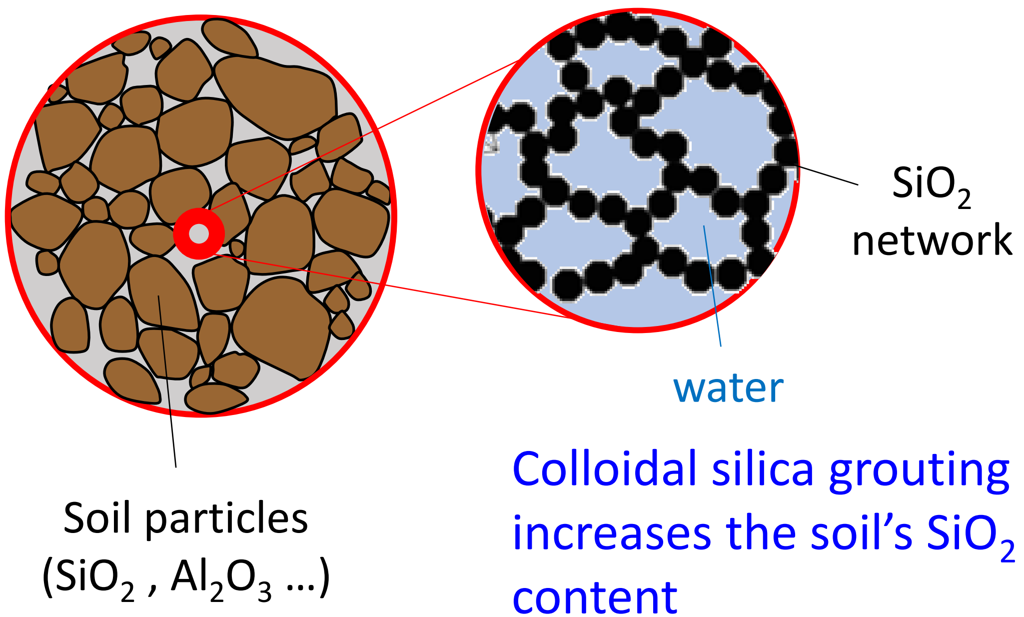

Colloidal silica grouting increases the soil's SiO_2 content

- Beneficial in terms of glass formation (SiO_2 is the most common glass former)
- Detrimental in terms of retention of contaminants (e.g. volatile radionuclides) as high SiO_2 contents lead to high melting temperatures

↓

glass-forming additives to lower melting temperatures

Assessing the feasibility of vitrification of CS-grouted soils

Colloidal silica grouted soil samples

Soil grouting:

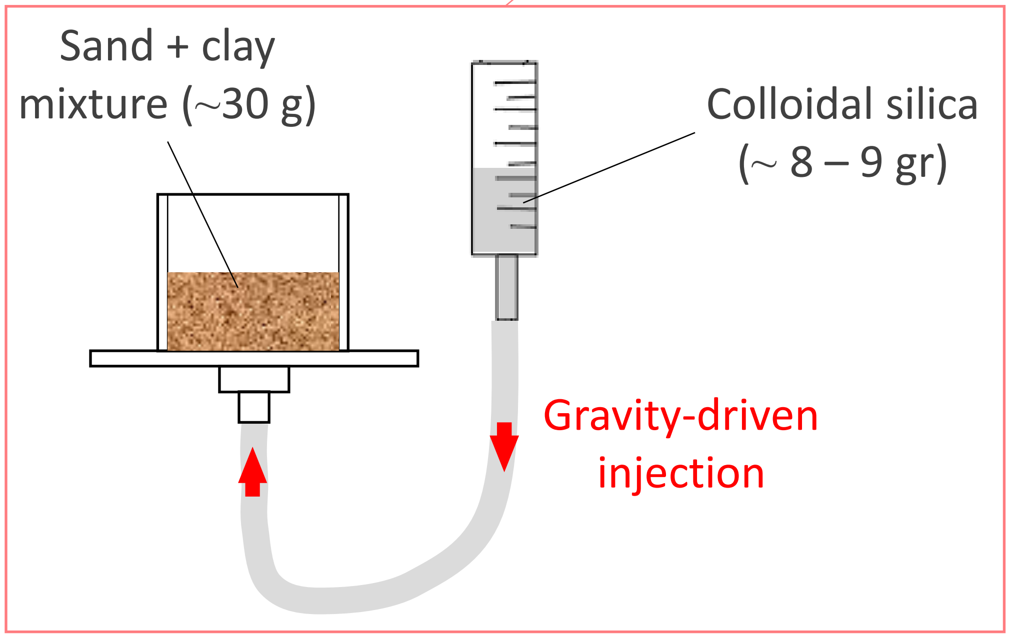

Assessing the feasibility of vitrification of CS-grouted soils

Approach

STAGE 1: Exploring the glass-forming ability of crushed-up soil/colloidal silica system (no contaminants)

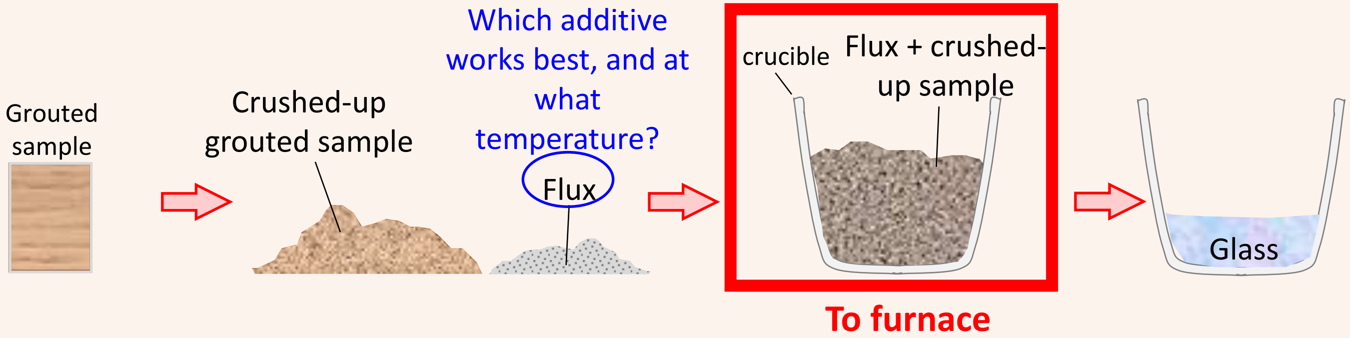

STAGE 2: Exploring the glass-forming ability of intact soil/colloidal silica system (no contaminants) -> operational challenge: how to add glass-forming additives?

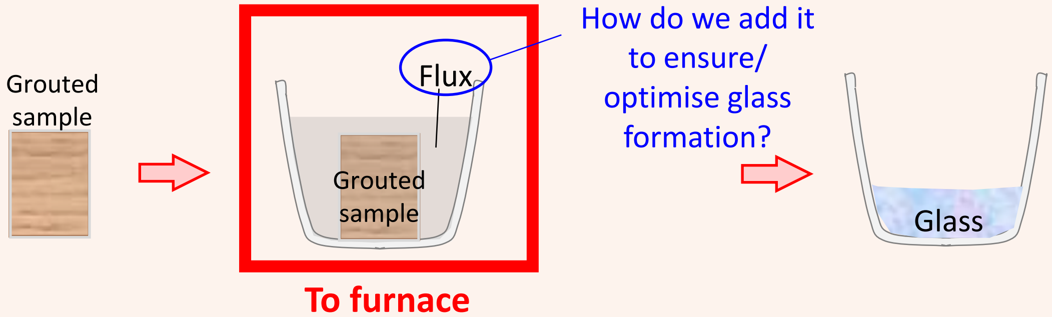

STAGE 3: Exploring the ability of contaminated soil/colloidal silica system to retain radionuclides upon glass formation

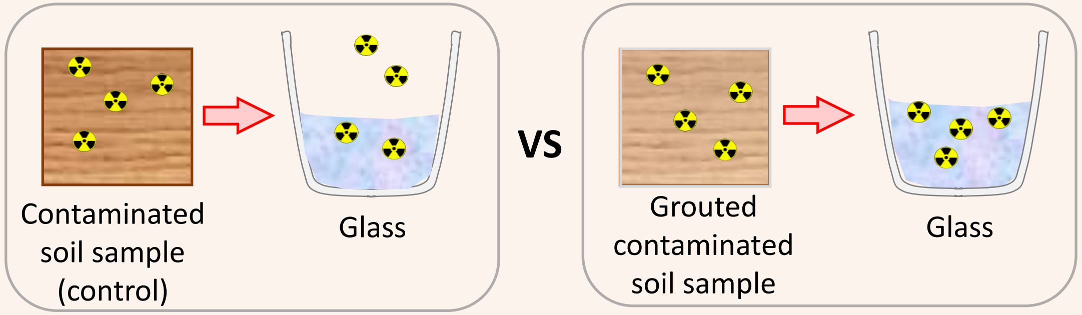

Work in progress!

Stage 1. Glass-forming ability of crushed-up grouted samples

Trial 1:

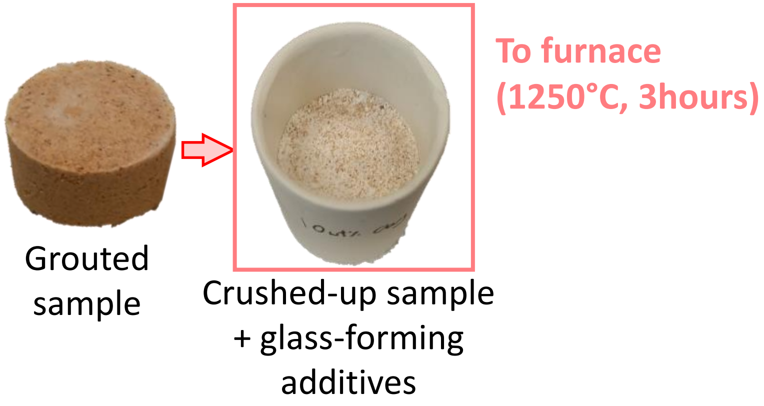

	Bacth composition		
Clay content in soil [%]	Grouted soil [wt%]	Na_2CO_3 [wt%]	$Al(OH)_3$ [wt%]
5	61.8	16.7	21.4
10	62.7	17.7	19.7
20	65.0	17.0	18.0

Not pourable, white inclusions

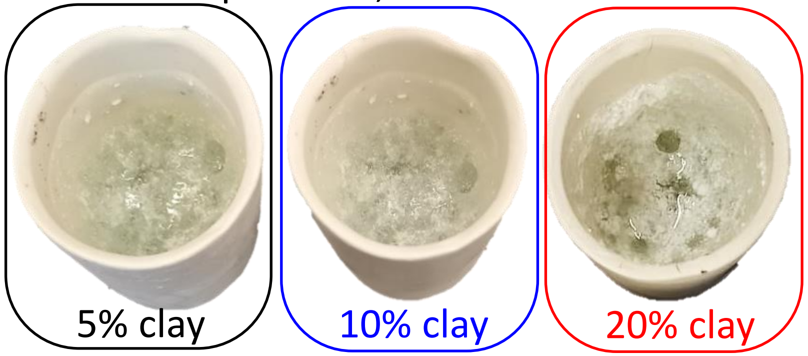

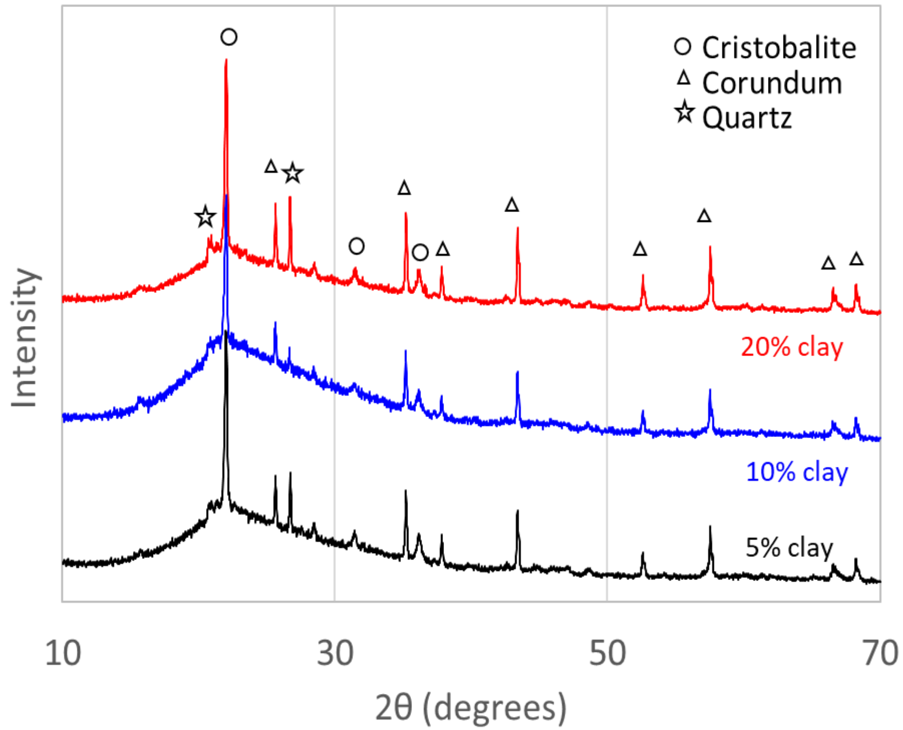

Stage 1. Glass-forming ability of crushed-up grouted samples

Trial 2: temperature increase

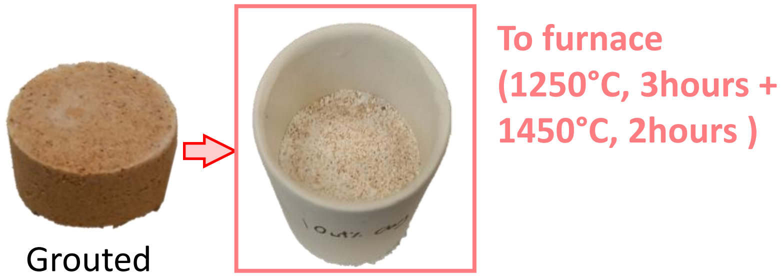

Grouted sample

Crushed-up sample + glass-forming additives

	Bacth composition		
Clay content in soil [%]	Grouted soil [wt%]	Na_2CO_3 [wt%]	$Al(OH)_3$ [wt%]
5	62.2	16.5	21.3
10	62.7	17.6	19.7
20	65.0	17.1	17.9

Not pourable, white inclusions

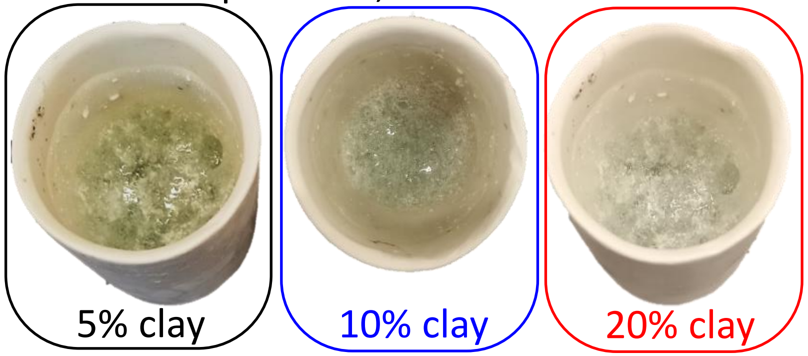

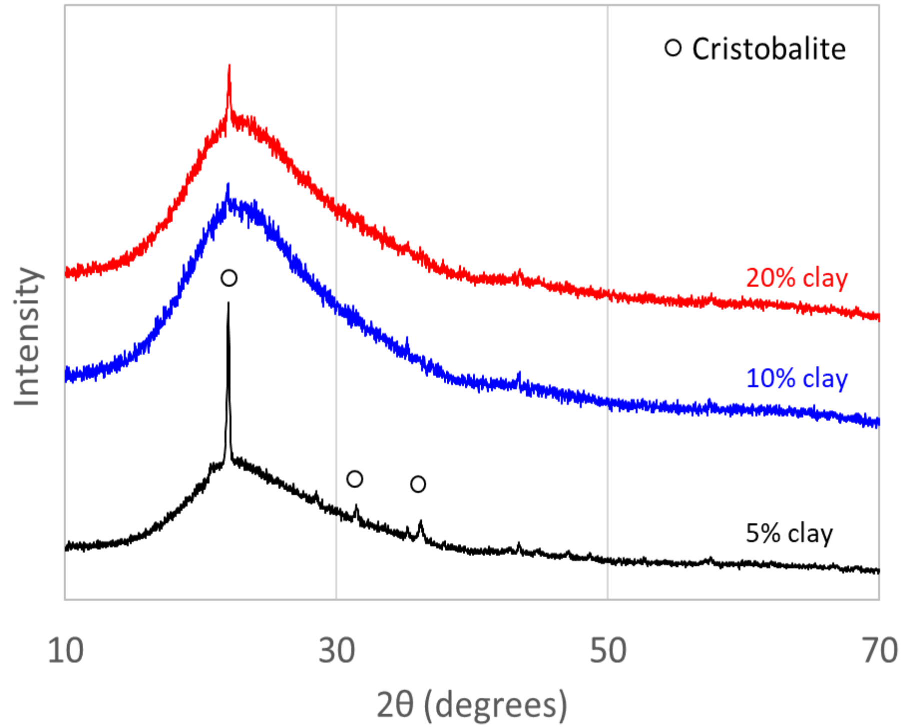

Stage 1. Glass-forming ability of crushed-up grouted samples

Trial 3: change of glass-forming additives

Grouted sample

Crushed-up sample + glass-forming additives

To furnace (1250°C, 3hours)

Glass-forming additives:

Clay content in soil [%]	Bacth composition		
	Grouted soil [wt%]	Na_2CO_3 [wt%]	Li_2CO_3 [wt%]
5	66	14	20
10	66	14	20
20	66	14	20

Pourable, homogenous

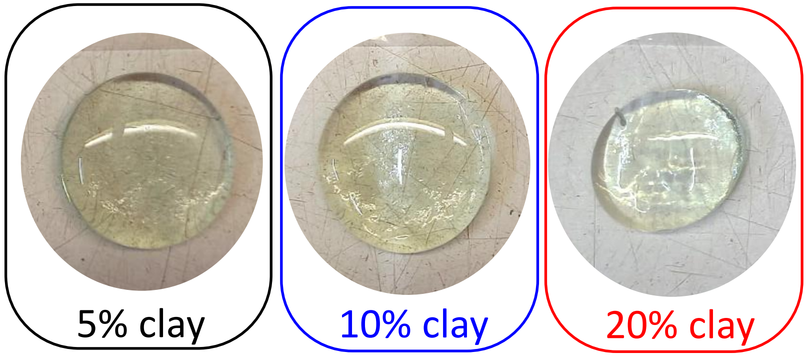

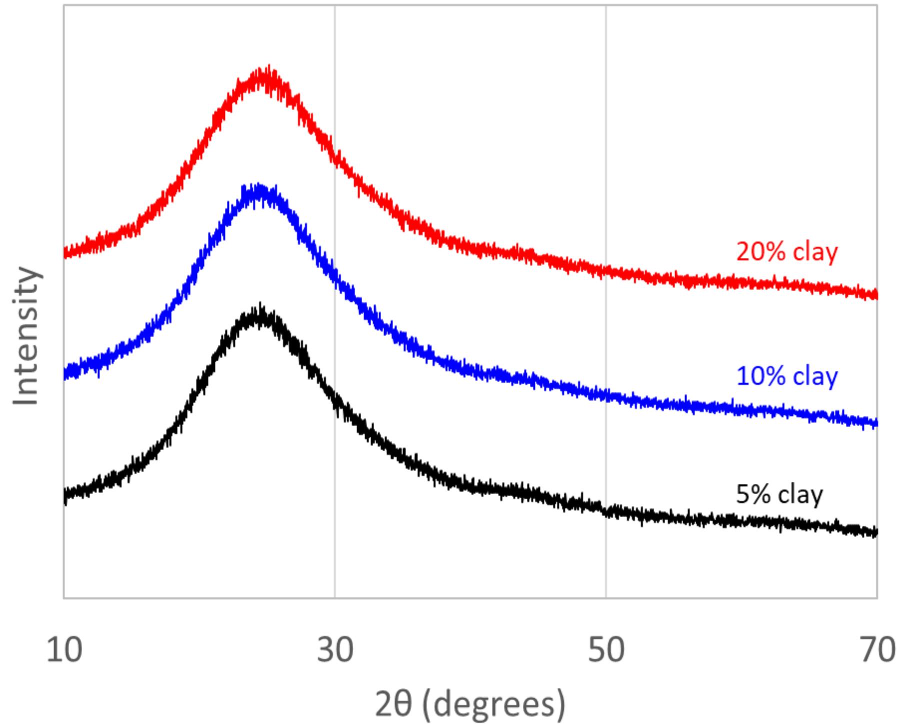

Stage 2. Glass-forming ability of intact grouted samples

How do we add glass-forming additives to intact samples?

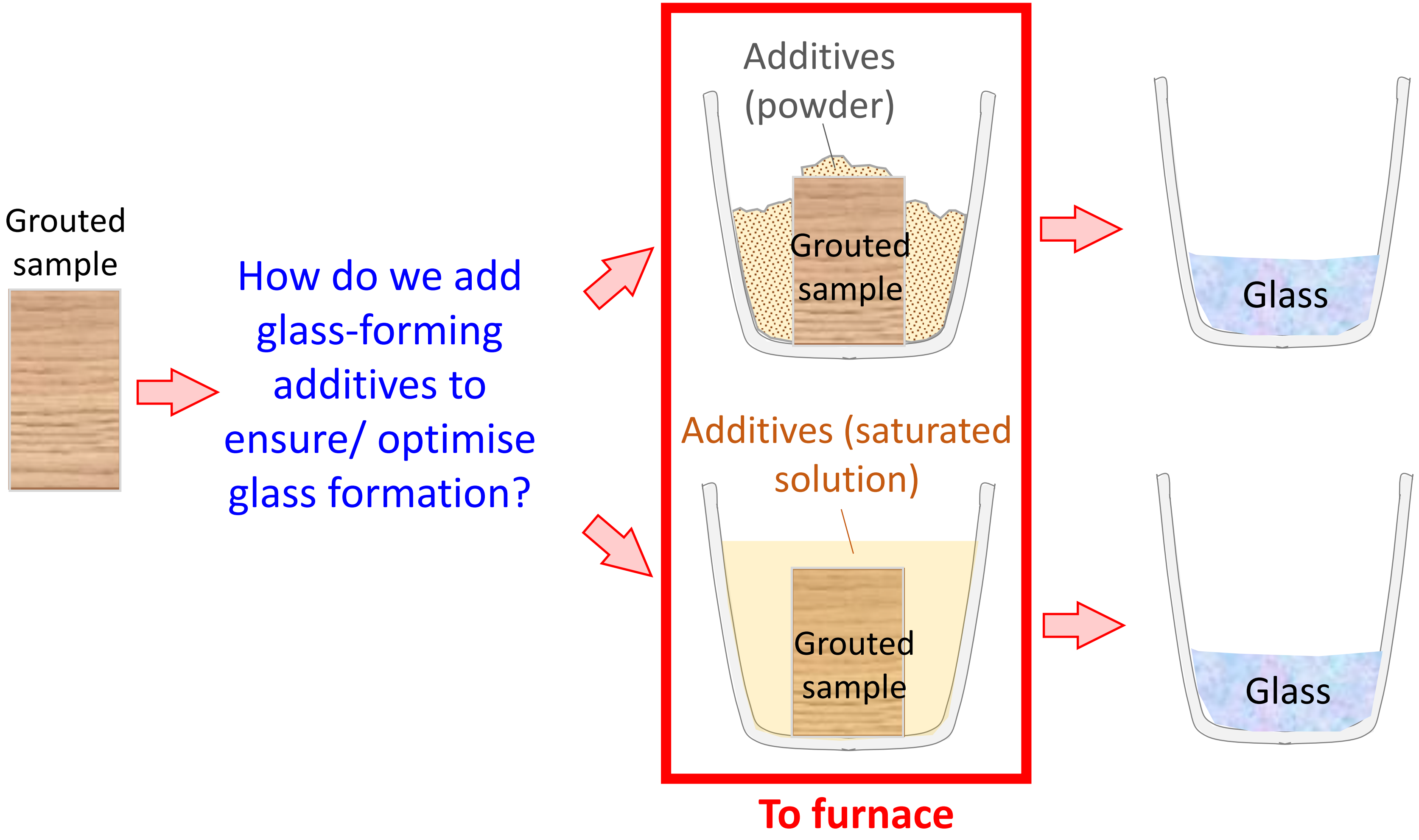

Stage 2. Glass-forming ability of intact grouted samples

Trial 2: Na_2CO_3 + $LiNO_3$ (powder and saturated solution)

Grouted sample

Powder Na_2CO_3 + $LiNO_3$

Saturated solution Na_2CO_3 + $LiNO_3$

To furnace (1250°C, 3hours)

Glass-forming additives:

Bacth composition		
Grouted soil [wt%]	Na_2CO_3 [wt%]	$LiNO_3$ [wt%]
55.8	11.9	32.2

Pourable, homogeneous

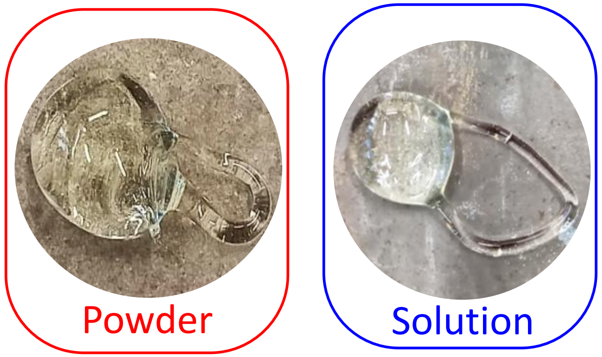

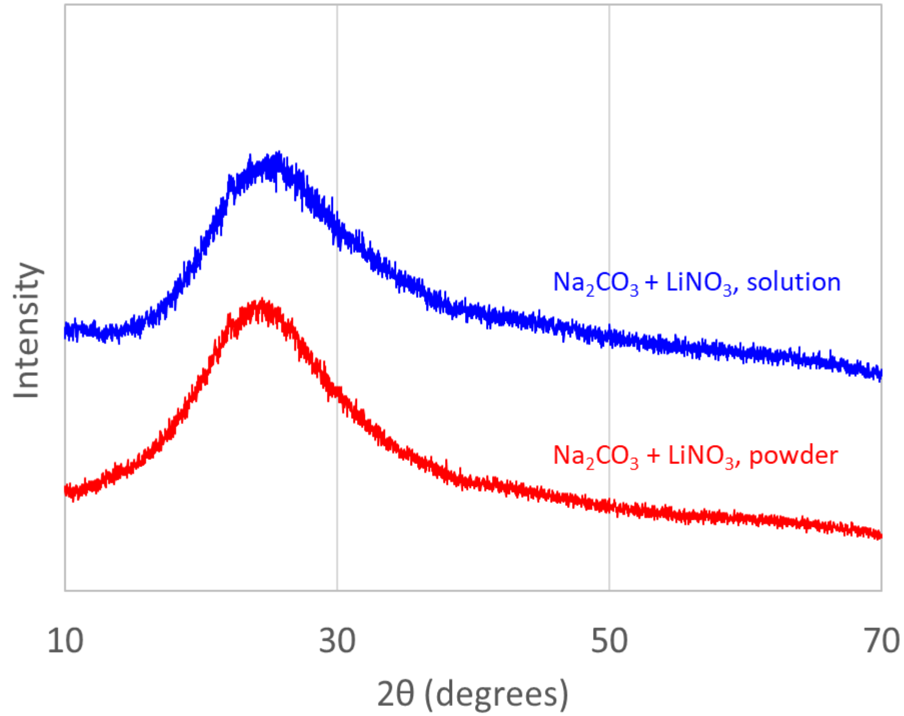

Stage 3. Cs and Sr retention of grouted samples upon glass formation

Cs Retention	Cs Retention
65.58	82.07

Ungrouted

Grouted

Spiked with Cs (1 wt% of total dry mass)

Ungrouted

Grouted

Spiked with Sr (1 wt% of total dry mass)

Sr Retention	Sr Retention
73.68	71.43

Analysed via XRF to determine Cs and Sr retention

Pourable, homogeneous and x-ray amorphous melts obtained by adding Na_2CO_3 + LiNO3 in solution (temperature 1250°C, 3 hours)

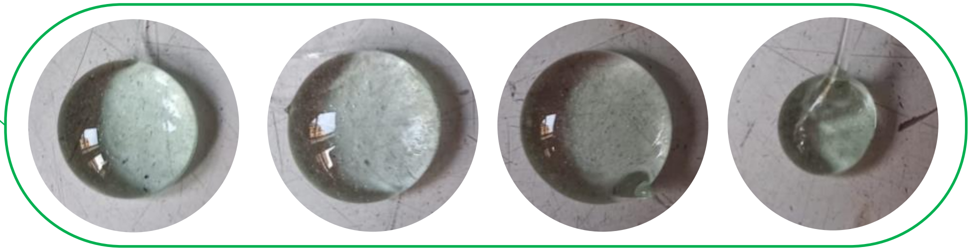

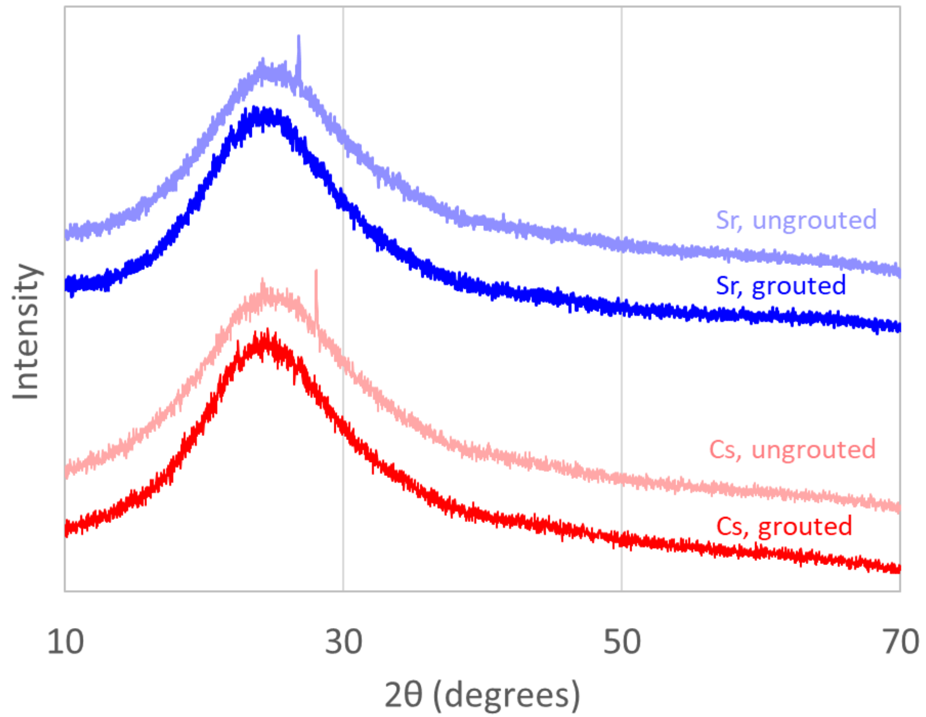

Conclusions

- Both crushed-up and intact colloidal silica grouted samples were successfully vitrified
- Na/Li based additives gave the best performance in terms of glass-forming ability at lower temperature (1250°C)
- Preliminary XRF analyses show an increased Cs retention capacity of soils grouted with colloidal silica

TRANSCEND

Transformative Science and Engineering for Nuclear Decommissioning

Thank you

arianna.pagano@strath.ac.uk

Transformative Science and Engineering for Nuclear Decommissioning

A theoretical study of NO and water co-reaction on PuO_2 (111) surface

Xiaoyu Han, Nik Kaltsoyannis
University of Manchester

2021, Harrogate

Energy
For a Low Carbon Future

Motivation

- UK strategy to net zero by 2050: reducing reliance on fossil fuels and move to **clean power**;
- One key area is to safely and securely manage and dispose the spent fuel;
- Currently, the Pu component in the spent fuel is in the form of **PuO_2** powder within inert steel canisters;
- To understand the water and other small molecules reaction within the canisters is still needed.

UK Overall Energy*

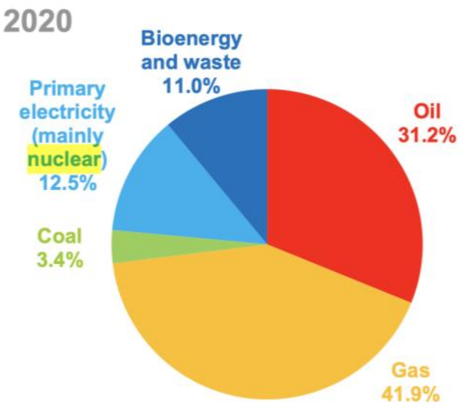

* UK Energy in Brief 2021, National Statistics

Challenges

- PuO_2 with radioactive nature, few experiment, especially surface study have been completed;
- Computationally, it's ill-treated correlated electron, controversy magnetic ordering, and uncertainty of relativistic contribution;
- Surface reaction need large number of atoms to represent the model is sufficient, which is computational demanding.
- Currently few study have done on the co-adsorption/reaction of more than one type of small molecule on the PuO_2 surfaces.

Method

- Periodic condition DFT: VASP;
- DFT+U: Dudarev approach;
- E cutoff 10^{-5} and F cutoff 0.01 eV/Å;
- Grimme-D3 method for vdW
- G-type AFM magnetic ordering for both bulk and surface;
- 3 X 3 with 6 repeated layer supercell for the surface;
- The reaction calculated at 300K, pH=7

$$\Delta G = \Delta E_{DFT} + \Delta E_{ZPE} - T\Delta S$$

The Hubbard *U* effect on PuO_2– projected Density of States

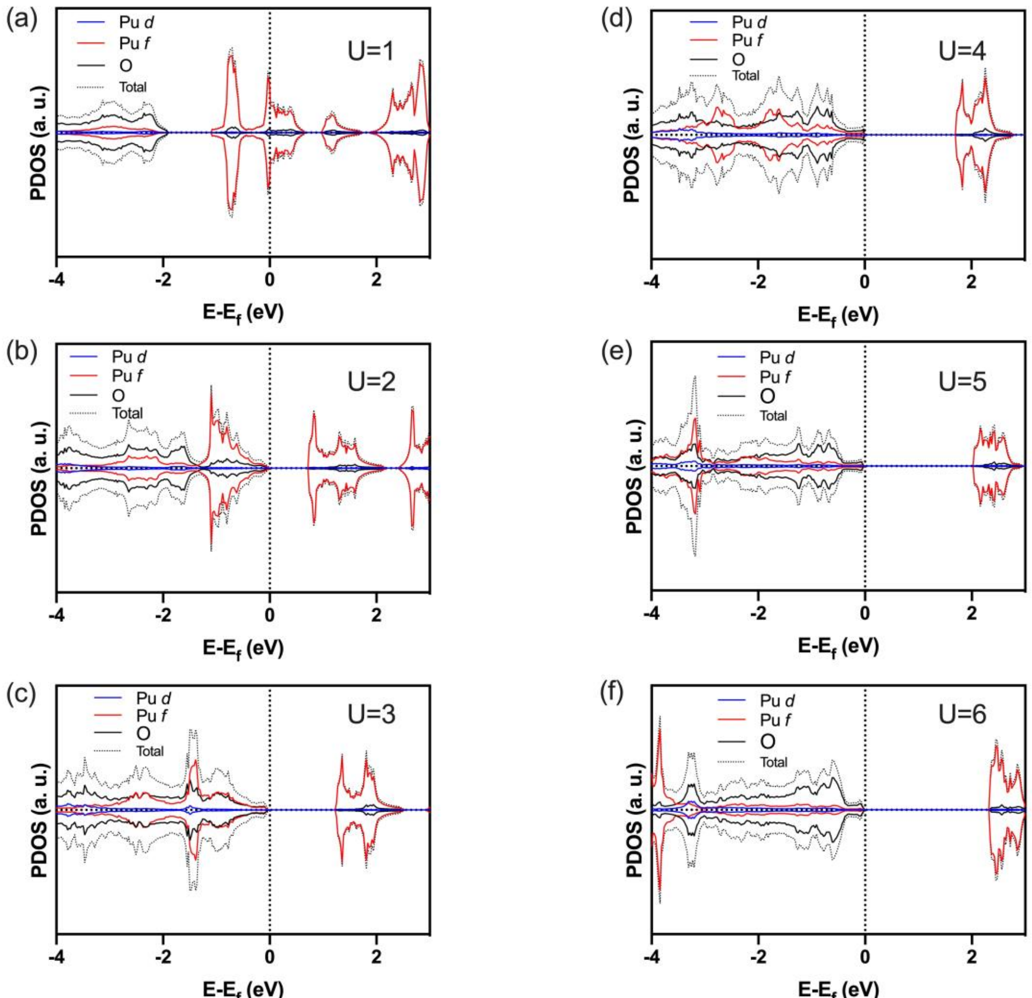

- ❖ Bandgap
- ❖ The contribution of the Pu in valence band

Experiments on **band gap**:

- 1.8 eV; electronic band gap;

C.E. McNeilly, J. of Nuclear Materials, **11**, 53, 1964;

- 2.80 eV; optical band gap;

T. Mark McCleskey, J. of Appl. Phys. **113**, 013515 (2013);

- 4.1 eV; optical band gap;

P. Roussel, *J. Electron Spectrosc. Relat. Phenom* **246** (2021), 147030

Band gap is not enough

ARPES for PuO_2 on a PAD film at 40.8 eV

LANL Research Quarterly, Issue 1, page 25, 2014

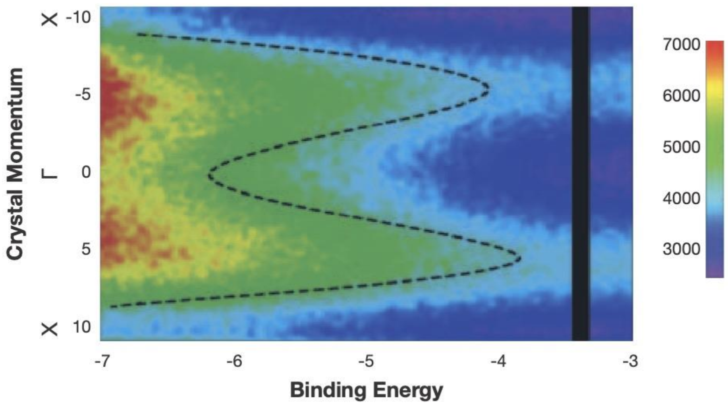

The peak split into **two peaks** represent **Pu 5*f* and O 2*p* hybridization**

PEECM hybrid functional

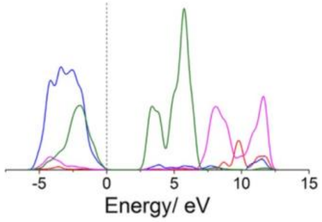

Fig. 4. PDOS of bulk AnO_2 (An = U (top), Np, Pu (bottom)) modelled as $An_{16}O_{32}$ clusters with the PEECM and the PBE0 functional. Vertical line shows the Fermi level. Vertical scale in arbitrary units.

Journal of Nuclear Materials 482 (2016) 124-134

Periodic DFT, PBE0

Our work

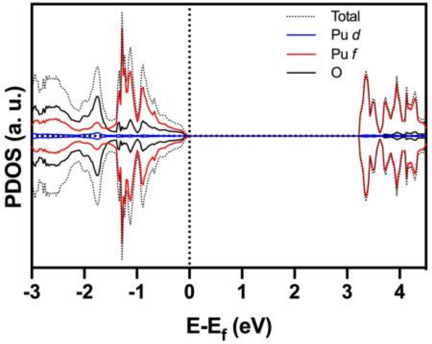

the characteristic of **the hybridization of 5f-2p orbitals in the first 2 eV range**

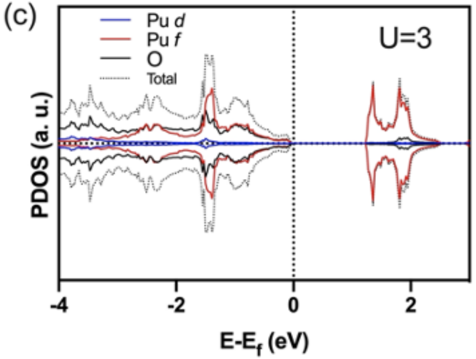

U=3 preserved the hybridization

H_2O on PuO_2 (111) --the most stable surface

Step 1 $H_2O + * \rightarrow H_2O*$

* denoted as the adsorption site on the surface

E_{ad} = -0.66 eV
$\Delta G_{1,300K}$= -0.68 eV

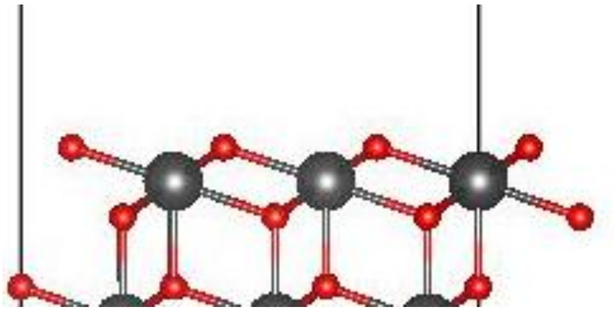

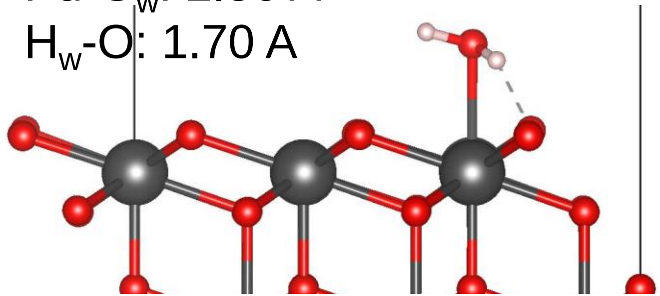

$Pu\text{-}O_w$: 2.56 A
$H_w\text{-}O$: 1.70 A

WF = 5.47 eV. (exp: 5.6 ±0.1 eV [1])
Bandgap = 1.613 eV

	1st layer Pu	Bonded Pu	Else Pu	H_2O
Magnetic moment	4.081	4.083	4.078	
Bader charge	2.403	2.420	2.408	8

physical adsorption through rearrangement of electrons of Pu

[1] P. Roussel, *J. Electron Spectrosc. Relat. Phenom* **246** (2021), 147030

H_2O on PuO_2 (111)

Step 1 $H_2O + * \rightarrow H_2O*$

Pu-O_w: 2.56 A
H_w-O: 1.70 A

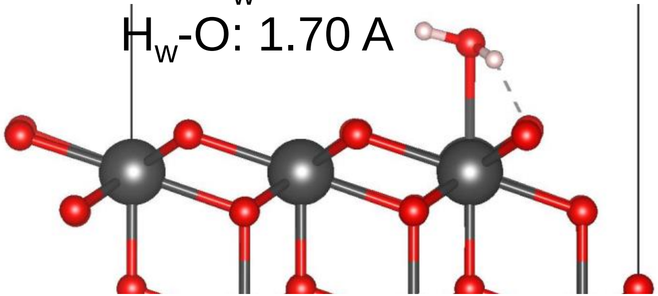

E_b =3.20 eV

Step 2 $H_2O* \rightarrow HO* + H*$

Pu-O_w: 2.20 A
H_w-O_w: 1.65 A

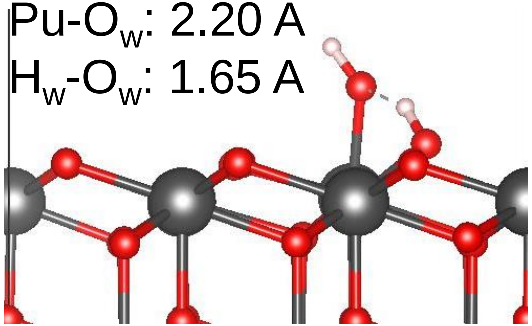

E_{ad} = -0.66 eV
$\Delta G_{1,300K}$= -0.68 eV

E_{ad} = -0.09 eV
$\Delta G_{2,300K}$= -0.62eV

even though **exothermal** reaction for overall splitting, but high reaction barriers

$H_2O@PuO_2$ (111) pDOS

$HO^*+H^*@PuO_2$ (111) pDOS

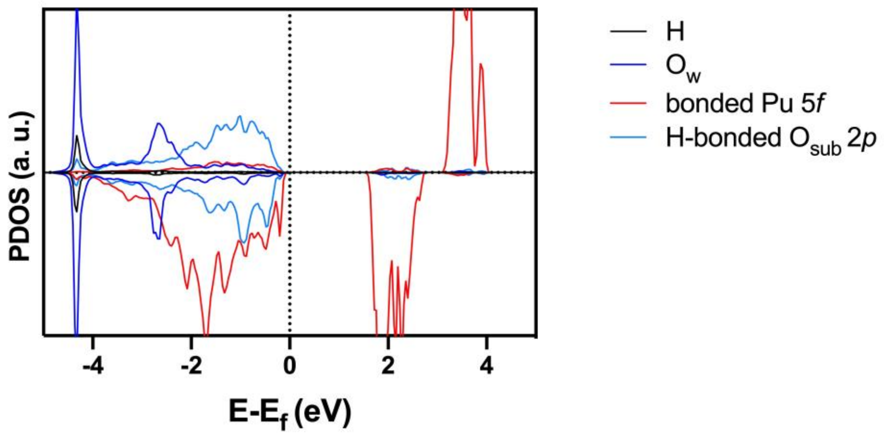

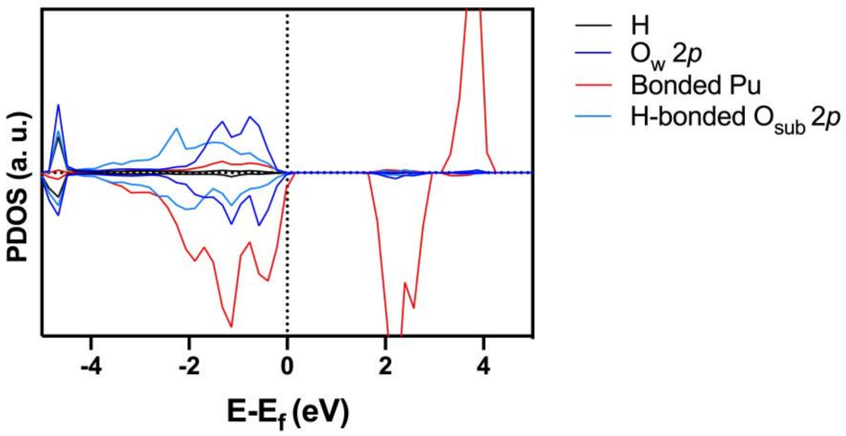

	$H_2O@PuO_2$ (111)	$HO^*+H^*@PuO_2$ (111)
The bonded Pu f band center in VB	-1.63 eV	-1.42 eV
O_w 2p	-2.68 eV	-1.82 eV
H	-4.32 eV	-4.67 eV

NO ⊥ PuO_2 (111) --- @Pu

NO+ * → NO*

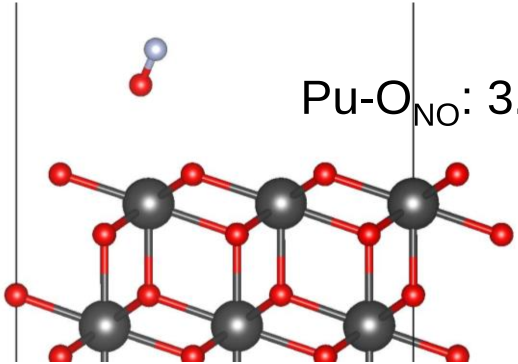

$\Delta G_{1,300}$= -0.29 eV

NO+ * → ON*

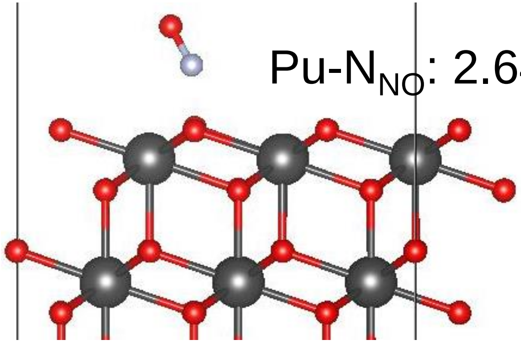

$\Delta G_{1,300}$= -0.60 eV

	1st layer Pu	NO*		ON*	
		Bonded Pu	Else Pu	Bonded Pu	Else Pu
Magnetic moment	4.081	4.065	4.082	4.039	4.085

Bonded Pu reduced

Z-direction profiles

NO+ * → NO*

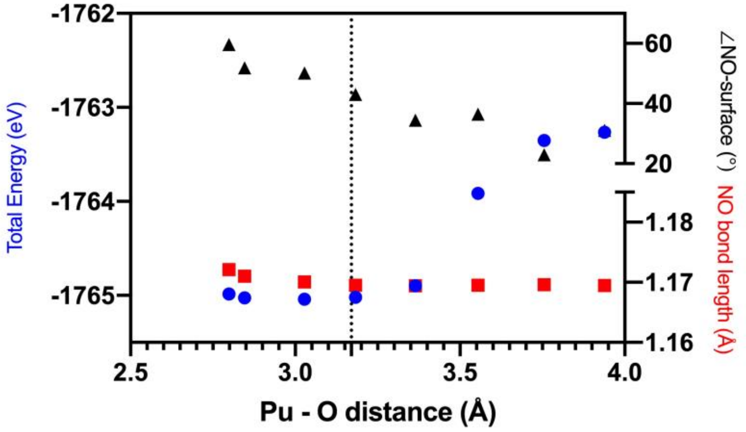

NO+ * → ON*

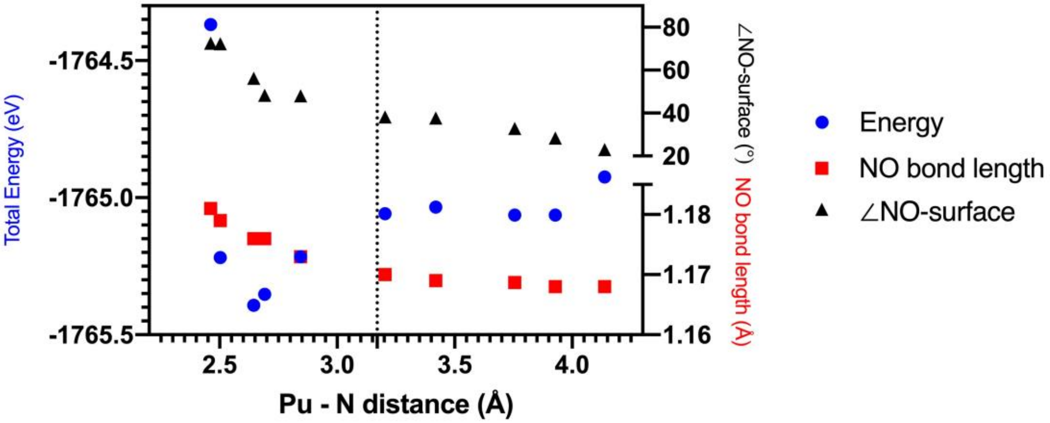

- For both approaching manner, the NO molecule adjust it **angle** with the surface from considerable parallel to perpendicular.
- When the distance reduced to its kinetic diameter, the N pointing downwards would further reduce the system energy by **stretching NO bond length**, whilst this behavior isn't significant when the O pointing downwards.

NO// PuO_2 ---@O_{sub}

Step 1 NO+ * → ON*

Step 2 ON* → * + NO_2

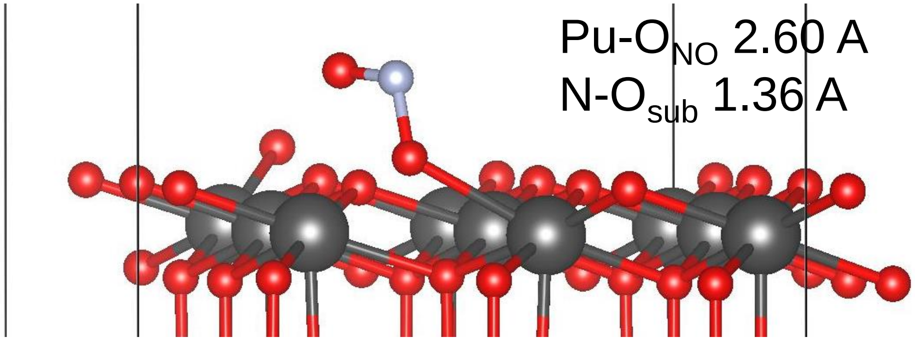

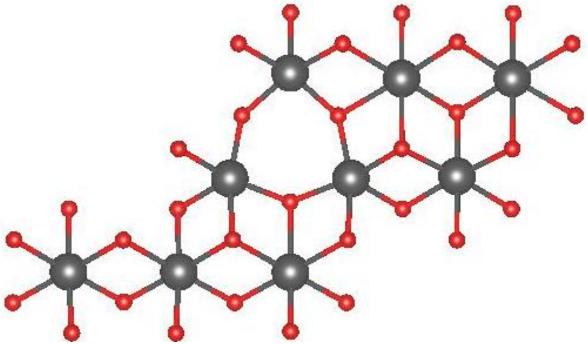

$\Delta G_{1,300}$= -0.60 eV

$\Delta G_{2,300}$= 3.91eV

Further reduction even harder!

H_2O @NO // PuO_2

Step 2 $H_2O + ON^* \rightarrow H_2O^* + ON^*$

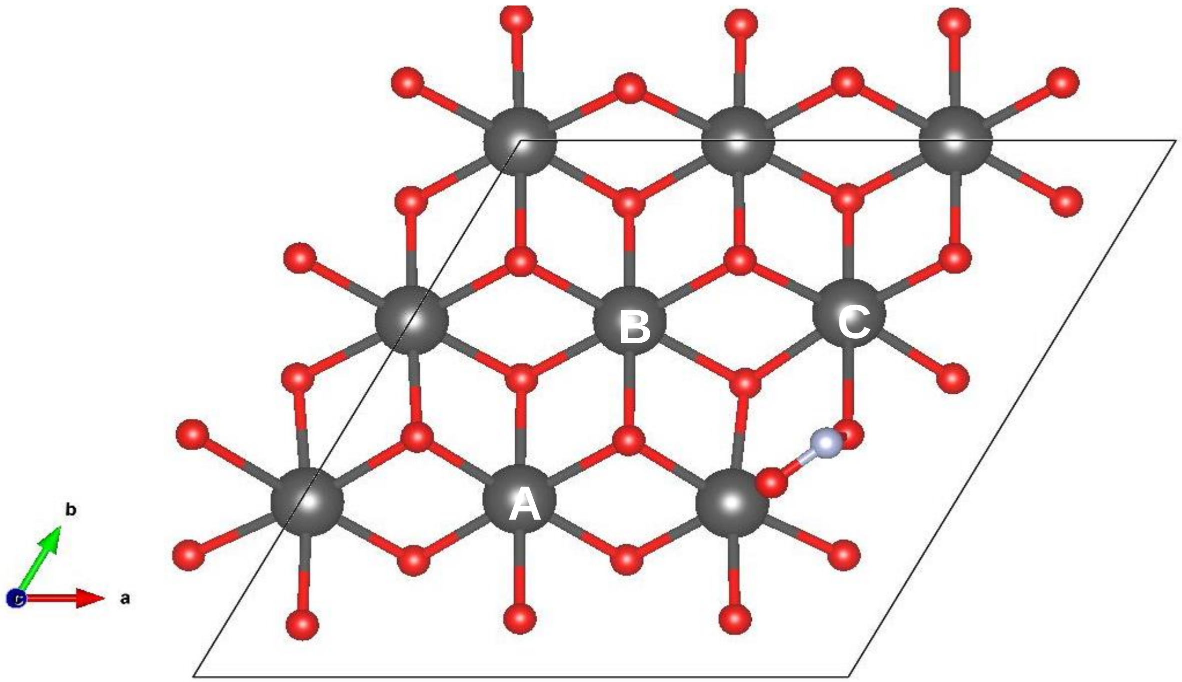

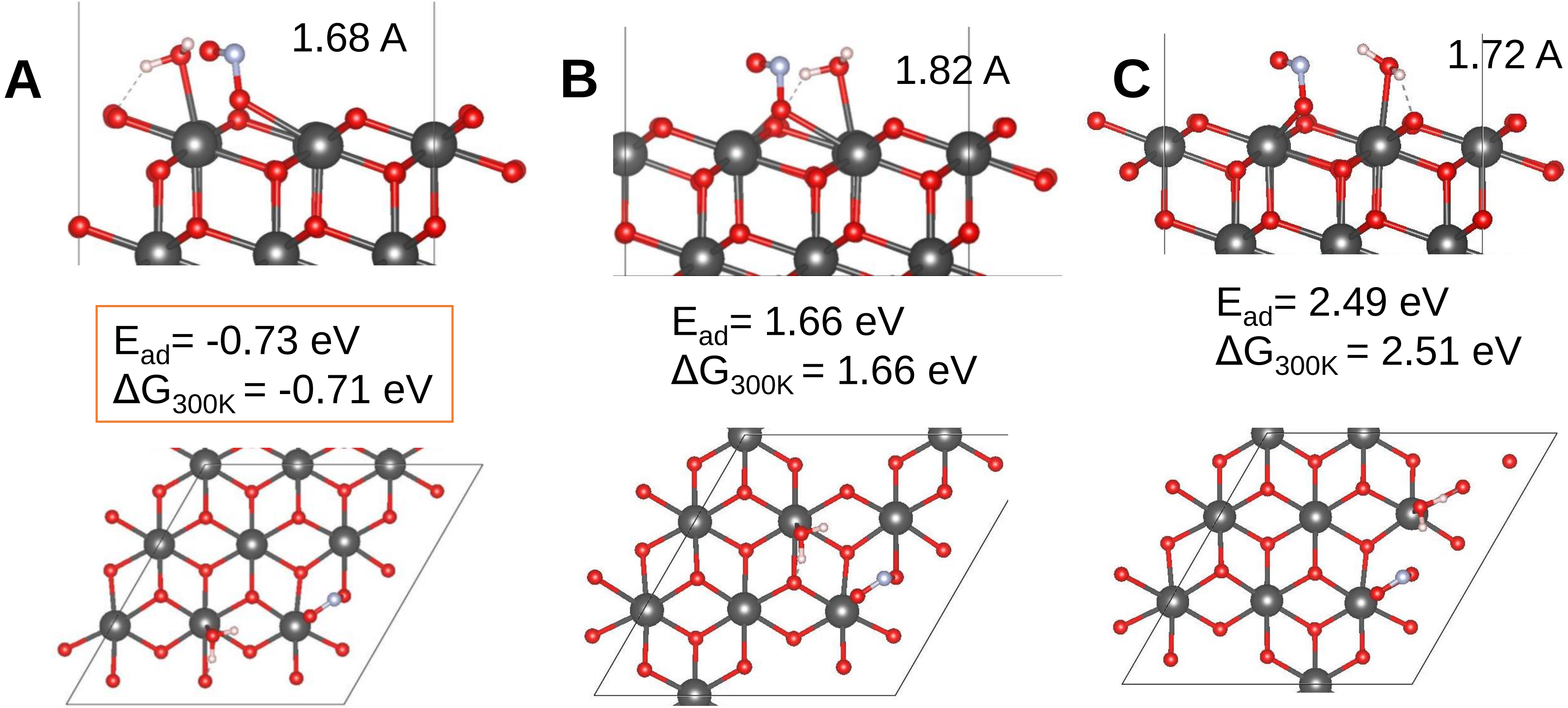

- H_2O adsorption is site-selective.
- A site is more energetic favourable than bare surface.

(A) H_2O dissociation

Step 3 $H_2O^* + ON^* \rightarrow HO^*+H^*+ON^*$

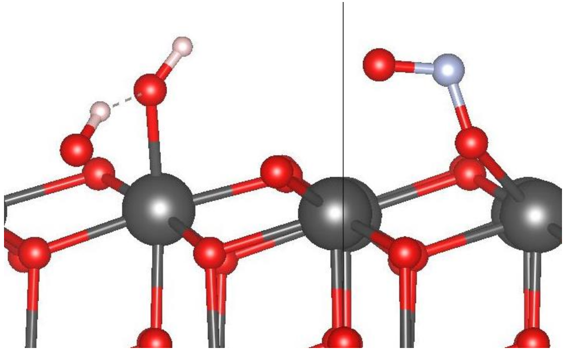

E_{ad}= -0.06 eV
$\Delta G_{3,300K}$ = -0.42 eV

(A) nitrous acid

Step 3 $H_2O^* + ON^* \rightarrow HO^*+HONO^*$

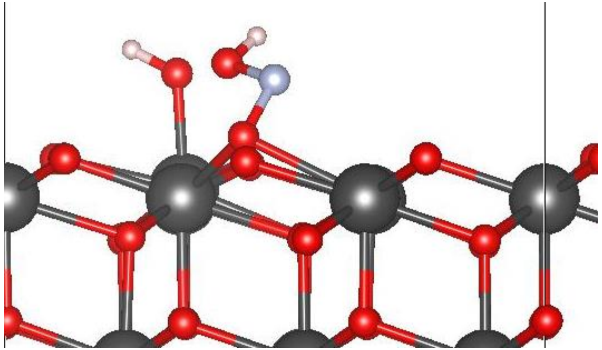

E_{ad}= 2.74 eV
$\Delta G_{3,300K}$ = 2.68 eV

Water affiliated A site prefer water dissociation

(B) H_2O dissociation

(B) nitroxyl

Step 3 $H_2O^* + ON^* \rightarrow HO^* + H^* + ON^*$

Step 3 $H_2O^* + ON^* \rightarrow HO^* + HONO^*$

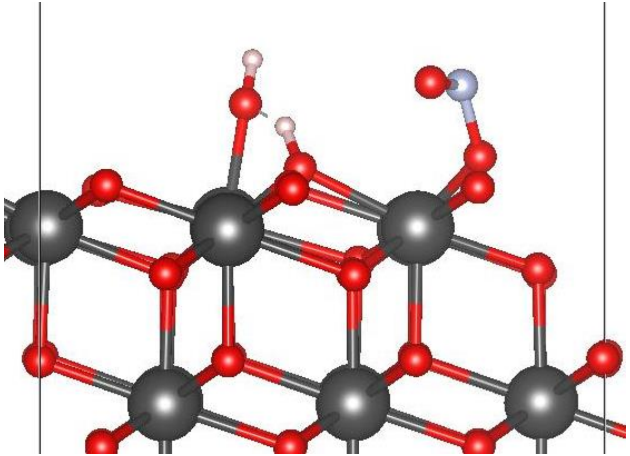

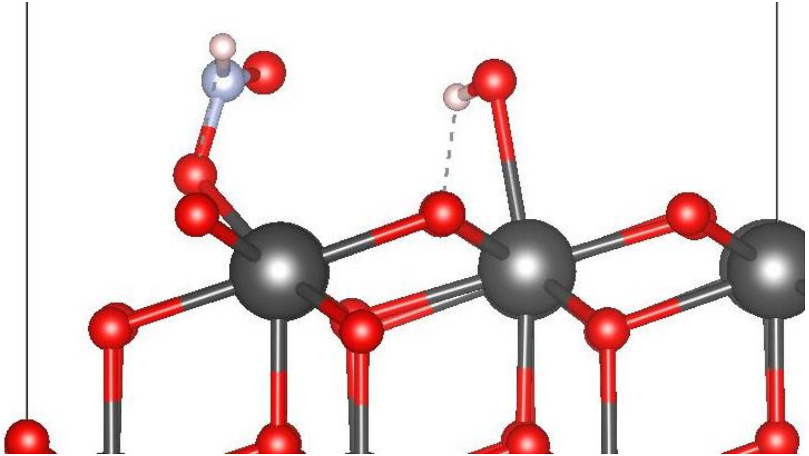

E_{ad}= 0.23 eV
ΔG_{300K} = -0.02 eV

E_{ad}= - 0.47 eV
ΔG_{300K} = - 0.66 eV

Water repulsing B site prefer to form nitroxyl

Conclusion

- Due to the wide range of experimental data on the bandgap, we selected **U=3**, which preserved the 5f and 2p **hybridization** on the VB to describe the PuO_2.
- The calculated {111} surface **work function** (5.47 eV) matched with the latest experimental one (5.6 ±0.1 eV);
- For individual water, **physical adsorption** of water achieved by rearrange of the oxidation on the first layer of Pu. High energy barrier for the water splitting;
- For individual NO, Pu is selective for the molecule direction, with N facing down prefered.
- After NO bonded with O_{sub}, further interaction with water and formation of **NO_2, HNO_2, and HNO** have been investigated.

Acknowledgement

- EPSRC: EP/S01019X/1;
- Archer HPC, CSF HPC in The University of Manchester and their associated services;
- Prof. N. Kaltsoyannis and the group members

Transformative Science and Engineering for Nuclear Decommissioning

Thank you

Xiaoyu.han@Manchester.ac.uk

Research and Development at Sellafield

‘*Where science never sleeps*’

Dr Katherine Eilbeck
Acting CTO
(Actual Head of R&D)

Where Science never sleeps ………….

& 25 years later ……….

https://youtu.be/Fm2hpD8C4ks

Science at Sellafield - WHY

- Act for Sellafield as a technical conscience and provide oversight
- Forward looking identification of technical options and opportunities and deliver innovative solutions to meet the need
- Maintain stakeholder confidence through recognition of our technical expertise
- Culture that embraces science and innovation
- Ensure we have the right people with the right skills in the right organisation at the right time

Science leads at Sellafield Ltd

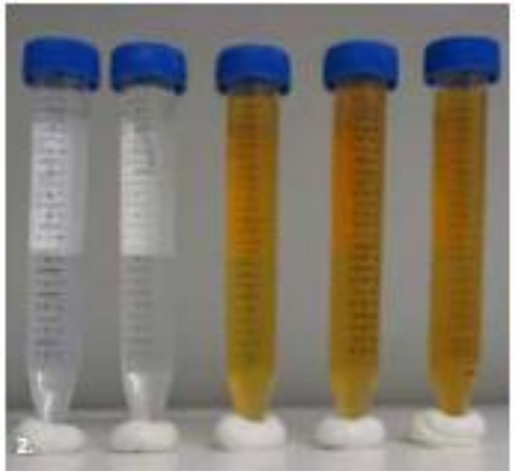

*Floc with 0.2g/L iron with increasing pH left to right – as part of r*esearch to adapt the Enhanced Actinides Removal Plant (EARP) to accept alternative waste streams from donor plants.

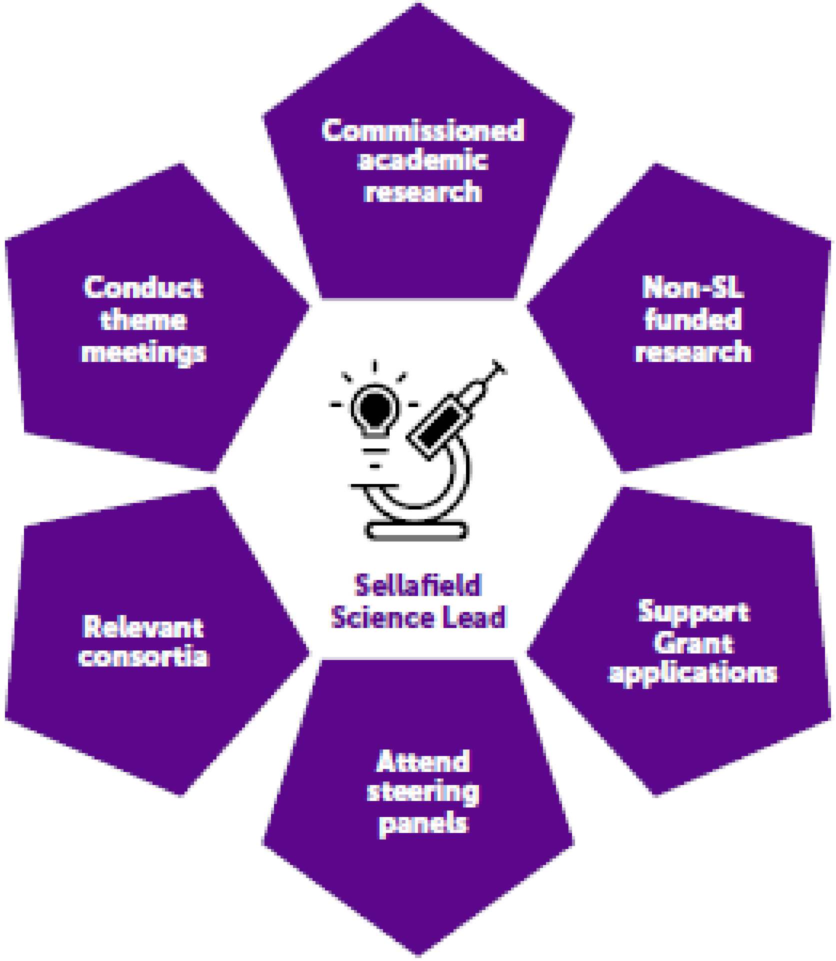

SCIENCE

Materials science

Understanding of the chemical, physical and engineering properties of current and new materials in their relevant operational environment to facilitate decisions in support of existing operations and design of new plants

Process chemistry

Underpinning science of current infrastructure of treatment and storage facilities so that they can be adapted to manage future wastes. Development of new processes to assist in the delivery of the changing mission

Particulate behaviour

Properties and behaviour of particulate materials, including sludges, slurries and suspended particulates or liquid droplets in gases to underpin design, abatement techniques, personnel protection and flowsheets

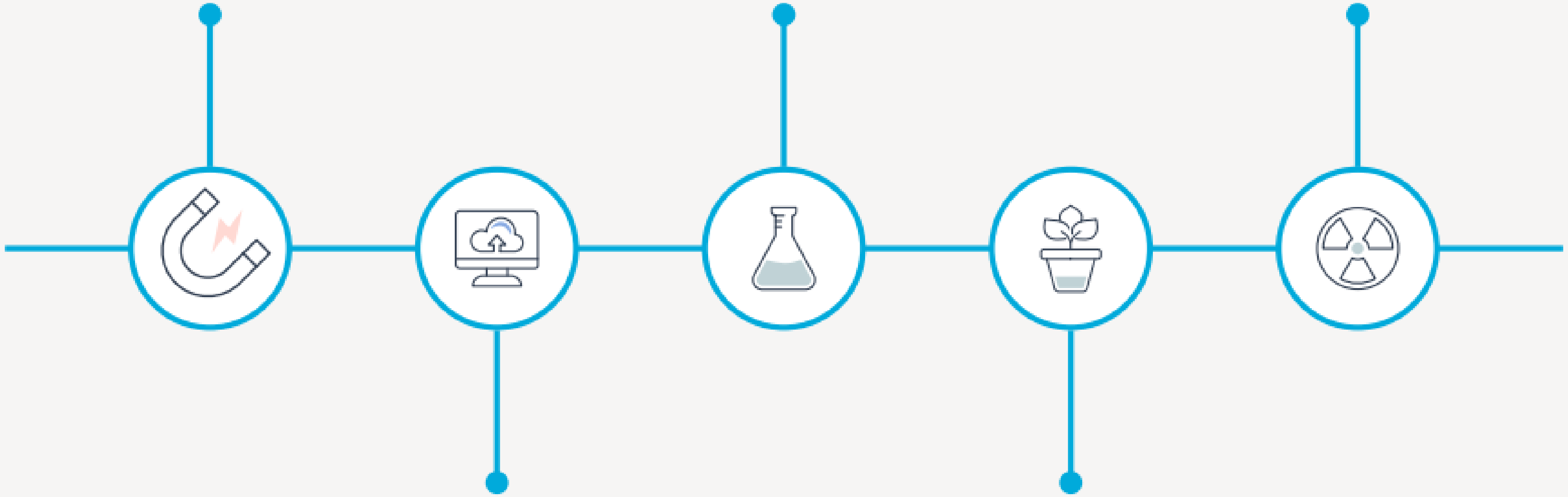

Data science

Data collection, processing and in depth data analysis to aid decision making

Environmental science

Understanding of the long term fate of radioactivity and its impact on the environment, as it changes

Underpinning science themes

INTEGRATED RESEARCH TEAMS

Waste treatment, conditioning & packages

Waste immobilisation strategies, including thermal technologies and low temperature processes and new, cost-effective waste container options for decommissioning

Future asset management & digital technologies

Application of Industry 4.0 (I4.0) and related technologies to asset management of aging and contaminated facilities

Protecting people

Improved personal protective equipment for the operator using modern materials, digital technologies and other human augmentation

Measurement & analysis

A range of measurement and deployment techniques to undertake analysis, detect signs of unexpected degradation and demonstrate control for extended storage periods

Post operational clean-out

Techniques for characterisation, decontamination, access and deployment whilst addressing effluent and waste treatment

Robotics & artificial intelligence

Building on existing remote handling capability to more autonomous systems. Development of a centralised route for the introduction of RAI to the site

Technology development themes

Sellafield Ltd

The Importance of sludge ……………………..

‘Chris Cunliffe’s thesis, which supports Slurry Transfers across site (potentially on many plants) in partially full and sloping pipes, has been received and reviewed by Technical. This provides important new engineering correlations and operational advice, replacing some major correlations used by engineers for over a hundred years, and new insights into slurry flow in sloping & part full pipes and was supported by Sellafield via CINDe with NNL.’

The results to date have substantiated our baseline strategy for washout of highly active tanks, so the value is in avoiding having to develop a new process for POCO & the consequent extension to our High Active Liquor programme. We’ve never tried to estimate the cost of developing and implementing plan B, but a cost of circa £550m is probably credible (this is based on a nominal estimate of costs for a 5 year extension to the HAL programme).

However, the biggest value realised from the phD has been Chris himself. He’s now working for NNL & is supporting the HALES/WVP slurry transport experiments.

Further information – R & D Needs…………

Sellafield_future_research_requirements_2021_LR.pdf (publishing.service.gov.uk)

Annual Research and Development Review

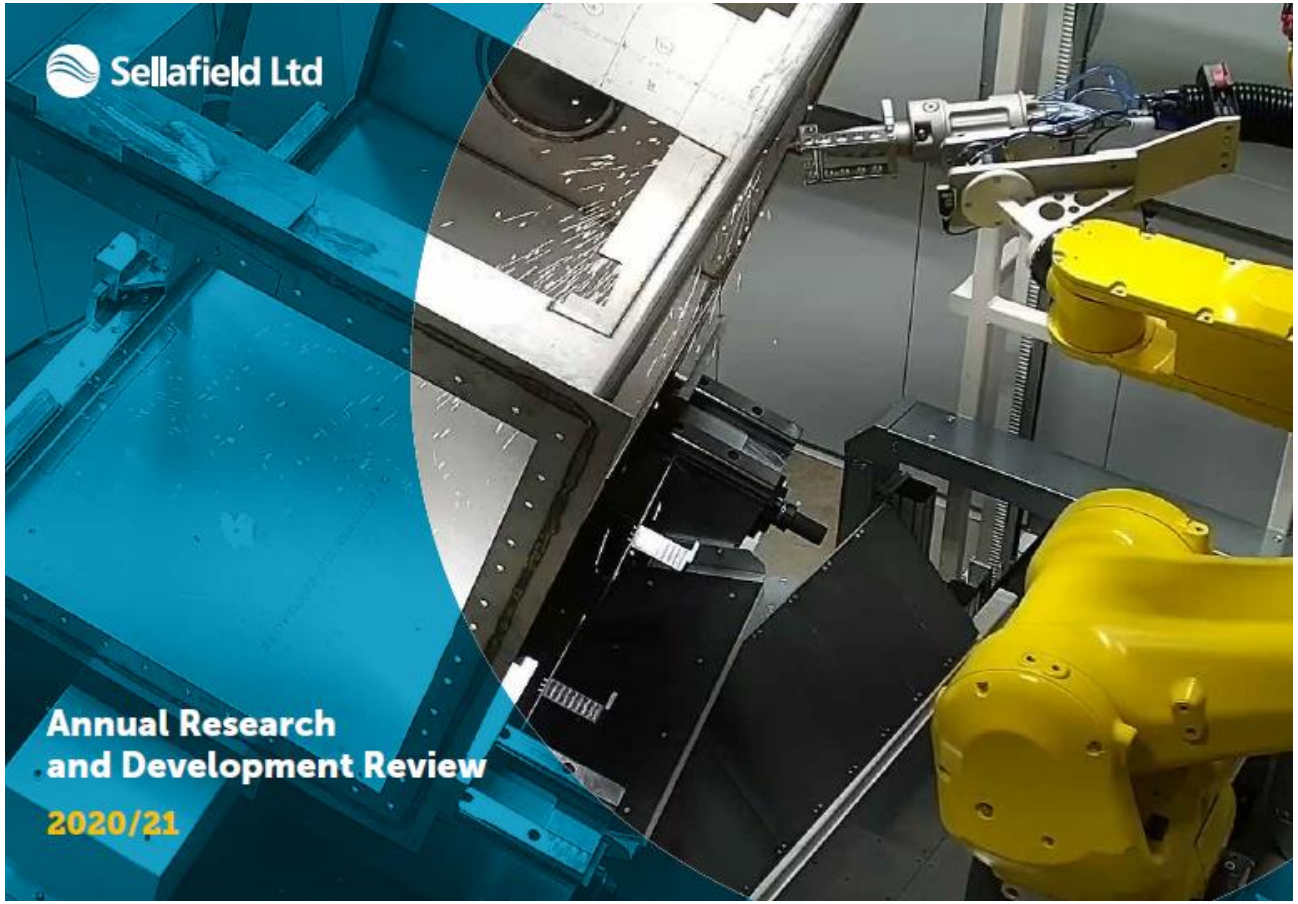

TRANSCEND

Transformative Science and Engineering for Nuclear Decommissioning

Imperial College London

Nanotechnology for effluent treatment and radionuclide assay and repair of ageing facilities

Dr. Gurpreet Singh

Imperial College London

Supervisors: Prof. Luc Vandeperre & Prof. Mary Ryan

10/11/2021
TRANSCEND Project

Energy
For a Low Carbon Future

Project Background

- Fortner's group (ref 1) had reported since 2015 about magnetic nanoparticles of mixed Mn/Fe oxide nanocrystals covered with a bilayered oleyl phosphate to adsorb/exchange uranyl ions in solution.
- Adsorption Capacity reported to be 1667 mg/g of mixed oxide nanocrystals.
- In 2017 DISTINCTIVE PhD student in our group (Ref 2) further enhanced the work by using magnetite coated with oleic acid (~12nm).
- The nanoparticles were further functionalised with phosphate groups to sequester uranium.
- The reported uptake capacity of Uranyl ions at neutral pH 7 was 1690 mg/g of nanoparticles in 200ppm U(VI) nitrate solution.
- This is the highest ever to be reported in the literature and also the fastest (within 1 minute).
- Mechanism of uptake unknown.
- Interesting interactions happen at physio-chemical interface.

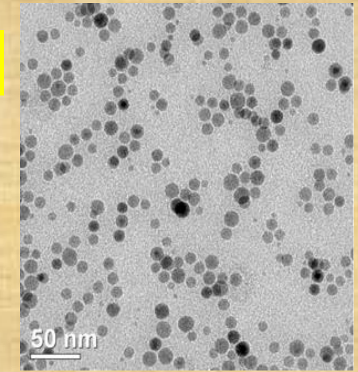

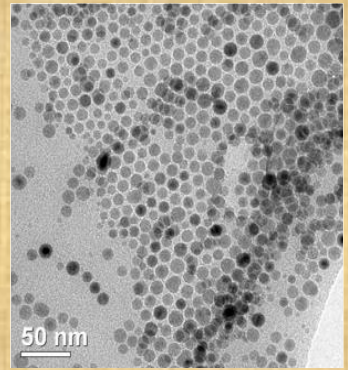

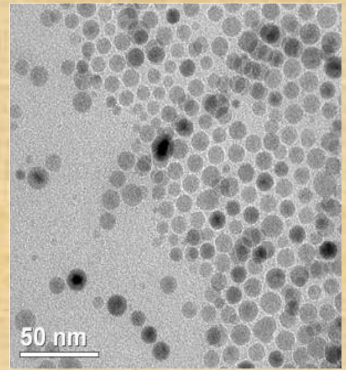

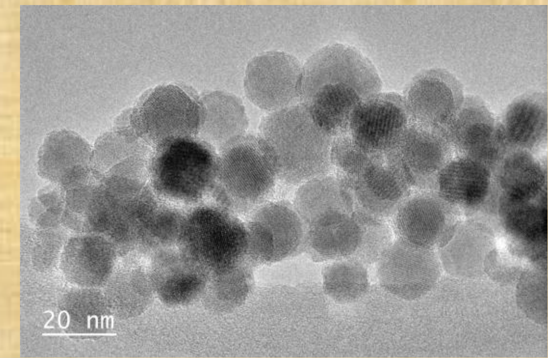

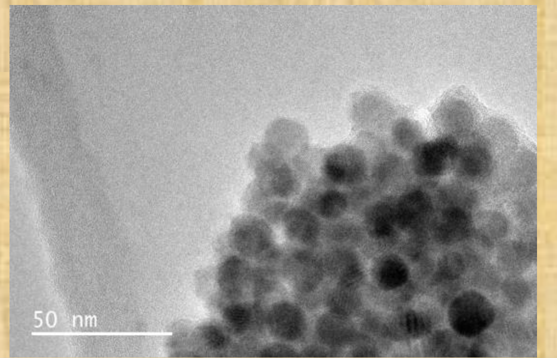

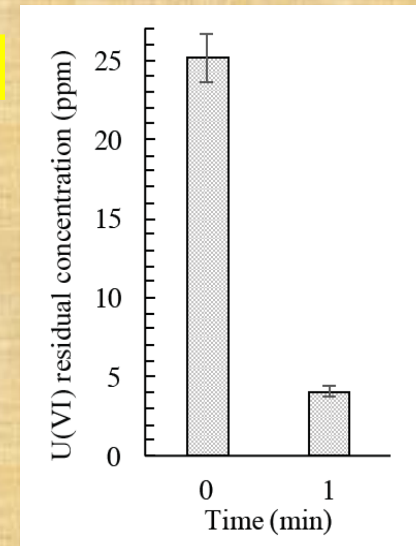

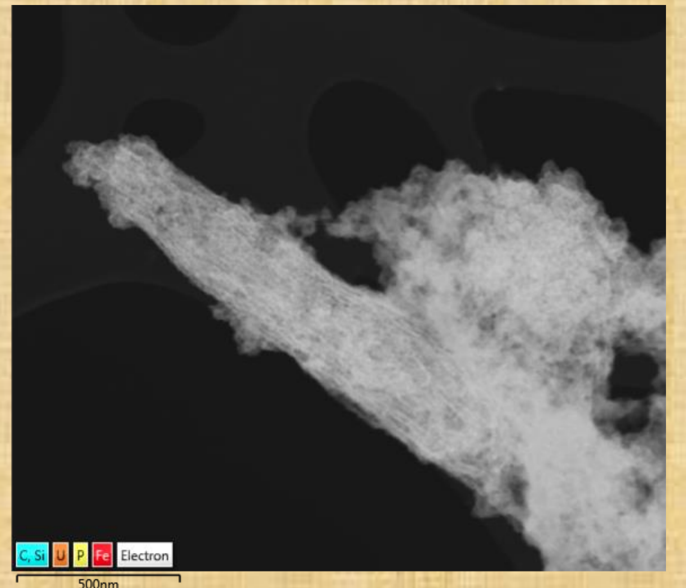

Current Strategy

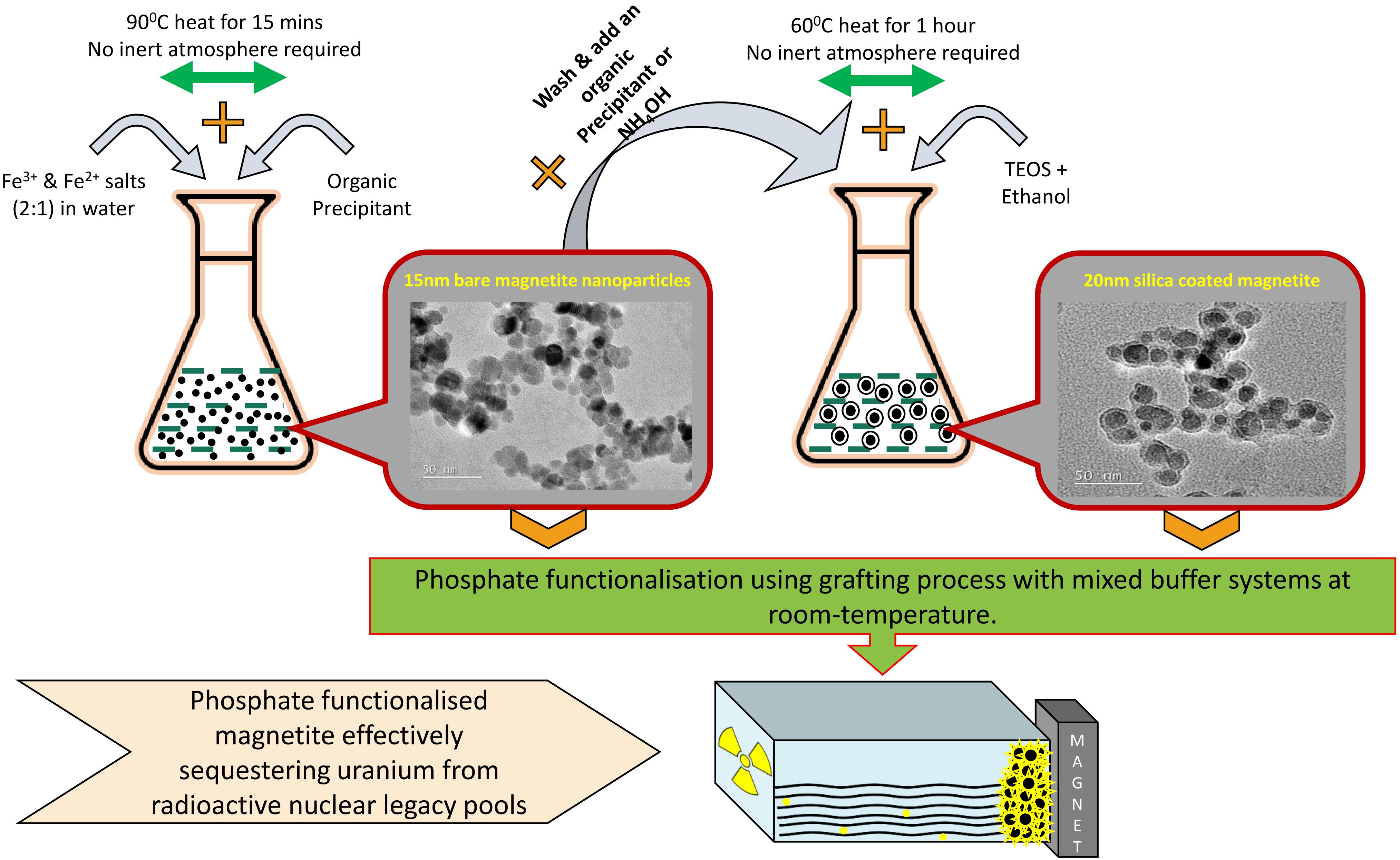

Analytical Results So Far….

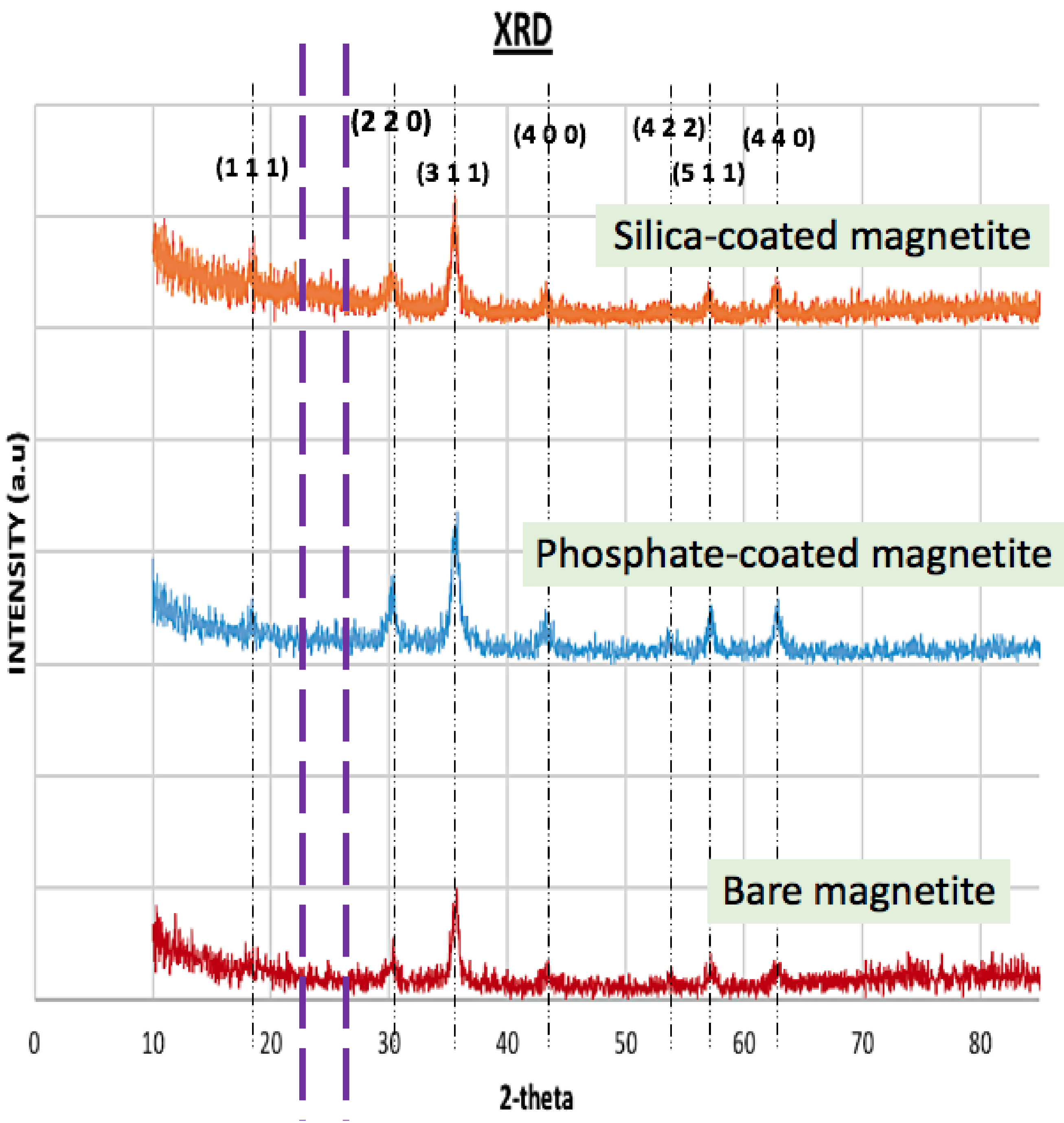

Bruker Cu-Kα 1.5406Å on a D2 Phaser Benchtop Diffractometer

Peaks identified with JCPDS Card 75-1610 to be magnetite

Typical maghemite (Ɣ-Fe_2O_3) peaks missing from the spectrum

Other techniques to confirm phase-purity, yet to be applied.

Silica and phosphate coating shows isostructural XRD patterns

Subtle differences in (1 1 1) reflection and crystallinity (P/N ratio)

TEM and EDX confirmations

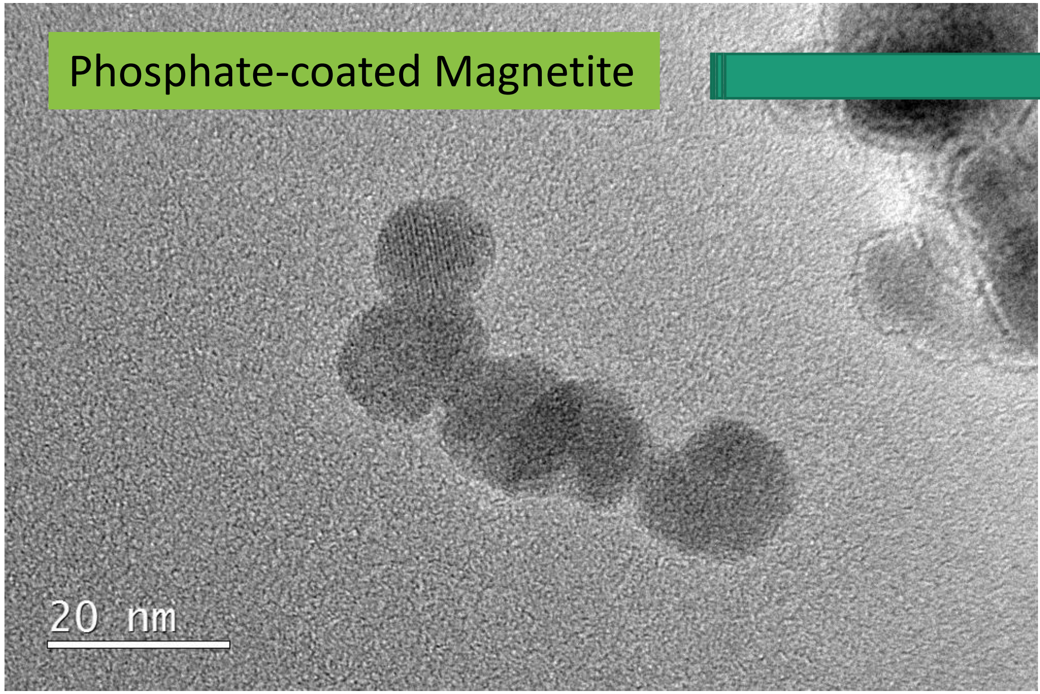

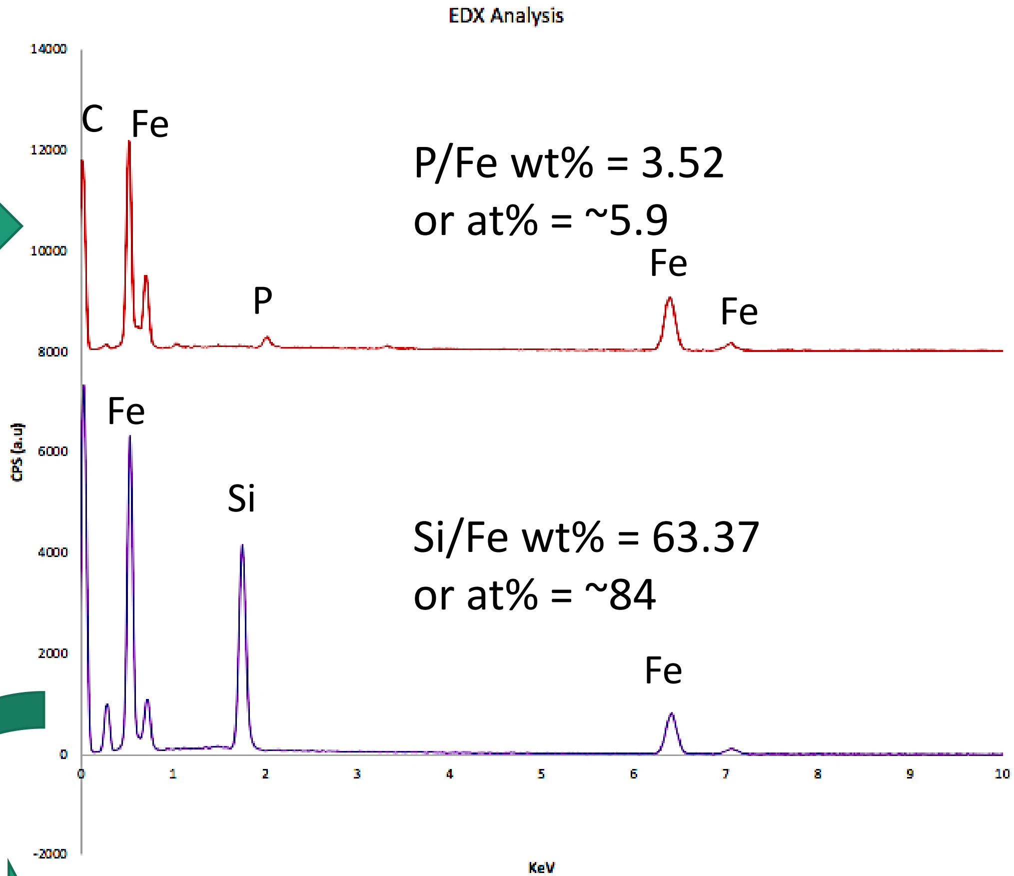

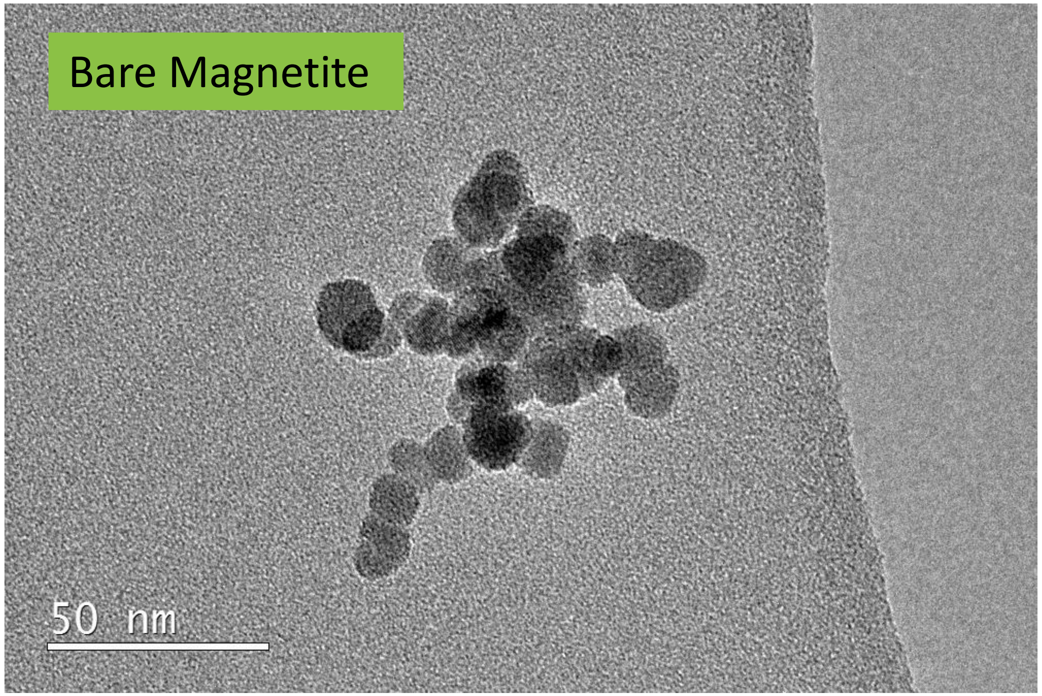

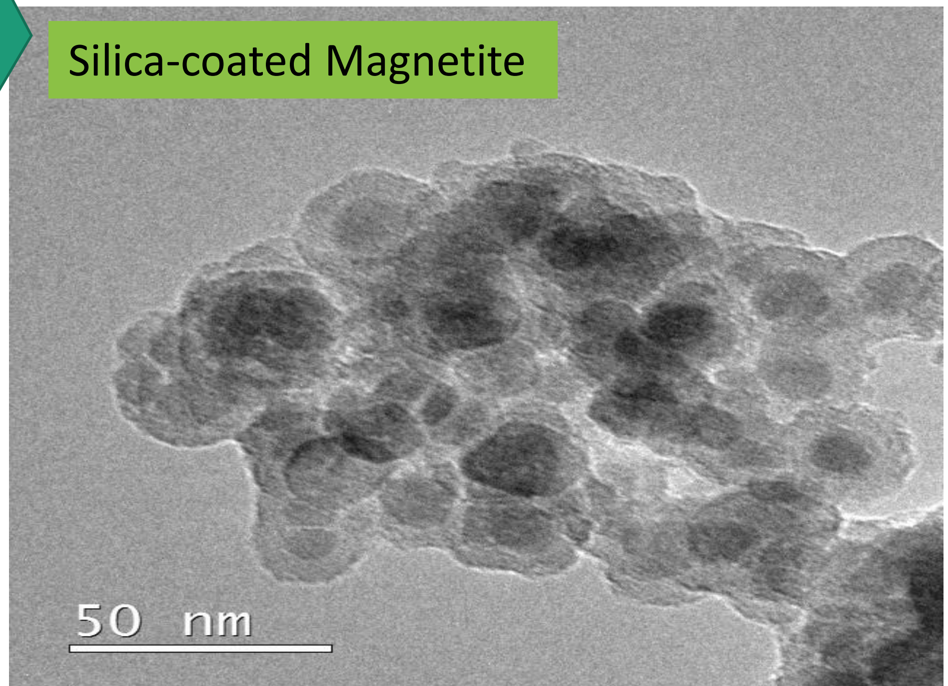

Zeta-potential & Surface Charge

			Mean (mV)	Area (%)	St Dev (mV)
Zeta Potential (mV):	-34.7	Peak 1:	-34.7	100.0	4.10
Zeta Deviation (mV):	4.10	Peak 2:	0.00	0.0	0.00
Conductivity (mS/cm):	0.0133	Peak 3:	0.00	0.0	0.00

Result quality : Good

Silica-coated magnetite in water

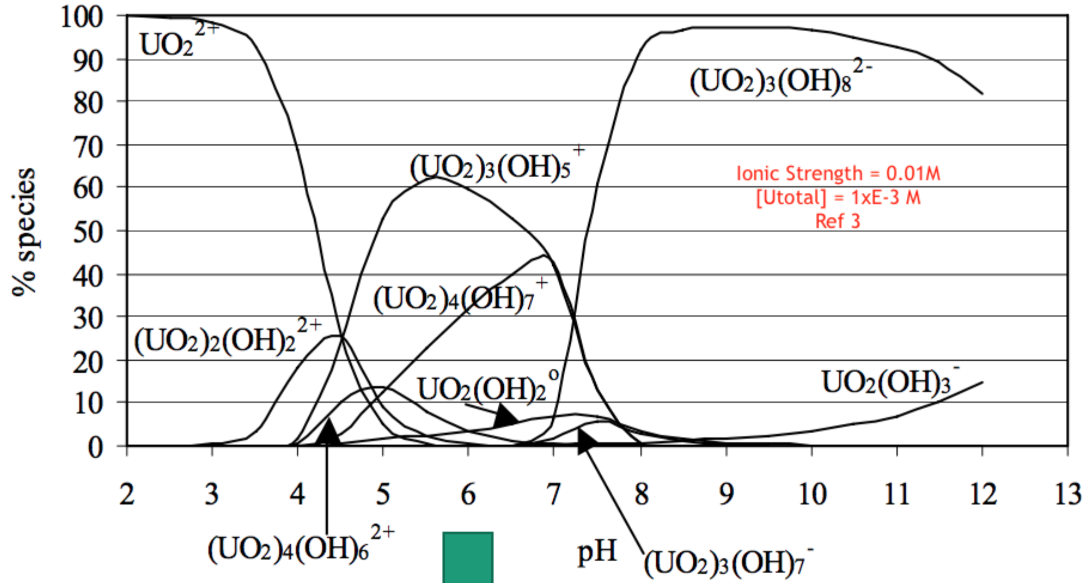

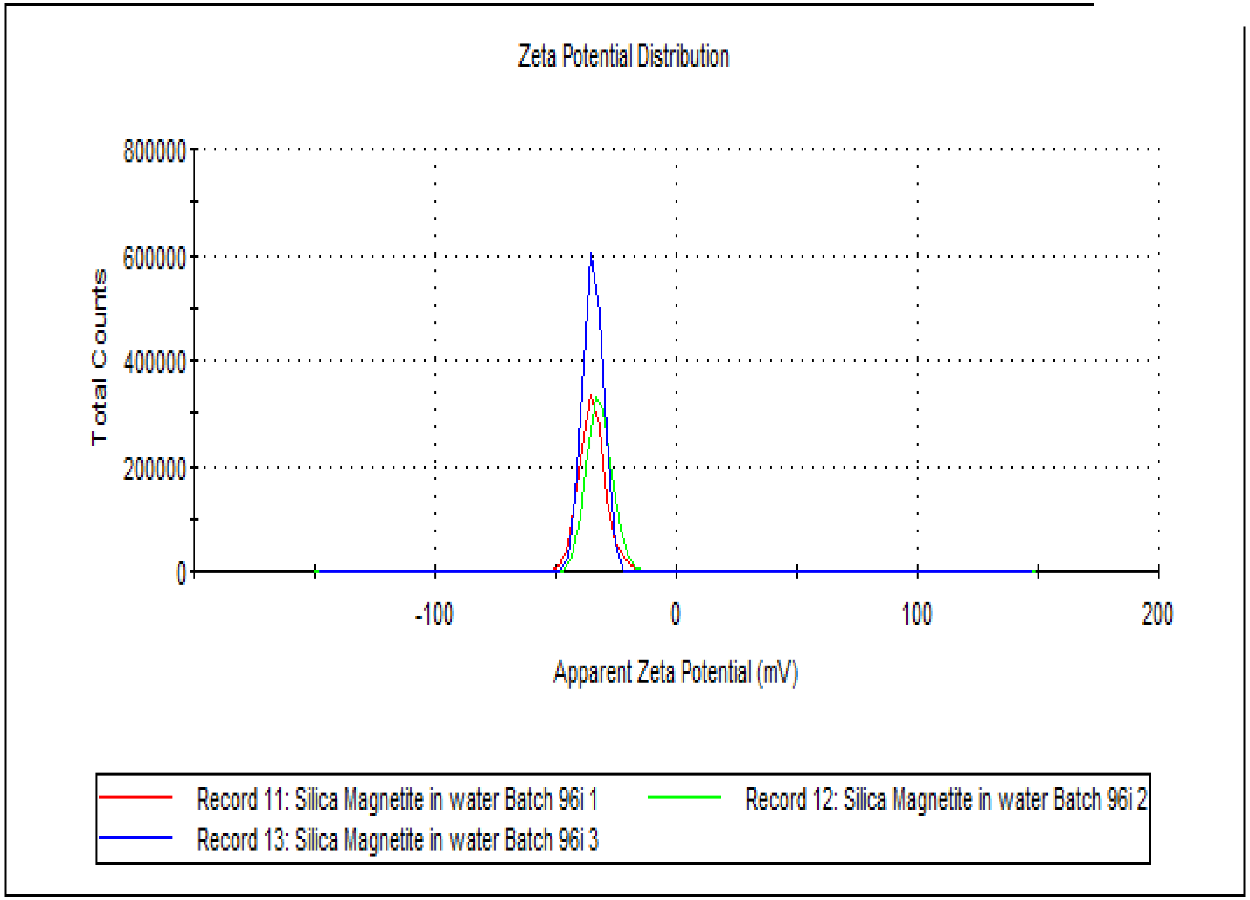

Unanswered questions on mechanism

The above chart is in the absence of any carbonates.

Real legacy pool samples will have interfering ions such as Cs, Sr, Co, etc

pH conditions are varied from highly acidic to highly basic, depending on stage of analysis.

Ongoing Work

- Optimisation of the processes to achieve maximum mono-dispersity
- Thorough characterisation w.r.t to surface energy, magnetisation values & quantification of coating layers.
- Upcoming studies at NNL for uranium adsorption experiments
- To deduce the mechanism of action by performing mixed-metal ion-exchanges
- Understanding gelation mechanism for repair of ageing facilities.

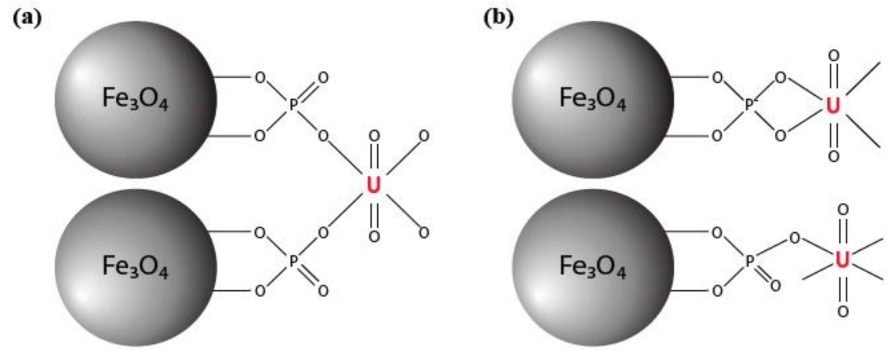

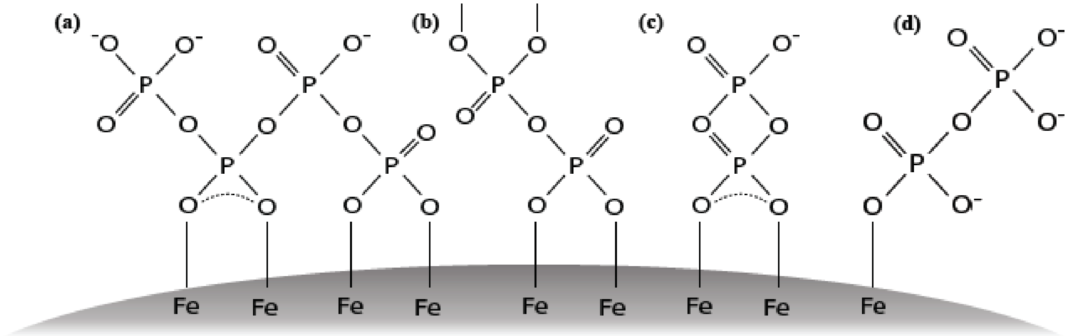

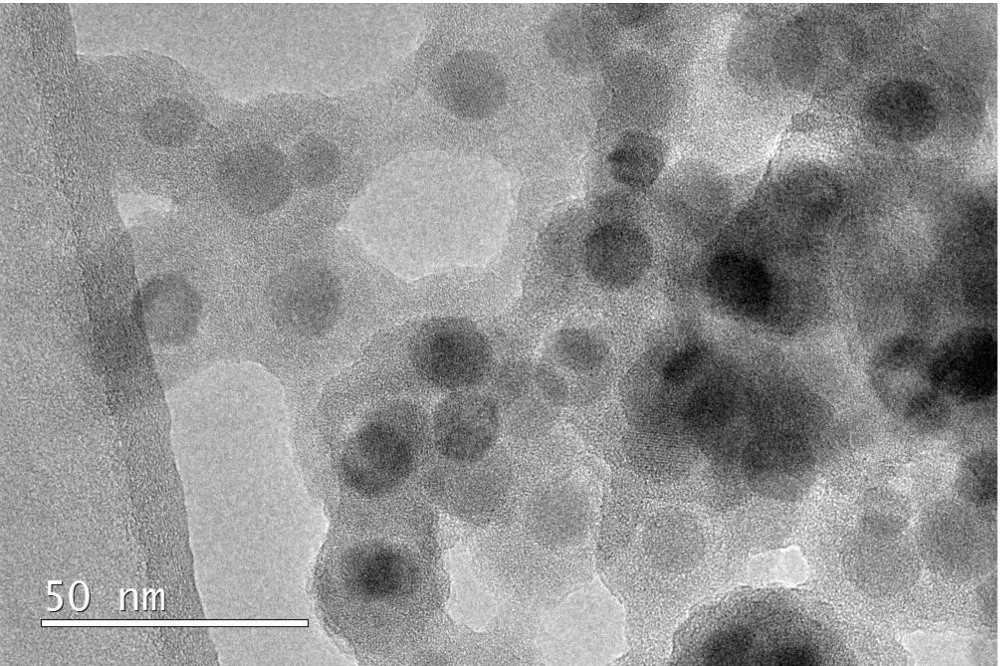

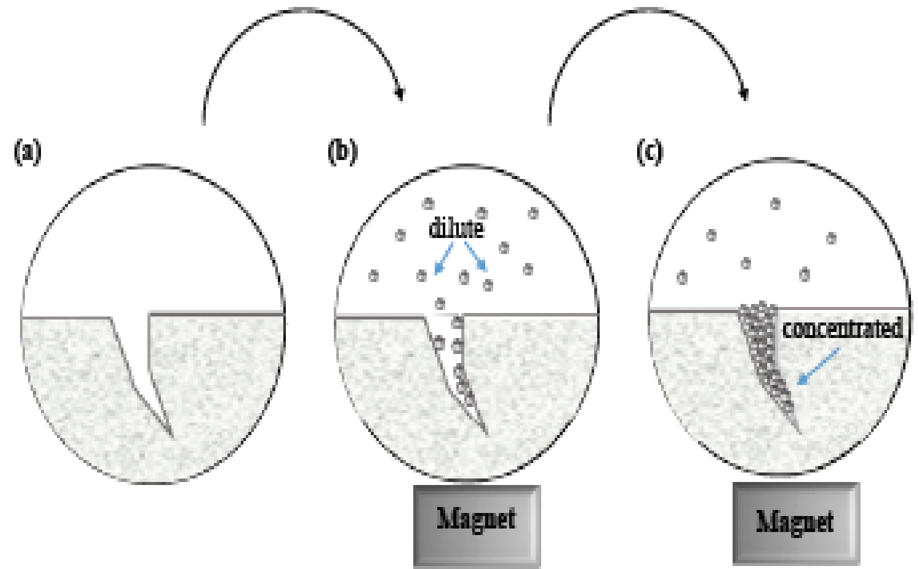

All pictures on this slide – Ref 2

REFERENCES

1. Wenlu Li, John T. Mayo, Denise N. Benoit, Lyndsay D. Troyer, Zuzanna A. Lewicka, Brandon J. La↵erty, Je↵rey G. Catalano, Seung Soo Lee, Vicki L. Colvin, and John D. Fortner. Engineered superparamagnetic iron oxide nanoparticles for ultra-enhanced uranium separation and sensing. J. Mater. Chem. A, 4(39):15022–15029, 2016.

2. Calì, E. & Qi, Jiahui & Preedy, O. & Chen, S. & Boldrin, D. & Branford, Will & Vandeperre, L. & Ryan, M.. (2018). Functionalised magnetic nanoparticles for uranium adsorption with ultra-high capacity and selectivity. Journal of Materials Chemistry A. 6. 10.1039/C7TA09240G.

3. A. Krestou and D. Panias. Uranium (VI) speciation diagrams in the UO2+ 2 /CO2− 3 /H2O system at 25 degC. The European Journal of Mineral Processing and Environmental, 4(2):pp. 113–129, 2004.

Thank you

Email: gsuri@ic.ac.uk

TRANSCEND

Transformative Science and Engineering for Nuclear Decommissioning

Electrokinetic Remediation – Where Next?

Dr. Jamie Purkis

J.M.Purkis@soton.ac.uk

University of Southampton

TRANSCEND Annual Meeting
Harrogate, November 2021

Energy
For a Low Carbon Future

Electrokinetic Remediation, EKR

electro kinetic

Electrical **movement (of ions, …)**

- Soil/groundwater/concrete
- Electromigration (**A**)
  → *movement of ions*
- Electrophoresis (**B**)
  → *movement of particles*
- Electro-osmosis (**C**)
  → *movement of water*

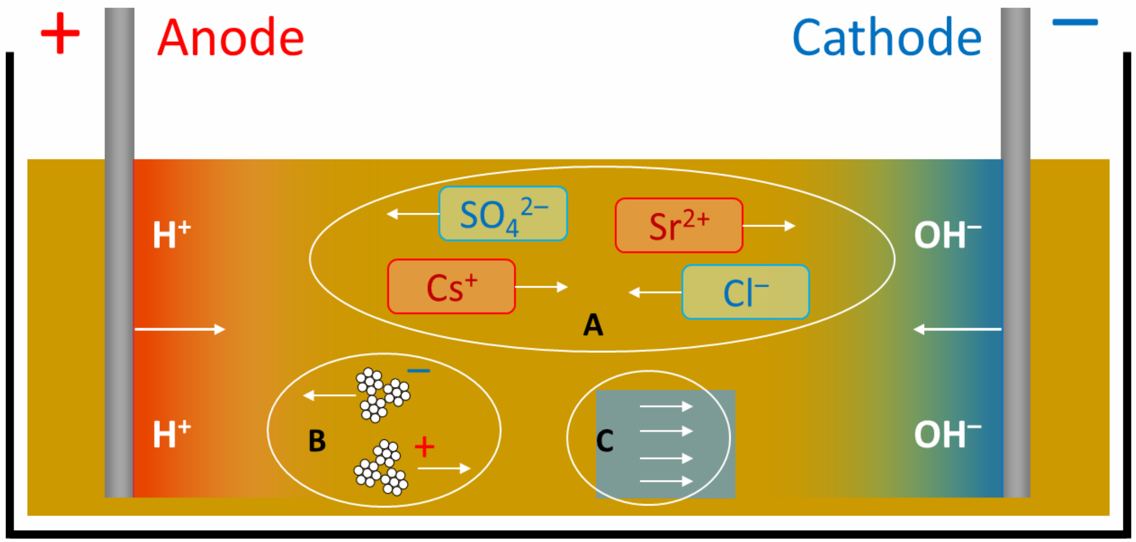

$H_2O \rightarrow 2\,H^+ + \frac{1}{2}\,O_2\,(\uparrow) + 2\,e^-$

$E^0 = -1.229$ V

$H_2O + 2\,e^- \rightarrow 2\,OH^- + H_2\,(\uparrow)$

$E^0 = -0.828$ V

Advantages of EKR

- ***In-situ*** **(or *ex-situ*)**

  Worker safety

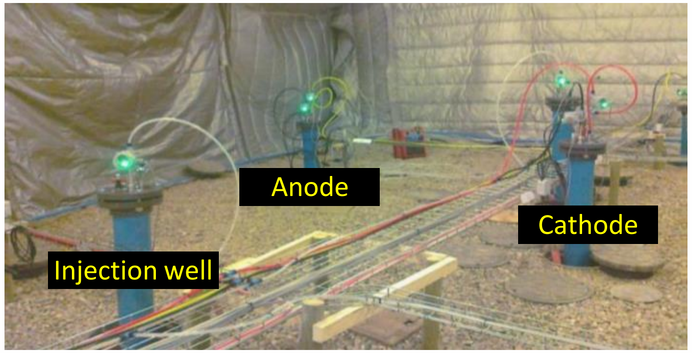

- **Cheap**

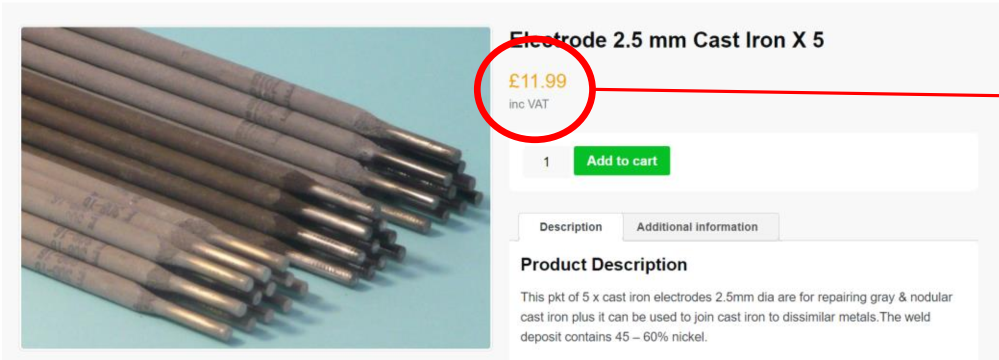

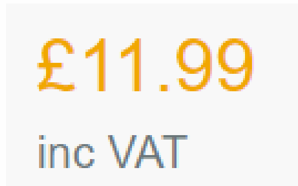

(+ next day delivery!)

- **Adaptable**

Electrode material
Electrode placement
Electrolyte
Voltage

Additives
Duration
(In-)organic + radionuclide
Combination (EKR-Bio…)

EKR for Nuclear Decommissioning

		TRL for nuclear	Duration?	Cost?	Comments	How can EKR help?
EKR		4 - 6	Variable	Low	✓ Flexible ✗ Unproven	--
Bio- and Phyto-	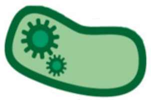 	5 - 7	High	Low	✓ Sustainable ✗ Slow	Faster nutrient movement
ISCO		4 - 6	Low	Variable	✓ Quick ✗ Permeability	***In-situ* barrier generation (FIRS)**
Colloids		5 +	Variable	High	✓ Immobilisation ✗ Unproven	**Colloidal Silica?**

Ferric Iron Remediation and Stabilisation

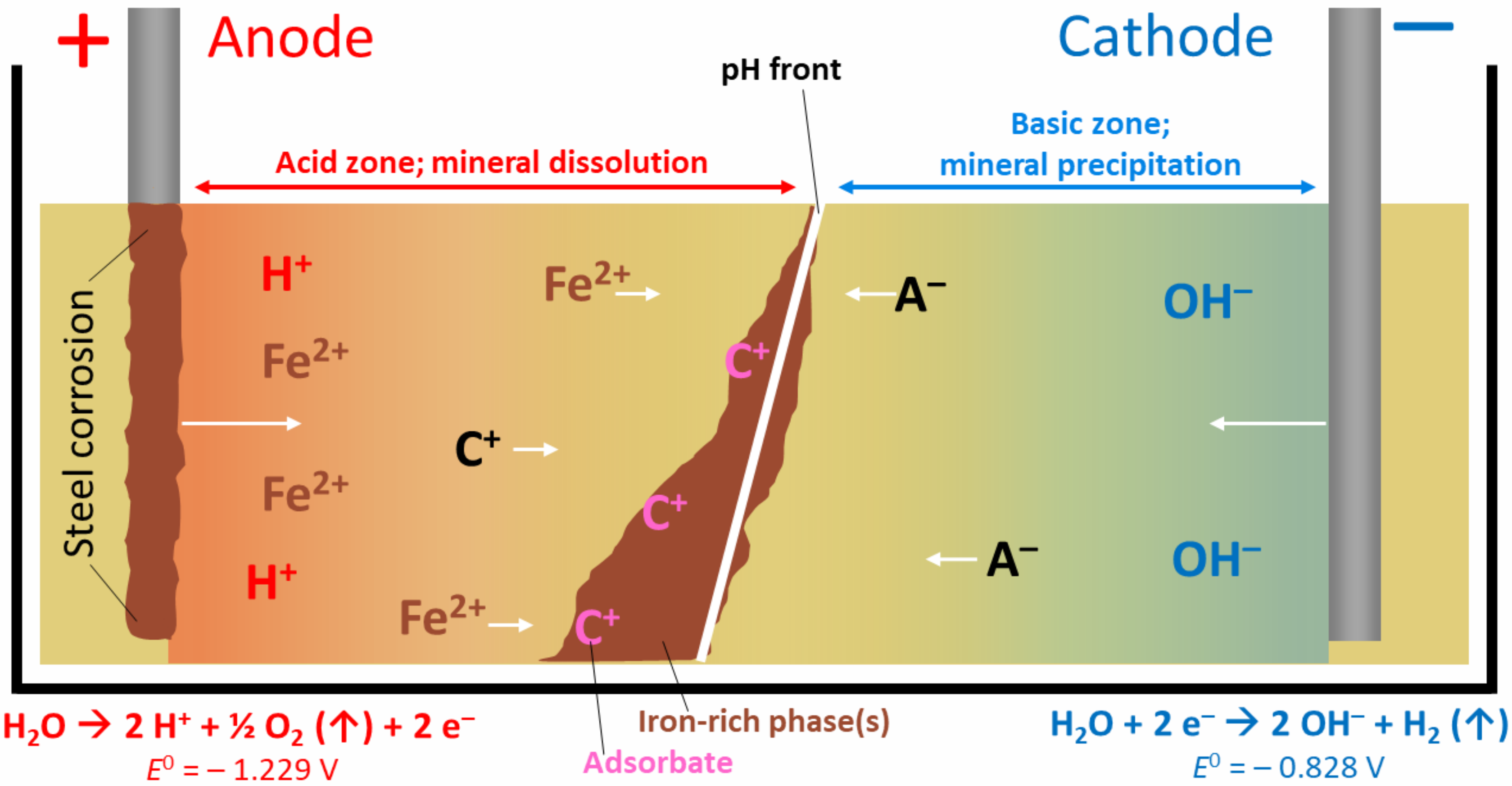

Purkis *et al*., ASCE J. Env. Engin., submitted; Cundy *et* al., Appl. Geochem., 2005, 20, 841

Case Study – FIRS

In-situ barrier growth in real materials?

1. Sellafield Sand/Groundwater (GW)
2. Sellafield Clay/GW
3. Sellafield Sand/Seawater (SW)
4. Sellafield Clay/SW

Steel electrodes, 0.5 V/cm

<u>Monitor</u>

- Barrier over time
- pH
- Changes before/after
- (Sorptive properties)

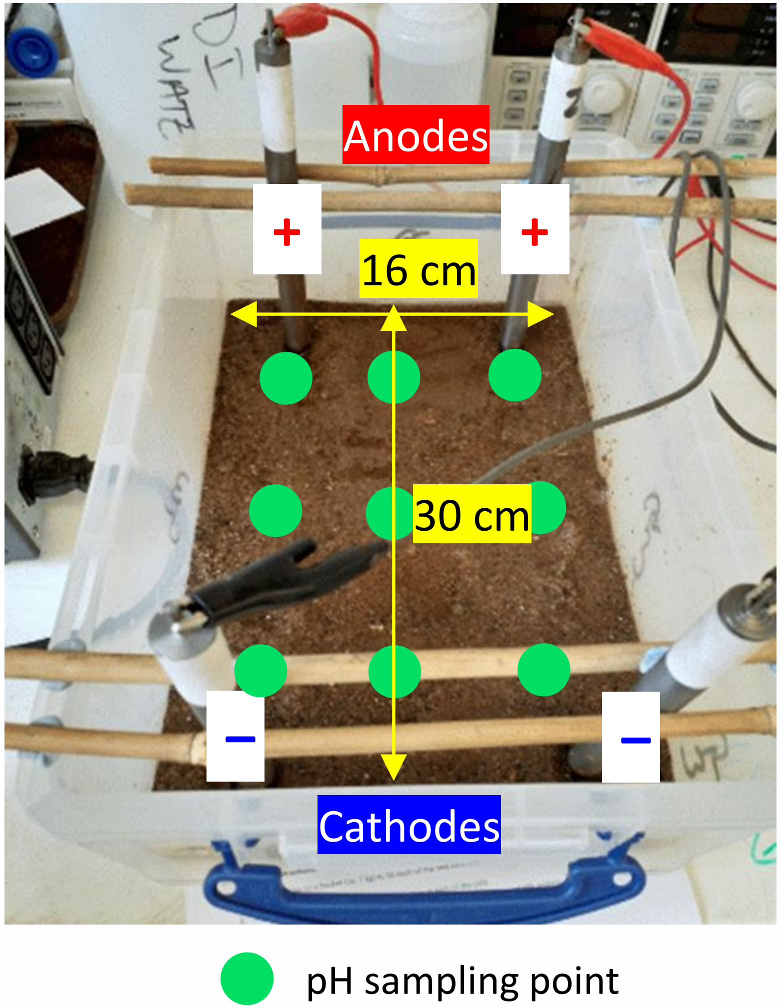

Purkis *et al.*, manuscript in preparation

Case Study – FIRS

- *In-situ* barrier growth in soil subsurface?

- Sellafield sand + simulant groundwater
- Steel electrodes
- Vary:
  - Electrode placement
  - Voltage
  - Duration

- Monitor:
  - Barrier over time
  - pH
  - Sorptive properties, *etc*…

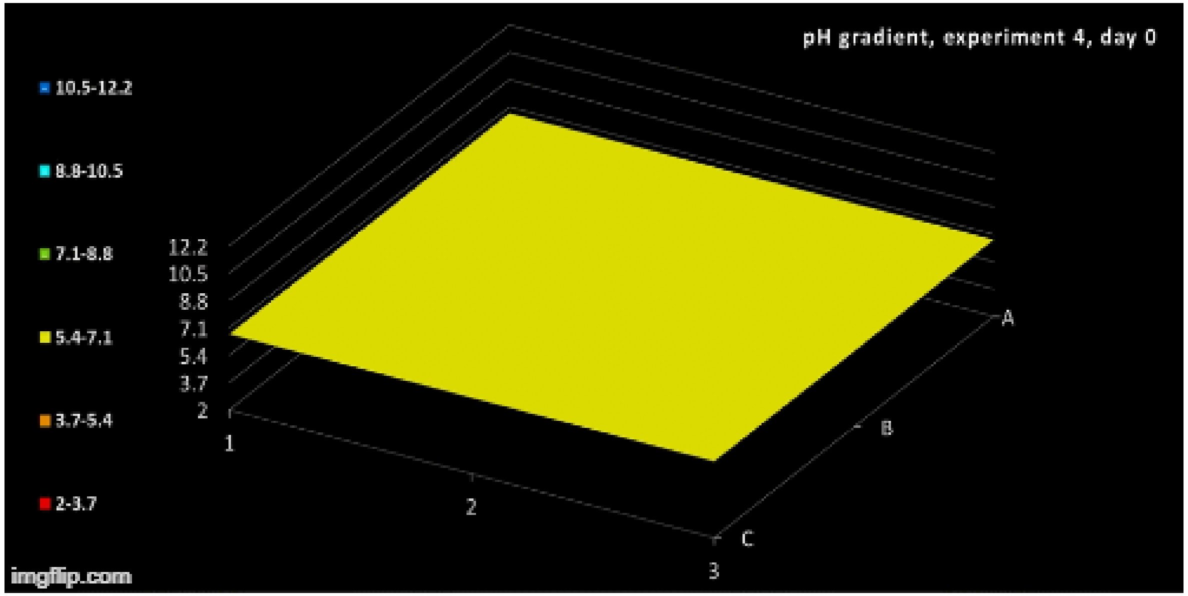

Purkis *et al.*, manuscript in prep.

Case Study – Element Distribution

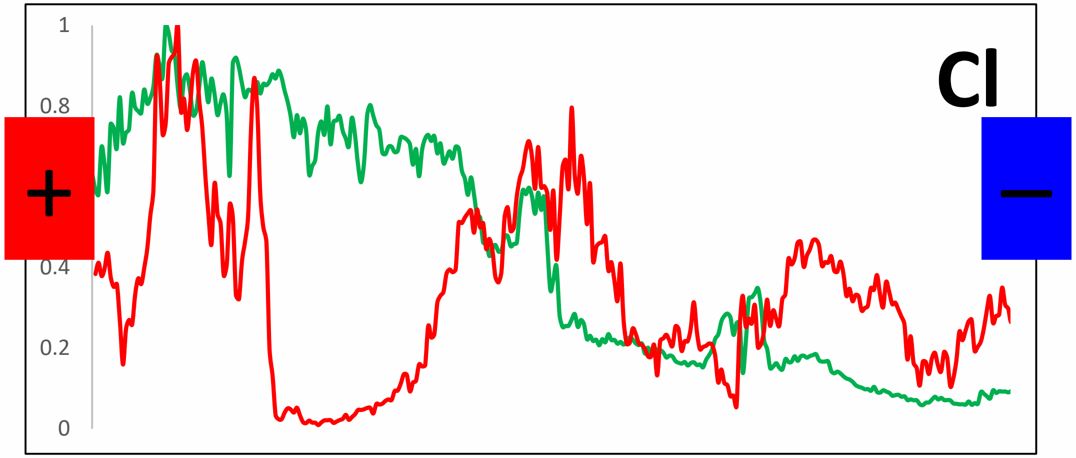

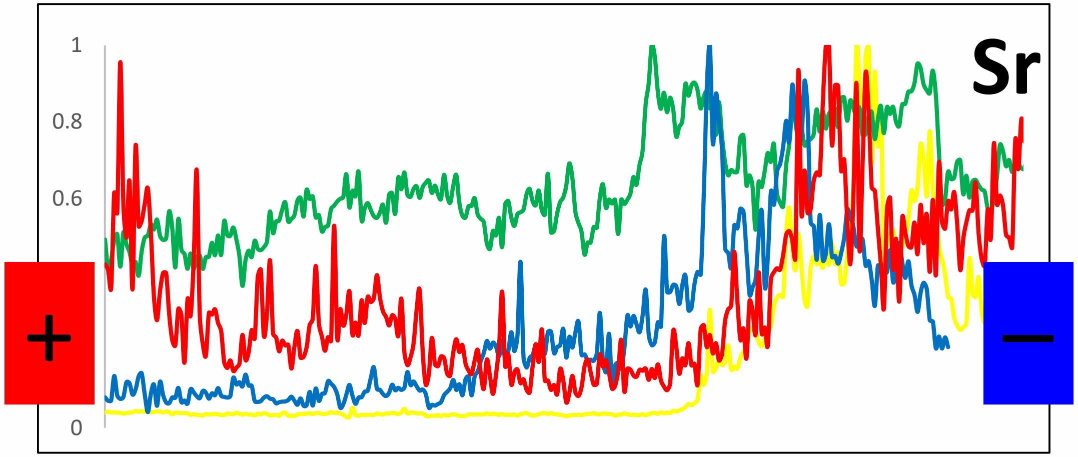

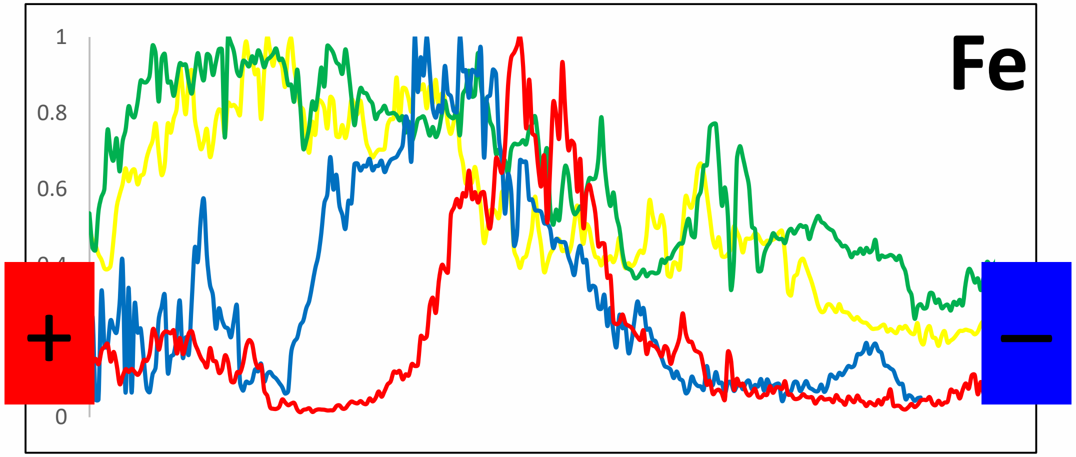

Clay/GW Clay/SW Sand/GW Sand/SW

Upcoming Publications

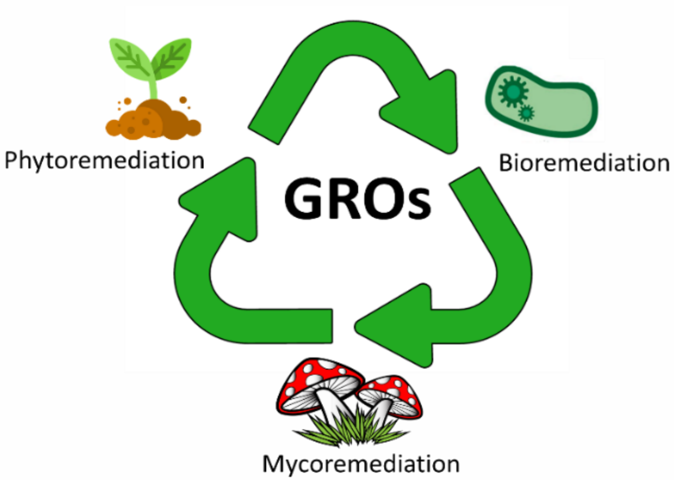

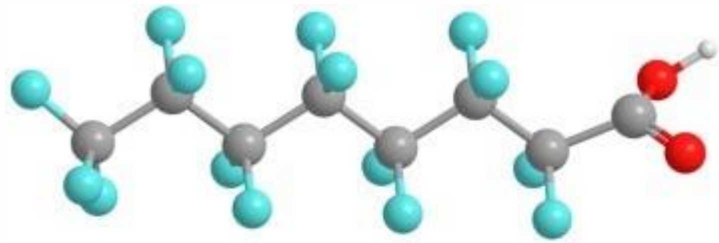

PFOA

“

Research Article | Full Access

Developing Effective Decision Support for the Application of “Gentle” Remediation Options: The GREENLAND Project

Andy Cundy, Paul Bardos, Markus Puschenreiter, Nele Witters, Michel Mench, Valerie Bert, Wolfgang Friesl-Hanl ... See all authors

First published: 10 June 2015 | https://doi.org/10.1002/rem.21435 |
Citations: 16

”

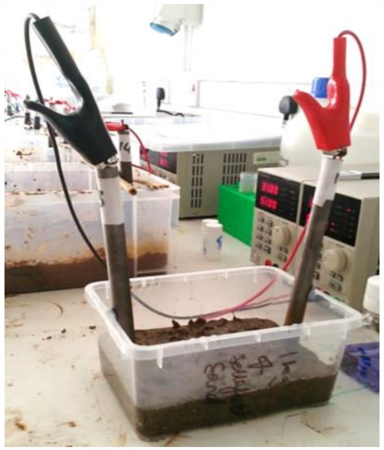

Colloidal Silica Grouting

- (Nano)-Particulate SiO_2

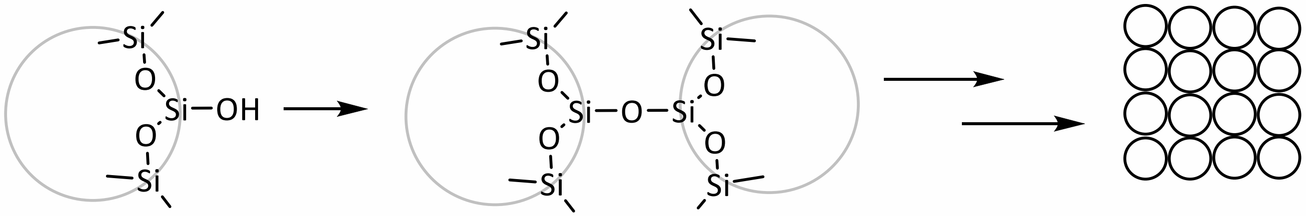

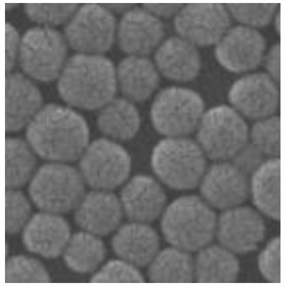

- Gelate with accelerant (NaCl)

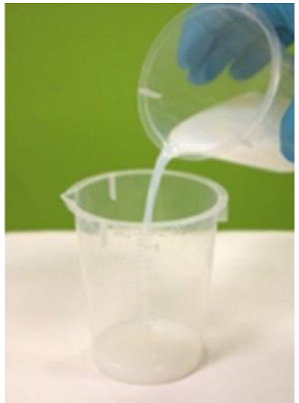

+

=

minutes

...

Dallari *et al.,* Sci. Adv., 2020, 6, eaaz2982; Wong *et al*., Eng. Geol., 2018, 243, 84

Colloidal Silica Grouting + EKR

- Inject into contaminated soil
- Impermeable ($10^{-10} – 10^{-8}$ m.s^{-1})
- Trap radionuclides – combined approach?

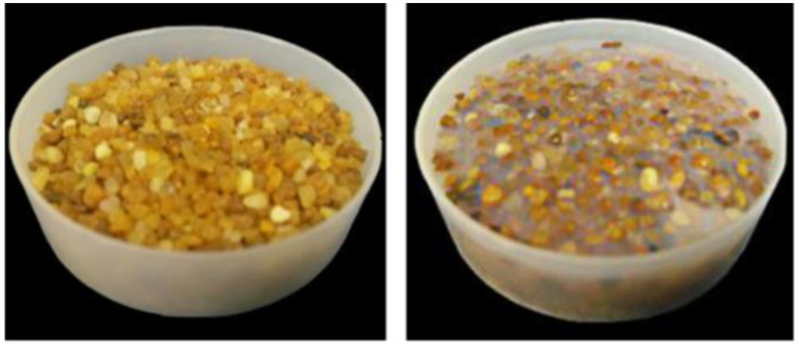

Sand before (L) and after (R) grouting

Pedrotti *et al.*, Eng. Geol., 2020, 270, 105579

TRANSCEND

Transformative Science and Engineering for Nuclear Decommissioning

EKR Decision Support Tools

i / ii

Properties of

Substrate **Contaminant**

Electrical conductivity?
Particle size?
Permeability and porosity?
Cation exchange capacity?
Redox chemistry?
Adsorption?
pH and buffering capacity?
Size and speed of contaminant plume?
Effect of biota?
Groundwater flow?
Hydraulic head?
Temperature?
Additives?
Ionic mobility?

↔

iii

Electrical inputs and electrodes

Voltage?
Current?
Electrode placement?
Electrode separation?
Electrode material?
Corrosion resistance?
Strength of pH gradient generated?
Energy consumption?
Electrolyte?
Dead zones?
Borehole engineering?
Electrode installation?
Depth?
Renewable *vs.* fossil fuel?

↔

iv

Cost and sustainability issues

Duration?
Batch *vs.* continuous?
Labour costs?
Source of materials?
Electricity pricing?
Cost saving by remediating?
Safety?
Electrode value?
In-situ vs. ex-situ?
Use of machinery?
Material disposal costs?
Material and labour transport?
Insurance?
Material storage pending remediation?
Possibility to achieve wider socio-economic and environmental benefits?

J. Haz. Mater., 2021, 413, 125274

Conclusions and Acknowledgements

- EKR: *in-situ*, cheap, flexible
- Limited at scale
- Combined approaches
  - *FIRS: iron barriering*
  - *Electro-grouting: colloidal Si*
- DSTs to avoid "valley of death"?
- Watch this space!






GAU Radioanalytical Laboratories

NATIONAL NUCLEAR LABORATORY

NDA

Case Study – FIRS

1. Barrier over time **2. pH over time** **3. Permeability** **4. SEM** **5. Mössbauer**

Clay with GW electrolyte

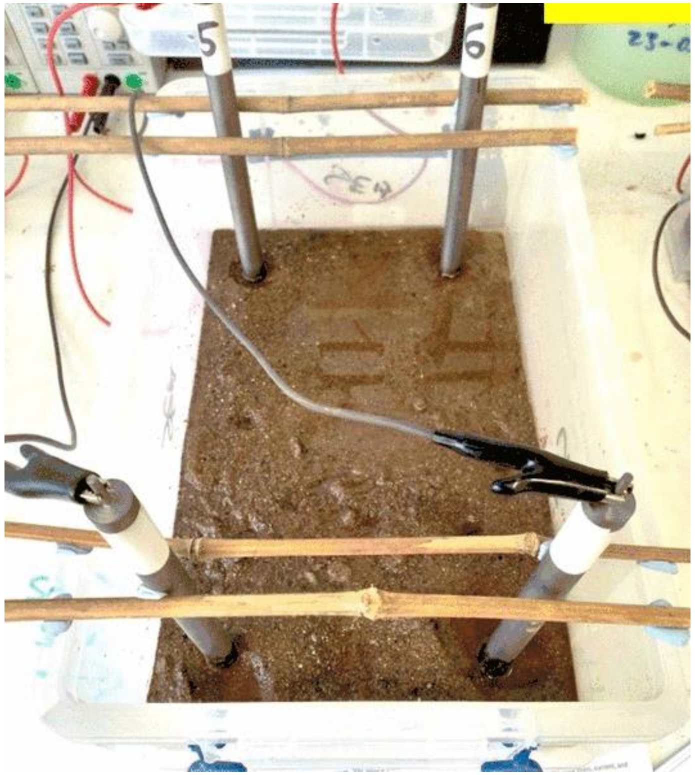

Sand with SW electrolyte
(GIF starts at day 0)

Iron barrier thicker and forms faster in SW electrolyte

Different composition?

Purkis *et al*., manuscript in preparation

Case Study – FIRS

1. Barrier over time   **2. pH over time**   3. Permeability   4. SEM   5. Mössbauer

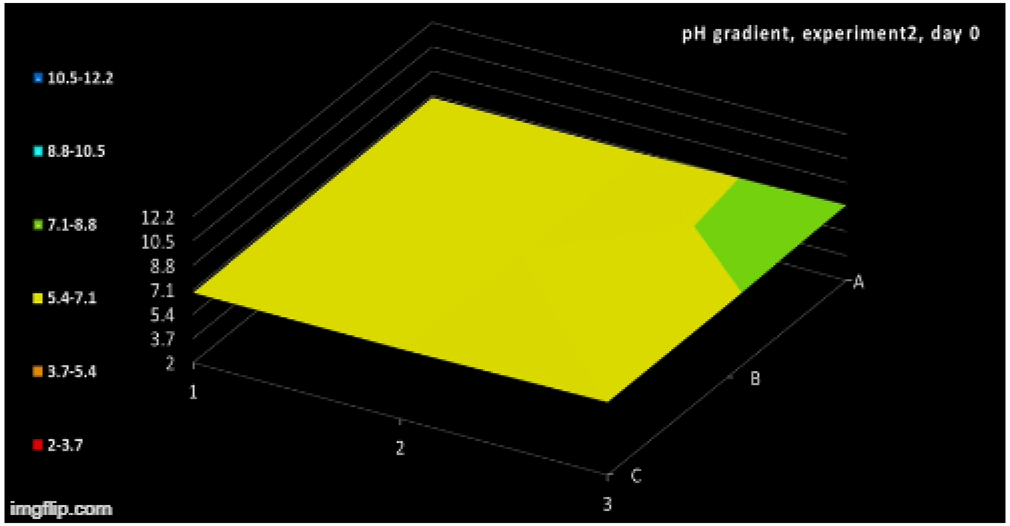

Clay/GW (shown to day 20)

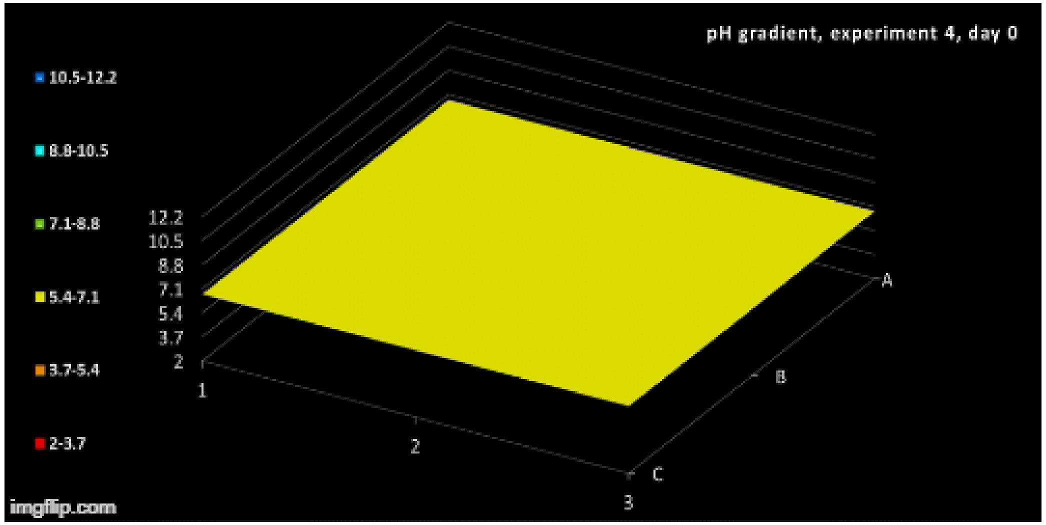

Sand/SW (shown to day 21)

GW has lower ionic strength; weaker pH gradient forms (and forms slower) than SW

Purkis *et al.*, manuscript in preparation

Case Study – FIRS

1. Barrier over time **2. pH over time** **3. Permeability** **4. SEM** **5. Mössbauer**

Sand/SW

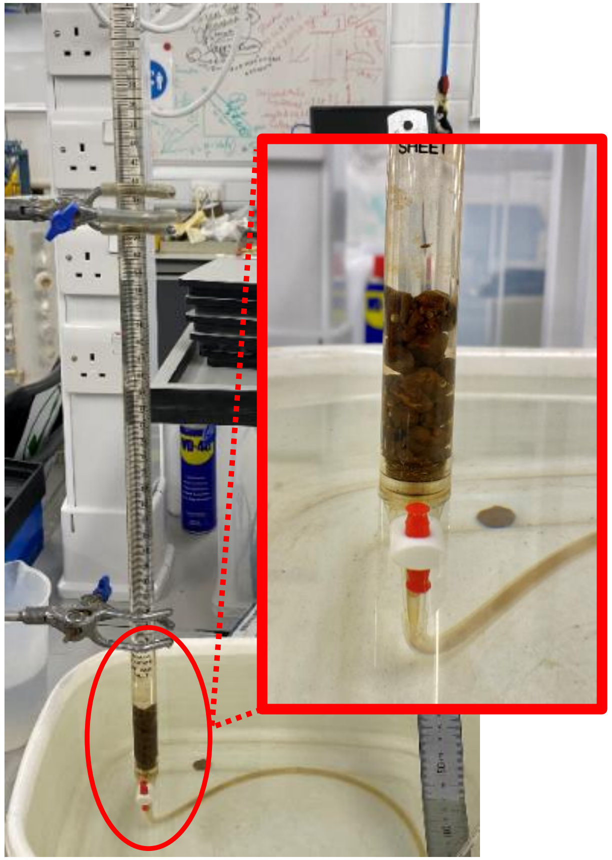

SAND (in m/s)

Parent	*1.1 x 10^{-3}*
GW	2.4 x 10^{-4}
SW	1.6 x 10^{-4}

CLAY (in m/s)

Parent	*1.3 x 10^{-10}*
GW	3.2 x 10^{-8}
SW	4.6 x 10^{-7}

Sand = ↓ permeability
Clay = ↑ permeability

Purkis *et al.*, manuscript in preparation

We acknowledge Prof. William Powrie and Mr. Jeerapat Sang-Iam (UoS) for data collection (BS EN ISO17892)

Case Study – FIRS

1. Barrier over time **2. pH over time** **3. Permeability** **4. SEM** **5. Mössbauer**

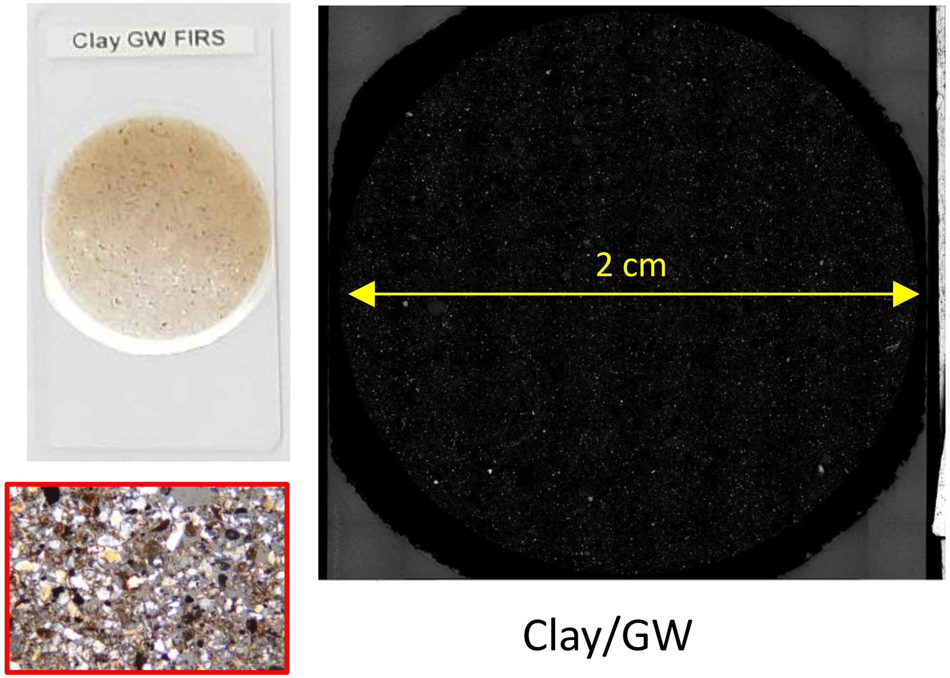

Clay/GW

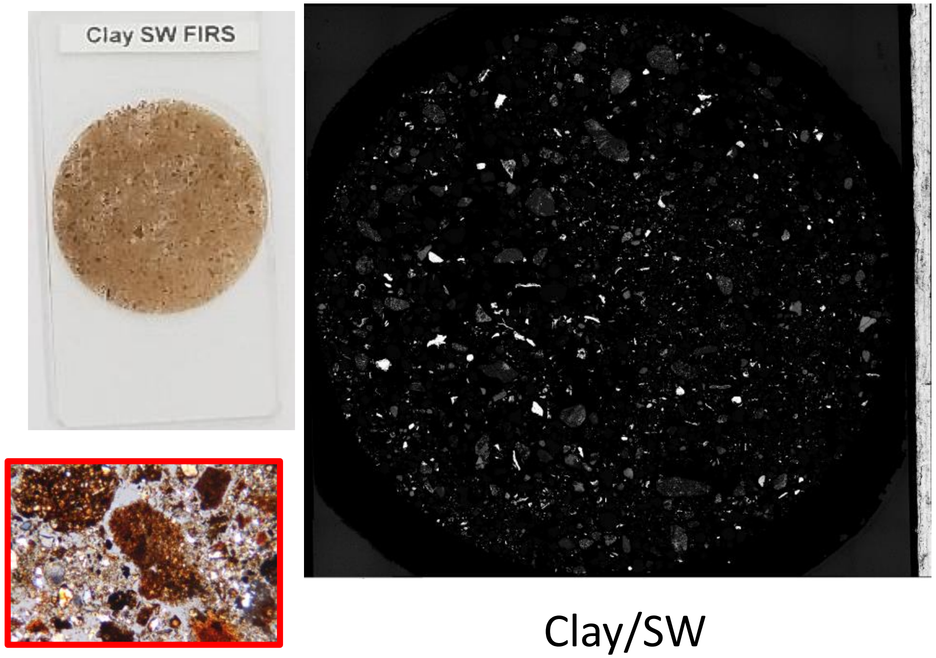

Clay/SW

SEM on thin sections of iron barrier material (+ microscopy)
High contrast (white areas; back-scattering) ∝ high [iron]

Differences in iron phase formation between GW/SW electrolyte

Work ongoing

Purkis *et al.*, manuscript in preparation; thanks to Dr. Richard Pearce (UoS)

Case Study – FIRS

1. Barrier over time **2. pH over time** **3. Permeability** **4. SEM** **5. Mössbauer**

Mössbauer Spectroscopy (ongoing)

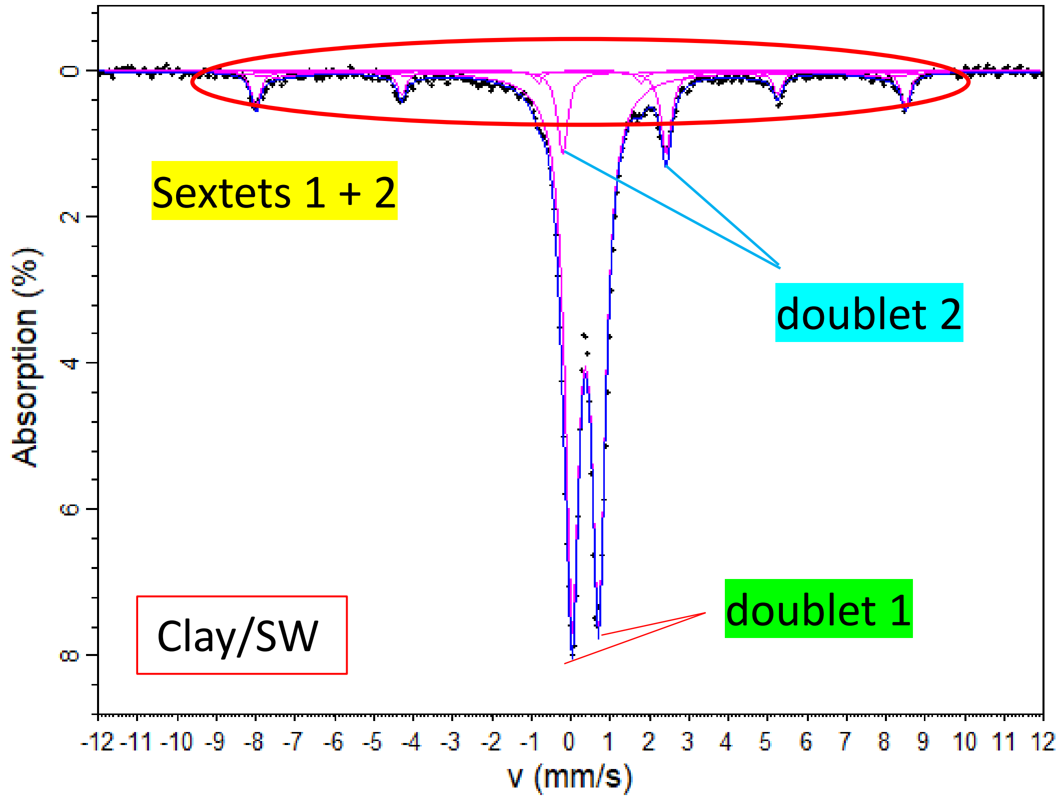

- Doublet 1 – likely Fe(III); oxide; O_h geometry
- Doublet 2 – likely Fe(II); oxide/hydroxide; likely O_h geometry
- Sextets – likely Fe(III); possibly (α-)Fe_2O_3 + ? *haematite*

Likely mix of iron oxides and oxyhydroxides, Fe(II) and Fe(III)

Work ongoing

Purkis *et al.*, manuscript in preparation.

We acknowledge Prof. Paul Bingham and Dr. Alex Scrimshire (Sheffield Hallam) for data collection and interpretation

Transformative Science and Engineering for Nuclear Decommissioning

Drying of Spent AGR Fuel

Thomas Bainbridge
pmtoba@leeds.ac.uk

TRANSCEND Annual Meeting 2021

Introduction

- Reprocessing has ceased and the current strategy is to wet store the fuel pending a permanent disposal option.
- Back up dry storage being considered as well as a prerequisite for disposal [1].
- Drying conducted to reduce the risks posed by radiolysis and corrosion.

AGR Fuel element [2]

[1] NDA Strategy Effective from March 2021, Nucelar Decomissioning Authority.
[2] . "AGR Fuel Element, c 1982. 1982-1575." Retrieved 12/05, 2021, from https://collection.sciencemuseumgroup.org.uk/objects/co5473/agr-fuel-element-c-1982-nuclear-fuel-fuel-rods.

Corrosion

- It is accepted that the corrosion occurring on the cladding is IGSCC.
- Thermal conditions in reactor and radiation induced segregation (RIS) cause sensitisation of the stainless steel.
- Chromium is depleted at grain boundaries leaving them susceptible to attack.

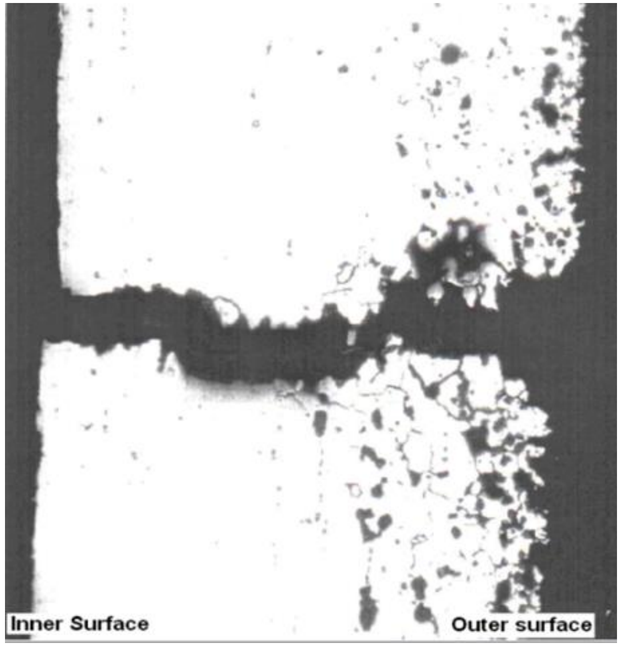

Failed AGR fuel cladding [3]

[3] Kyffin, J. and A. Hillier (2015). Technological Development to Support a Change in the United Kingdom's Strategy for Management of Spent AGR Oxide Fuel. Proceedings of the International Conference on Management of Spent Fuel from Nuclear Power Reactors, IAEA Vienna.

My Project

- To produce a process model to inform the drying.
- Two main areas – computational and experimental.
- Computational – modelling the flow through the cracks.
- Experimental – producing representative cracks to validate the model.

Computational Model

- Various methods considered:
  - Treat sections of the crack as orifices.
  - The narrowest section acting as a restrictor.
  - Model the whole crack.

- Literature narrowed down to models by:
  - Bomelburg [4]
  - Beck et al [5]
  - Taggart & Budden [6]

- Initial validation performed.

[4] Bomelburg, H. J. (1977). Estimation of gas leak rates through very small orifices and channels, Battelle Pacific Northwest Labs.
[5] Beck, S., et al. (2005). "Explicit equations for leak rates through narrow cracks." International journal of pressure vessels and piping **82**(7): 565-570.
[6] Taggart, J. and P. Budden (2008). "Leak before break: Studies in support of new R6 guidance on leak rate evaluation." Journal of pressure vessel technology **130**(1).

Bomelburg Capillary Method

- Developed for leak rate calculations involving PuO_2 containers in accident conditions.
- Most simplistic of the models considered.
- Does not account for pressure losses from friction or turns in the crack.
- Disregards molecular flow.

$$Q = 54.8\, m \frac{d^4}{\mu l}\left(p_u^2 - p_d^2\right)$$

m – molecular weight
d – diameter
μ - absolute viscosity
l – length
p_u – upstream pressure
p_d – downstream pressure

Bomelburg, H. J. (1977). Estimation of gas leak rates through very small orifices and channels, Battelle Pacific Northwest Labs.

Beck et al Method

- Developed for leak-before-break assessments
- For calculating the flow through narrow cracks with high tortuosity
- Considers viscosity, roughness and tortuosity.

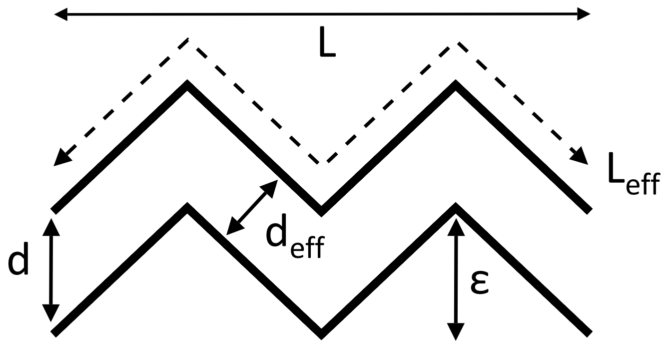

$$Q = ud_{eff}$$

$$0 = \frac{\rho u^2}{2}\left[N\left(1 - \left(\frac{d_{eff}}{d}\right)^2\right)\right] + \frac{2u}{\rho}\left[\frac{12\mu l_{eff}}{d_{eff}^2}\right] - \Delta P$$

Q – flow rate through crack
u – mean flow velocity
d_{eff} – adjusted hydraulic diameter / adjusted mean crack width
d – hydraulic diameter / mean crack width
ρ – density
N – number of grain faces along crack
L_{eff} – adjusted length of arc of flow around crack tip
P – pressure
ε – perpendicular grain height

Beck, S., et al. (2005). "Explicit equations for leak rates through narrow cracks." International journal of pressure vessels and piping **82**(7): 565-570.

Taggart & Budden Method

- Another leak-before-break model.
- Considers pressure losses due to both local and global roughness.
- Also accounts for frictional, inertial and recirculation pressure losses.

$$\boldsymbol{Q = C_D (P\rho)^{1/2} W_c L}$$

Q – flow rate
C_D – discharge coefficient
P – pressure
ρ – density
W_c – mean width
L - length

Taggart, J. and P. Budden (2008). "Leak before break: Studies in support of new R6 guidance on leak rate evaluation." Journal of pressure vessel technology **130**(1).

Results - Air

- Pinhole diameter of 227µm
- Initially modelled for the just air flowing through the pinhole.
- No one method best across the whole test period.
- Decided to try averaging the 3 approaches.
- Average method may not be the best at a single point but overall was the best approach.

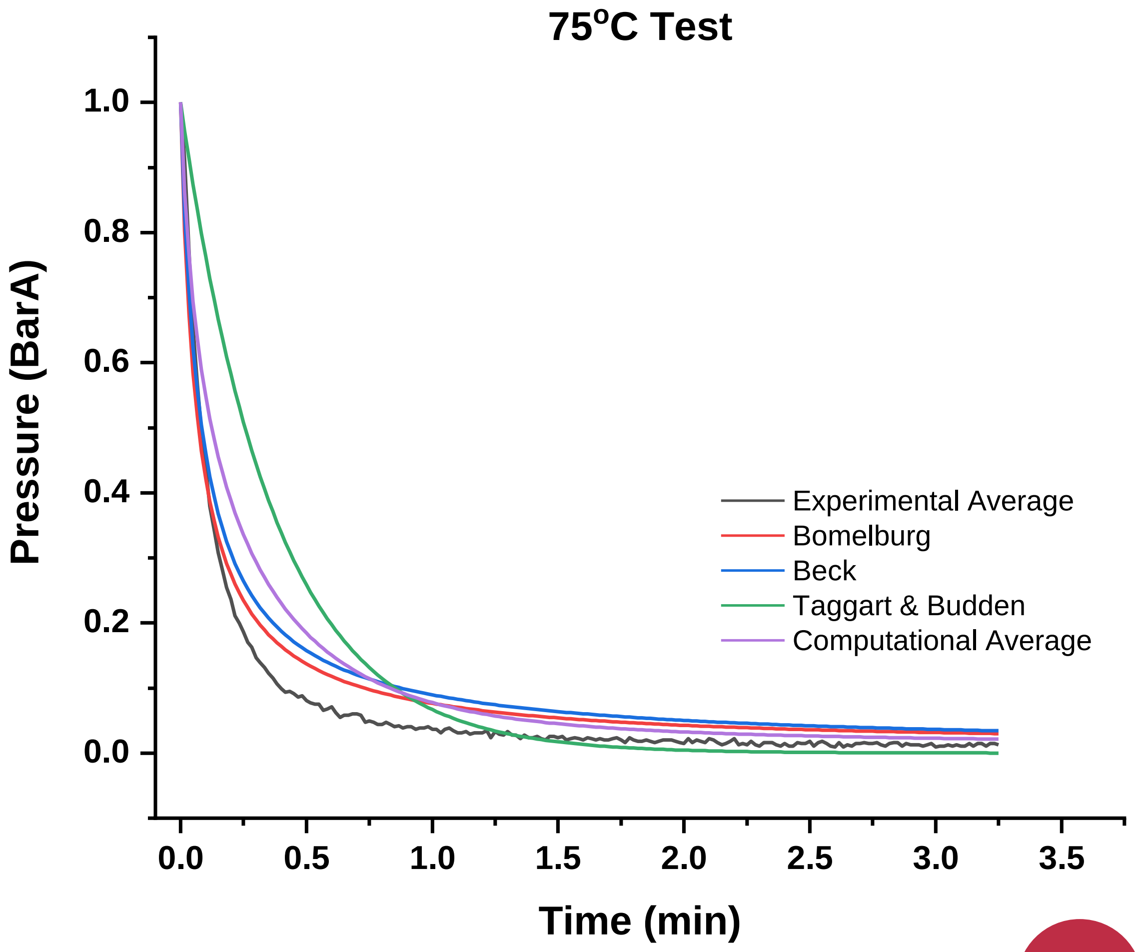

Results – Water Vapour

- Assuming single phase flow through the crack.
- Plot the experimental results against the results from each of the methods used to model the flow.
- Now the method by *Beck et al* is the most suitable.
- Residuals and standard deviations for the methods have been calculated.

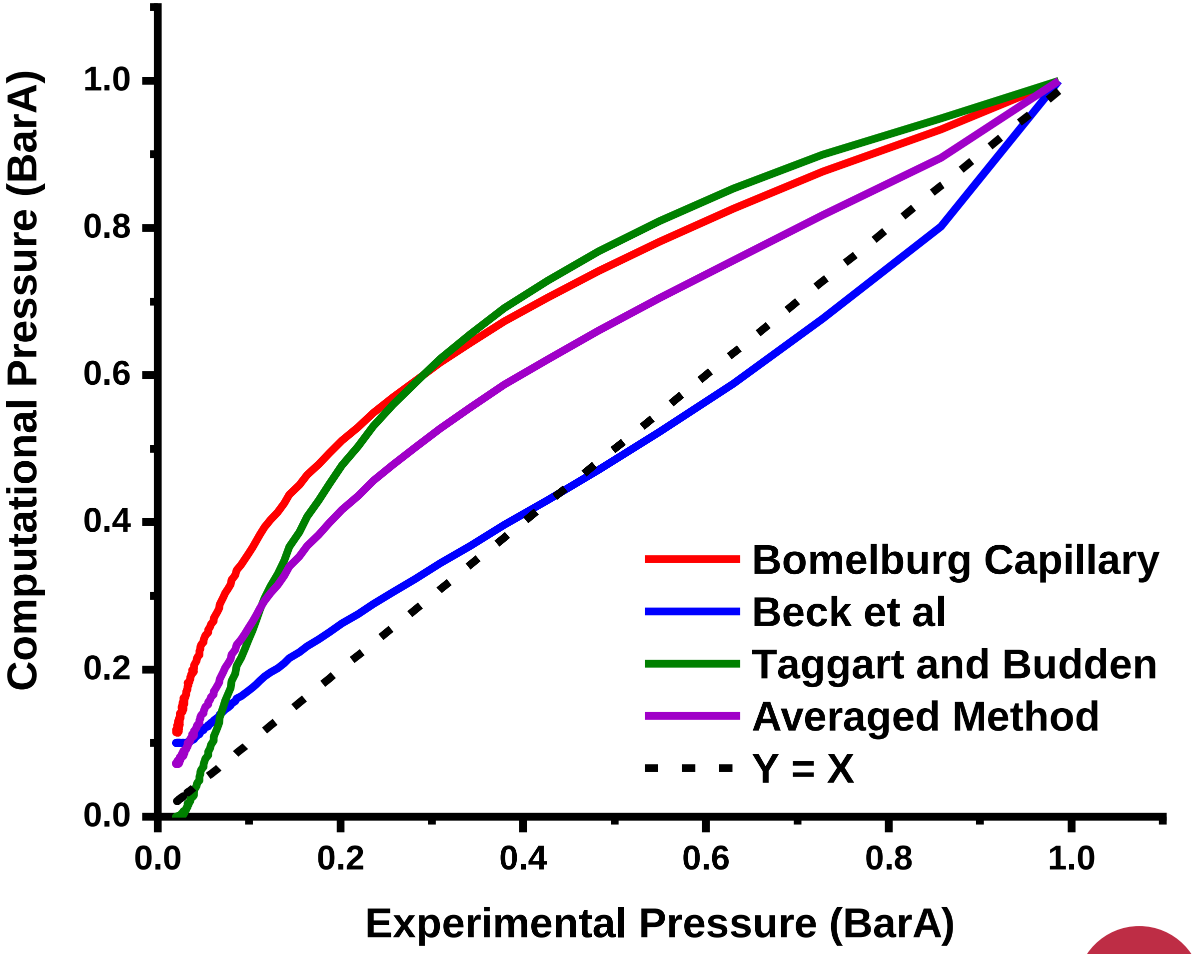

Residuals – Water Vapour

Method	33°C		69°C		75°C		98°C	
	Average Residual	Standard Deviation	Average Residual	Standard Deviation	Average Residual	Standard Deviation	Average Residual	Standard Deviation
Bomelburg	0.090	0.077	0.080	**0.051**	0.056	0.072	0.061	0.081
Beck et al	**0.010**	**0.014**	0.045	0.062	**0.013**	**0.017**	**0.014**	**0.020**
Taggart & Budden	0.051	0.079	0.044	0.060	0.059	0.075	0.066	0.097
Average Method	0.038	0.053	**0.038**	**0.051**	0.036	0.052	0.047	0.065

Image Analysis

- The models require parameters such as the width and the length.
- MATLAB used to perform image analysis.
- Image first needs to be “tidied” up first.
- Image skeletonised then path length and average width calculated.

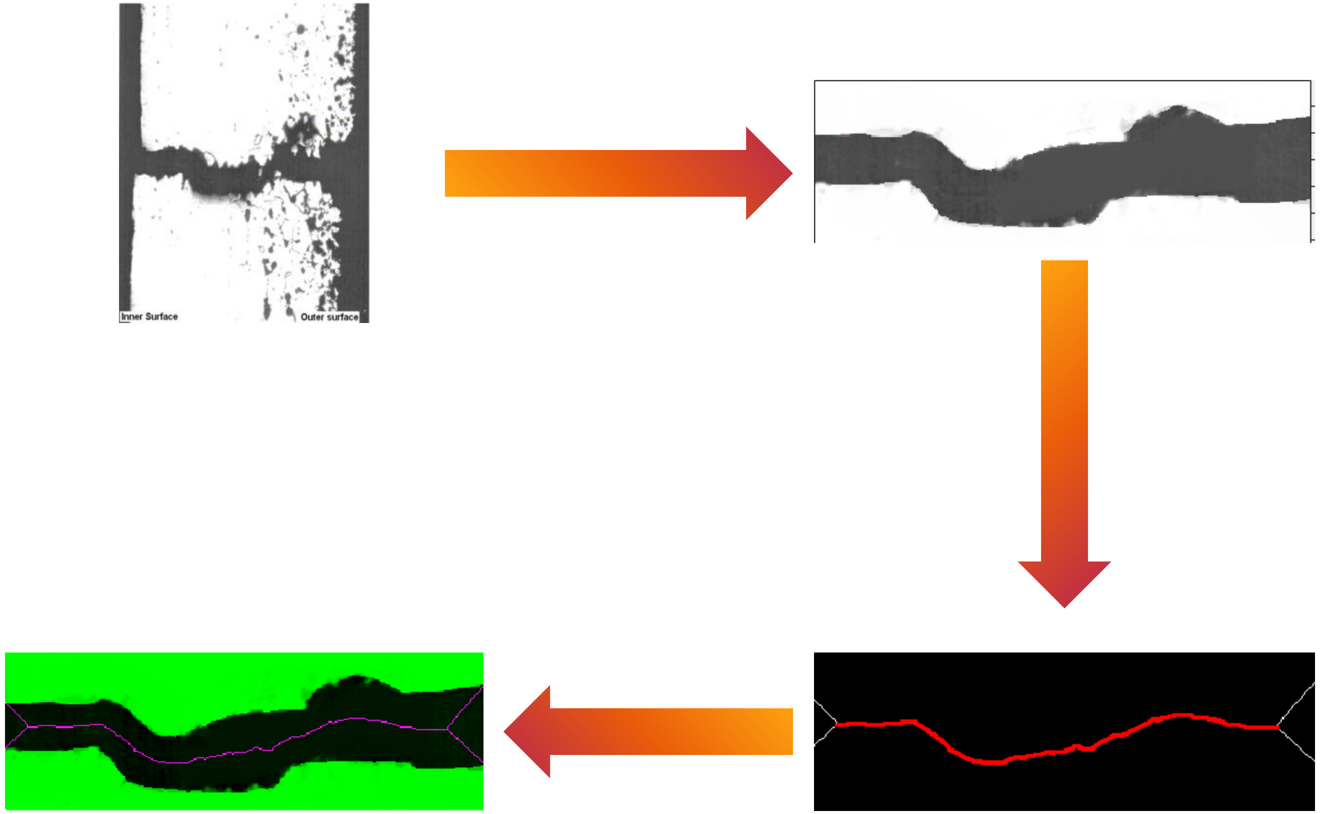

Image Analysis - Validation

Sample	Measured		Calculated		% Variation	
	Length	Width	Length	Width	Length	Width
	29.88	8.03	29.89	8.43	0.04	4.98
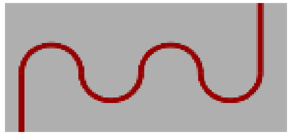	58.10	0.63	60.68	0.62	4.45	1.45
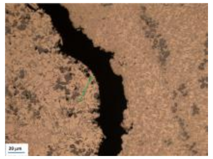	257.50	61.15	222.93	58.37	13.43	4.54
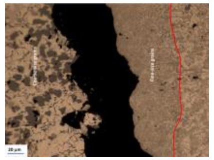	215	25.88	220.82	29.02	2.71	12.15

Haghshenas, M. and J. Jamali (2017). "Assessment of circumferential cracks in hypereutectic Al-Si clutch housings." Case studies in engineering failure analysis **8**: 11-20.

Future Work – Cracking Stainless Steel

- Plan to use drop evaporation.
- Sample will be stressed and heated.
- Chloride solution will be dripped onto the sample with each drop allowed to evaporate before the next drop.
- This concentrates the chloride and produce representative cracks.

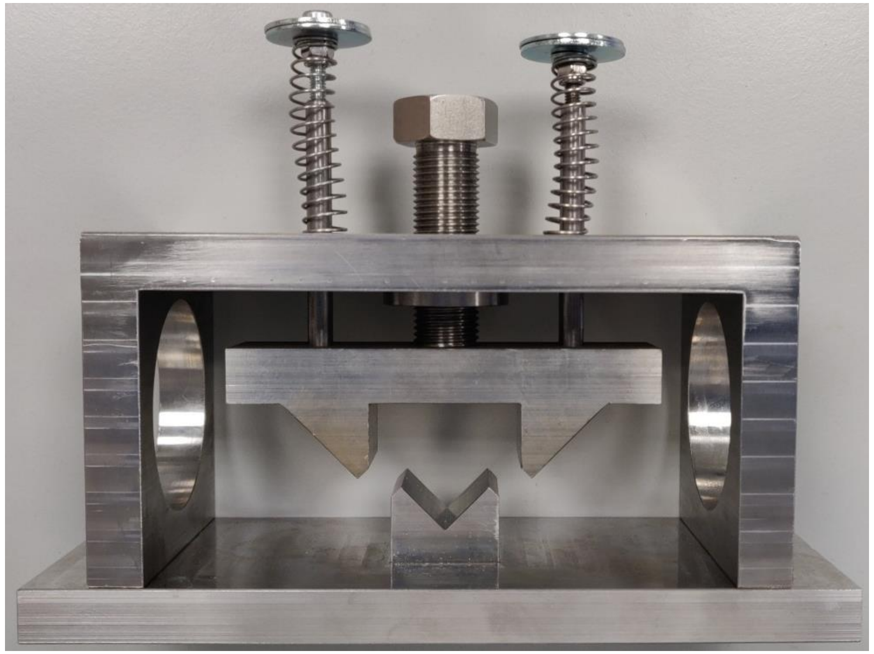

Drop evaporation rig

Future Work – Fluid Flow

- Pinholes of known diameter being used.
- Capped section of stainless steel pipe.
- Flow rate measured in the drying rig.
- Second rig to measure more precisely measure the flow being built.
- Both rigs will eventually allow for the representative cracks to be used

Drying rig test piece

Acknowledgments

- Academic Supervisor: Prof. Bruce Hanson

- Industrial Supervisor: Dr Carlos de la Fontaine

Thank you

TRANSCEND

Transformative Science and Engineering for Nuclear Decommissioning

Computational Studies of Helium Incorporation in PuO_2

Elanor Murray

University of Birmingham

NATIONAL NUCLEAR LABORATORY

NDA

TRANSCEND

Transformative Science and Engineering for Nuclear Decommissioning

Atomistic Simulation of Helium Incorporation in PuO_2

How much helium can the lattice accommodate?

What are the likely trapping sites?

Is helium diffusion vacancy assisted?

How does helium aggregate?

What is the mechanism for bubble formation?

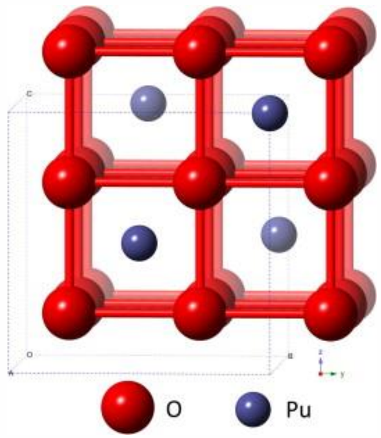

Atomistic Simulation of Helium Incorporation in PuO_2

Migration pathways

He diffusion

He cluster analysis

TRANSCEND

Transformative Science and Engineering for Nuclear Decommissioning

Bulk PuO_2

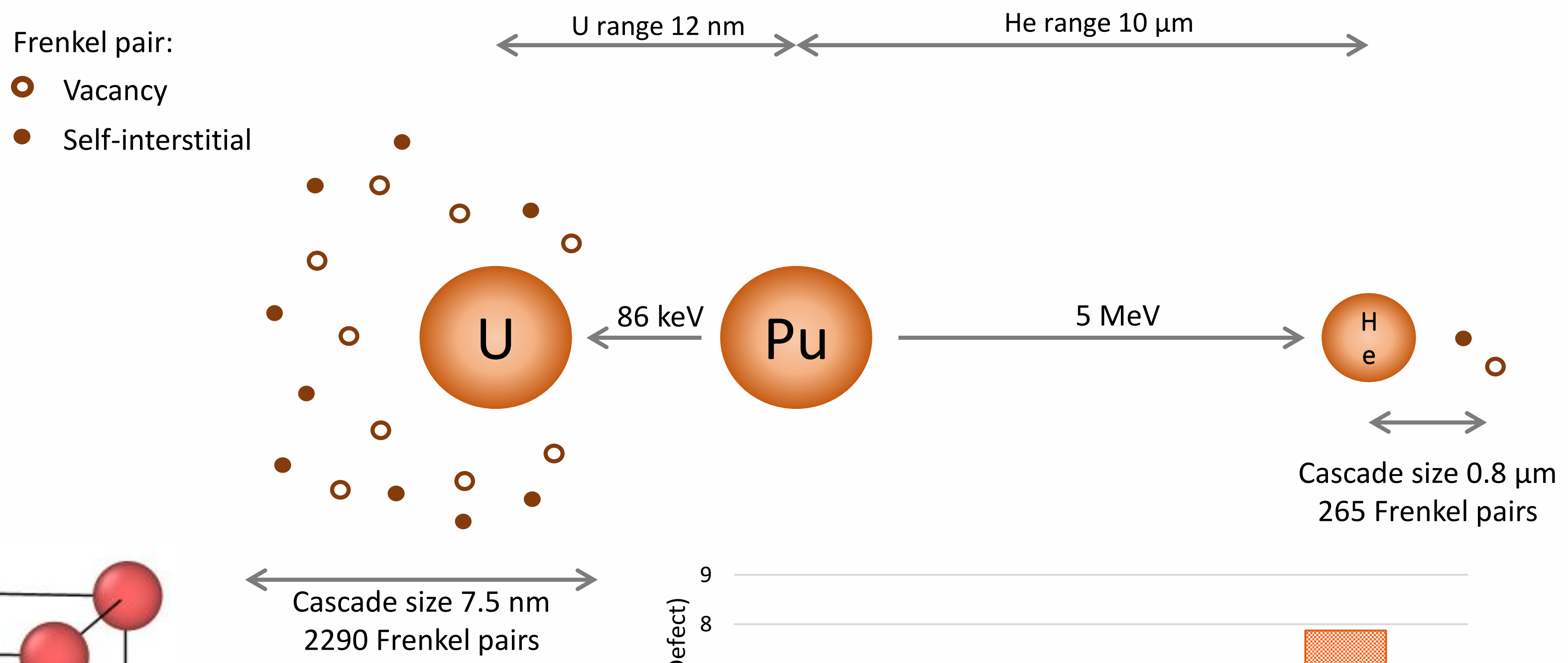

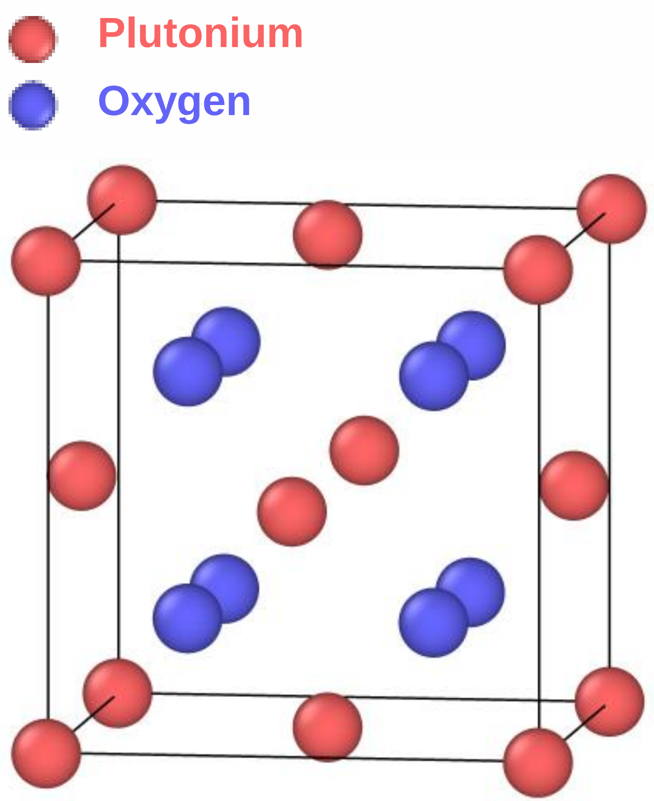

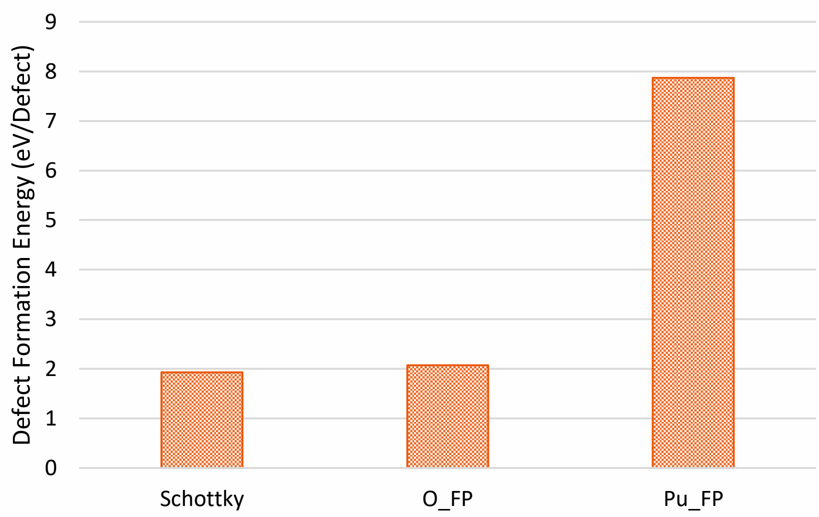

Found Schottky and Oxygen Frenkel Pairs to be most energetically favourable defects

Interstitial Sites

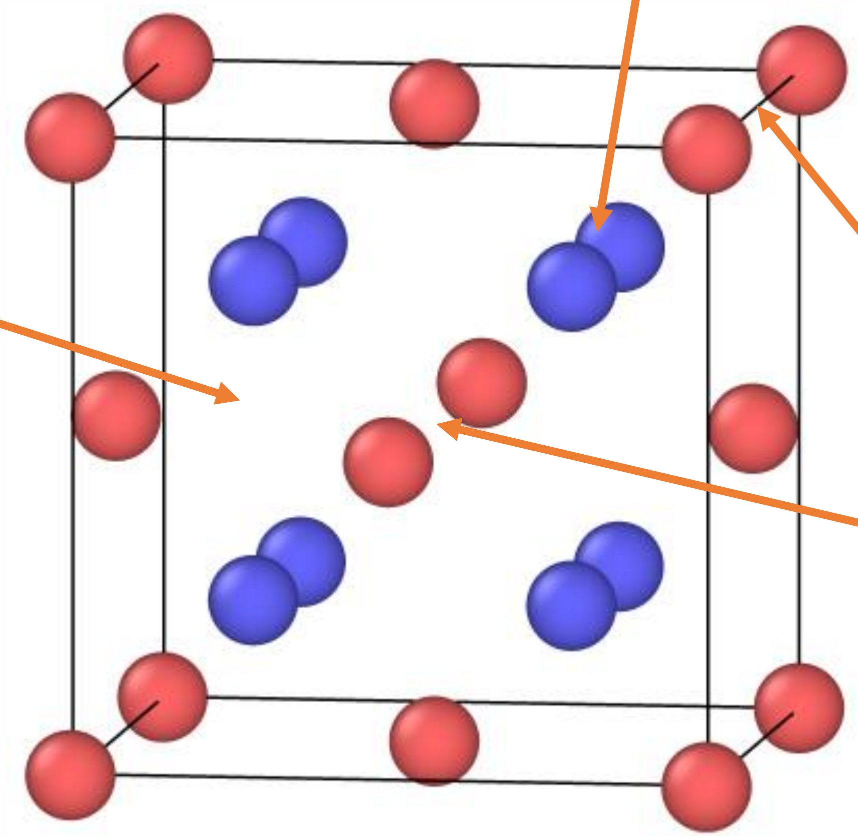

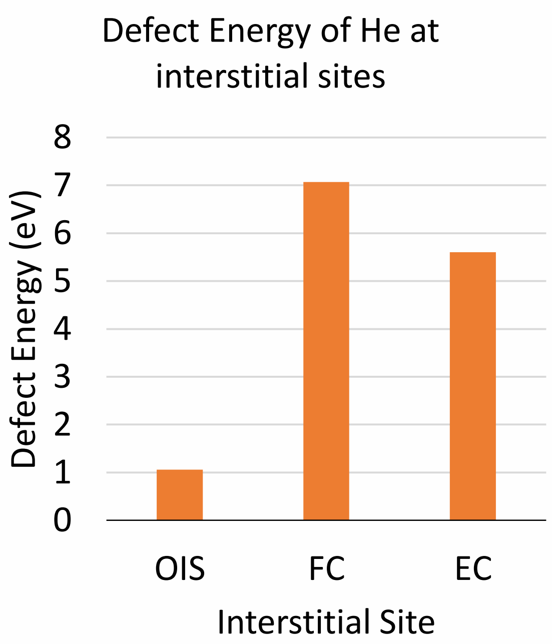

TRANSCEND

Migration pathways

Migration pathways

OIS → OIS

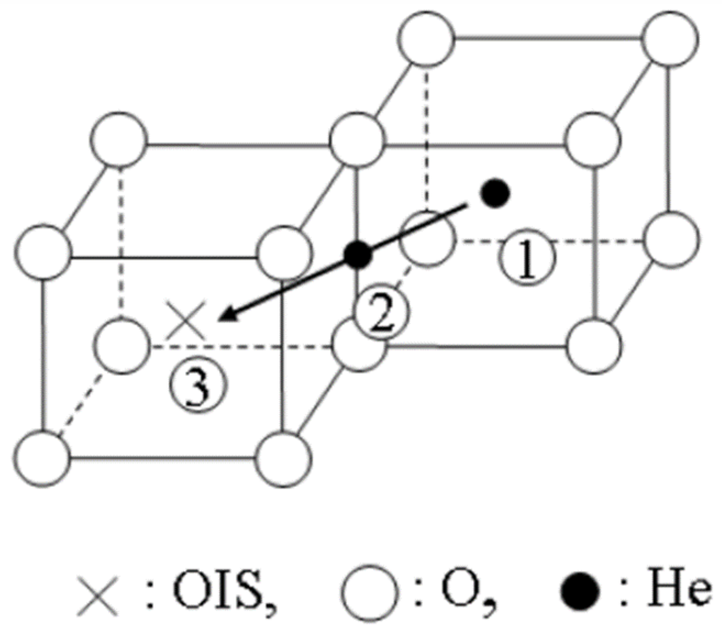

When at edge centre position

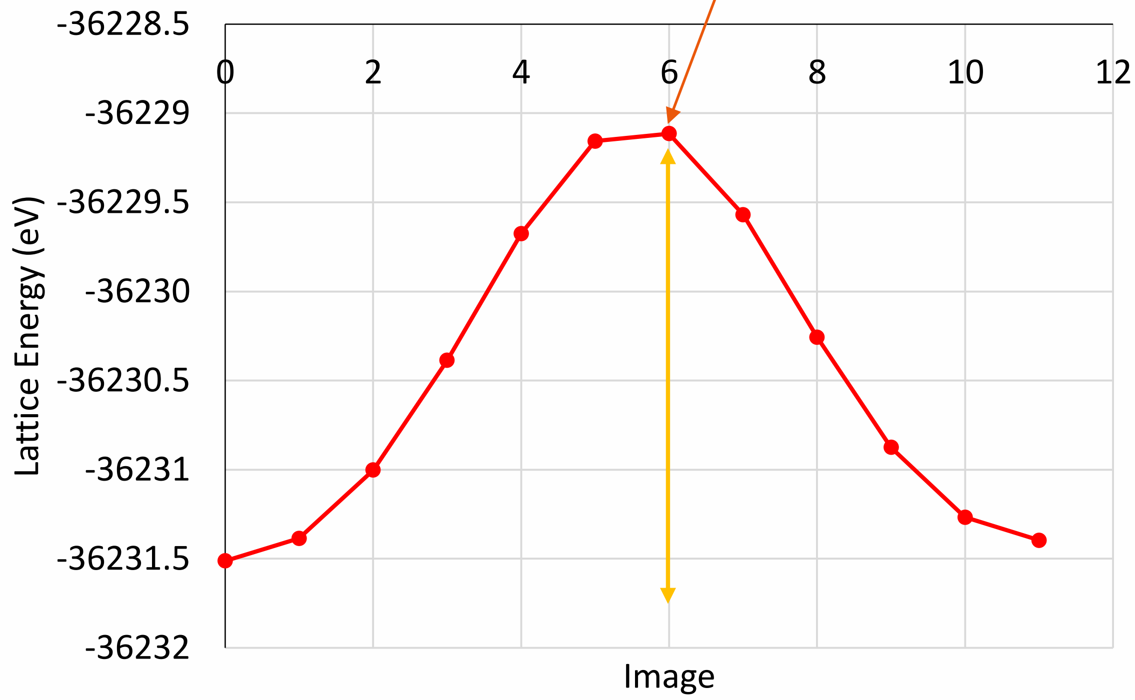

Migration barrier: 2.4 eV

Transformative Science and Engineering for Nuclear Decommissioning

Migration pathways

OIS → OIS

Plutonium

Oxygen

Via O vacancy

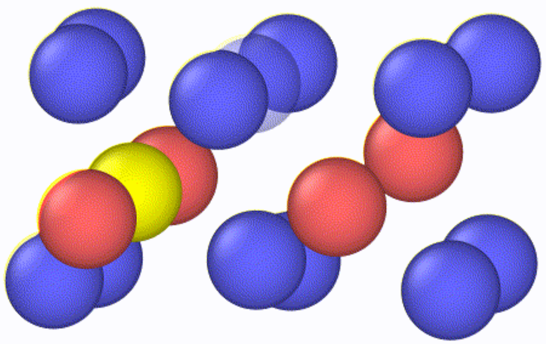

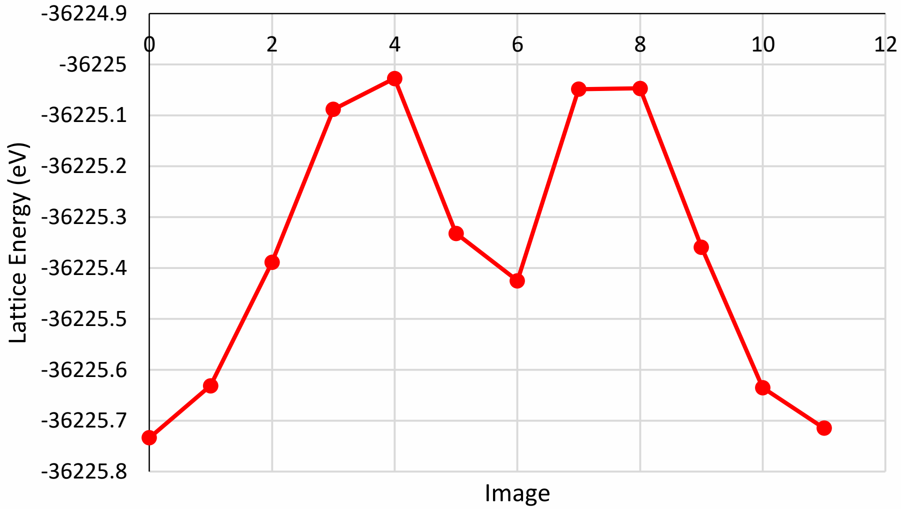

Via Pu vacancy

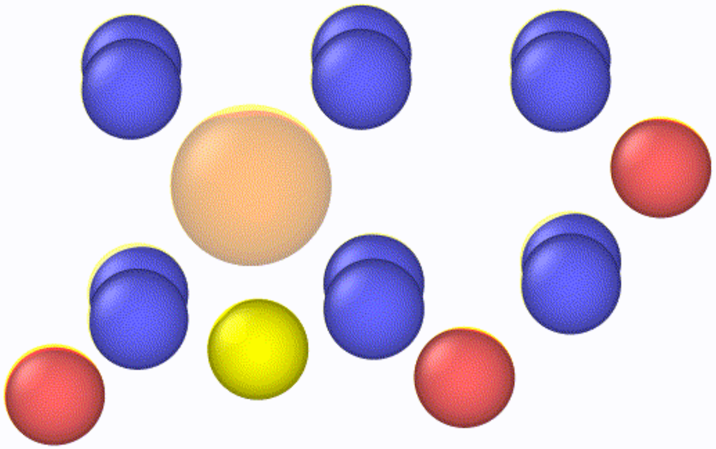

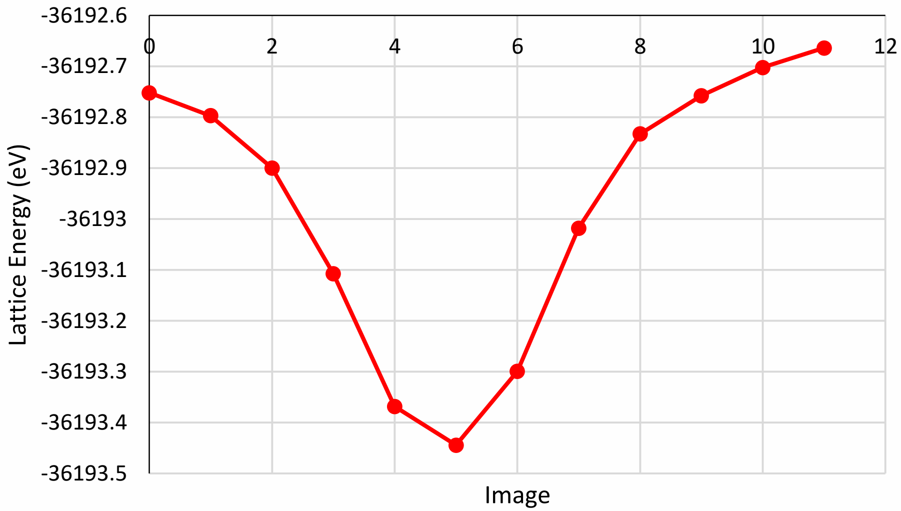

Migration pathways

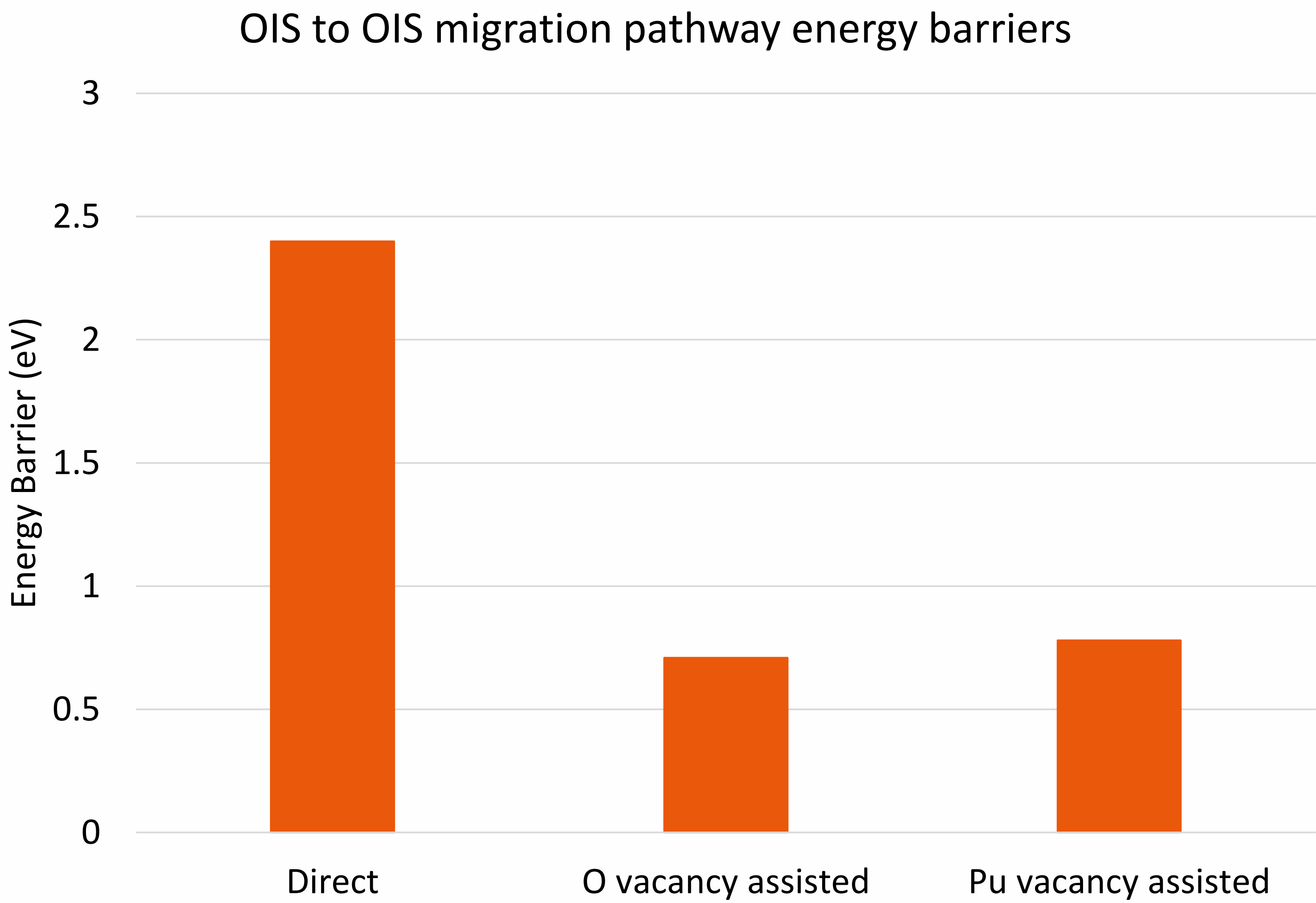

Migration pathways

He in OIS, 500K, 1ns

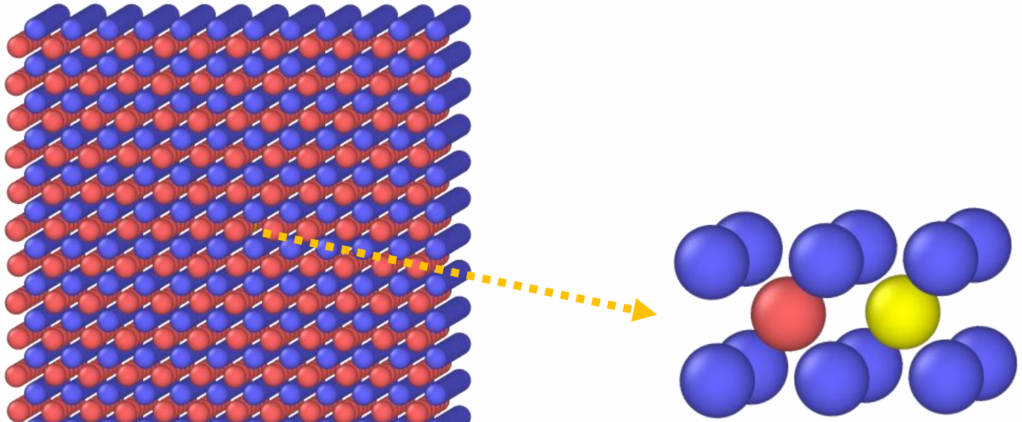

Defect	Trajectory
Pure	
Oxygen Vacancy	
Plutonium Vacancy	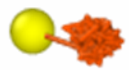

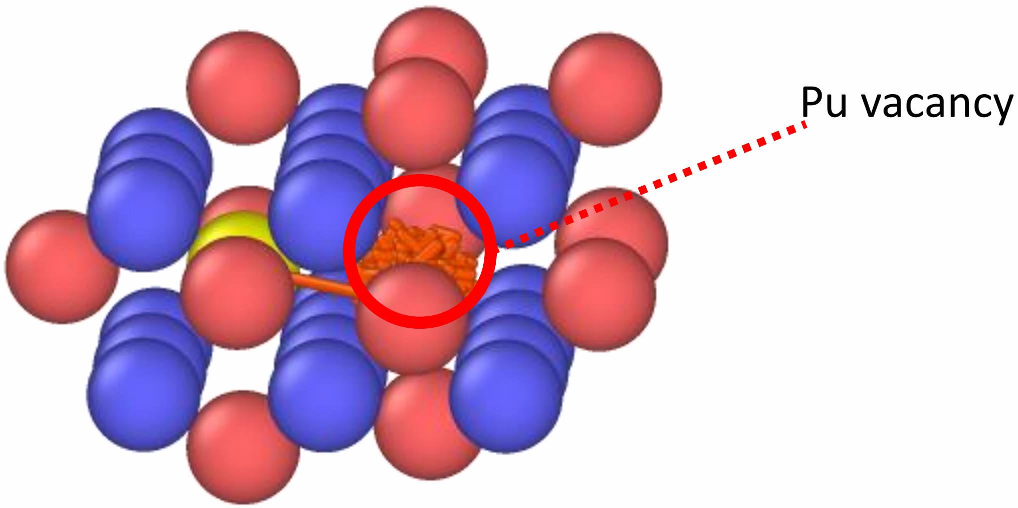

He diffusion

TRANSCEND

Transformative Science and Engineering for Nuclear Decommissioning

He diffusion

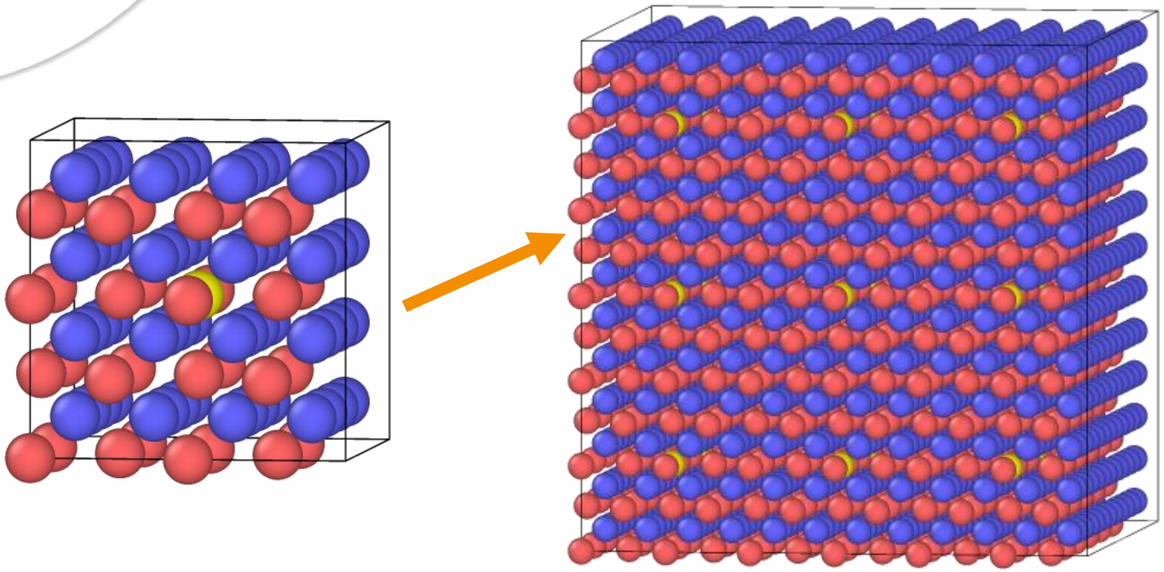

27 He atoms, 0.04%

2000K, 1 He trajectory

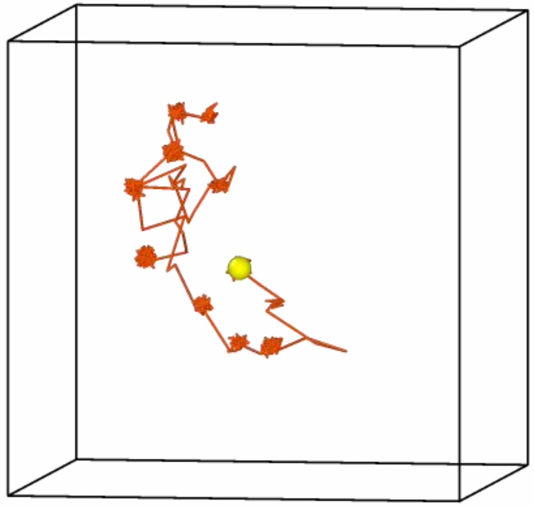

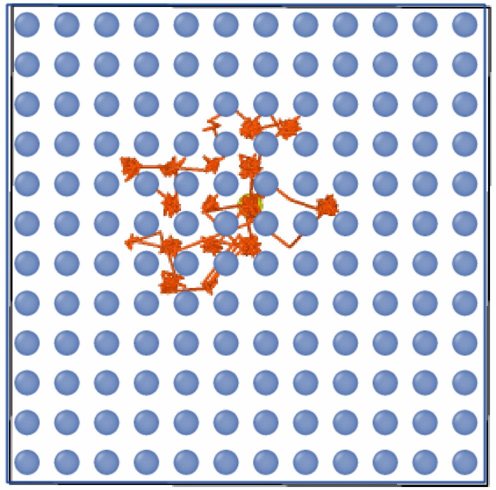

He moving OIS position

750K

1250K

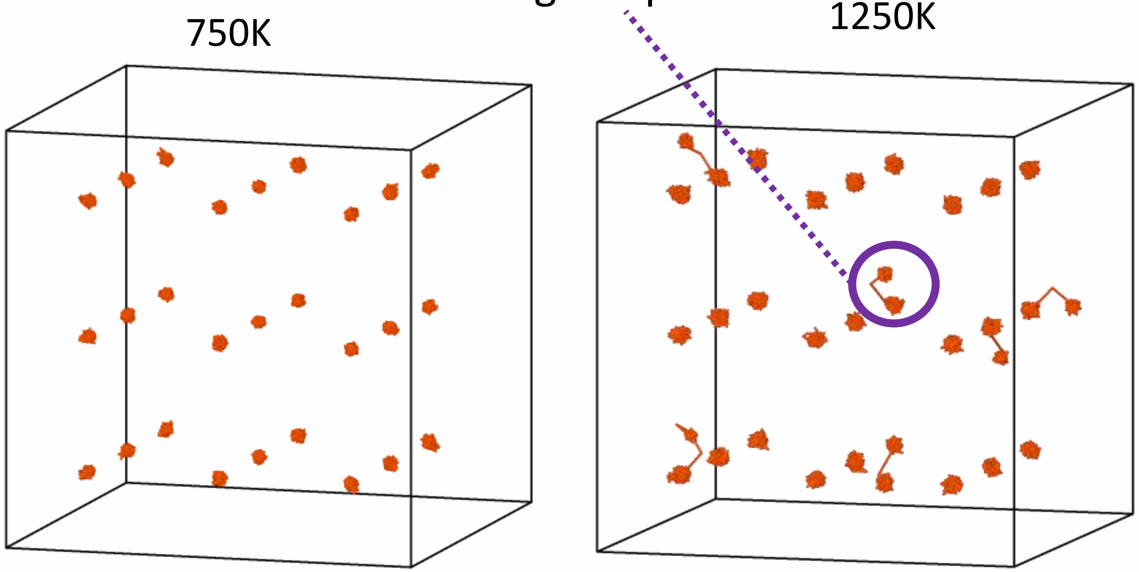

Trajectory of 27 He in OIS over 1ns

He diffusion

4% Schottky, 2500K

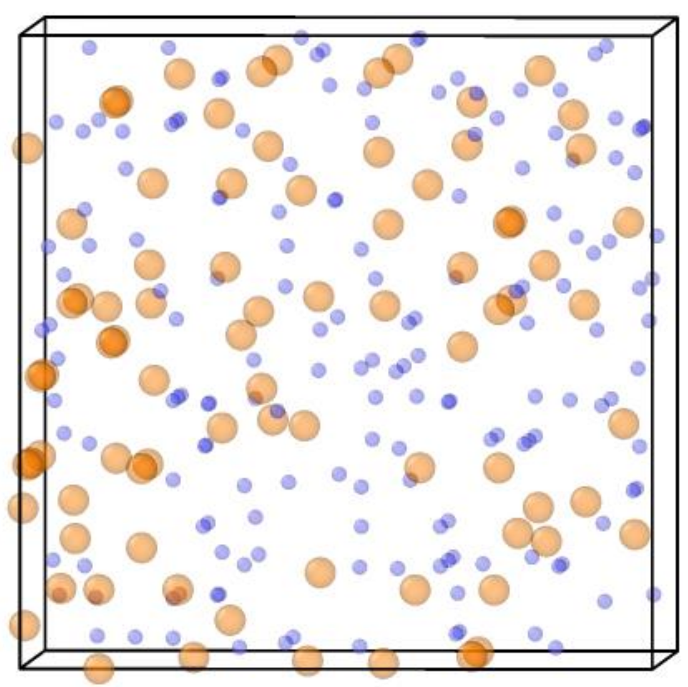

Pu vacancy

O vacancy

He interstitial

Trajectory of He atoms starting in OIS

Trajectory of He atoms starting in O vacancy

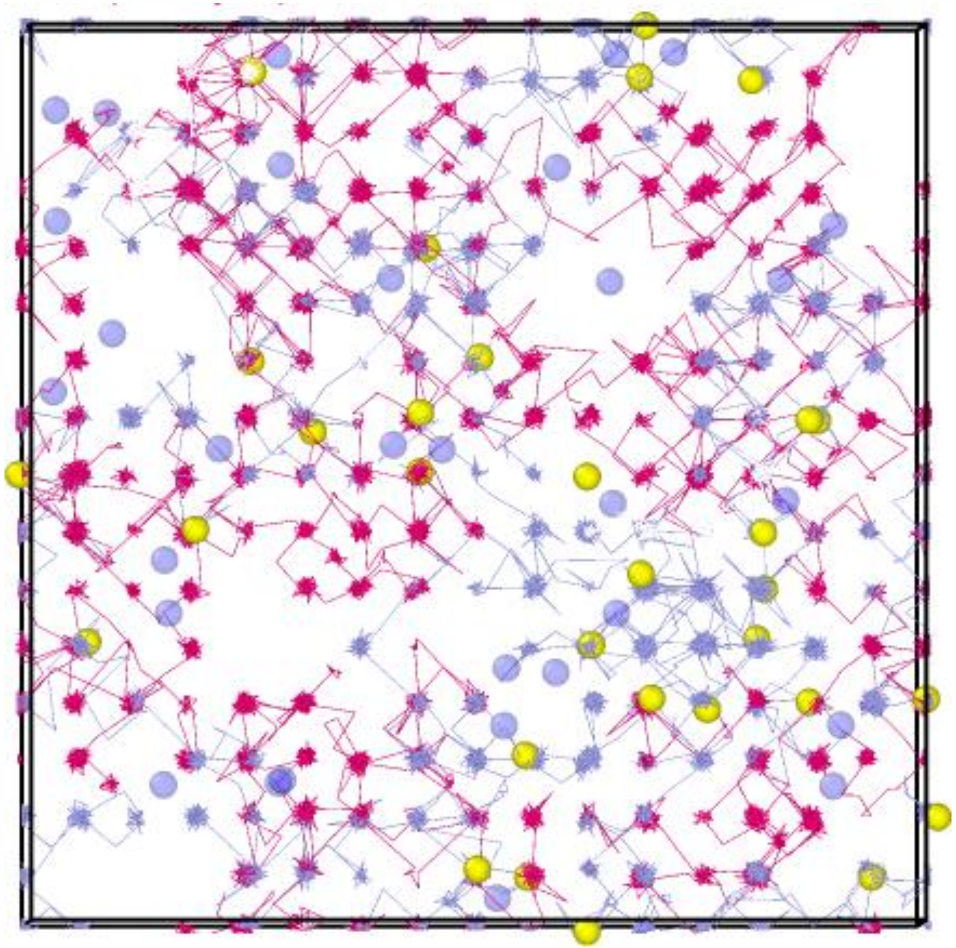

Regardless of start in OIS or O vacancy, lots of inter-site hopping.

2% Schottky, 2000K

Trajectory of He atoms starting in OIS

Trajectory of He atoms starting in Pu vacancy

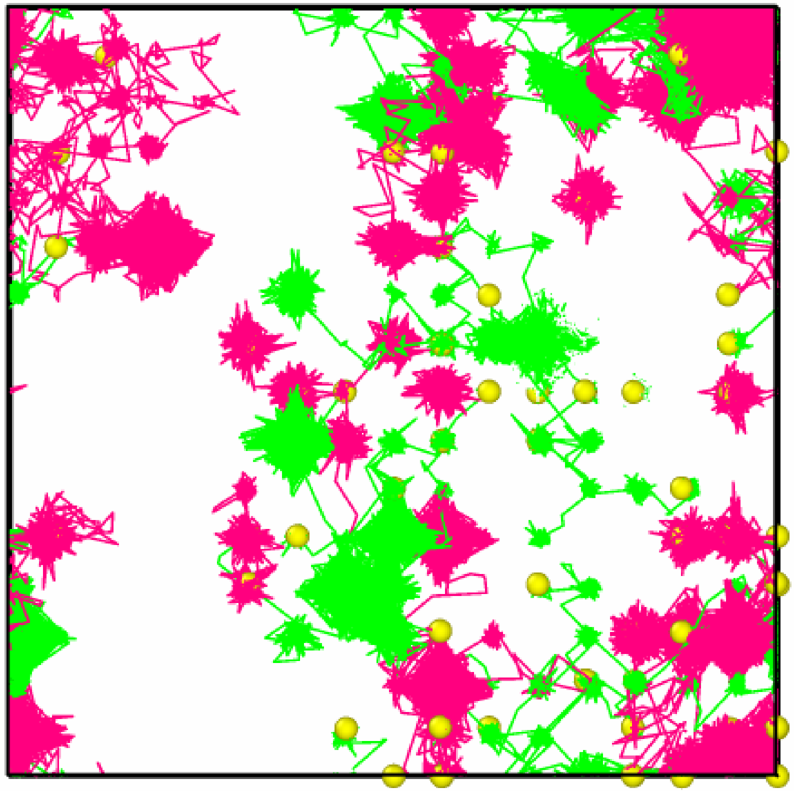

Much more OIS hopping when initial started in OIS. With Pu tend to oscillate about the empty Pu site. More space to move.

Pu FPs, 2000K

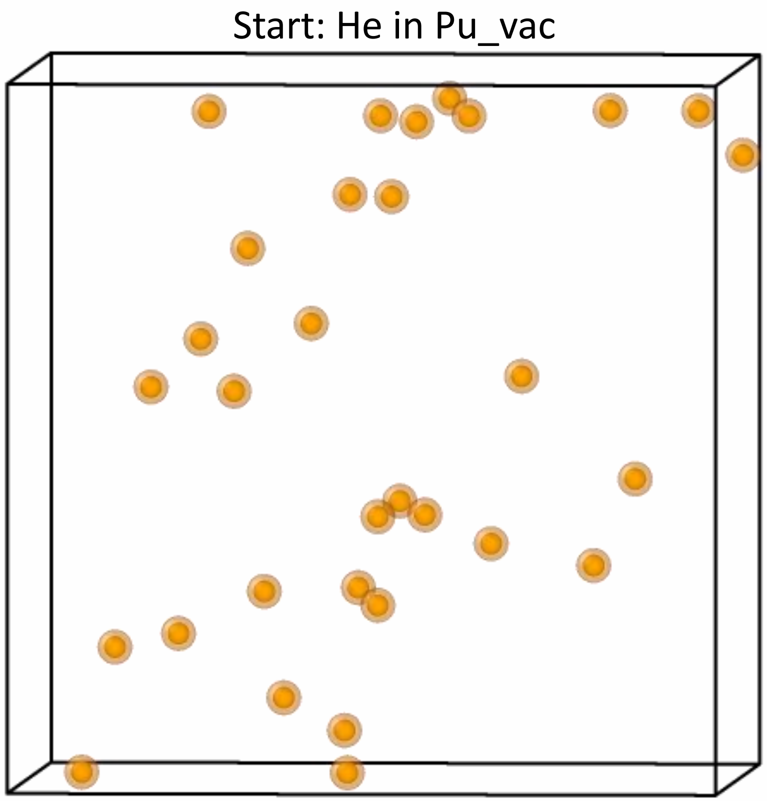

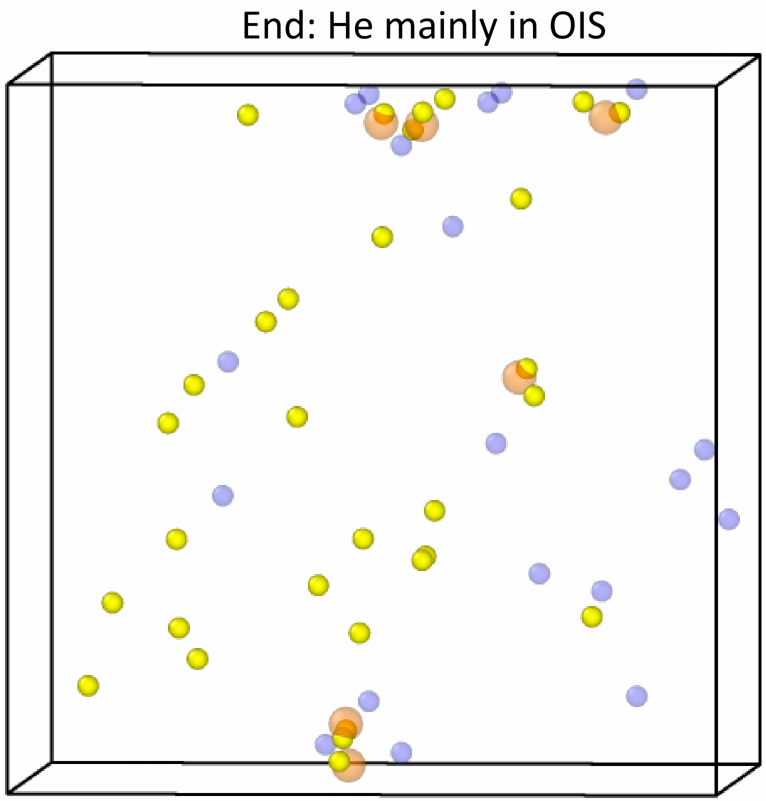

At end, very few Pu vacancies – the **Frenkel pairs have recombined**.

0.5% Pu vac, 2250K

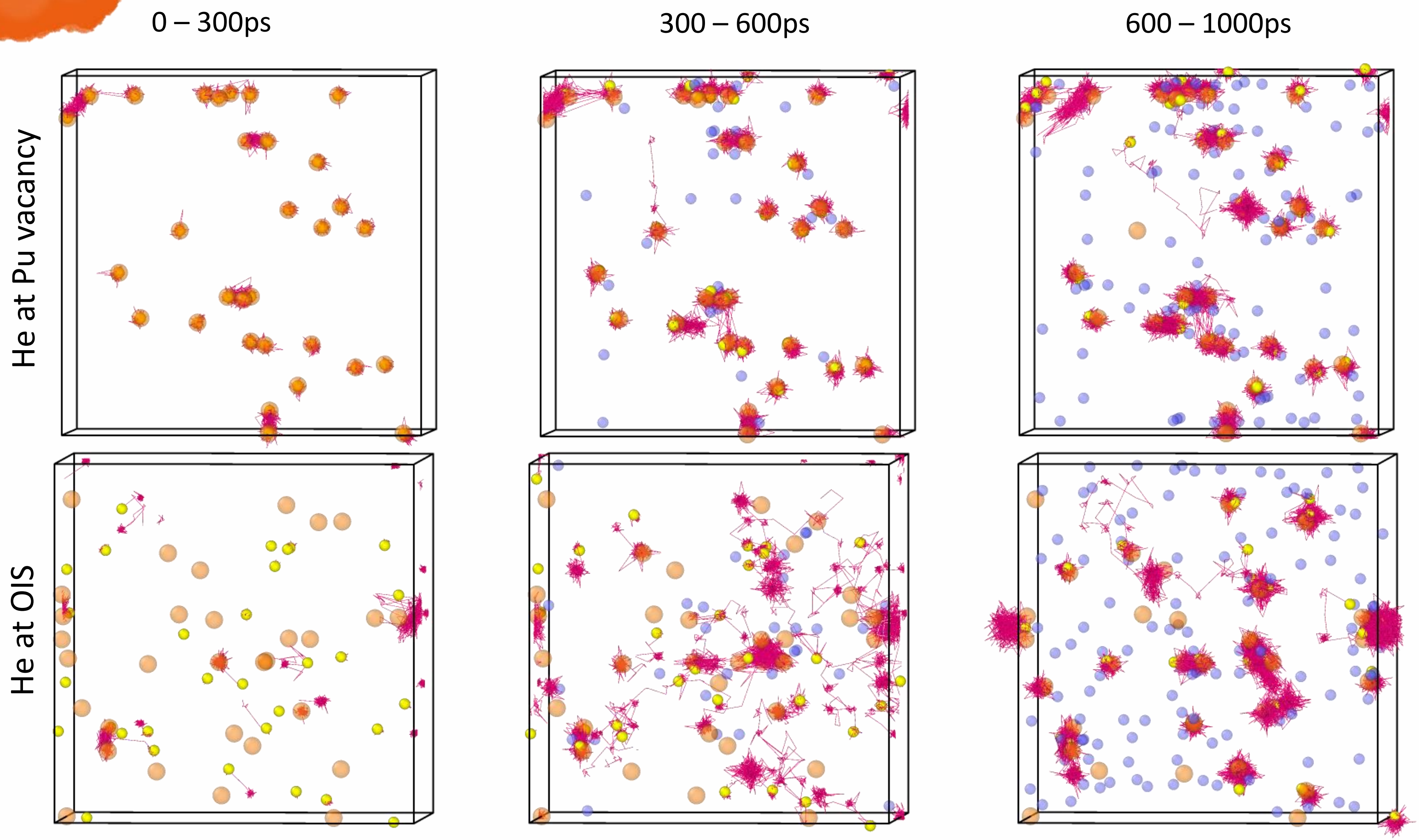

He diffusion

He migration to join another He at a Pu vacancy

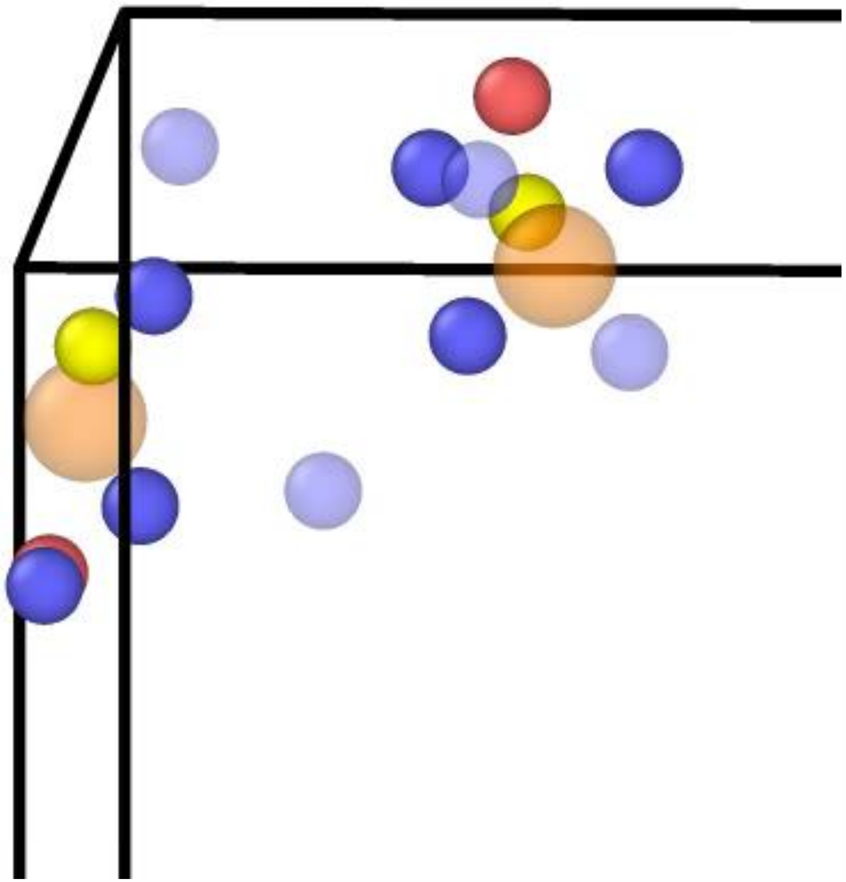

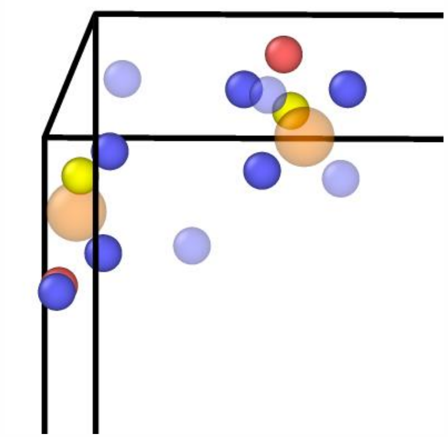

1. 2 He atoms in separate Pu vac

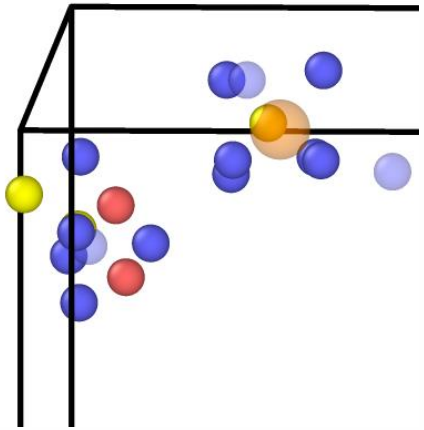

2. Pushed out by Pu interstitial

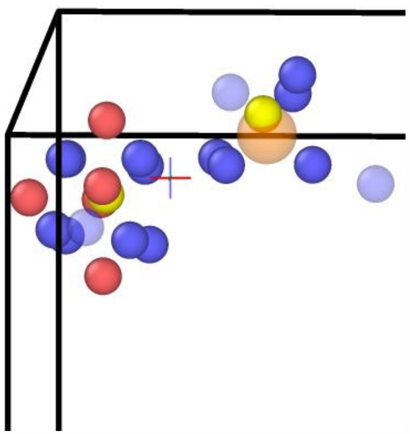

3. He in OIS, stays here for ~5 ps

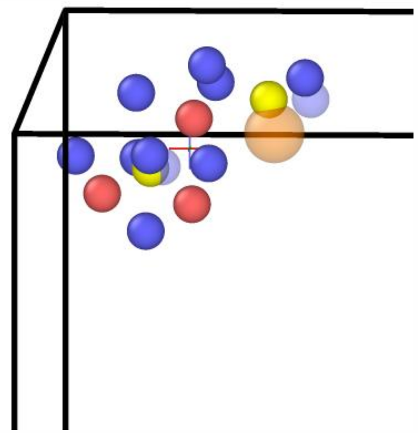

4. Hop to oxygen vacancy

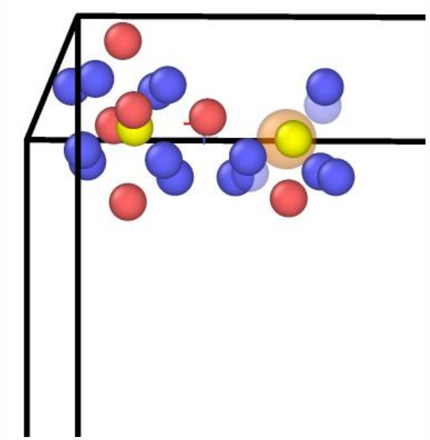

5. To next OIS (Ovac assisted diffusion)

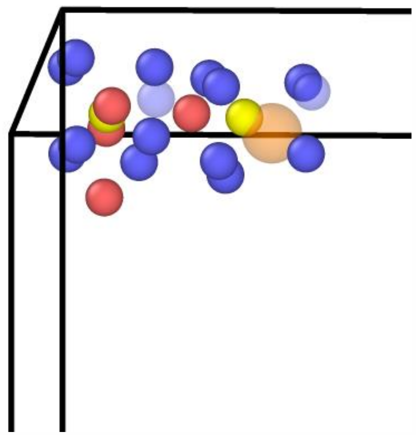

6. Neighbouring Oxygen vacancy

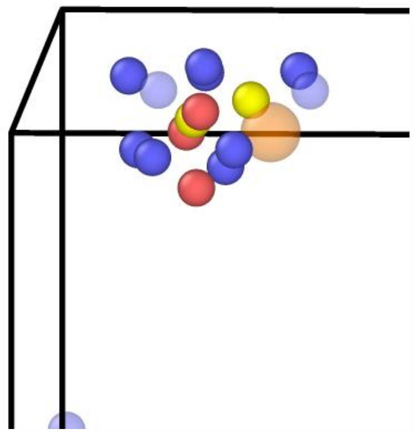

7. OIS jump via Ovac

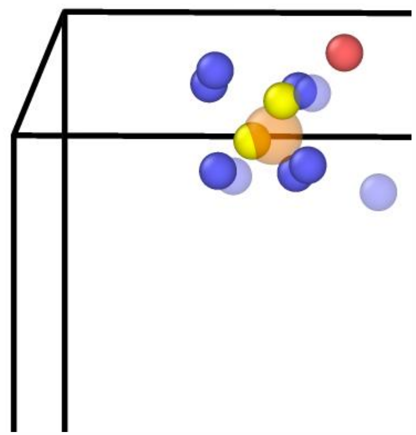

8. 2 He in Pu vac

He cluster analysis

Energy minimisation — What size clusters can form?

NEB — Will the clusters form?

Molecular dynamics — Do the clusters form?

TRANSCEND

Transformative Science and Engineering for Nuclear Decommissioning

He cluster analysis

Helium:vacancy ratio

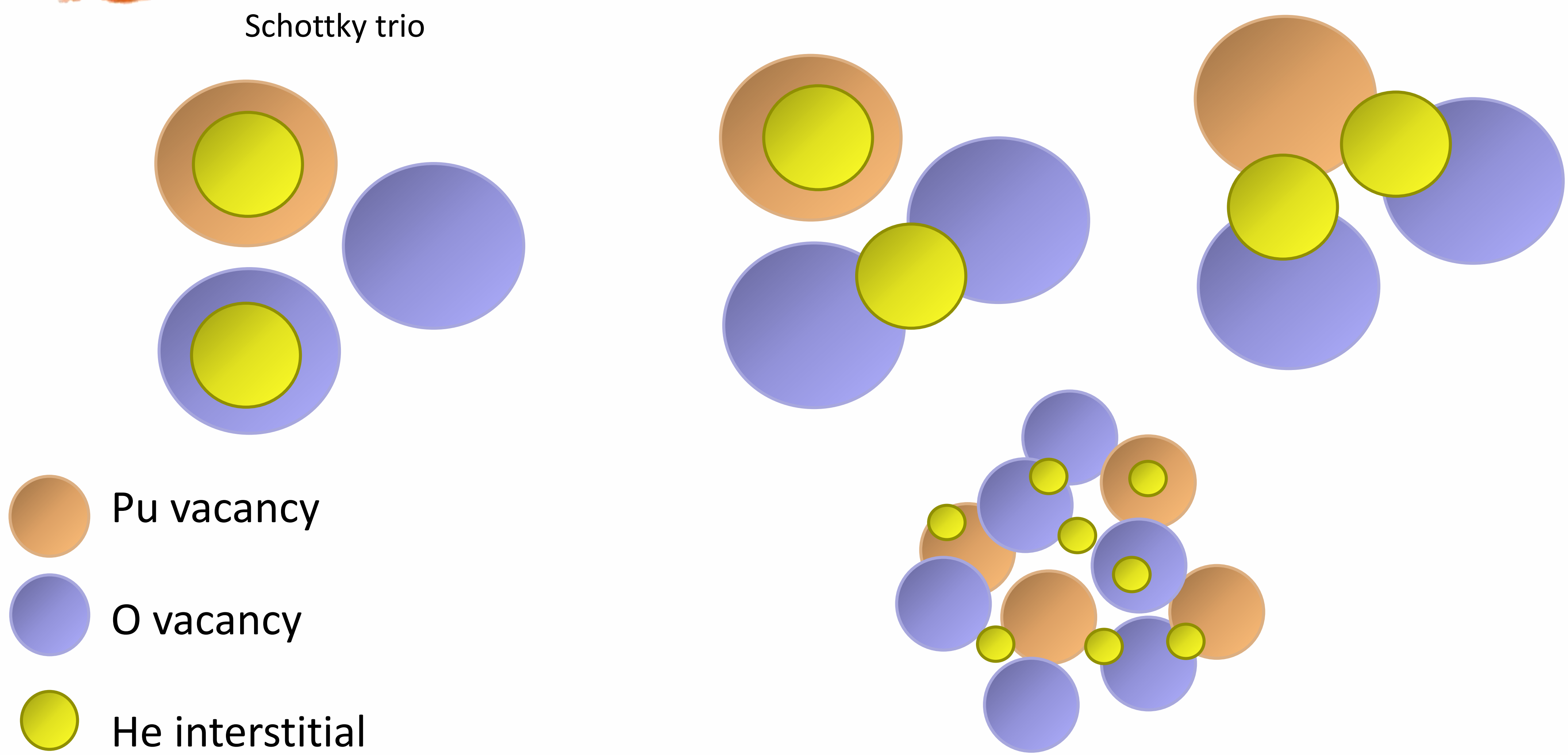

Transformative Science and Engineering for Nuclear Decommissioning

He cluster analysis

Energy minimisation

Energy of Incorporation vs. He:Vacancy ratio

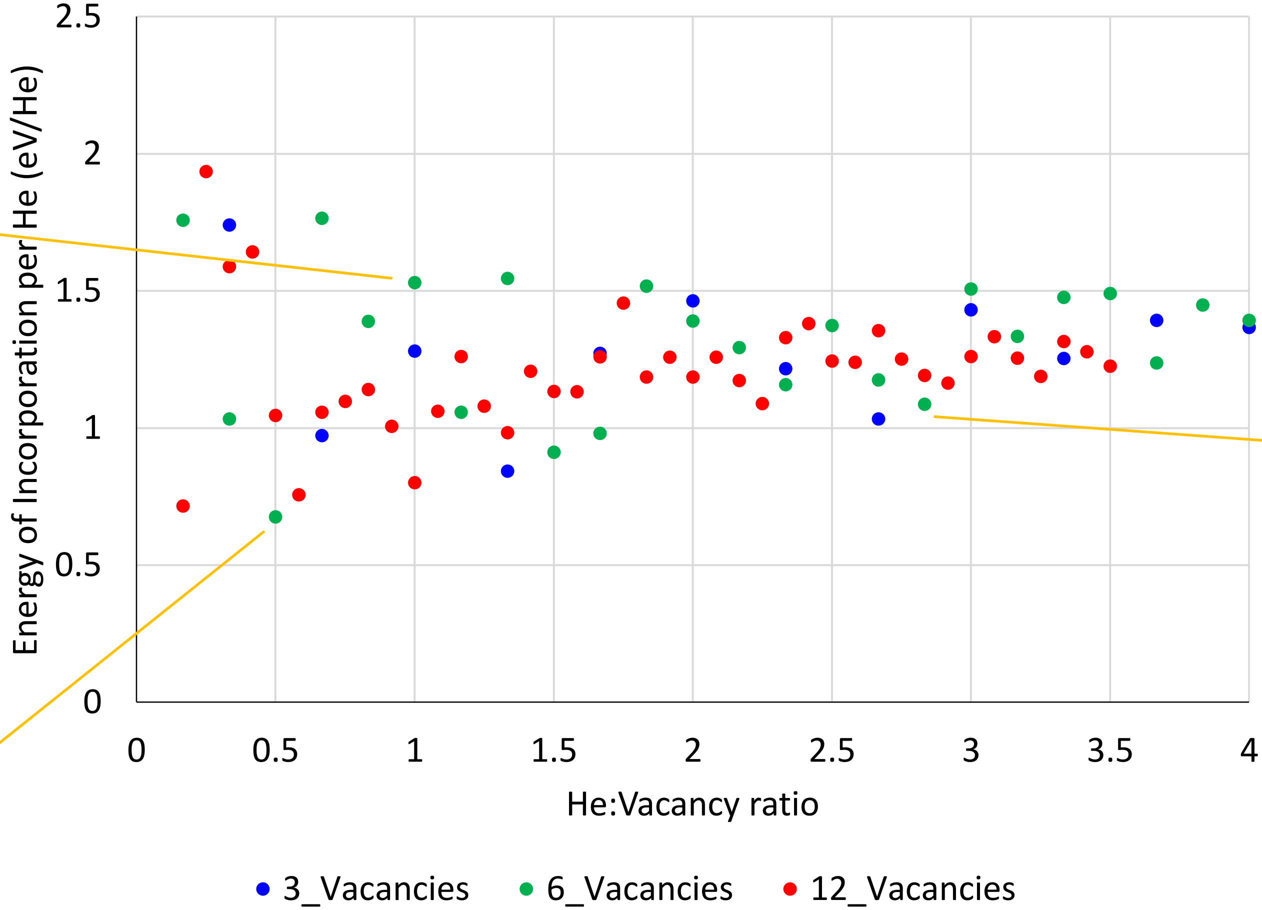

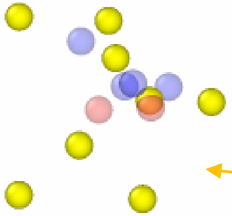

He_8V_6

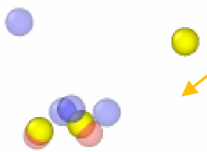

He_3V_6

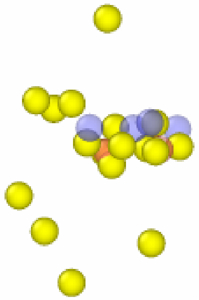

$He_{17}V_6$

Instead be He_9V_6 with 8 interstitials

He cluster analysis

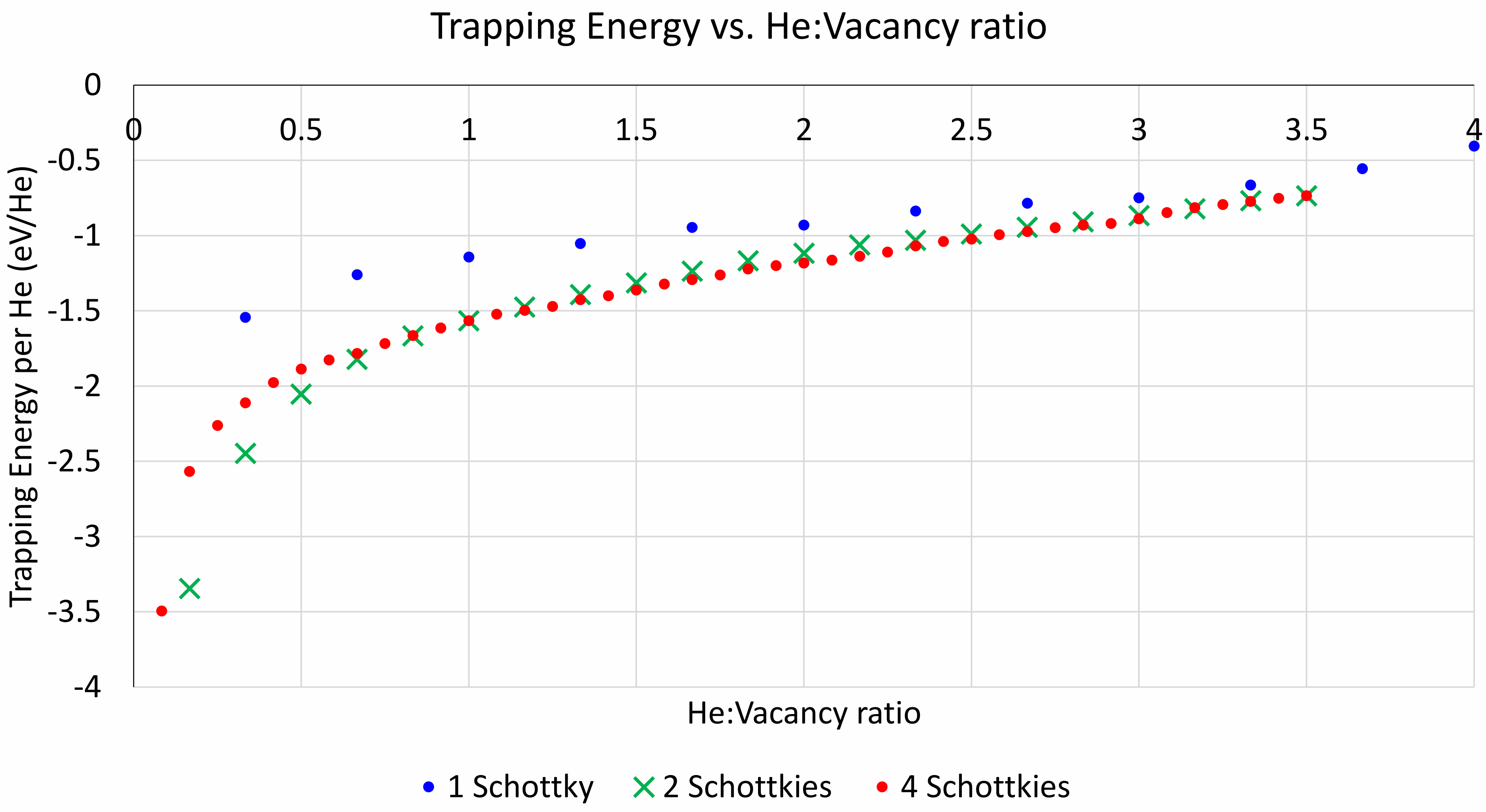

TRANSCEND

Transformative Science and Engineering for Nuclear Decommissioning

He cluster analysis

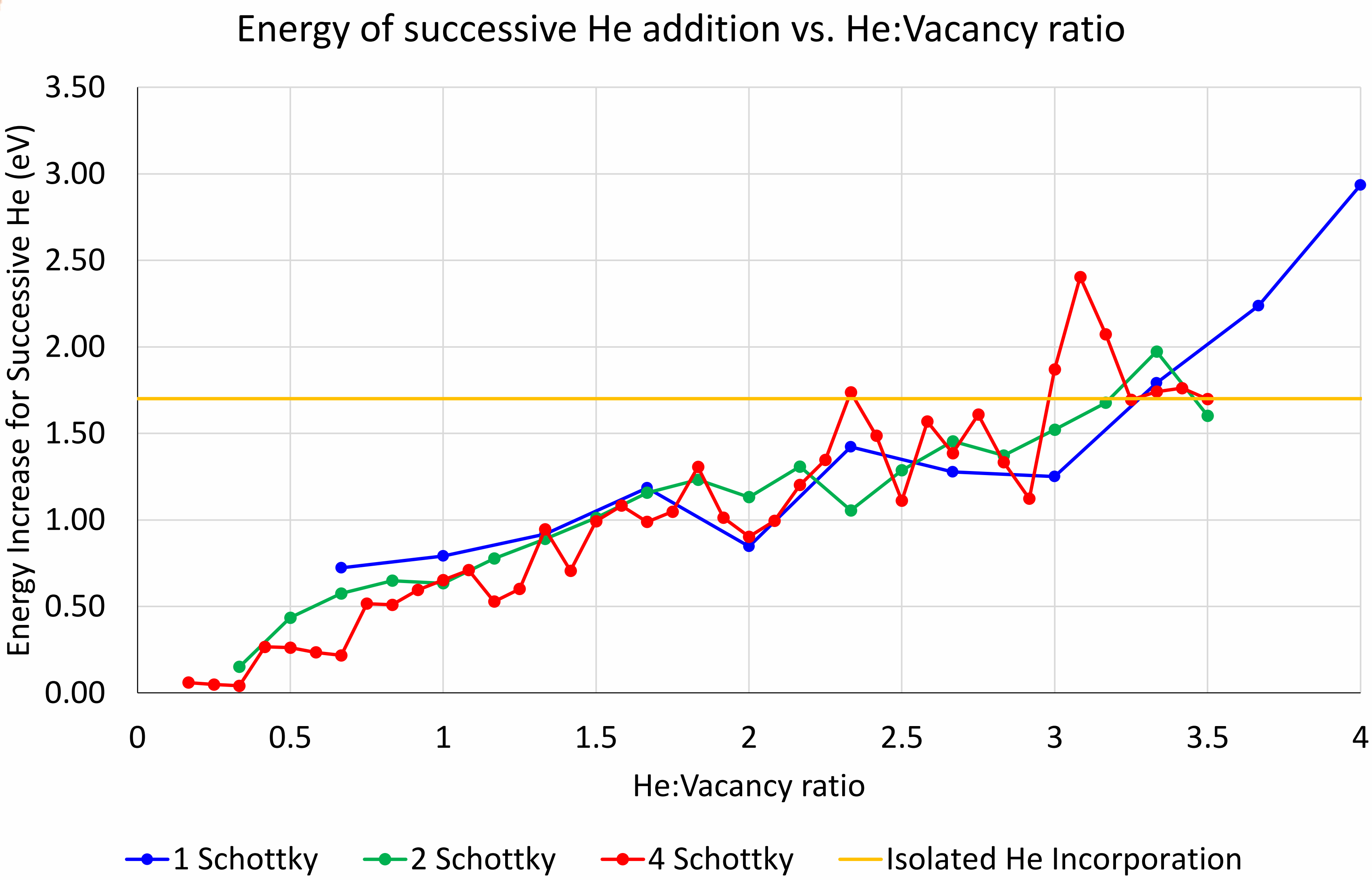

TRANSCEND

Transformative Science and Engineering for Nuclear Decommissioning

He cluster analysis

NEB

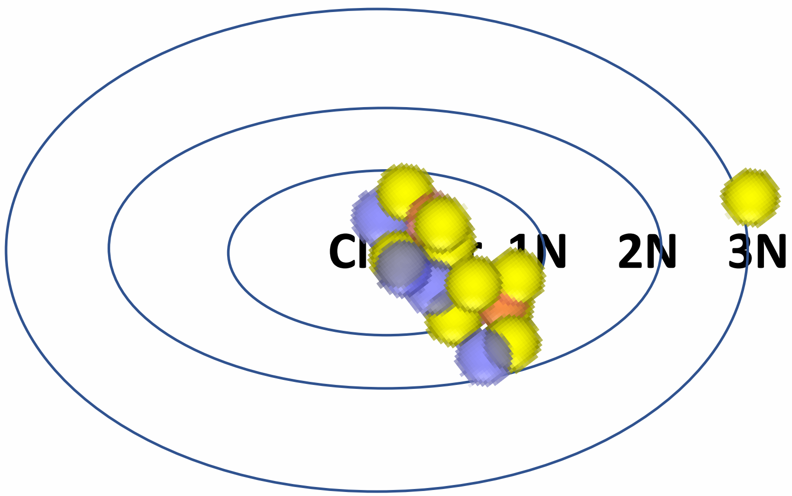

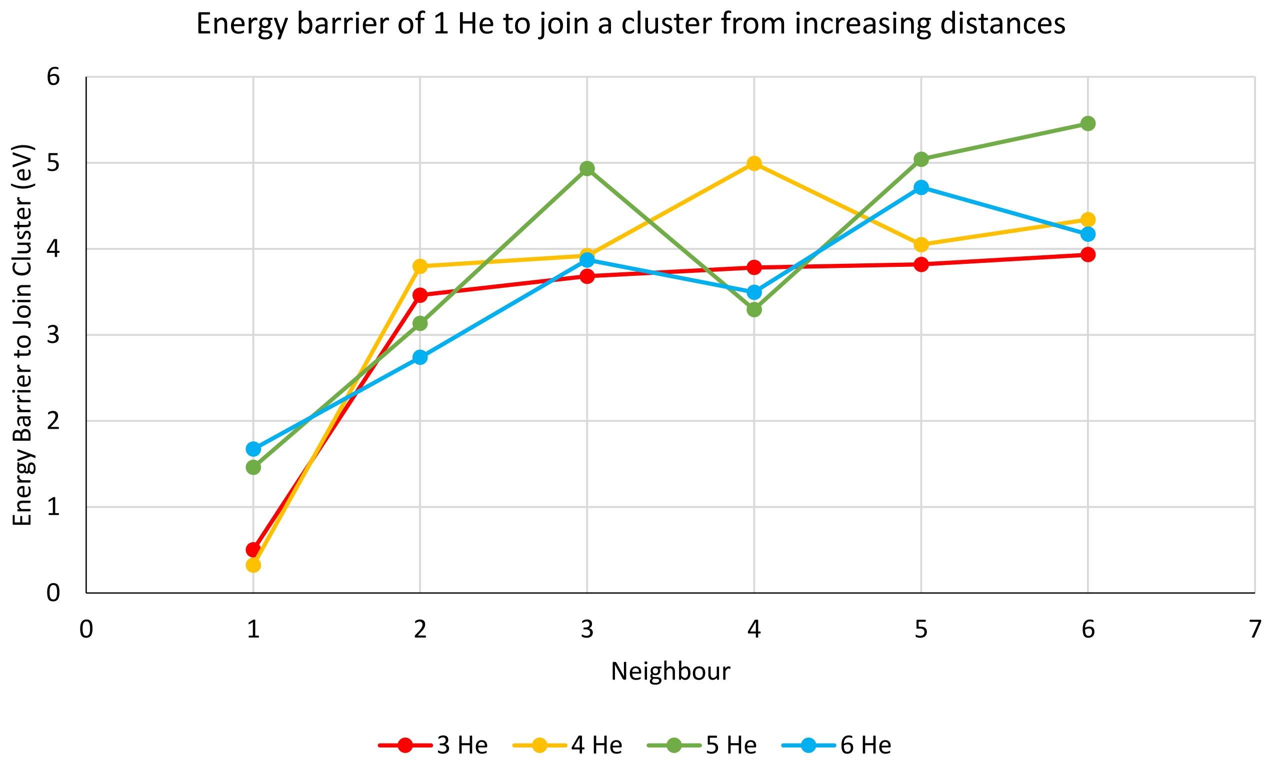

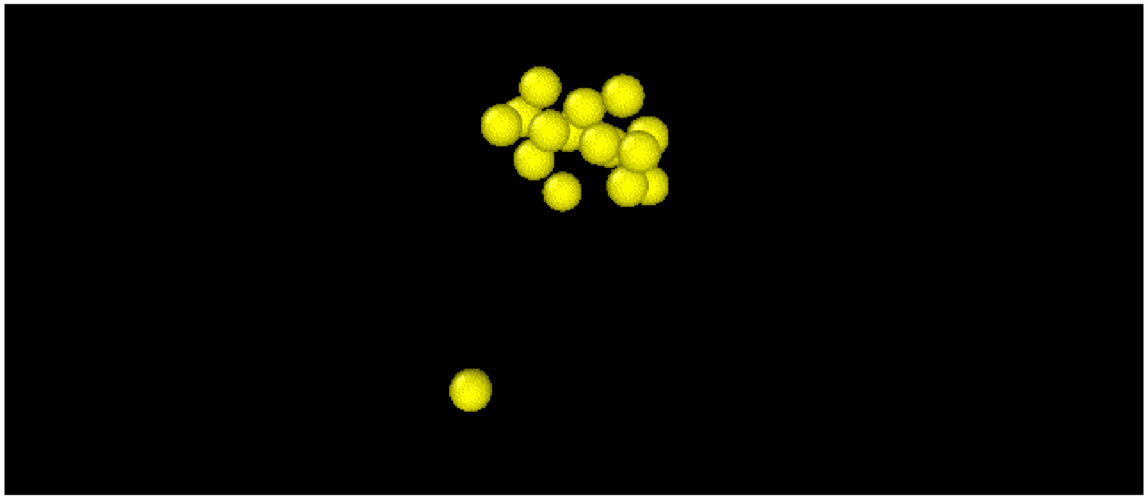

TRANSCEND

Transformative Science and Engineering for Nuclear Decommissioning

He cluster analysis

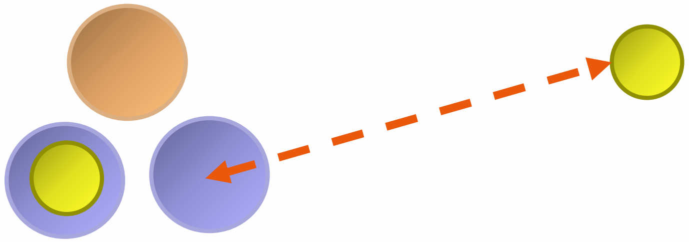

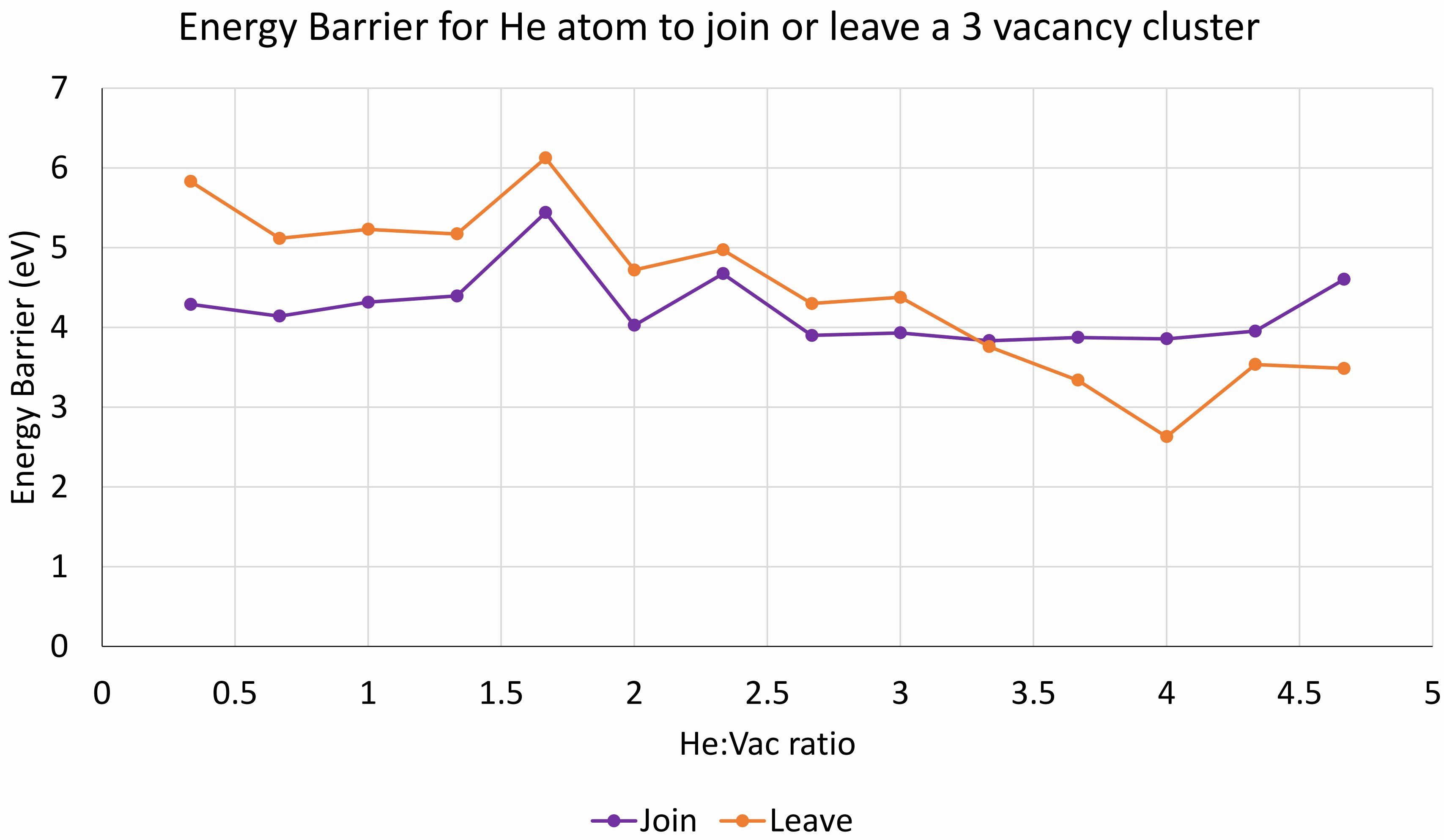

He cluster analysis

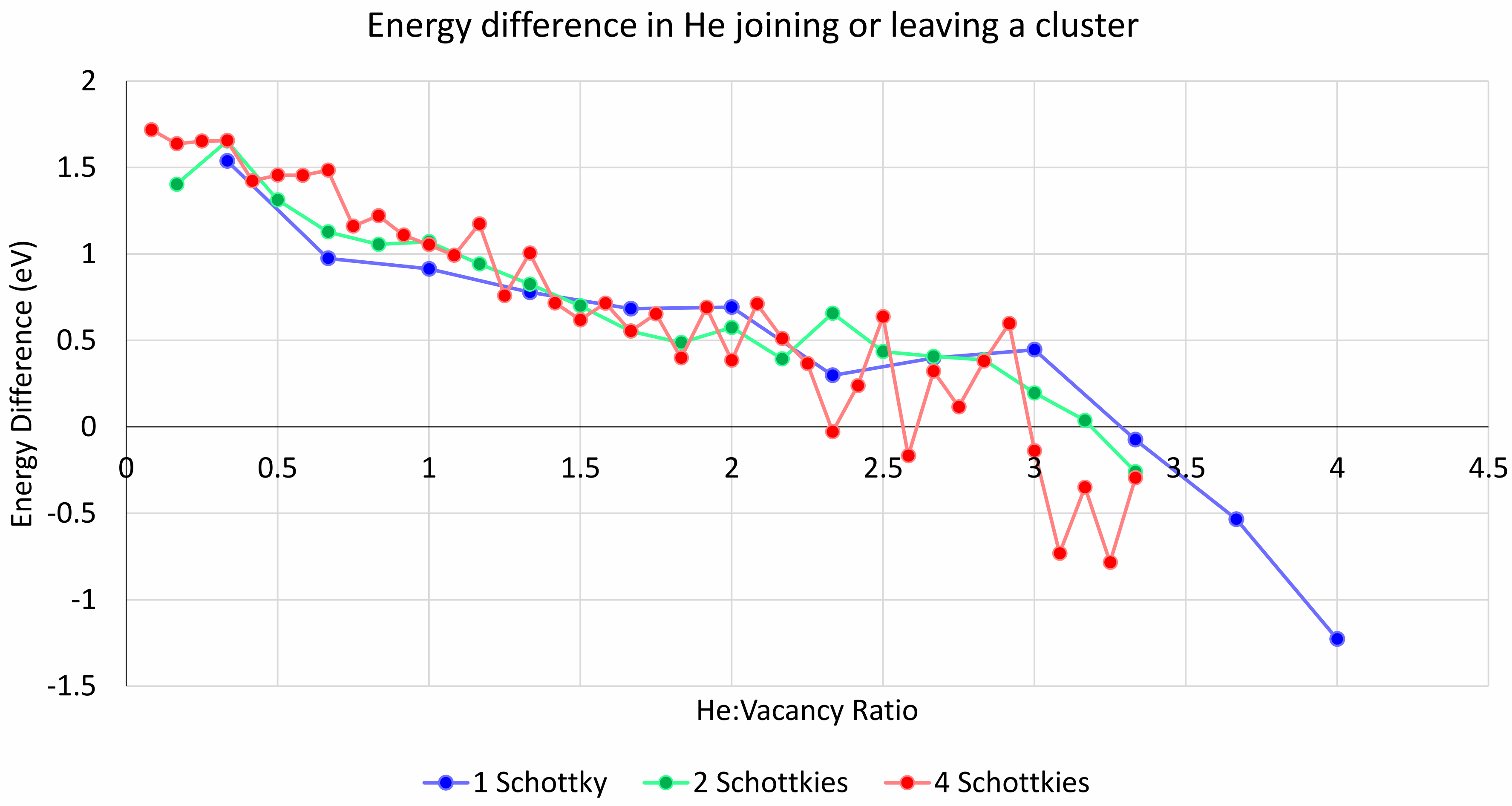

TRANSCEND

Transformative Science and Engineering for Nuclear Decommissioning

He cluster analysis

Molecular dynamics

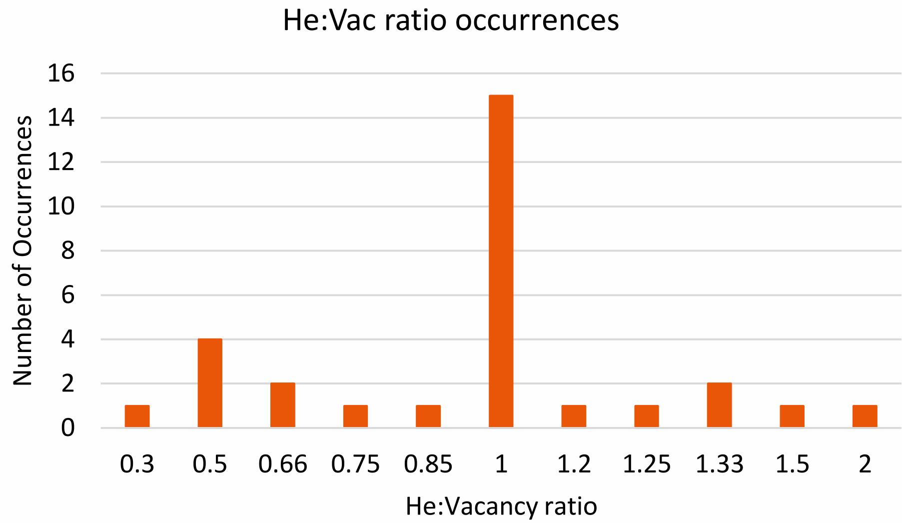

1:1 1500K

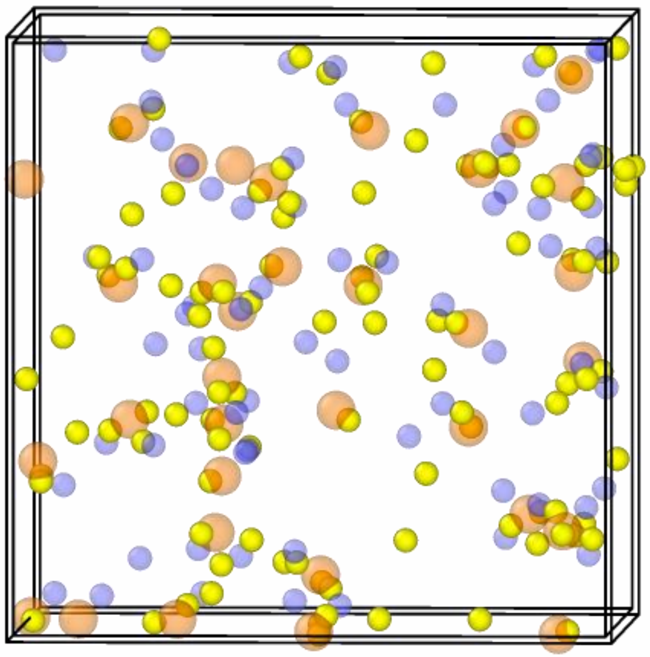

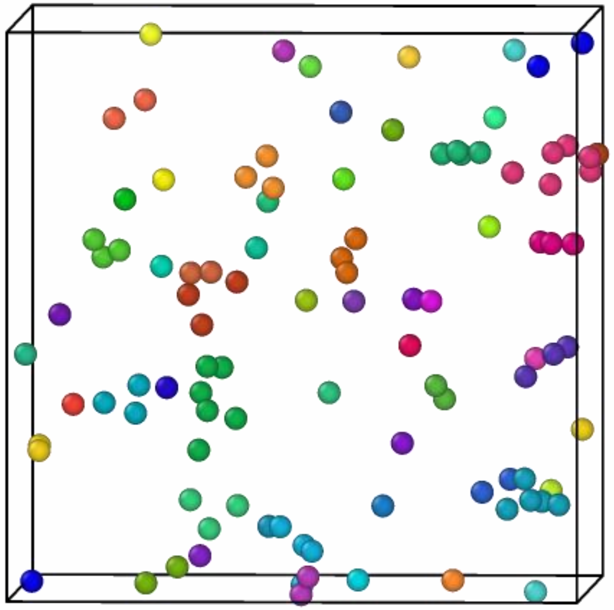

Atomistic Simulation of Helium Incorporation in PuO_2

Migration pathways Interstitial hopping assisted by vacancies

He diffusion Pu vacancies act as ‘traps’ and drastically reduce diffusion

He cluster analysis Maximum energetically favourable cluster is ~4:1 He:Vacancy ratio

Transformative Science and Engineering for Nuclear Decommissioning

Acknowledgements

- Peter Slater (University of Birmingham)
- Pooja Goddard, Ying Zhou, Roger Smith (University of Loughborough)
- Rob Jackson (University of Keele)
- Helen Steele (SL)
- Robin Orr, Mark Read (NNL)

TRANSCEND

Transformative Science and Engineering for Nuclear Decommissioning

Thank you

exm350@student.bham.ac.uk

TRANSCEND

Transformative Science and Engineering for Nuclear Decommissioning

A Monte Carlo Study of Nanoparticles Relevant to Nuclear Waste

Ella Schaefer, The University of Manchester

Integrated Waste Management – Theme 1

10.11.21

ella.schaefer@postgrad.manchester.ac.uk

Energy

For a Low Carbon Future

Background

What type of NPs?

Nuclear – light metal hydroxides/oxides

(e.g. Al_2O_3 and $Mg(OH)_2$)

Why Oxides/Hydroxide NPs?

- **Present in waste storage ponds**
- **From corrosion of the cladding on nuclear fuel rods in the nuclear waste storage ponds in Sellafield**

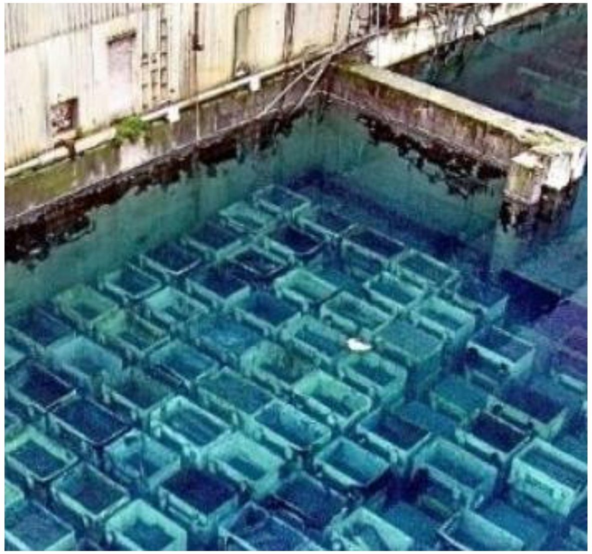

Figure 1 – a) Photograph of a legacy pond at *Sellafield* and b) Close up of a legacy pond at *Sellafield* showing cloudy water containing particulates

Background

Why Nanoparticles (NPs)?

- Irradiated NPs produce chemical changes in the surrounding media
- Including •OH, low E e^-s and H_2
- In healthcare •OH and low E e^-s are used in radiotherapy
- H_2 formation is relevant to nuclear safety cases – due to it’s flammable and potentially explosive nature

A Simplified View of an Irradiated NP

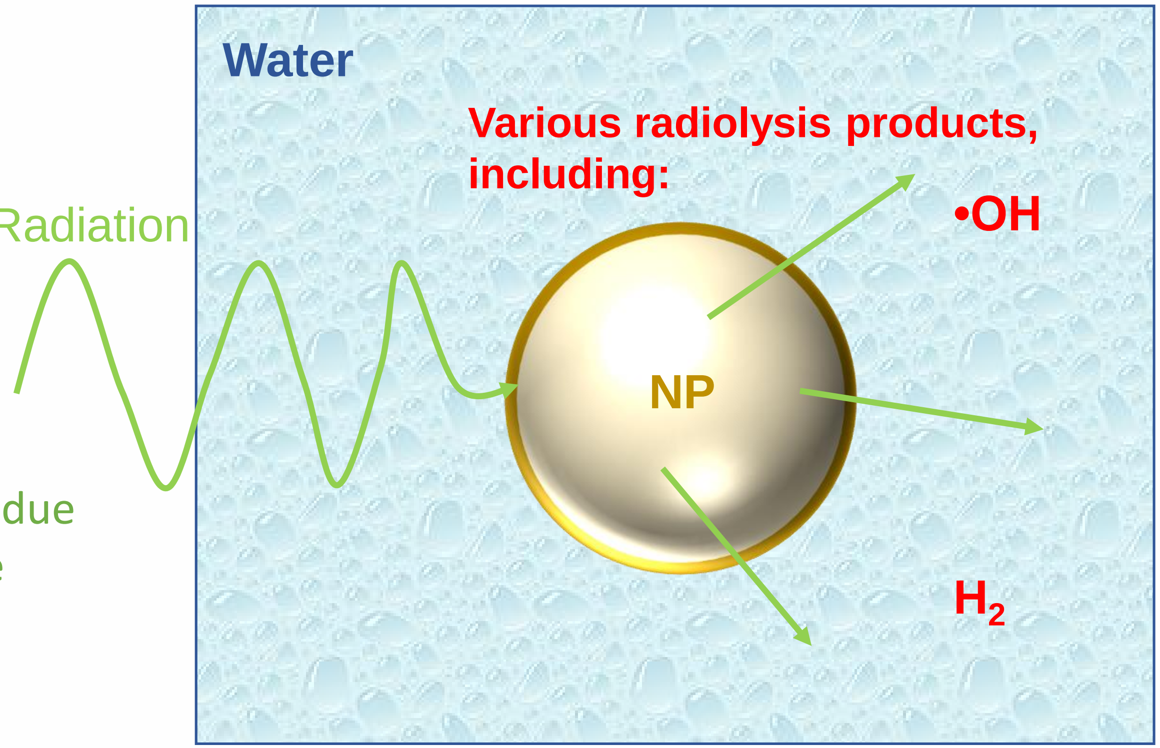

Figure 2 – Diagram showing the irradiation of a NP resulting in various radiolytic species, noting two of interest; the hydroxyl radical and gaseous molecular hydrogen.

Radiation Interaction with NP

A few important processes that occur when a NP is irradiated:

a) Photoelectric effect

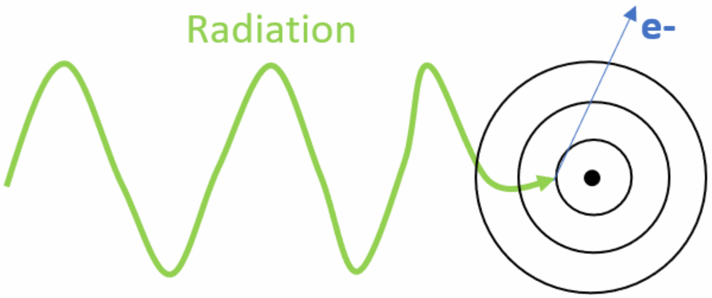

c) Compton effect

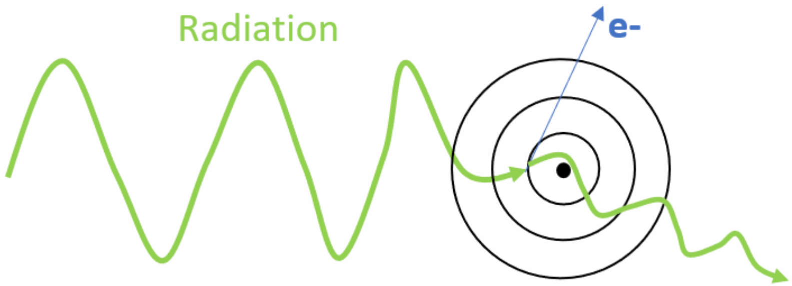

d) Exciton generation

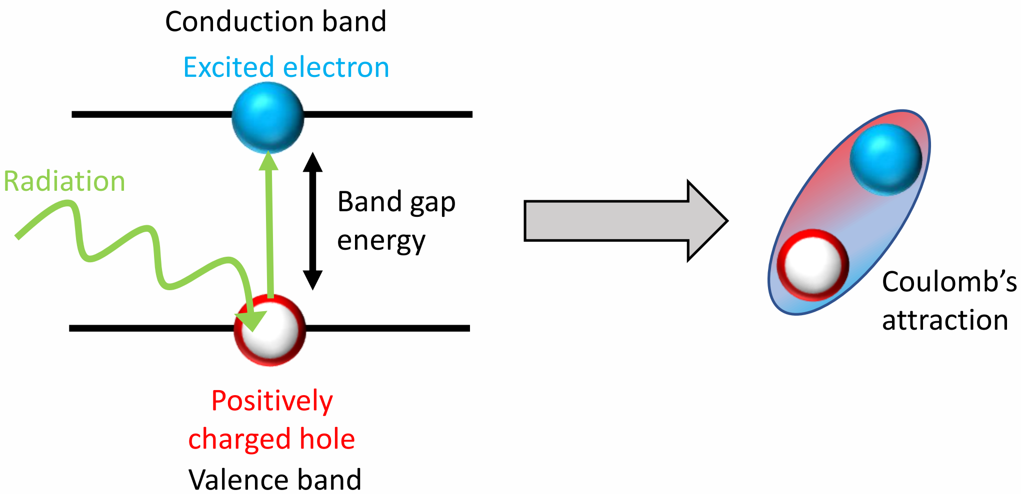

b) Auger effect

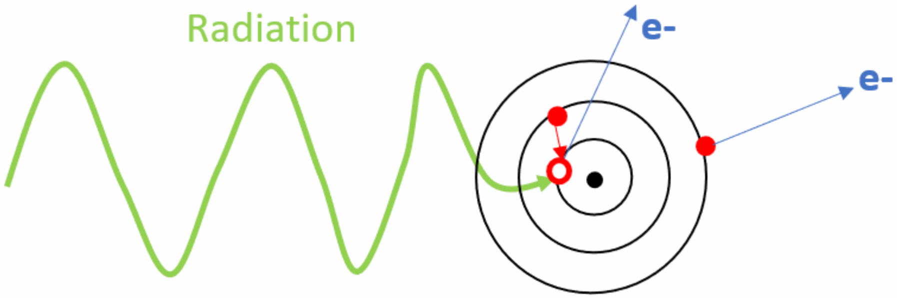

Figure 3 – Diagram depicting a) the Photoelectric effect, b) the Auger effect c) the Compton effect and d) exciton generation

Method

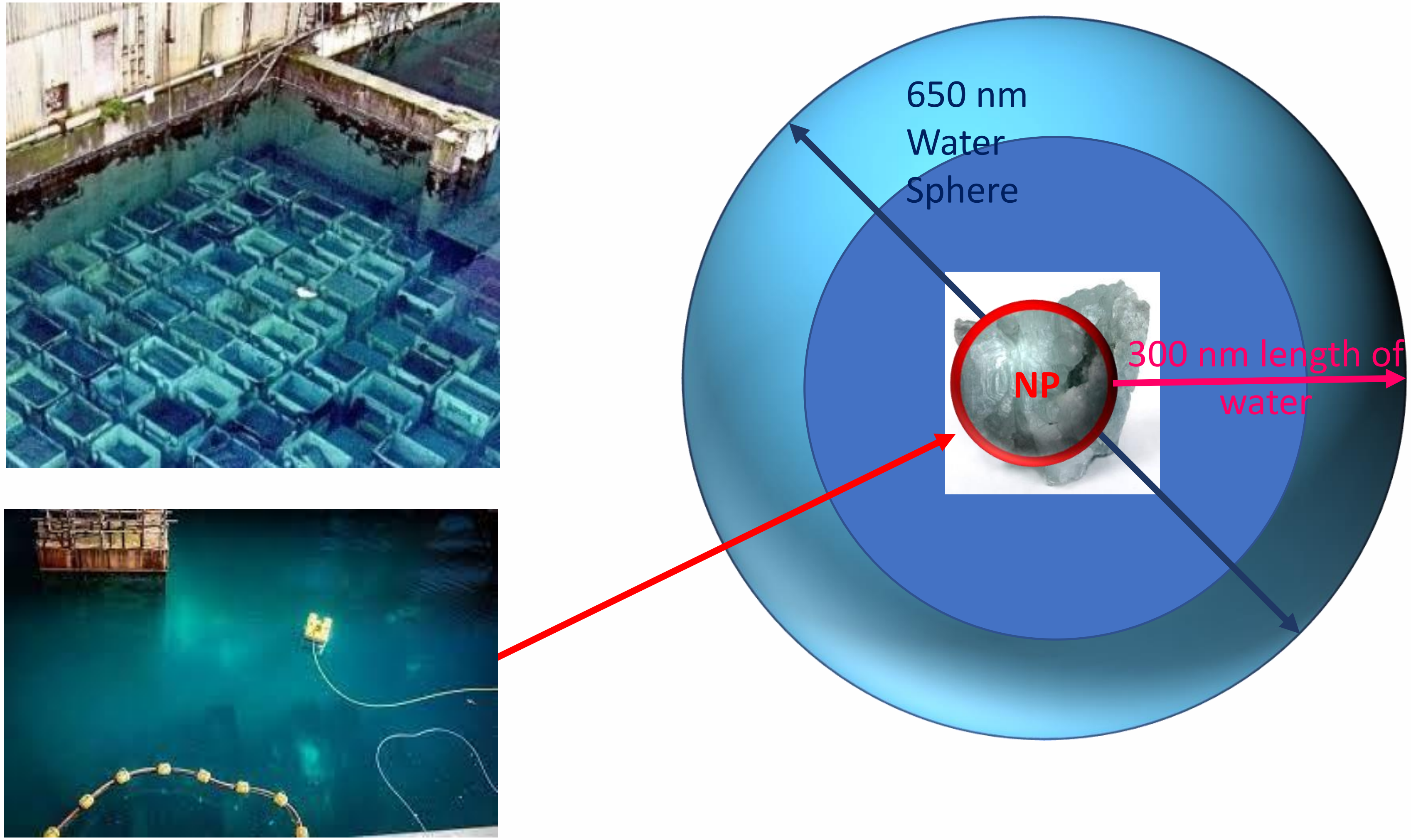

Radial Dose Distribution –
Dose is measured in 1nm sections from the NP surface to the edge of the water sphere

Figure 4 – Visualisation of the method

Radial Dose Distributions (RDDs)

- 20 – 60 keV relates to specific measurements that can be performed at the Synchrotron
- Although E in ponds is much greater, after ~60 keV the underlying physics is the same, MeV can be calculated but require much longer times/computational power
- At lower E dose is higher for a longer range
- Al_2O_3 deposits greater dose than $Mg(OH)_2$

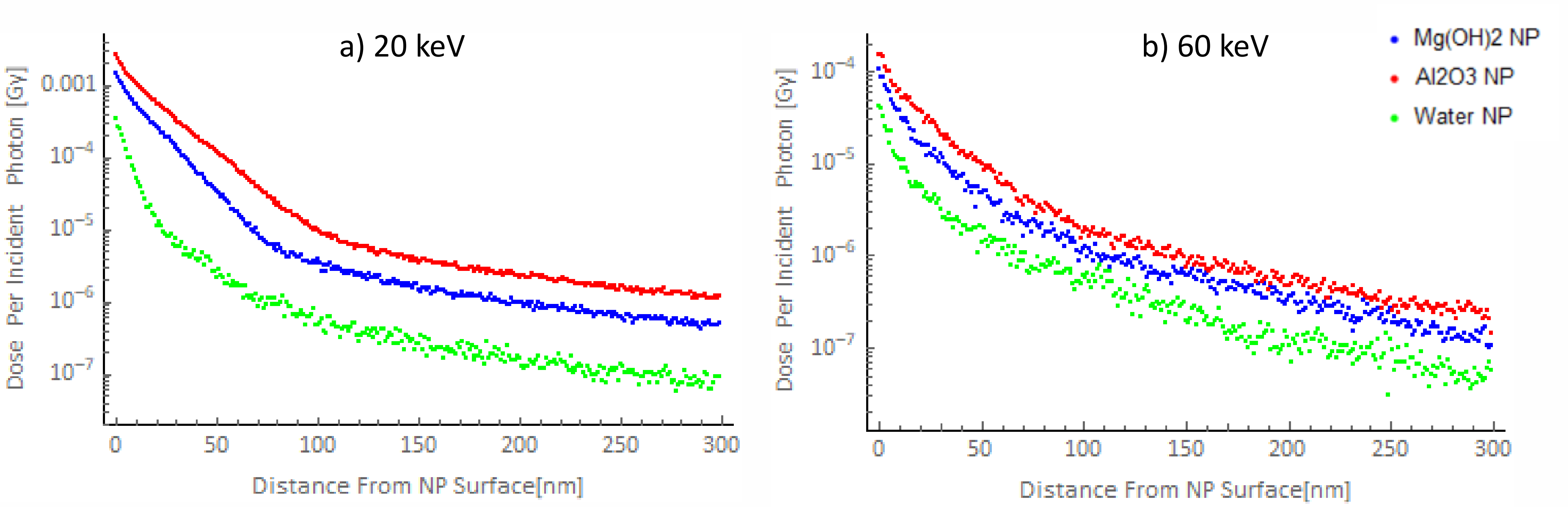

Figure 5 – Graphs showing the radial dose distributions per incident photon for Al_2O_3, $Mg(OH)_2$ and water NPs irradiated by a) 20 and b) 60 keV

RDDs as Ratios

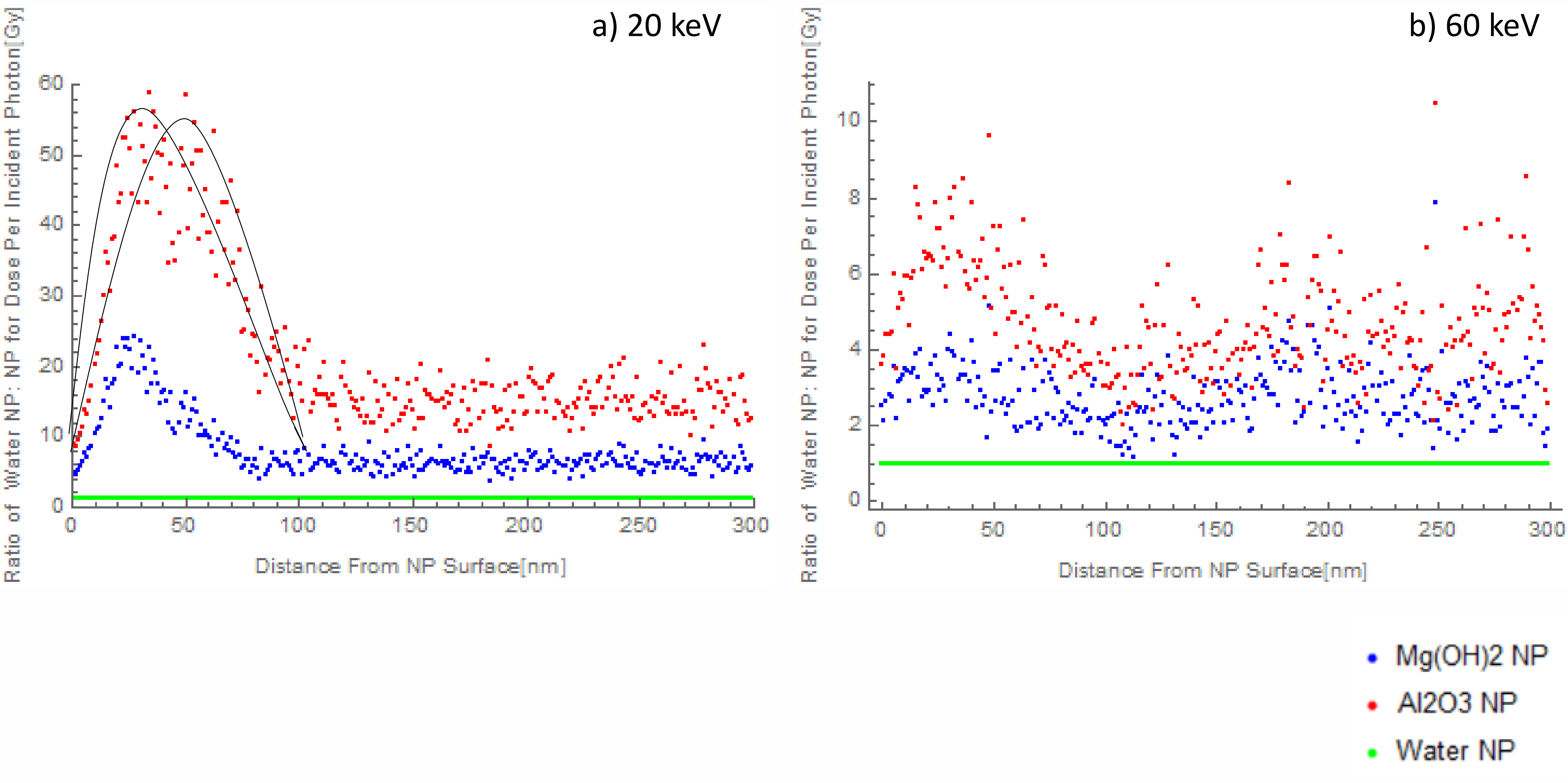

Figure 6 – Graphs showing the radial dose distributions per incident photon for Al_2O_3 and $Mg(OH)_2$ NPs as ratios to Water NPs irradiated by a) 20 and b) 60 keV

Al_2O_3 Scorer

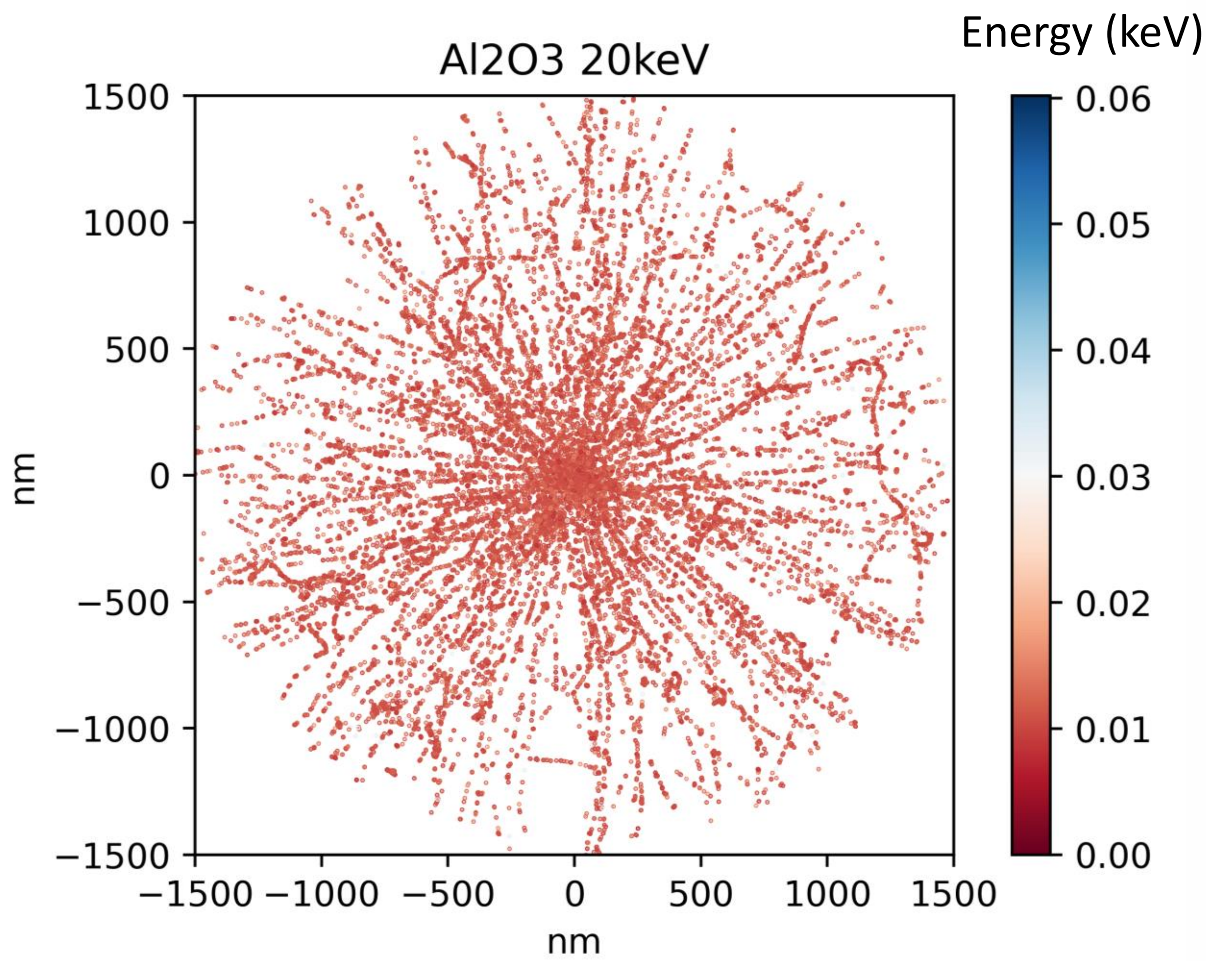

- Simulation was further developed to detect when an ionisation or excitation occurs
- When an ionisation/excitation occurs the process, position and energy of the generated e^- is recorded

Figure 7 – Figure showing the ionisations and excitations occurring in a 1500nm world following the irradiation of an Al_2O_3 NP by photons of 20 keV

Al_2O_3 Scorer

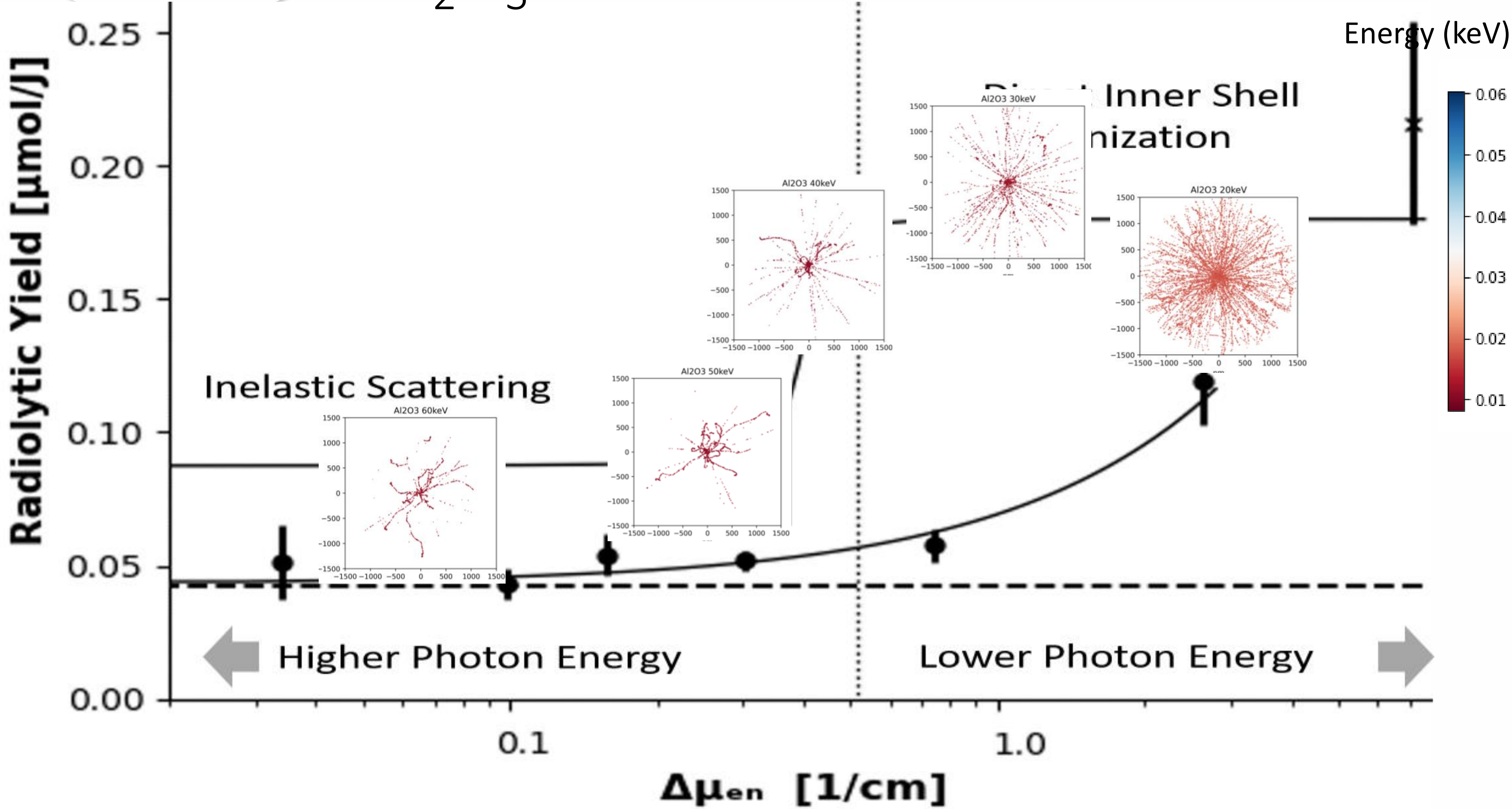

Figure 8 – Plot of the measured radiolytic hydrogen yields against the difference between energy absorption coefficients of the particulate phase and the aqueous phase [M. O'leary] overlayed with figures showing the ionisations and excitations occurring in a 1500nm world following the irradiation of an Al_2O_3 NP by photons of energies a) 20, b) 30, c) 40, d) 50 and e) 60 keV

$Mg(OH)_2$ Scorer

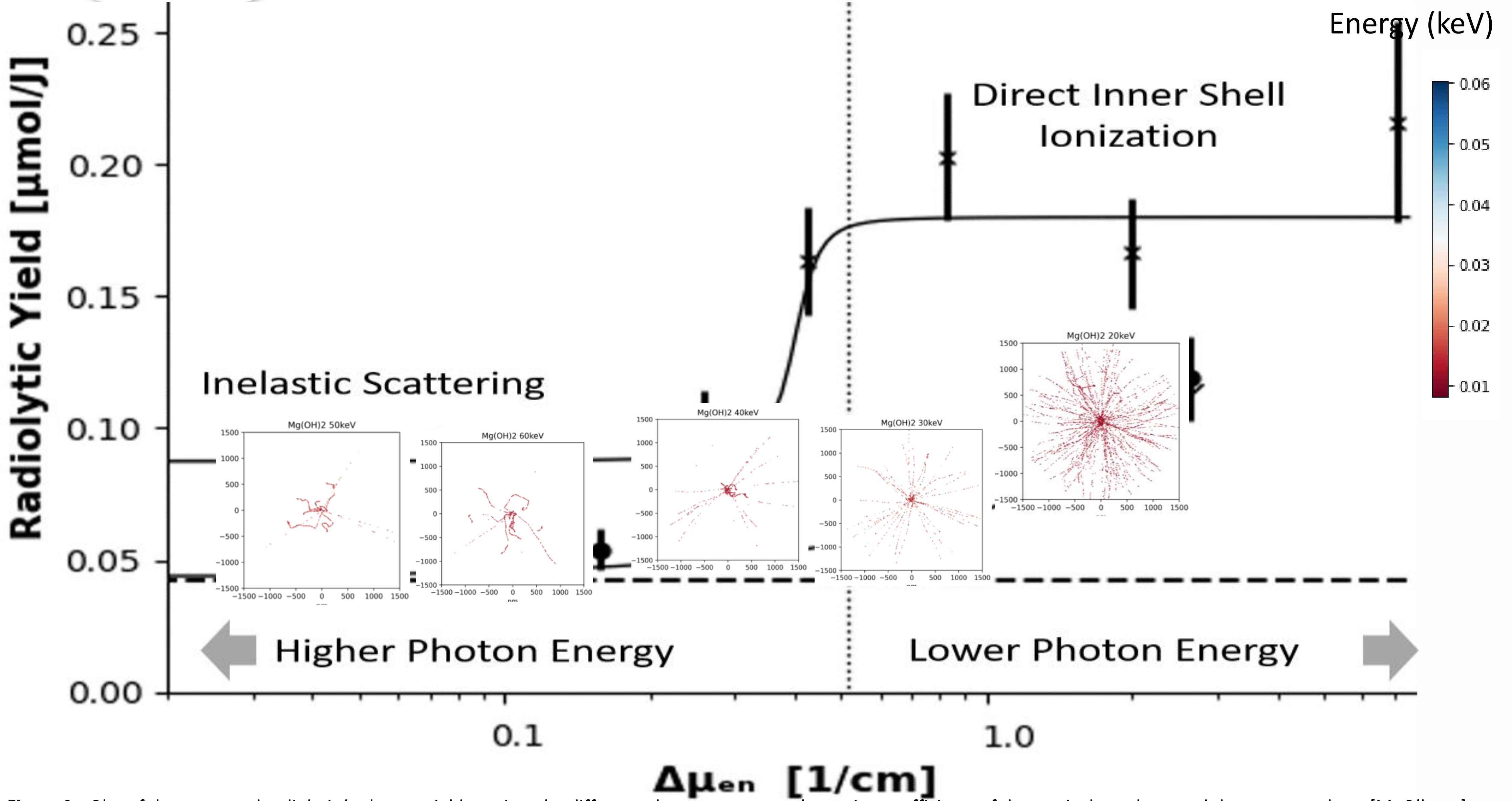

Figure 9 – Plot of the measured radiolytic hydrogen yields against the difference between energy absorption coefficients of the particulate phase and the aqueous phase [M. O'leary] overlayed with figures showing the ionisations and excitations occurring in a 1500nm world following the irradiation of an $Mg(OH)_2$ NP by photons of energies a) 20, b) 30, c) 40, d) 50 and e) 60 keV

Discussion

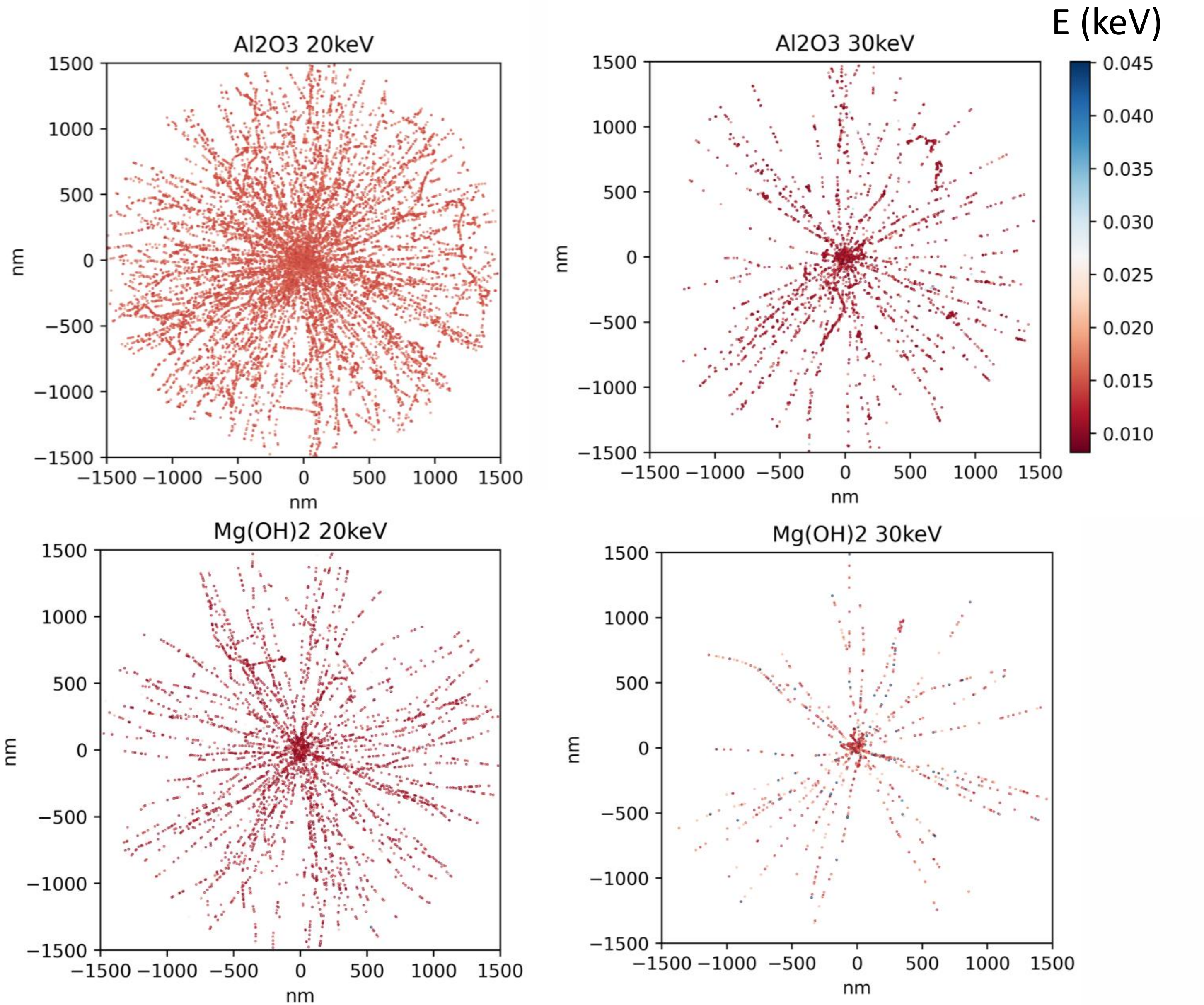

- Difference in colour shows the difference in E
- Much greater activity and E in Al_2O_3
- Especially noticeable at 20 and 30 keV – which is where the switch from Compton to photoelectric processes occur
- Likely due to Auger cascade

Figure 10 – Figures showing the ionisations and excitations occurring in a 1500nm world following the irradiation of an Al_2O_3 NP by a) 20 and b) 30 keV and a $Mg(OH)_2$ NP by c) 20, and d) 30 keV

Process RDDs

- Specific versions of the RDDs were run where the particles escaping the NP were filtered by the generation process

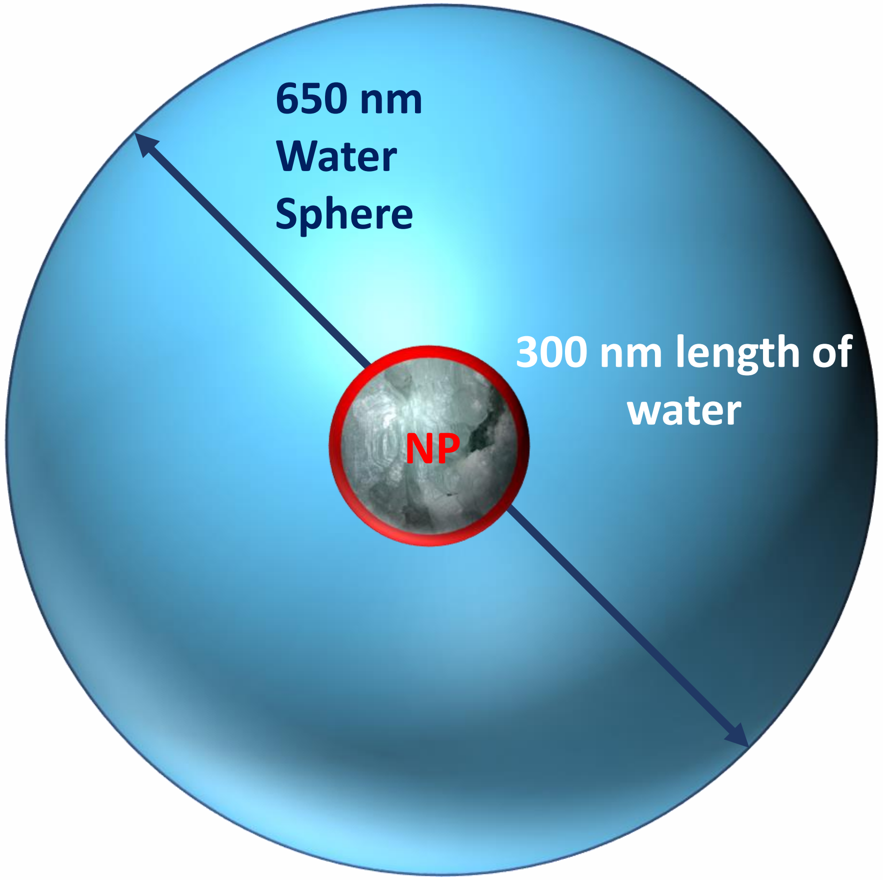

Radial Dose Distribution –
Dose is measured in 1nm sections from the NP surface to the edge of the water sphere

Figure 11 – Visualisation of method

TRANSCEND

Transformative Science and Engineering for Nuclear Decommissioning

Process RDDs

Al_2O_3 NP

$Mg(OH)_2$ NP

Photoelectric

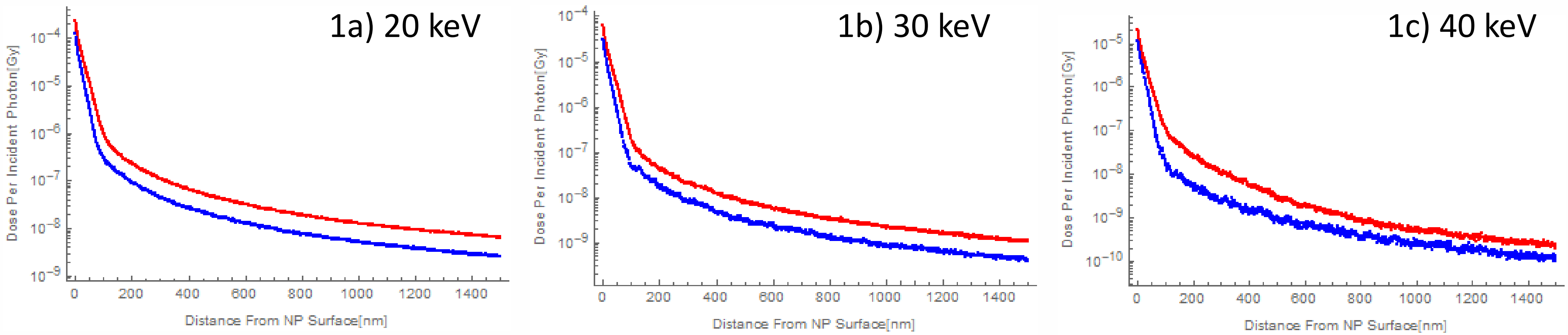

Compton

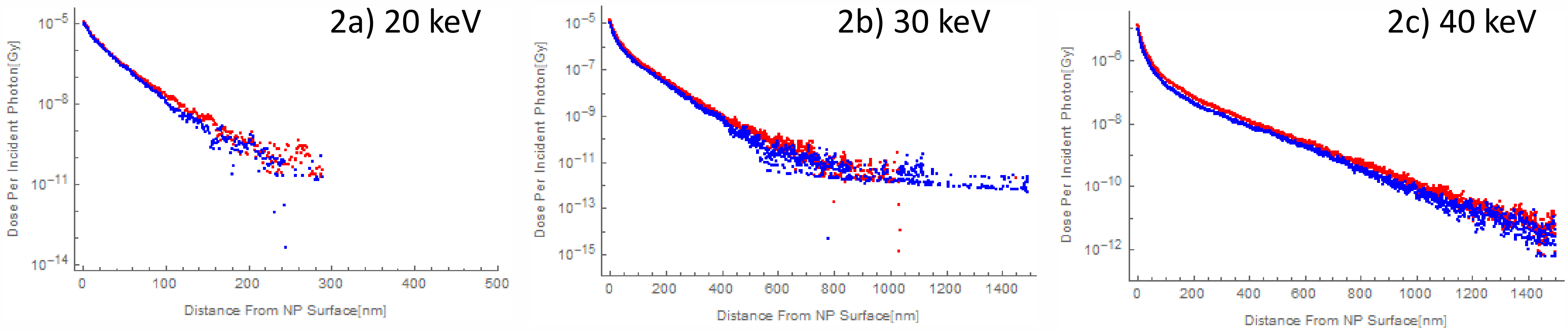

Figure 12 – Graphs showing the radial dose distributions per incident photon for Al_2O_3 and $Mg(OH)_2$ NPs irradiated by a) 20 b) 30 and c) 40 keV photon beam, filtered by 1) the photoelectric effect and 2) the Compton effect

Transformative Science and Engineering for Nuclear Decommissioning

Process RDDs

■ Al_2O_3 NP
■ $Mg(OH)_2$ NP

Photoelectric

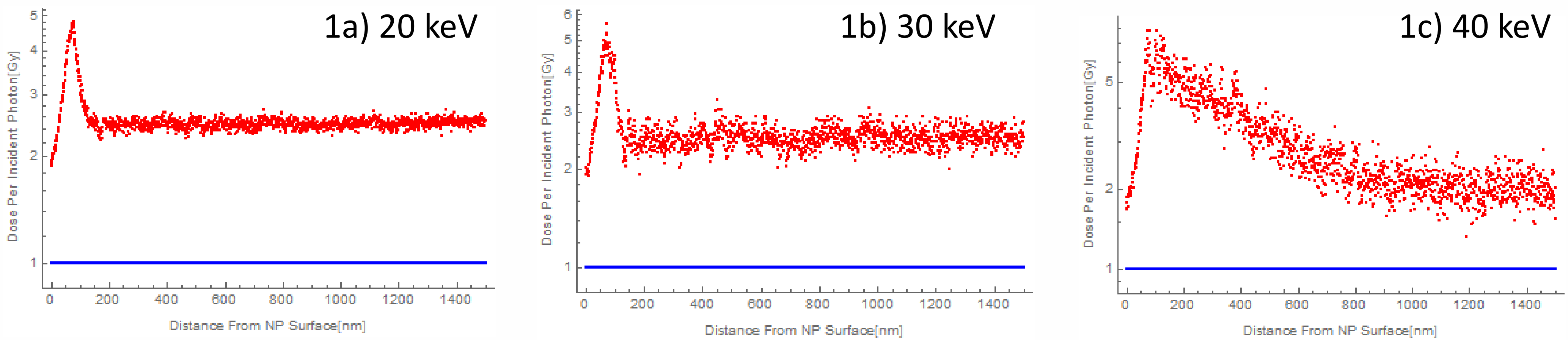

Compton

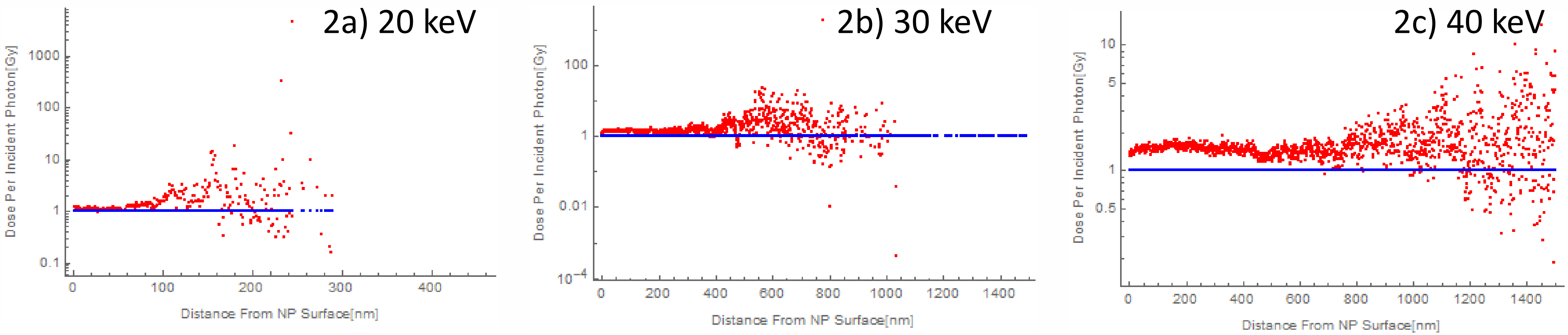

Figure 13 – Graphs showing the radial dose distributions per incident photon for Al_2O_3 as a ratio to $Mg(OH)_2$ NPs irradiated by a) 20 b) 30 and c) 40 keV photon beam, filtered by 1) the photoelectric effect and 2) the Compton effect

Conclusions

- Unique insight into the fundamental processes occurring on the nano-scale in irradiated NP aqueous systems
- Following photon beam irradiation Al_2O_3 NPs exhibit a greater dose than $Mg(OH)_2$ NPs
- Theorised to be due to photoelectric effects (i.e. Auger cascade)

Future Work

- Apply the model to other oxide/hydroxide NPs – to build a systematic survey
- Accounting for excitons
- Incorporate Geant4-DNA Chemistry into the current model - permits simulations of radiolytic products diffusion and mutual interactions

TRANSCEND

Transformative Science and Engineering for Nuclear Decommissioning

MANCHESTER 1824
The University of Manchester

NATIONAL NUCLEAR LABORATORY

Thank you

Ella Schaefer
ella.schaefer@postgrad.manchester.ac.uk

TRANSCEND

Transformative Science and Engineering for Nuclear Decommissioning

Safe Interim Storage of plutonium: Electrochemical investigations on doped plutonium oxide

Transcend Research Consortium

Dr. Dominic Laventine, Prof. Colin Boxall
Lancaster University

Energy – For a Low Carbon Future

Lancaster University

NATIONAL NUCLEAR LABORATORY

Lloyd's Register Foundation

Plutonium interim storage in the UK

Ca. 250 tonnes of separated Pu currently stockpiled worldwide. Approx. 137 tonnes is in interim storage in UK whilst the Government "develops its options".
Interim storage of PuO_2 involves sealing in nested steel containers, under a partial argon atmosphere with (PVC) packing material.

PuO_2 is hydroscopic and picks up water during the packaging process. The disposition of this water under the storage conditions is unclear: It may exists in a gaseous state, or be weakly or strongly bound to the PuO_2 surface.

Radiolytic and catalytic processes may also result in formation of radicals and other chemical species with high oxidative potential (H_2O_2, $\cdot OH$)

Need to understand how the structure and properties of PuO_2 change with time under storage condition, including under oxidative conditions.

Cannister pressurisation

Over time a small number of cannisters have been observed to deform due to pressurisation: this makes storage and efficient heat transfer difficult 5 routes to gas production have been suggested that could contribute to this pressurisation:

(i) Helium accumulation from a decay
(ii) Decomposition of polymeric packing material
(iii) H_2O desorption (steam) from hygroscopic PuO_2
(iv) Radiolysis of adsorbed water
(v) Generation of H_2 by chemical reaction of PuO_2 with H_2O, producing a PuO_{2+x} phase.

The last route, forming hyperstoichiometric PuO_{2+x}, was suggested by Hashke to explain experimental results, and has been supported by computational studies, but has not been spectroscopically observed and has been disputed on thermodynamic grounds.

Thus, we propose to use electrochemical techniques to study interrogate the possible solid-state oxidation of PuO_2 to PuO_{2+x} directly using PuO_2 thin layer-coated microelectrodes.

- **Introduction to plutonium electrochemistry**
- **Synthesis of thin-layer actinide coatings**
- **Electrochemistry of doped-U and Pu layers**

- **Introduction to actinide electrochemistry**
- Synthesis of thin-layer actinide coatings
- Electrochemistry of doped-U and Pu layers

Doped UO_2 cyclic voltammetry

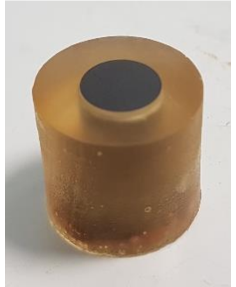

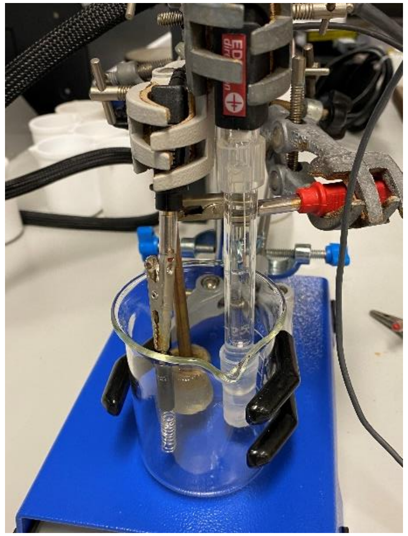

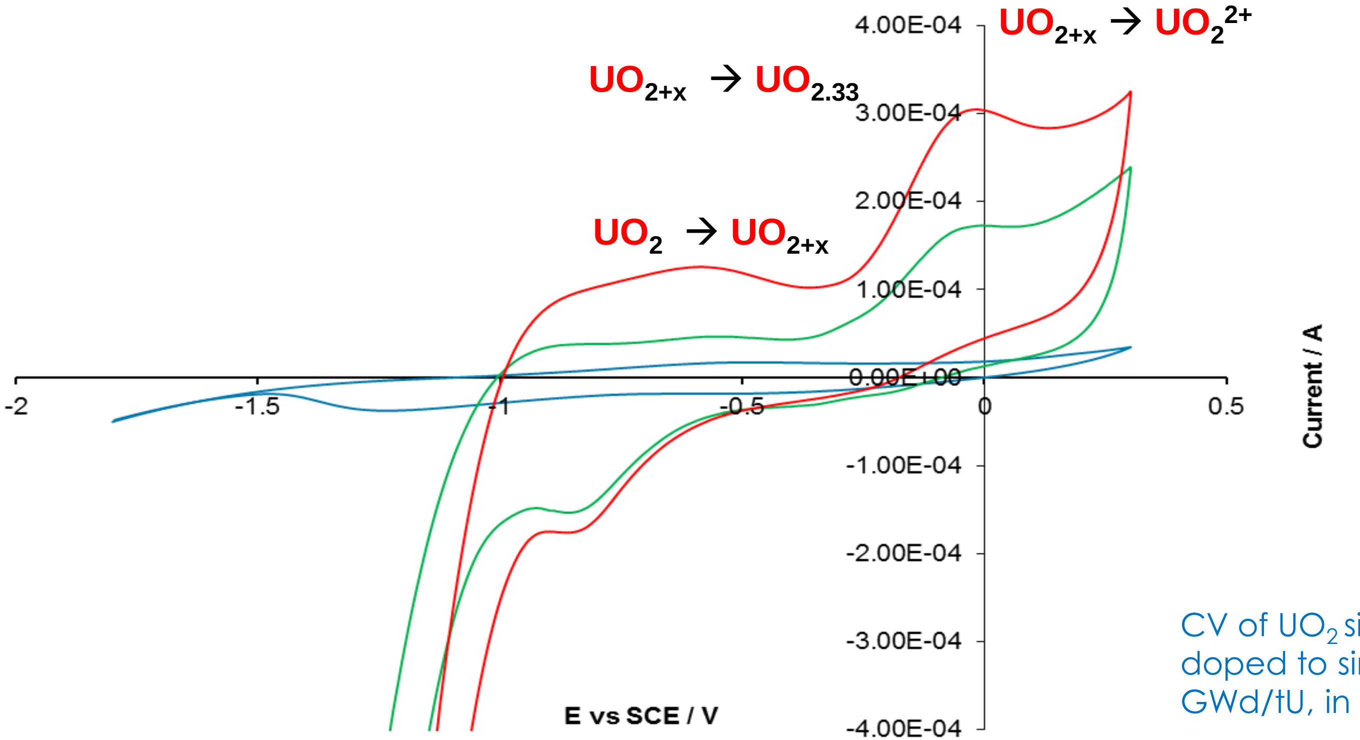

CV of UO_2 simfuel pellet, doped to simulate 43 GWd/tU, in 0.1 M Na_2SO_4

- Voltammetry of AGR SIMFUELs in aqueous systems show them to be susceptible to electrochemical oxidation, due to semi-conductor properties introduced by dopants.
- Aqueous electrochemical limited to approx. max 1.23 V due to water oxidation.

TRANSCEND NATIONAL NUCLEAR LABORATORY Lancaster University

Actinide oxide electron energies

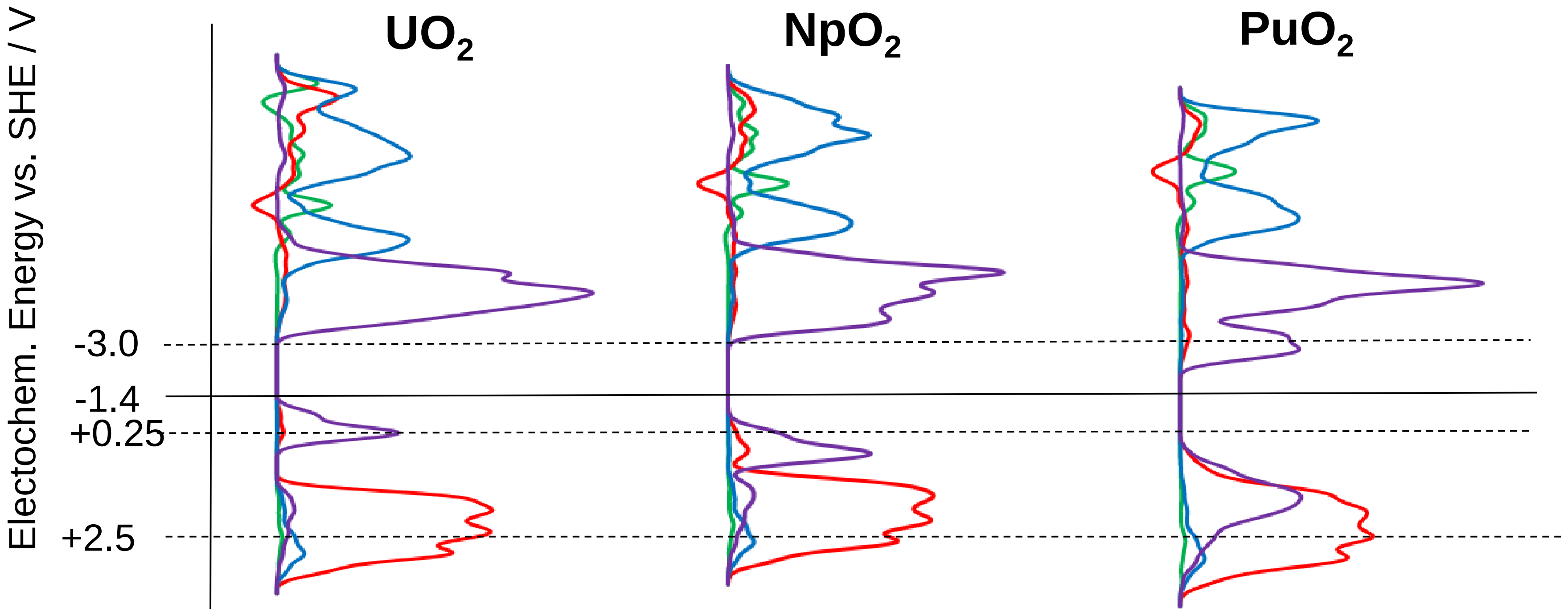

- Electronic structure of bulk AnO_2 clusters calculated with PBE0 function (Joseph Wllington, Uni. Manchester), then converted to electrochemical potentials.
- UO_2 and NpO_2 predicted to be Mott-Hubbard insulators, PuO_2 predicted to be a charge transfer insulator.
- UO_2 IV -> V occurs at ~ -0.25 V vs SHE, where the energy is sufficient to access the 5f.
- PuO_2 requires greater voltage to oxidise, and therefore solvent with higher electrochemical limit e.g. butyrolactone

TRANSCEND NATIONAL NUCLEAR LABORATORY Lancaster University

Electrochemical window for Pu^{IV} -> Pu^{V}

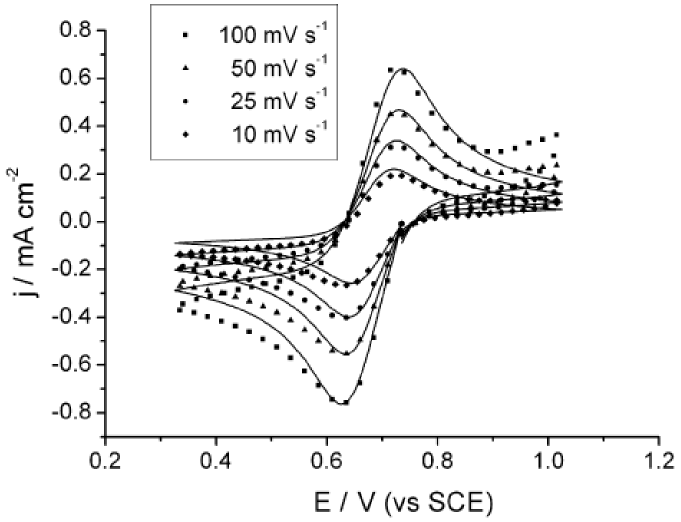

Literature CV of Pu solution in HNO_3 aq., showing Pu^{III} -> Pu^{IV} transition, with no further oxidation up to 1.0 V.

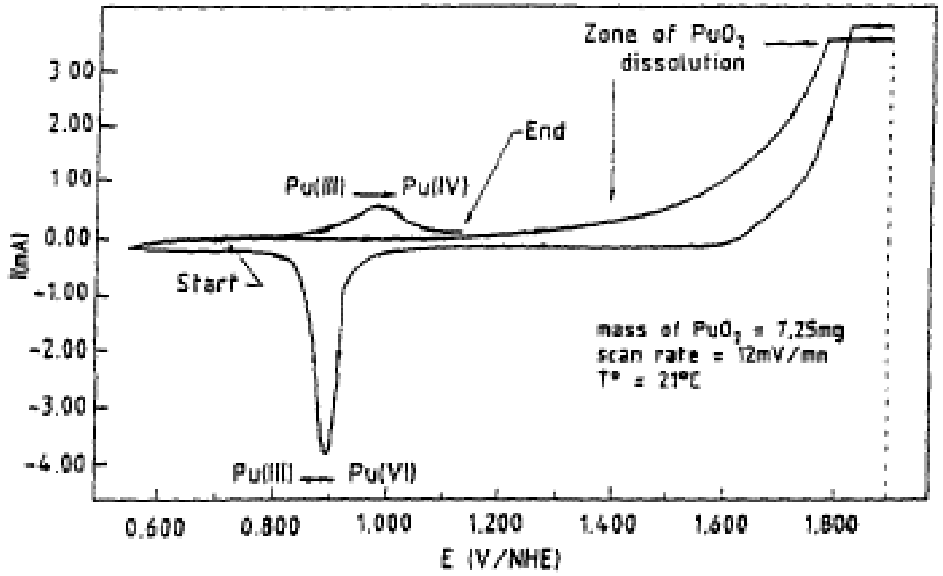

Literature CV of PuO_2 on carbon paste electrode (7.25 mg of PuO_2; 1 M $HClO_4$ aq.). Further oxidation occurs along with PuO_2 dissolution at > 1.4 V, but is hidden by water oxidation wave.

- Literature redox potentials (in acidic aq.) Pu^{III} -> Pu^{IV} at 0.7-1.0 V vs SCE.
- Pu^{IV} -> Pu^{V} expected to be higher, possible above ~1.4 V vs NHE.
- Water oxidation occurs ~1.2 V under standard conditions. Too low to see Pu^{V} formation.
- There, we planned to use organic solvents to allow access to higher voltages e.g. MeCN, GBL

- Introduction to plutonium electrochemistry
- **Synthesis of thin-layer actinide coatings**
- Electrochemistry of doped-U and Pu layers

PuO_2 coated microelectrodes

- PuO_2 coated microelectrodes made, minimising Pu required for coating.
- *Via* dip-coating electrode in $Pu(NO_3)_x$ solution (Pu-239), in HNO_3 (aq) / EtOH with surfactant 5% triton-X) added, followed by evaporation of ~ 10 μL droplet.
- Calcine at 400°C

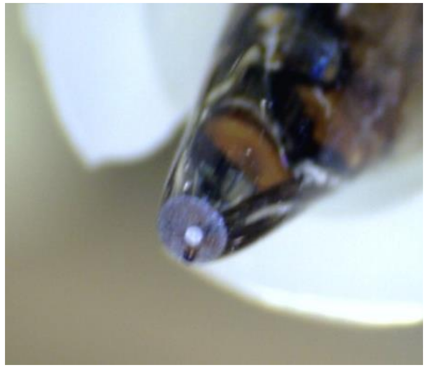

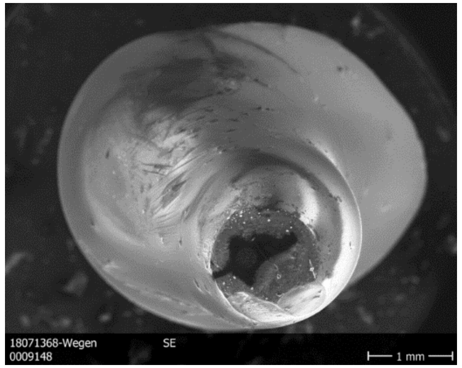

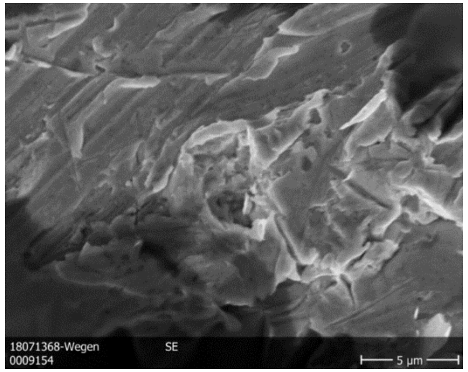

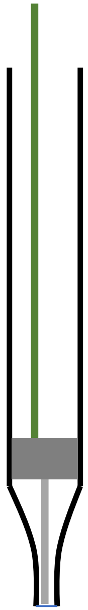

- Vary $Pu(NO_3)_x$ solution (8, 40 mM) to give ~ 200 nm – 1 μm layers
- Dope with Eu (1-10%) to increase p-type semiconductor behaviour
- Test 4 electrolyte systems: $NaClO_4$ (aq), $NaClO_4$ (MeCN), Bu_4NF_4B (MeCN), Bu_4NF_4B (GBL).

TRANSCEND NATIONAL NUCLEAR LABORATORY Lancaster University

- Introduction to plutonium electrochemistry
- Synthesis of thin-layer actinide coatings
- **Electrochemistry of doped-U and -Pu layers**

Electrochemical window for Pu^{IV} -> Pu^{V}

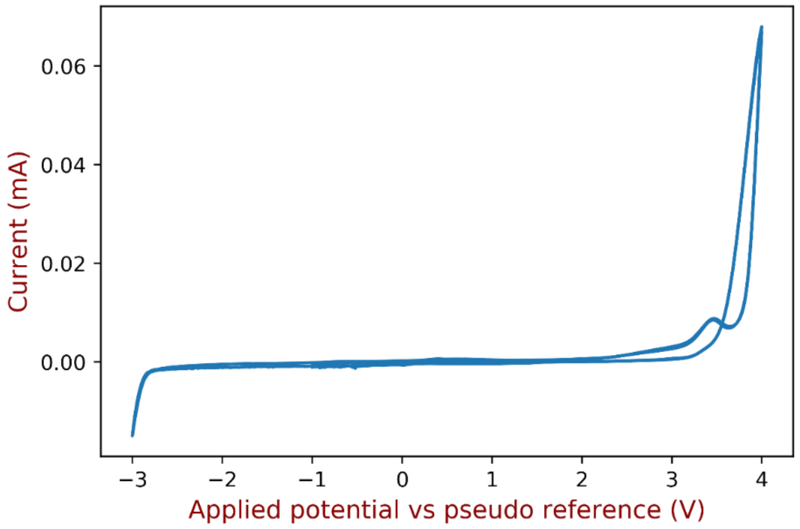

CV of Pt microelectrode in TBATFB / GBL, showing large potential window without electrolyte breakdown.

- TBATFB electrolyte in GBL allows a wide electrochemical window to > 2.0 V.
- GBL has low vapour pressure and flammability, and is non-toxic.

UO_2 CV in GBL

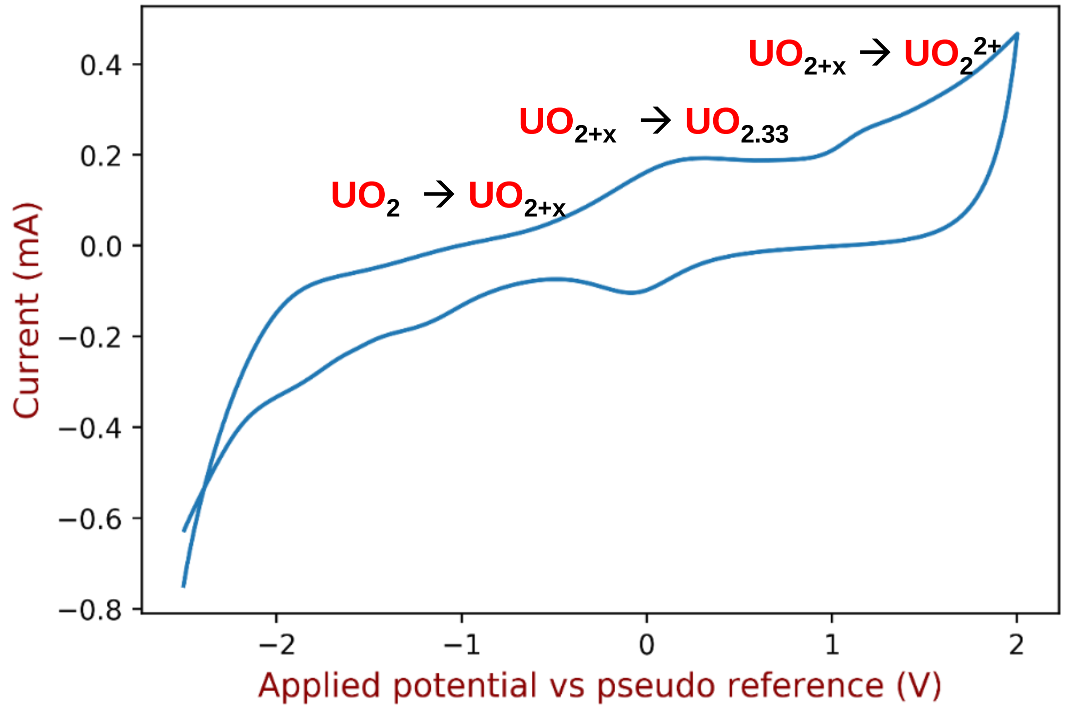

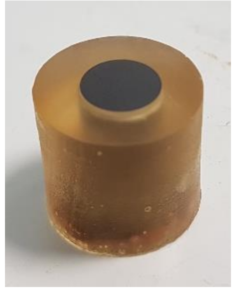

CV of UO_2 simfuel pellet, doped to simulate 43 GWd/tU, in 1 M TBATFB / GBL electrolyte, using a Pt pseudo reference.

- Voltammetry of AGR SIMFUELs in organic system (1 M TBATFT / GBL) show the same redox peaks as the aqueous CVs.
- Similar current passes (~ 0.5 mV) as aqueous system.
- Aqueous electrochemical limited to approx. max 1.23 V due to water oxidation.

TRANSCEND NATIONAL NUCLEAR LABORATORY Lancaster University

Initial PuO_2 CVs

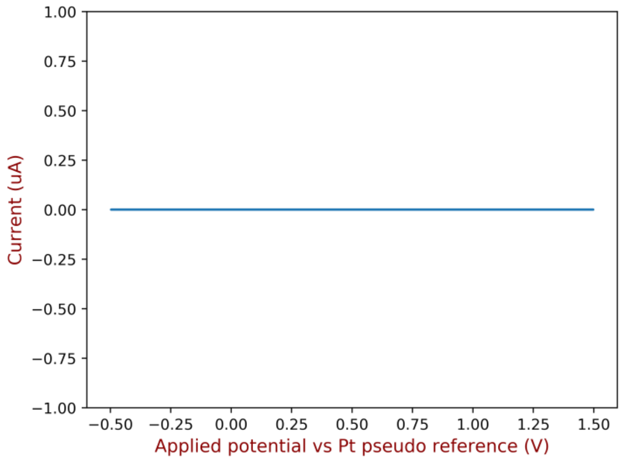

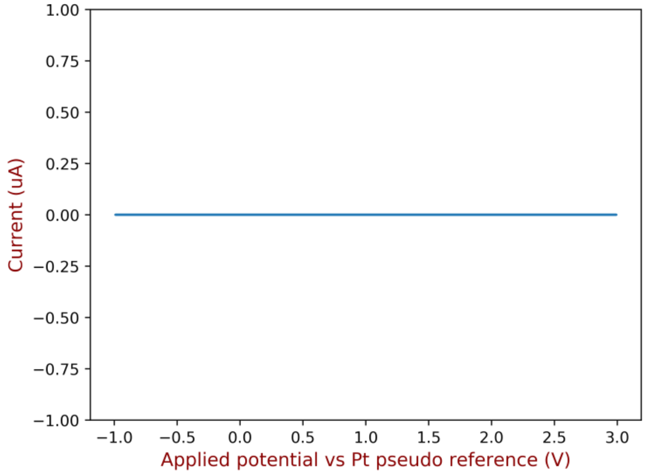

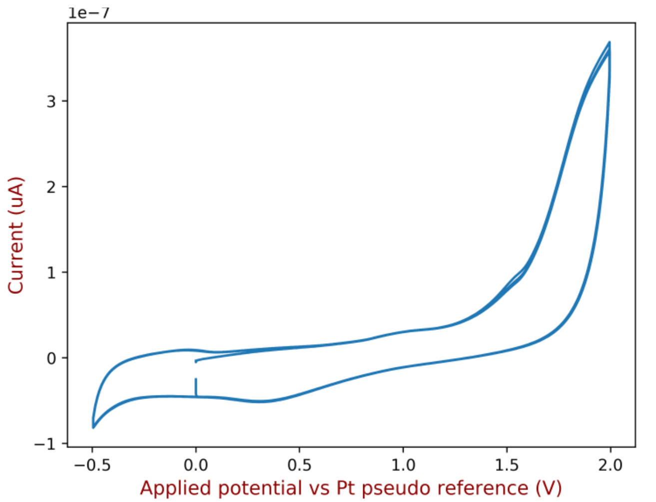

- Thicker PuO_2 layers (~1 um) were found to pass no current in measurable range, in aqueous or organic systems.
- Eu-doping of thicker PuO_2 layers (~1 um, 1-10% Eu) also did not allow sufficient current to pass.
- Reducing the thickness of the Eu-doped of PuO_2 layers (~200 nm, 10% Eu) resulted in layers that did pass current (10 nA range).

PuO_2 CV in GBL

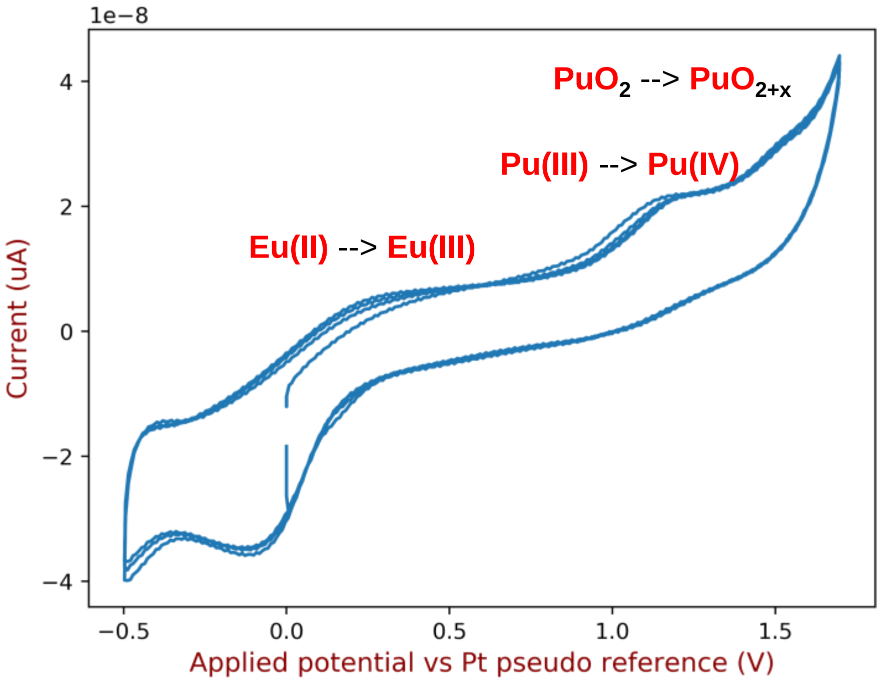

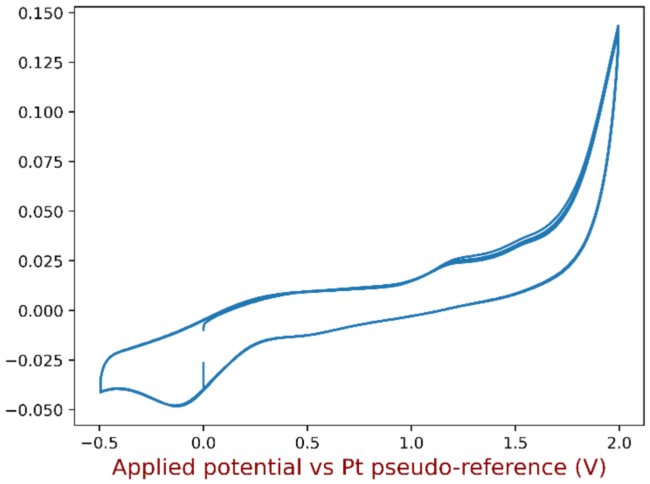

CV of 10% Eu-doped PuO_2, in 1 M TBATFB / GBL electrolyte, using a Pt pseudo reference.

- Redox peaks observed were assigned by comparison to the UO_2 CVs in the same electrolyte and to literature values for Pu oxidations.
- Oxidation at ~ 1V assigned to a Pu_{III} -> Pu^{IV} transition.
- Oxidation at ~ 1.5V assigned to a Pu^{IV} -> Pu^{V} transition.

PuO_2 Impedance

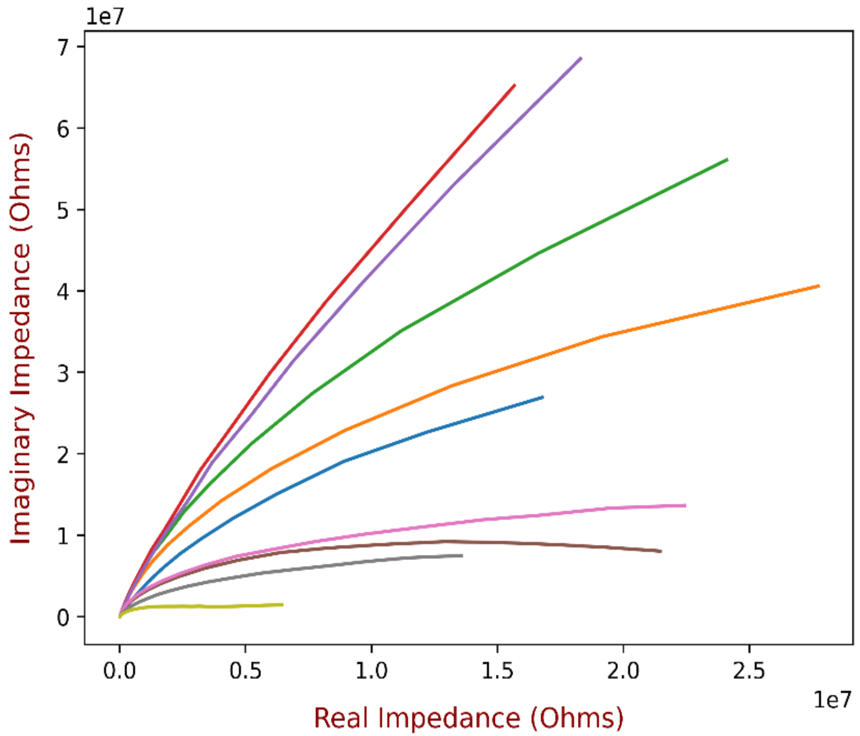

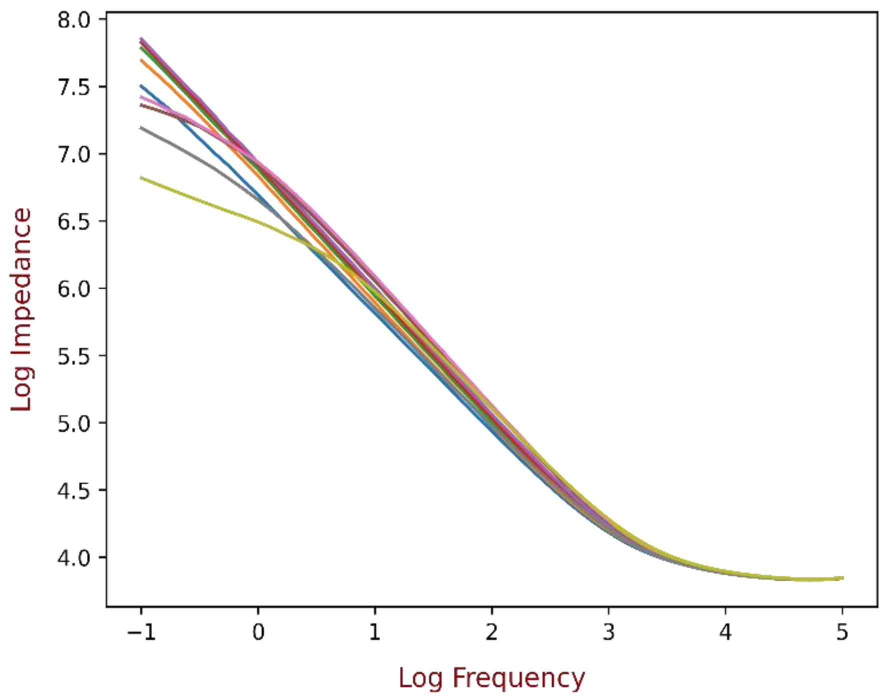

- Impedance of 10% Eu-doped PuO_2 was measured at a range of applied potentials (-1.0 – 3.0 V) in TBATFB / GBL.

- Bode plot shows one dominant time constant (indicating one component in the circuit dominates the impedance), with the Nyquist plot showing a well defined curve.

PuO_2 Impedance

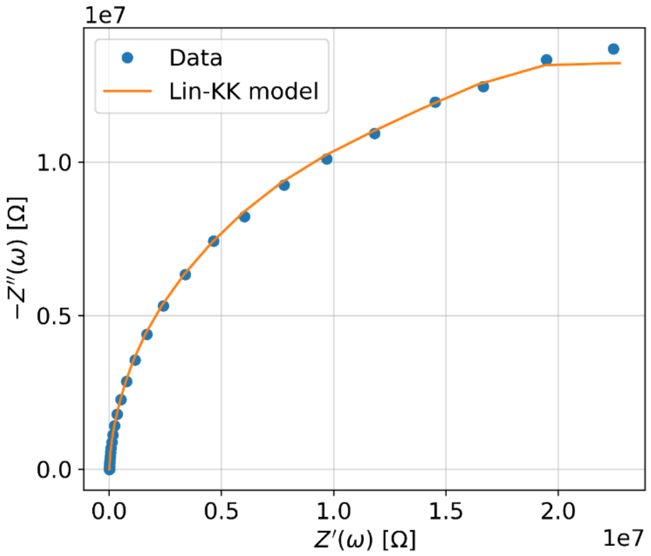

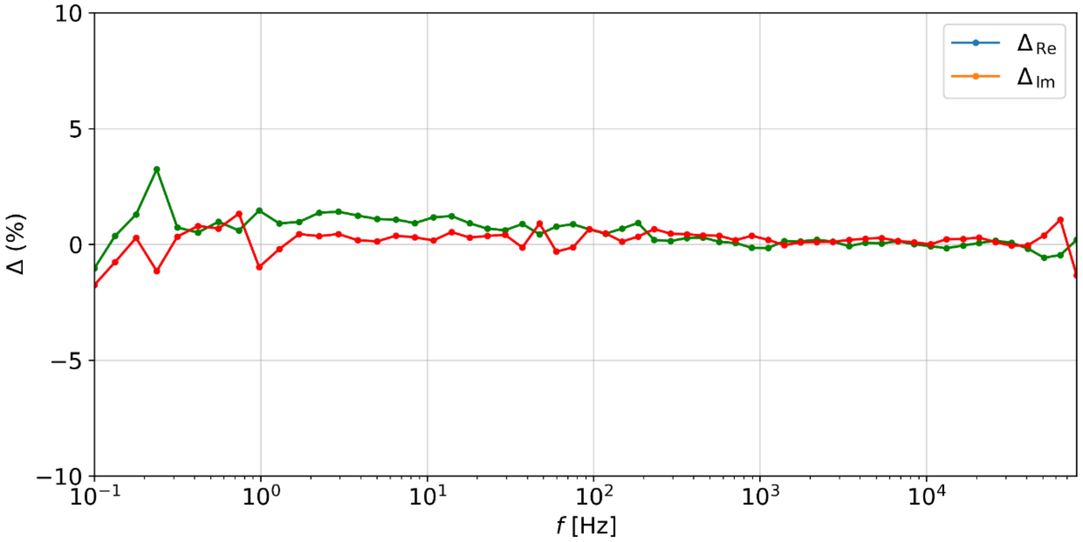

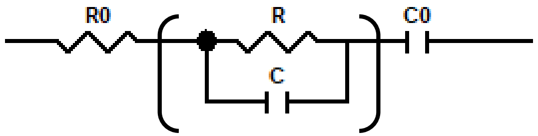

- Fitting of data to various serial and parallel Randles circuits.
- KK-plot predicts "2.6" Randles circuits required.

- Fitted models give values for the resistances and capacitances or each component (resistance/capacitance pair) in the circuit.

TRANSCEND NATIONAL NUCLEAR LABORATORY Lancaster University

PuO_2 Impedance

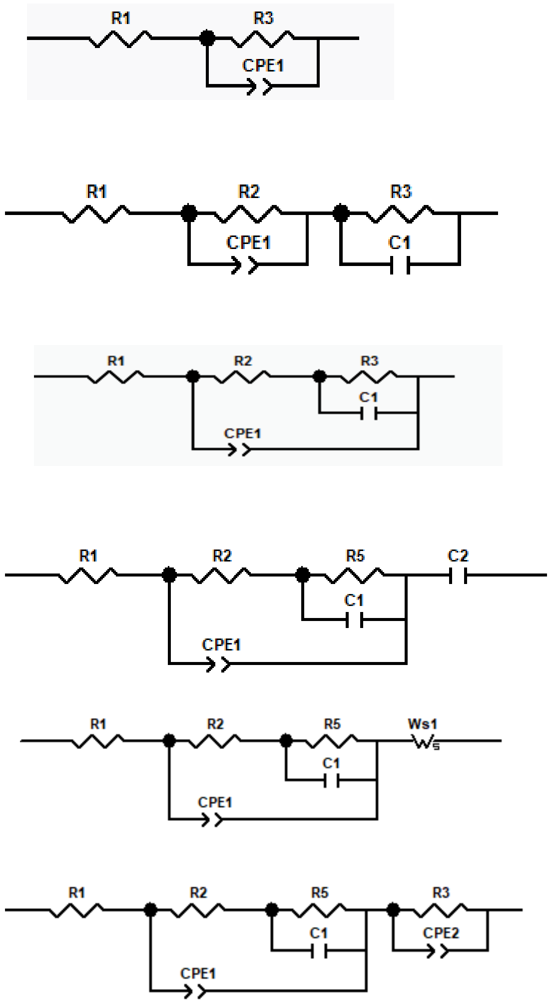

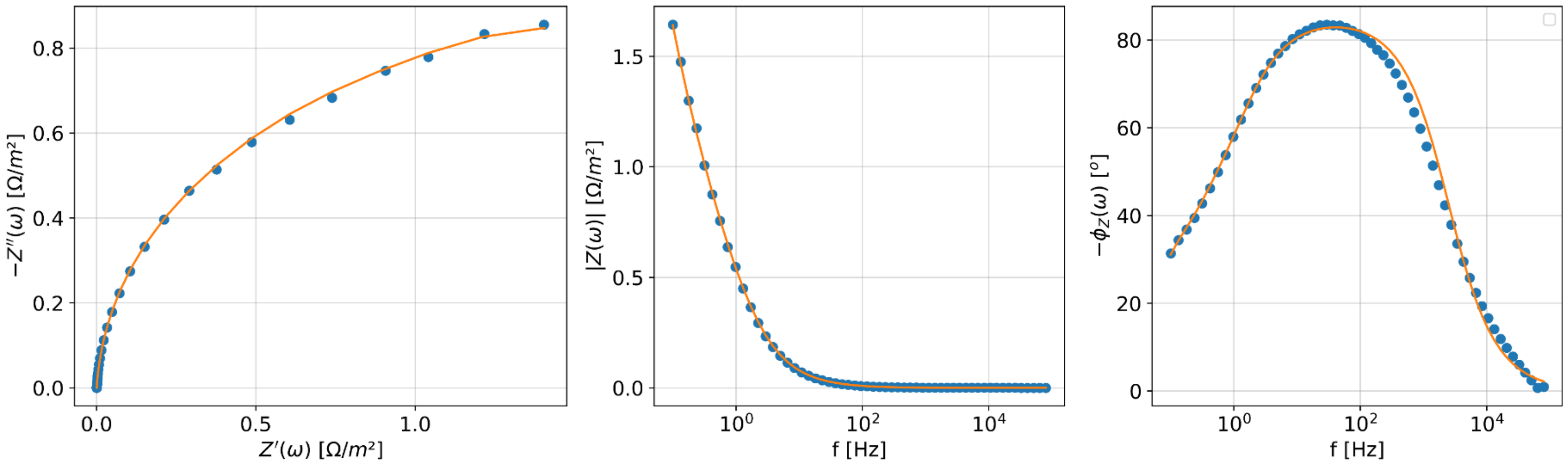

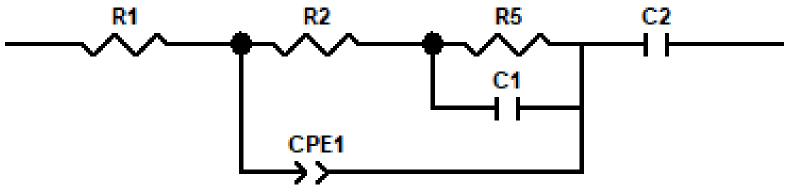

TRANSCEND
NATIONAL NUCLEAR LABORATORY
Lancaster University

Mott-Schottky plot 1

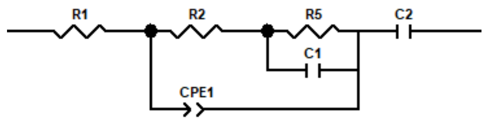

$$\frac{1}{C^2} = \frac{2}{\varepsilon\varepsilon_0 A^2 q N_D}\left(-E + E_{FB} + \frac{k_B T}{q}\right)$$

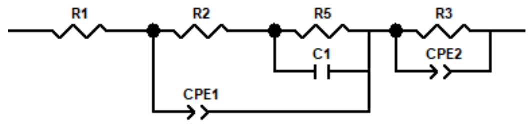

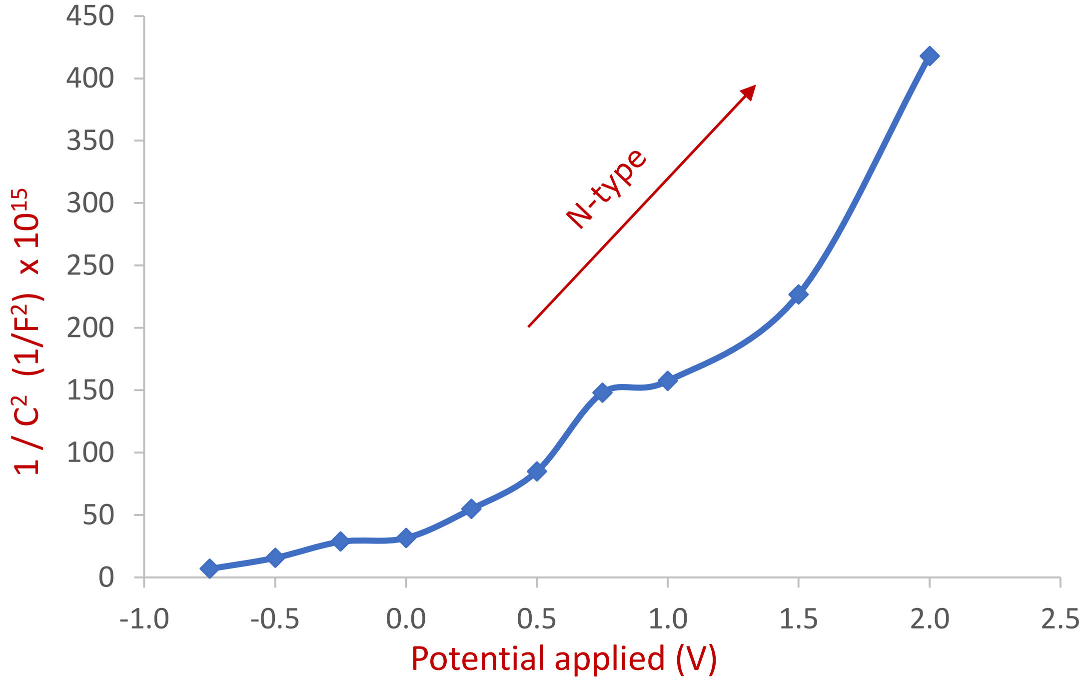

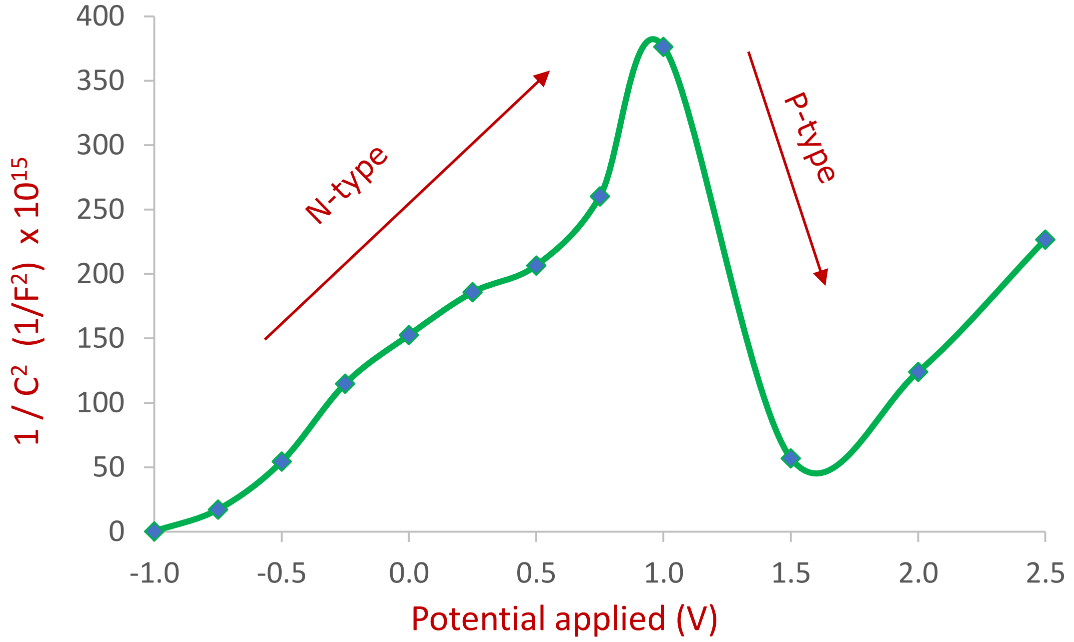

- Capacitance of PuO_2 coating obtained from Randles circuit fit was plotted (as inverse square) against the applied potential to produce a 'Mott-Schottky' plot.
- Mott-Shottky plot shows reflex point between 1.0-1.5 V, indicating change in semi-conductor type from N-type to P-type.
- More data needed

Conclusions

- Thin-layers of ceria, urania and plutonia produced through dip-coating process onto gold and platinum electrodes.

- Cyclic voltammetry of doped UO_2 measured in aqueous and organic solvent systems, showing current can be passed in both, and redox chemistry of solid UO_2 to be explored.

- PuO_2 layers found to be insulators as expected, but reducing thickness to nano-scale and doping with europium found to allow current to pass.

- Cyclic voltammetry of Eu-doped PuO_2 measured in organic solvent systems, allowing redox chemistry of solid PuO_2 to be explored at potential higher than are possible in aqueous systems, showing an oxidation at ~1.5 V assigned to PuO_2 -> PuO_{2+x}.

- Impedance spectrometry of Eu-doped PuO_2 measured in organic solvent systems at a range of potentials allowed capacitance of the layers to be measured, and show a change in semiconductor character, possibly due to to the observed PuO_2 -> PuO_{2+x}. More modelling underway.

TRANSCEND NATIONAL NUCLEAR LABORATORY Lancaster University

Lancaster University

Elizabeth Howett

Richard Wilbraham

ITU

Detlef Wegen

Nadya Rauff-Nisthar

Thanks for your attention

Mott-Schottky plots 2

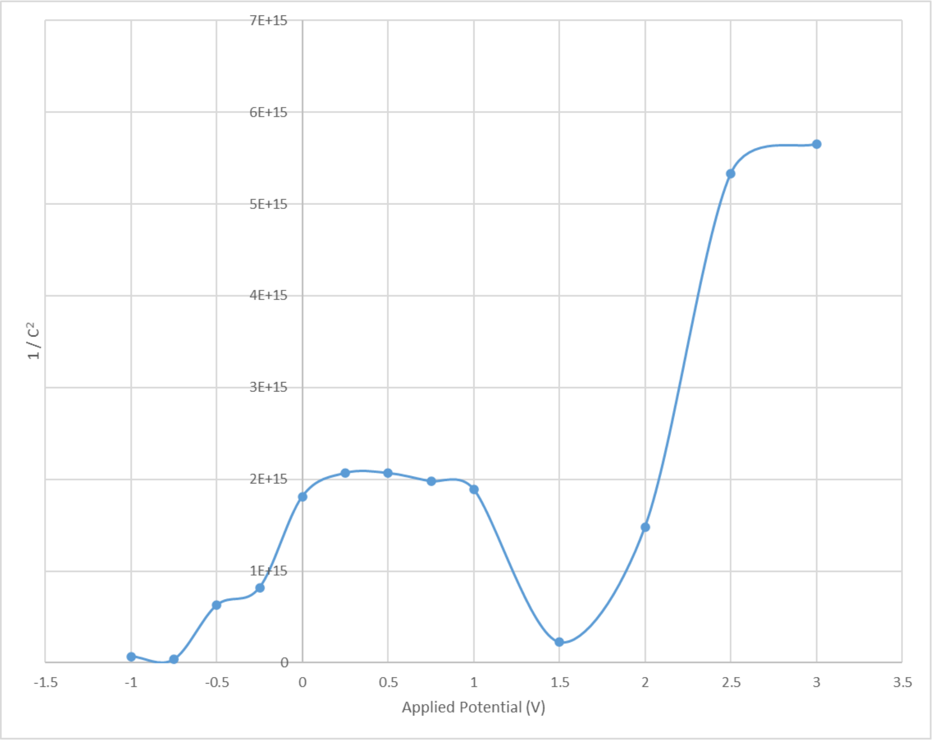

Mott Schottky plot using 2 Randles circuits

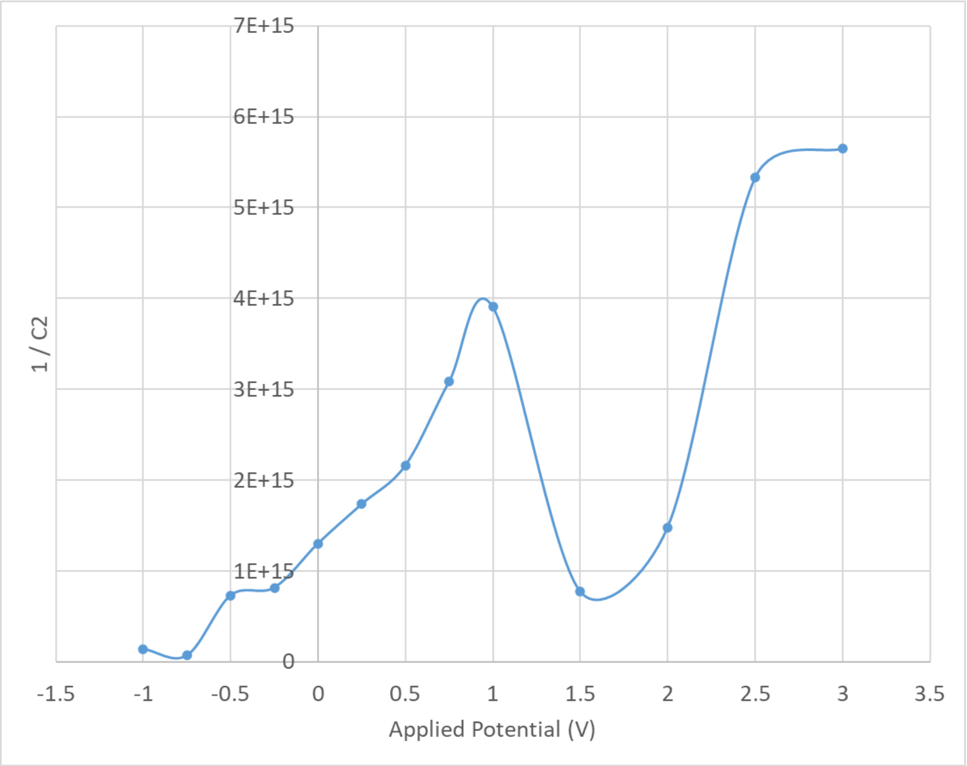

Mott Schottky plot using 2 Randles circuits and limiting data to above 0.5 Hz throughout

Improve fit

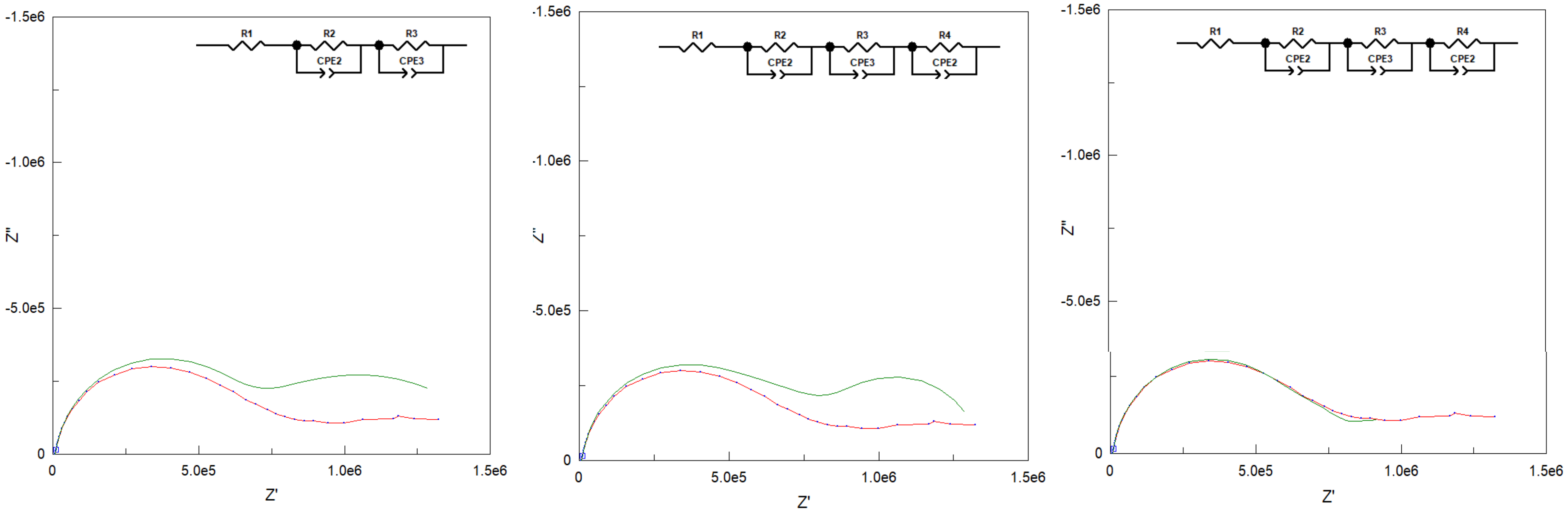

- Zview does not give good fit for 2 or 3 Randles circuits.
- Improved fit by manually fitting to 3 Randles.

TRANSCEND NATIONAL NUCLEAR LABORATORY Lancaster University

Improve fit

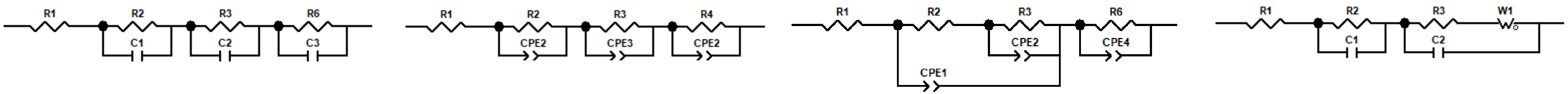

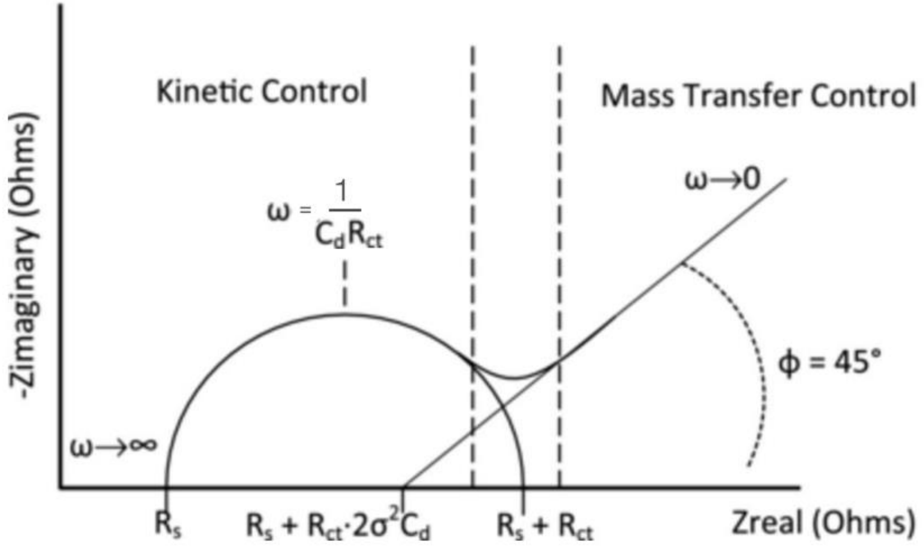

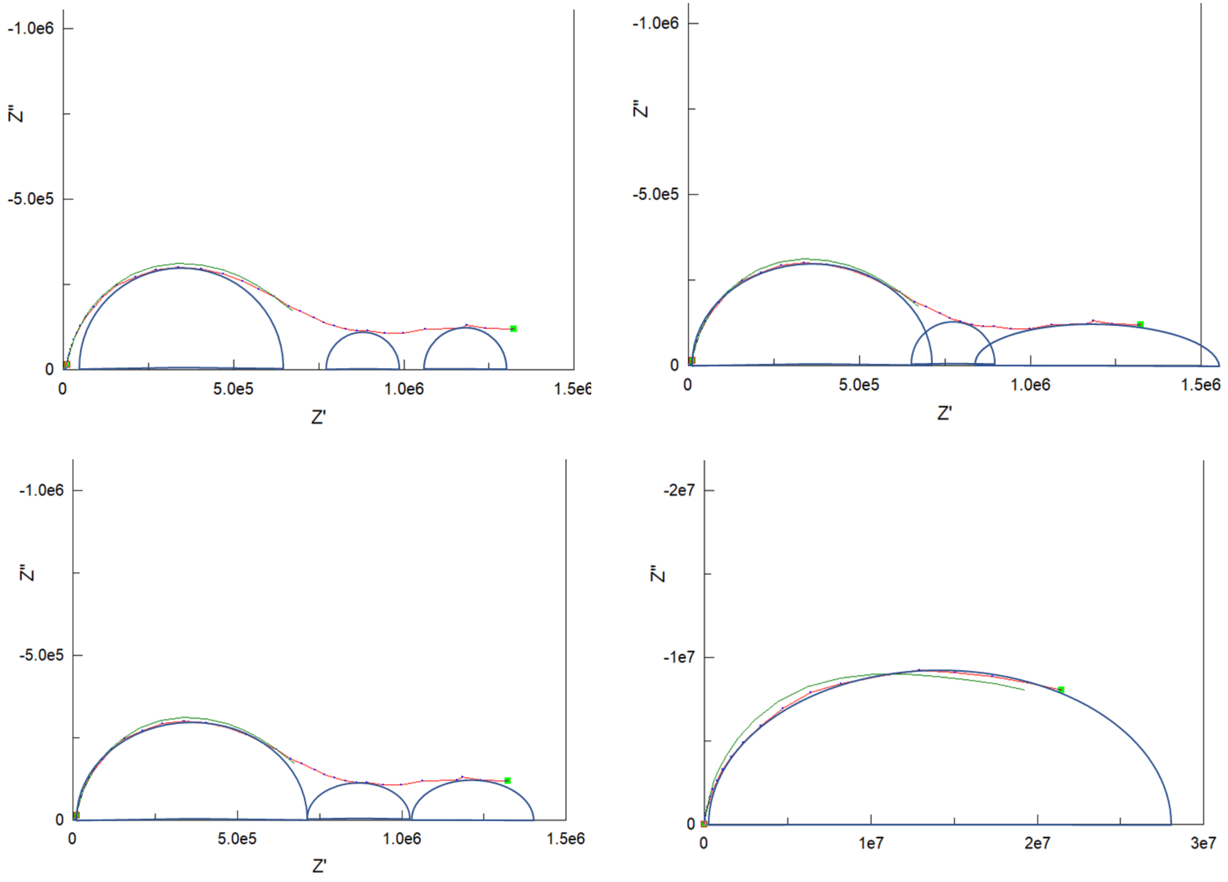

- Add additional Randles circuits. 3 or 4?
- Compare series versus nested circuits
- Warburgs or CPEs